

# **Stony Brook University**



OFFICIAL COPY

**The official electronic file of this thesis or dissertation is maintained by the University Libraries on behalf of The Graduate School at Stony Brook University.**

**© All Rights Reserved by Author.**

# **Mechanistic Studies of the Photoactive Protein AppA**

A Dissertation Presented

by

**Allison Haigney**

to

The Graduate School

in Partial Fulfillment of the

Requirements

for the Degree of

**Doctor of Philosophy**

in

**Chemistry**

Stony Brook University

**May 2012**

**Stony Brook University**

The Graduate School

**Allison Haigney**

We, the dissertation committee for the above candidate for the  
Doctor of Philosophy degree, hereby recommend  
acceptance of this dissertation.

**Peter J. Tonge – Dissertation Advisor  
Professor of Chemistry**

**Erwin London – Chairperson of Defense  
Professor of Biochemistry and Cell Biology**

**Lisa M. Miller – Committee Member of Defense  
Biophysicist, National Synchrotron Light Source, Brookhaven National Laboratory**

**Robert Callender – External Committee Member of Defense  
Professor of Biochemistry, Albert Einstein College of Medicine**

This dissertation is accepted by the Graduate School

Charles Taber  
Interim Dean of the Graduate School

Abstract of the Dissertation

**Mechanistic Studies of the Photoactive Protein AppA**

by

**Allison Haigney**

**Doctor of Philosophy**

in

**Chemistry**

Stony Brook University

**2012**

The blue light using flavin (BLUF) domain proteins are a novel class of photosensors that bind flavin noncovalently in order to sense and respond to high intensity blue (450 nm) light. The transcriptional antirepressor AppA, is a BLUF photosensor that utilizes a non-covalently bound flavin chromophore which is unable to undergo large scale structural change upon light absorption in contrast to most photoreceptors such as rhodopsin, which undergo structural alterations such as trans/cis isomerization upon irradiation. It is thus of great interest to understand how the BLUF protein matrix senses and responds to flavin photoexcitation. In order to probe the mechanism of photoactivation, the excited state photochemistry of wild-type and mutant AppA proteins has been analyzed using ultrafast time resolved infrared (TRIR) spectroscopy. Reconstitution of the protein with isotopically labeled flavin has permitted unambiguous assignment of the ground and excited state modes associated with the flavin C2=O and C4=O groups which participate in a hydrogen bonding network that surrounds the flavin. This approach has allowed us to probe the role of the hydrogen bonding network in AppA activation. Isotope labeling of the Q63E mutant allowed assignment of a protein mode that



appears within 100 fs of excitation, demonstrating that the protein matrix responds instantaneously to flavin excitation. These data have led to a detailed understanding of the photoexcitation mechanism, which involves a tautomerization followed by rotation of residue Q63. Additional insight into photoactivation of AppA has also been obtained by replacing a key tyrosine in the hydrogen bonding network with unnatural fluorotyrosine analogs that have altered pKa values. These data have established the acidity of residue Y21 is crucial in stabilizing the light activated form of the protein.

## **Dedication Page**

To my parents for their unconditional love, continuous support and for always believing in me.

## Table of Contents

Abstract.....	iii
Table of Contents.....	vi
List of Figures and Tables.....	x
List of Abbreviations .....	xvi
Acknowledgement .....	xx
List of Publications .....	xxi
Chapter 1. Introduction to AppA and Methodologies of Study .....	1
A. Photoreceptors- Light to Chemical Energy Blue Light Using FAD Domain.....	1
B. Blue Light Using FAD Domains .....	2
C. AppA, A BLUF Domain Protein .....	4
D. Methods to Incorporate Unnatural Amino Acids.....	14
E. Ultrafast Studies of AppA- Time Resolved Spectroscopy .....	17
F. Specific Aims.....	20
G. References.....	21
Chapter 2. Assignments of Vibrational Modes by FAD and Riboflavin Isotopologue Incorporation into AppA <sub>BLUF</sub> .....	26
A. Introduction.....	26
B. Materials and Methods.....	29
B.1. Over expression and Purification of AppA.....	29
B.2. Binding of Riboflavin and FAD Isotopologues to AppA .....	30
B.3. Time Resolved Infrared Spectroscopy.....	31

B.4. Density Functional Theory Calculations .....	32
C. Results and Discussion .....	33
C.1. Isotopically Labeled Carbonyls of Flavin. [4,10a- <sup>13</sup> C <sub>2</sub> ]riboflavin and [2- <sup>13</sup> C <sub>2</sub> ]-FAD.....	33
C.2. Additional Assignments of Flavin Vibrational Modes. [[uniform- <sup>13</sup> C <sub>17</sub> ]-FAD, [xylene- <sup>13</sup> C <sub>8</sub> ]-FAD, [uniform- <sup>15</sup> N <sub>4</sub> ]-FAD and [4- <sup>18</sup> O <sub>1</sub> ]-FAD.....	49
D. Conclusions.....	66
E. References.....	68
Chapter 3. Reorganization of the Hydrogen Bonding Network Surrounding the Flavin Chromophore of AppA .....	73
A. Introduction.....	73
B. Materials and Methods.....	73
B.1. Overexpression and Purification of AppA and its Mutants .....	73
B.2. Photoconversions .....	75
B.3. Steady State Raman Spectroscopy.....	76
B.4. Time Resolved Fluorescence Measurements.....	76
B.5. Time Resolved Infrared Spectroscopy.....	77
B.6. Transient Absorption Spectroscopy.....	78
C. Results and Discussion .....	79
C.1. Photoexcitation of the Blue Light Using FAD Photoreceptor AppA Results in Ultrafast Changes to the Protein Matrix (Q63E AppA <sub>BLUF</sub> ).....	79

C.2. Reorganization of the Hydrogen Bonding Network Reveals the Significance of Residue W104 in the Stabilization of lAppA and Shows No Evidence for Electron Transfer During Photoactivation (The W104M and Y21W Mutants).....	98
D. Conclusions.....	108
E. References.....	110
Chapter 4. Modulating the Environment of the Hydrogen Bonding Network of AppA to Probe Time Dependant Structural Changes that Occur with Photoactivation .....	113
A. Introduction.....	113
B. Materials and Methods.....	116
B.1. Tyrosine Phenol Lyase Purification.....	116
B.2. Enzymatic Synthesis of Fluorinated Tyrosine Analogs.....	117
B.3. AppA Overexpression Protocols for Mutants and Fluorotyrosine Incorporation.....	118
B.4. Incorporation of Cyanophenylalanine using the Amber Codon Methodology....	120
B.5. Time-Resolved Infrared Spectroscopy .....	122
C. Results and Discussion .....	124
C.1. Y21 Mutants (Y21C, Y21S and Y21I) .....	124
C.2. Tyrosine Phenol Lyase- Enzymatic Production of Fluorinated Tyrosine.....	129
C.3. Y56F AppA <sub>BLUF</sub> .....	130
C.4. Incorporation of Fluorinated Tyrosine into Y56F AppA.....	132
C.5. Incorporation of 3,5-difluorotyrosine into residue Y21 .....	136
C.6. Incorporation of 3-fluorotyrosine into residue Y21 .....	136
C.7. Incorporation of 2-fluorotyrosine into residue Y21 .....	139

C.8. Incorporation of 2,6-difluorotyrosine into residue Y21 .....	144
C.9. Major Conclusions from Fluorotyrosine Incorporation .....	145
C.10. Cyanophenylalanine Incorporation .....	149
D. Conclusions .....	158
E. References .....	160
Chapter 5. Summary of Proposed Models for Dark to Light Formation and Light to Dark Recovery of AppA <sub>BLUF</sub> .....	164
Bibliography .....	169

## List of Figures and Tables

### Chapter 1

<b>Figure 1.1.</b> Photoreceptor families with chromophore structure and proposed photochemistry ....	2
<b>Figure 1.2.</b> The biological role of AppA .....	4
<b>Figure 1.3.</b> Crystal structure of AppA <sub>BLUF</sub> bound to the flavin chromophore .....	5
<b>Figure 1.4.</b> Photoconversion of dAppA to lAppA .....	6
<b>Figure 1.5.</b> AppA's photocycle .....	6
<b>Figure 1.6.</b> Anderson <i>et. al.</i> crystal structure of AppA .....	7
<b>Figure 1.7.</b> Jung <i>et. al.</i> crystal structure of AppA .....	8
<b>Figure 1.8.</b> Steady state Raman difference spectra of AppA bound to riboflavin .....	9
<b>Figure 1.9:</b> Proposed mechanisms for the formation of lAppA from dAppA .....	11
<b>Figure 1. 10.</b> Crystal structure of AppA highlighting glutamines .....	15
<b>Figure 1.11:</b> Schematic of time resolved infrared spectroscopy.....	18

### Chapter 2

<b>Figure 2.1.</b> Environment of the isoalloxazine chromophore in AppA .....	34
<b>Figure 2.2.</b> TRIR and calculated spectra of unlabeled FAD and [2- <sup>13</sup> C <sub>1</sub> ]FAD in H <sub>2</sub> O .....	35
<b>Figure 2.3.</b> TRIR and calculated spectra of [2- <sup>13</sup> C <sub>1</sub> ]-FAD in H <sub>2</sub> O and D <sub>2</sub> O .....	36
<b>Figure 2.4.</b> TRIR and calculated spectra of unlabeled FAD in H <sub>2</sub> O and D <sub>2</sub> O.....	38
<b>Figure 2.5.</b> TRIR and calculated spectra of unlabeled riboflavin and [4,10a- <sup>13</sup> C <sub>2</sub> ]riboflavin in D <sub>2</sub> O .....	40
<b>Figure 2.6.</b> TRIR spectra and kinetic data of dAppA <sub>BLUF</sub> and lAppA <sub>BLUF</sub> bound to riboflavin or FAD in D <sub>2</sub> O .....	42

<b>Figure 2.7.</b> TRIR spectra of FAD and [2- <sup>13</sup> C <sub>1</sub> ]-FAD bound to dAppA <sub>BLUF</sub> and lAppA <sub>BLUF</sub> .....	44
<b>Figure 2.8.</b> TRIR spectra of FAD and [4,10a- <sup>13</sup> C <sub>2</sub> ]riboflavin bound to dAppA and lAppA .....	47
<b>Figure 2.9.</b> Isotopologues incorporated into AppA.....	49
<b>Figure 2.10a.</b> TRIR spectra of unlabeled FAD and [4- <sup>18</sup> O <sub>1</sub> ]-FAD in D <sub>2</sub> O .....	51
<b>Figure 2.10b.</b> Calculated spectra of unlabeled FAD and [4- <sup>18</sup> O <sub>1</sub> ]-FAD .....	52
<b>Figure 2.10c.</b> ES-API in negative mode for [4- <sup>18</sup> O <sub>1</sub> ]-FAD.....	53
<b>Figure 2.11a.</b> TRIR spectra of unlabeled FAD and [1,3,5,10- <sup>15</sup> N <sub>4</sub> ]-FAD in D <sub>2</sub> O .....	54
<b>Figure 2.11b.</b> Calculated spectra of unlabeled FAD and [1,3,5,10- <sup>15</sup> N <sub>4</sub> ]-FAD .....	54
<b>Figure 2.12a.</b> TRIR spectra of unlabeled FAD and [Xylene- <sup>13</sup> C <sub>8</sub> ]-FAD in D <sub>2</sub> O .....	55
<b>Figure 2.12b.</b> Calculated spectra of unlabeled FAD and [Xylene- <sup>13</sup> C <sub>8</sub> ]-FAD .....	56
<b>Figure 2.13a.</b> TRIR spectra of unlabeled FAD and [Uniform- <sup>13</sup> C <sub>17</sub> ]-FAD in D <sub>2</sub> O .....	57
<b>Figure 2.13b.</b> Calculated spectra of unlabeled FAD and [U- <sup>13</sup> C <sub>17</sub> ]-FAD .....	58
<b>Figure 2.14.</b> TRIR spectra of unlabeled FAD and [4- <sup>18</sup> O <sub>1</sub> ]-FAD bound to AppA .....	59
<b>Figure 2.15.</b> TRIR spectra of unlabeled FAD and [1,3,5,10- <sup>15</sup> N <sub>4</sub> ]-FAD bound to AppA .....	60
<b>Figure 2.16.</b> TRIR spectra of unlabeled FAD and [Xylene- <sup>13</sup> C <sub>8</sub> ]-FAD bound to AppA.....	62
<b>Figure 2.17.</b> TRIR spectra of unlabeled FAD and [Uniform- <sup>13</sup> C <sub>17</sub> ]-FAD bound to AppA .....	64
<b>Table 2.1.</b> Observed and calculated vibrational modes of FAD, [2- <sup>13</sup> C <sub>1</sub> ]-FAD, riboflavin and [4,10a- <sup>13</sup> C <sub>2</sub> ]riboflavin in H <sub>2</sub> O and D <sub>2</sub> O .....	48
<b>Table 2.2.</b> Observed and calculated vibrational modes of FAD, [4- <sup>18</sup> O <sub>1</sub> ]-FAD, [U- <sup>15</sup> N <sub>4</sub> ]-FAD, [U- <sup>13</sup> C <sub>17</sub> ]-FAD and [xylene- <sup>13</sup> C <sub>8</sub> ]-FAD in D <sub>2</sub> O Buffer .....	65

### Chapter 3

<b>Figure 3.1.</b> Hydrogen bonding network in dAppA and lAppA .....	79
--	----



<b>Figure 3.2.</b> Absorption spectra of wild-type d and lAppA <sub>BLUF</sub> and Q63E AppA <sub>BLUF</sub> .....	80
<b>Figure 3.3.</b> Raman spectra of wild-type d and lAppA <sub>BLUF</sub> and Q63E AppA <sub>BLUF</sub> .....	82
<b>Figure 3.4.</b> TRIR spectra of wild-type d and lAppA <sub>BLUF</sub> and Q63E AppA <sub>BLUF</sub> measured at 3 ps .....	84
<b>Figure 3.5.</b> Kinetics of the ground state recovery for wild-type d and lAppA <sub>BLUF</sub> and the Q63E AppA <sub>BLUF</sub> .....	85
<b>Figure 3.6.</b> Transient absorption spectra of wild-type d and lAppA <sub>BLUF</sub> and the Q63E AppA <sub>BLUF</sub> .....	86
<b>Figure 3.7.</b> Kinetics of the ground state recovery for wild-type and the Q63E AppA <sub>BLUF</sub> .....	87
<b>Figure 3.8.</b> TRIR spectra of unlabeled and <sup>13</sup> C labeled Q63E AppA <sub>BLUF</sub> .....	89
<b>Figure 3.9.</b> TRIR spectra of unlabeled and <sup>13</sup> C labeled d and lAppA <sub>BLUF</sub> .....	90
<b>Figure 3.10.</b> Proposed hydrogen bonding structure of Q63E AppA <sub>BLUF</sub> .....	94
<b>Figure 3.11.</b> Proposed model for formation of lAppA from dAppA .....	95
<b>Table 3.1:</b> Kinetics of dAppA <sub>BLUF</sub> , lAppA <sub>BLUF</sub> and Q63E AppA <sub>BLUF</sub> determined by TRIR and transient absorption spectroscopy .....	96
<b>Figure 3.12.</b> Electronic absorption spectra of W104M photoconversion bound to riboflavin ....	99
<b>Figure 3.13.</b> Electronic absorption spectra of W104M light to dark recovery .....	99
<b>Figure 3.14.</b> TRIR spectra of W104M bound to riboflavin .....	100
<b>Figure 3.15.</b> TRIR spectra wild-type d and lAppA <sub>BLUF</sub> and the Y21W AppA <sub>BLUF</sub> .....	102
<b>Figure 3.16.</b> Kinetics of the excited state decay and ground state decay for Y21W AppA <sub>BLUF</sub>	103
<b>Figure 3.17.</b> Kinetics of the excited state decay and ground state decay for lAppA <sub>BLUF</sub> .....	104
<b>Figure 3.18.</b> Kinetics of the excited state recovery for dAppA <sub>BLUF</sub> .....	105

<b>Figure 3.19.</b> Kinetics of the ground state recovery for wild-type d and lAppA <sub>BLUF</sub> and the Y21W AppA <sub>BLUF</sub> .....	105
<b>Figure 3.20.</b> The two crystal structure of AppA .....	106
 <b>Chapter 4</b>	
<b>Figure 4.1.</b> TRIR spectra of wild-type d and lAppA <sub>BLUF</sub> and Y21C AppA <sub>BLUF</sub> .....	125
<b>Figure 4.2.</b> TRIR spectra of wild-type d and lAppA <sub>BLUF</sub> and Y21S AppA <sub>BLUF</sub> .....	125
<b>Figure 4.3.</b> TRIR spectra of wild-type d and lAppA <sub>BLUF</sub> and Y21I AppA <sub>BLUF</sub> .....	126
<b>Figure 4.4.</b> Kinetics of the ground state recovery for wild-type d and lAppA <sub>BLUF</sub> and the Y21 AppA <sub>BLUF</sub> mutants .....	127
<b>Figure 4.5.</b> Protein configuration of residues Y21 and Q63 in wild-type d and lAppA <sub>BLUF</sub> .....	128
<b>Figure 4.6.</b> 15% PAGE gel of Tyrosine Phenol Lyase Purification .....	129
<b>Figure 4.7.</b> Mass spectrum of 2,6-difluorotyrosine.....	130
<b>Figure 4.8.</b> Electronic absorption spectra of Y56F AppA <sub>BLUF</sub> .....	131
<b>Figure 4.9.</b> TRIR spectra of Y56F d and lAppA <sub>BLUF</sub> .....	131
<b>Figure 4.10.</b> MALDI mass spectra of fluorotyrosine incorporation .....	133
<b>Figure 4.11.</b> MALDI mass spectra of peptide containing fluorotyrosine .....	134
<b>Table 4.1.</b> Fluorotyrosine analogs incorporated into residue Y21 .....	135
<b>Figure 4.12.</b> Electronic absorption spectra of 3FY21 AppA <sub>BLUF</sub> recovery from light to dark state .....	137
<b>Figure 4.13.</b> TRIR spectra of d and l3FY21 AppA <sub>BLUF</sub> .....	138
<b>Figure 4.14.</b> Kinetics of the ground state recovery for wild-type d and lAppA <sub>BLUF</sub> and d and l3FY21 AppA <sub>BLUF</sub> .....	138

<b>Figure 4.15.</b> An example of a kinetic measurement of wild-type AppABLUF at pH 7 .....	139
<b>Figure 4.16a.</b> Electronic absorption spectra of 2FY21 AppA <sub>BLUF</sub> light to dark state recovery..	140
<b>Figure 4.16b.</b> Electronic absorption spectra of wild-type AppA <sub>BLUF</sub> light to dark state recovery at various pH values.....	141
<b>Figure 4.17.</b> TRIR spectra of 2FY21 d and lAppA <sub>BLUF</sub> .....	142
<b>Figure 4.18.</b> Kinetics of the ground state recovery for wild-type d and lAppA <sub>BLUF</sub> and d and l2FY21 AppA <sub>BLUF</sub> .....	143
<b>Figure 4.19.</b> Photoconversion of 2,6-difluoroY21 AppA <sub>BLUF</sub> .....	144
<b>Figure 4.20.</b> Hydrogen bonding network in dAppA and lAppA .....	146
<b>Figure 4.21.</b> Bronsted plot of log k versus the pKa of residue Y21.....	147
<b>Figure 4.22.</b> Proposed model for the recovery of lAppA to dAppA .....	148
<b>Figure 4.23.</b> The gene sequence of AppA <sub>BLUF</sub> in pBAD myc His vector.....	150
<b>Figure 4.24.</b> The crystal structure of AppA <sub>BLUF</sub> showing positions where cyanophenylalanine was inserted.....	151
<b>Figure 4.25.</b> Overexpression gel of wild-type and F101cyanophenylalanine AppA <sub>BLUF</sub> expressed in BL21AI cells.....	152
<b>Figure 4.26.</b> MALDI mass spectra of peptide containing cyanophenylalanine.....	153
<b>Figure 4.27.</b> Absorption spectra of wild-type d and lAppA <sub>BLUF</sub> .....	154
<b>Figure 4.28.</b> Absorption spectra of d and lY56cyanophenylalanine AppA <sub>BLUF</sub> .....	155
<b>Figure 4.29.</b> Absorption spectra of d and lY56cyanophenylalanine AppA <sub>BLUF</sub> .....	155
<b>Figure 4.30.</b> Absorption spectra of d and lF101cyanophenylalanine AppA <sub>BLUF</sub> .....	156
<b>Figure 4.31.</b> FTIR spectrum of cyanophenylalanine in buffer.....	157

## Chapter 5

**Figure 5.1.** Proposed Model for Formation of lAppA from dAppA .....166

**Figure 5.2.** Proposed Model for the recovery of lAppA to dAppA .....168

## List of Abbreviations

2FY	2-Fluorotyrosine
2,6FY	2,6-difluorotyrosine
3FY	3-Fluorotyrosine
3,5FY	3,5-difluorotyrosine
Ala (A)	Alanine
Amp	Ampicillin
AppA	Activation of photopigment and puc expression
AppA <sub>BLUF</sub>	AppA blue light using FAD domain
Arg (R)	Arginine
Asn (N)	Asparagine
Asp (D)	Aspartic acid
BLUF	Blue light using FAD
BBO	Barium borate
C	Celcius
CCD	Charge coupled device
cm	Centimeter
cm <sup>-1</sup>	Wavenumbers
Cys (C)	Cysteine
D	Deuterium
Da	Dalton

dAppA	Dark AppA
DMSO	Dimethyl sulfoxide
DFT	Density functional theory
ESI	Electrospray ionization
FAD	Flavin adenine dinucleotide
FMN	Flavin mononucleotide
fs	Femtosecond
FTIR	Fourier transform infrared
g	Grams
GFP	Green fluorescent protein
Gln (Q)	Glutamine
Glu (E)	Glutamic acid
Gly (G)	Glycine
H-Bond	Hydrogen bond
HSQC	Heteronuclear single quantum coherence
His (H)	Histidine
His-tag	Hexa histidine tag
Ile (I)	Isoleucine
IPTG	Isopropyl-beta-D-thiogalactopyranoside
IR	Infrared
L	Liter
lAppA	Light AppA
LB	Luria broth

Leu (L)	Leucine
LOV	Light oxygen voltage
Lys (K)	Lysine
MALDI	Matrix assisted laser desorption/ionization
Met (M)	Methionine
Mg	Milligram
Min	Minute
mL	Milliliter
mM (mmol)	Millimolar
MS	Mass spectrometry
MW	Molecular weight
MWCO	Molecular weight cut off
nm	Nanometer
ns	Nanosecond
NTA	Nitrilotriacetic acid
OD <sub>600</sub>	Optical density at 600 nm
OPA	Optical parametric amplifier
PAC	Photoactivated adenylyl cyclase
PAGE	Polyacrylamide gel electrophoresis
PCET	Proton coupled electron transfer
Phe (F)	Phenylalanine
PMSF	Phenylmethanesulfonylfluoride
Pro (P)	Proline

ps	Picosecond
RPM	Revolutions per minute
Rf	Riboflavin
SDS	Sodium dodecyl sulfate
Ser (S)	Serine
TA	Transient absorption
TPL	Tyrosine phenol lyase
Thr (T)	Threonine
TRIR	Time resolved infrared
Trp (W)	Tryptophan
Tyr (Y)	Tyrosine
UTRF	Ultrafast time resolved fluorescence
UV	Ultraviolet
Val (V)	Valine
WT	Wild-type



## **Acknowledgments**

I owe my deepest gratitude to my advisor Professor Peter Tonge for his guidance and support throughout my time as a graduate student. I am grateful to have had such a kind and patient mentor who is undoubtedly a brilliant scientist and my role model. I am also grateful to my mentor Professor Stephen Meech whose encouragement and guidance have contributed to the success of my project and to my personal development as a scientist. I am appreciative to have had the opportunity to collaborate with him and spend time working in his lab at the University of East Anglia. Without both Peter and Steve's encouragement and effort, this dissertation would not have been written. I would like express my sincere appreciation to Dr. Sabrina Sobel, my undergraduate research advisor, for her encouragement and enthusiasm. She is a great friend and the reason I decided to become a graduate student.

I would also like to thank my thesis committee; Dr. Erwin London, Dr. Lisa Miller, Dr. Robert Callender and the late Dr. Michelle Millar for their encouragement and providing constructive guidance for this project.

I am indebted to many of my colleagues who have supported me over the years and will miss working with you all very much. It is an honor for me to thank the other individuals who have contributed to this project; Professor Adelbert Bacher, Dr. Ian Clark, Dr. Gregory Greetham, Dr. Minako Kondo, Dr. Andras Lukacs, Dr. Eduard Melief, Dr. Allison Stelling, Dr. Deborah Stoner-Ma, Dr. Michael Towrie, Richard Brust, and Rui-Kun Zhao.

Finally I would like to thank my family and friends for their continuous support throughout the years. I am so grateful to have been blessed with such remarkable people in my life. There are too many of you to name individually but I would like to specifically thank my parents, my sister Julia and my boyfriend Carl for always believing in me.

## List of Publications

“Excited State Structure and Dynamics of the Neutral and Anionic Flavin Radical Revealed by Ultrafast Transient Mid IR to Visible Spectroscopy.” A. Lukacs, RK. Zhao, **A. Haigney**, R. Brust, GM. Greetham, M. Towrie, PJ. Tonge and SR. Meech, *The Journal of Physical Chemistry*, In Press.

“Ultrafast Transient Mid IR to Visible Spectroscopy of Fully Reduced Flavins.” RK. Zhao, A. Lukacs, **A. Haigney**, R. Brust, GM. Greetham, M. Towrie, PJ. Tonge and SR. Meech, *Physical Chemistry Chemical Physics*, 2011, 13, 17642-17648.

“Photoexcitation of the BLUF Photoreceptor AppA Results in Ultrafast Changes to the Protein Matrix.” A. Lukacs\*, **A. Haigney\***, R. Brust, RK. Zhao, AL. Stelling, I. Clark, M. Towrie, GM. Greetham, PJ. Tonge and SR. Meech, *Journal of the American Chemical Society*, 2011, 133, 16893–16900.

“Ultrafast Infrared Spectroscopy of an Isotope-Labeled Photoactivatable Flavoprotein.” **A. Haigney**, A. Lukacs, RK. Zhao, AL. Stelling, R. Brust, RR. Kim, I. Clark, M. Towrie, GM. Greetham, B. Illarionov, A. Bacher, M. Fischer, SR. Meech and PJ. Tonge, *Biochemistry*, 2011, 50, 1321–1328.

“The complexation of aqueous metal ions relevant to biological applications. 2. Reactions of copper(II) citrate and copper(II) succinate with selected amino acids.” SG. Sobel, **A. Haigney**, M. Kim, D. Kim, G. Theophall, J. Nuñez, D. Williams, B. Hickling, J. Sinacori, *Chemical Speciation and Bioavailability*, 2010, 22, 2, 109-114.

“The complexation of aqueous metal ions relevant to biological applications. 1. Poorly soluble zinc salts and enhanced solubility with added amino acid.” SG. Sobel, **A. Haigney**, T. Concepcion, M. Kim, *Chemical Speciation and Bioavailability*, 2008, 20, 2, 93-97.

“Mössbauer spectroscopy of 151 europium dicarboxylates.” CI. Wynter, DH. Ryan, O. Trichtchenko, CJ. Voyer, DE. Brown, SG. Sobel, **A. Haigney**, L. May, BR. Hillery and NS. Gajbhiye, *Hyperfine Interactions*, 2008, 185, 123-127.

# Chapter 1

## Introduction to AppA and Methodologies of Study

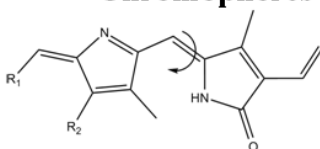
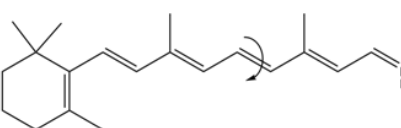
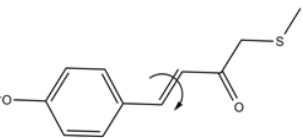
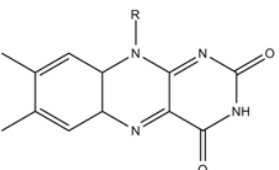
### I. Photoreceptors – Light Energy to Chemical Energy.

As the base energy source for the food chain, all life on Earth depends on light from the sun. Light is used in a multitude of processes across all domains of life and is necessary for photosynthesis, circadian rhythms, phototropism and visual signal transduction. In order for these processes to occur, a system responsible for sensing and responding to light is necessary within the organism.

Photoreceptors are photoactive proteins that function to detect light and respond by regulating light driven processes such as photosystem biosynthesis. Some known classes of photoreceptors include the rhodopsins (4, 5), xanthopsins (6), phytochromes (7) and three classes of flavoproteins. Within the class of flavoproteins are light-oxygen-voltage (LOV) domain proteins (8, 9), photolyase-like cryptochromes (10) and the blue-light using FAD (BLUF) domain proteins (4). Each of these photoreceptors has a conserved domain that binds a small molecule chromophore that is sensitive to specific wavelengths of light. Upon light absorption by the chromophore there is a structural change that occurs in the photoreceptor referred to as the signaling state.

The mechanism leading to the signaling state in each class of photoreceptor is unique and for each class there is a desire to understand how the absorption of light leads to the signaling state of the protein. The rhodopsins, xanthopsins and phytochromes undergo a large structural change resulting from E/Z photoisomerization of the bound small molecule chromophore when light absorption occurs. In the LOV domain proteins, a cysteinyl-flavin adduct is transiently formed in the signaling state and in the cryptochromes light absorption results in a single-electron transfer leading to the reduction of the flavin to

a neutral radical semiquinone signaling intermediate. The BLUF proteins undergo a much more subtle change in the chromophore configuration and it is speculated that the absorption of light causes a rearrangement of a hydrogen bonding network which leads to the formation of the signaling state of the protein (11).

Photoreceptor Family	Chromophores	Photochemistry
Phytochromes		trans ↔ cis isomerization
Rhodopsins		trans ↔ cis isomerization
Xanthopsins		trans ↔ cis isomerization
Cryptochromes		
Phototropin		electron transfer
BLUF proteins		

**Figure 1.1:** Photoreceptor families with the chromophore structure and proposed photochemistry

## II. Blue Light Using FAD Domains

Blue light using FAD (BLUF) domain proteins exist in many species and have a variety of functions. This class of photoreceptor proteins have been found and characterized in species including the green algae *Euglena* (12), the cyanobacteria *Synechocystis* and *Thermosynechococcus elongatus* (13) and in the purple bacterium *Rhodobacter sphaeroides* (4).

BLUF proteins fall into two categories, complex multidomain and simple single domain proteins. Simple BLUF proteins consist of a single domain responsible for sensing blue light but have the potential to communicate this blue light signal to other catalytic proteins. Multidomain BLUF proteins, in addition to having a blue light sensing domain also contain catalytic domains that can be responsible for a variety of functions. Photoactivated adenylyl cyclase (PAC) is a modular protein in *E. gracilis* with both a photoreceptor domain that binds to flavin and a catalytic adenylyl cyclase domain. These domains enable PAC to act as a photoreceptor in order to regulate photophobic, phototactic responses and to synthesize cAMP depending upon light conditions (12). The PixD proteins in cyanobacteria, Tll0078 from *Thermosynechococcus elongates* and Slr1694 from *Synechocystis*, also bind flavin in order to regulate phototaxis via a blue light signaling mechanism (14). BlrB in *R. sphaeroides* is a small single domain BLUF protein (140 residues) with unknown function that undergoes a similar photocycle as other BLUF proteins described above (15). Another single domain BLUF protein exists in *E. coli* called YcgF. YcgF is 47 kDa with a distinct photocycle but unknown function (16). It is postulated that YcgF and BlrB control blue light responses when they are bound to separate binding partner proteins that have not been identified.

BLUF domain proteins bind flavin noncovalently in order to sense and respond to high intensity blue (450 nm) light. The structure of the BLUF domain has been crystallized and shows a conserved ferredoxin-like fold that consists of 5  $\beta$ -strands and 2  $\alpha$ -helices. The isoalloxazine ring of the flavin is located in between the two  $\alpha$ -helices (3). In addition, the hydrogen bonding network of the flavin to amino acid side chains of a tyrosine and glutamine is also conserved (**Figure 1.6**). Blue light excitation of the BLUF domain leads to a characteristic red shifted electronic spectrum of FAD in comparison to non-irradiated protein. This process is reversible in

BLUF proteins and the light or signaling state will return to the dark, non-signaling form, decaying through a monoexponential process.

### III. AppA – A BLUF domain Protein

The first and best characterized BLUF domain photoreceptor is AppA from *Rhodobacter sphaeroides* where it acts as an antirepressor of photosystem biosynthesis. In the dark AppA binds PpsR, a transcription factor, forming an AppA-PpsR<sub>2</sub> complex. When irradiated with high intensity blue light, the complex dissociates releasing PpsR and enabling PpsR to bind to DNA

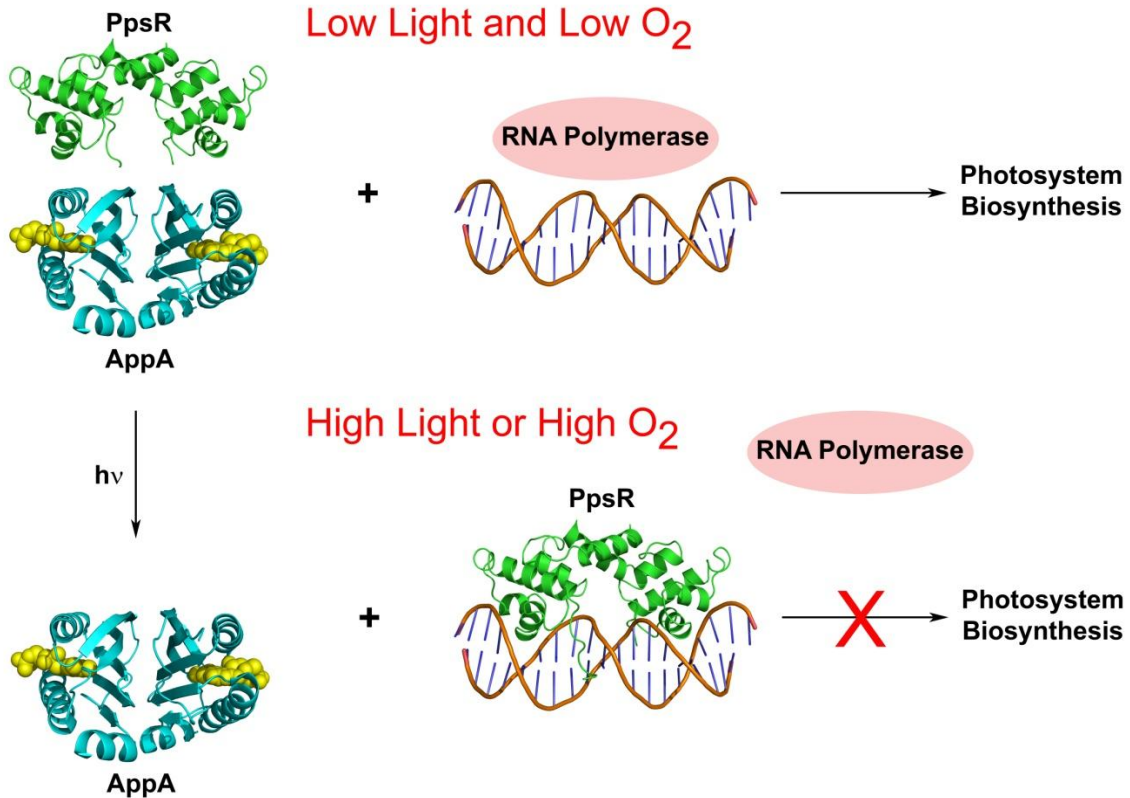


**Figure 1.2:** The biological role of AppA. Under low light and low oxygen conditions, AppA will bind to the transcription factor PpsR. Once exposed to high light or high oxygen conditions, a structural change in AppA occurs and the protein can no longer bind to PpsR turning of photosystem biosynthesis.

and repress photosystem biosynthesis (4).

In order to understand the mechanism by which AppA regulates photosynthetic processes, it is possible to look at the structure-function relationship of the protein. AppA has two domains, the amino terminal light sensing domain and the carboxy terminal PpsR repressor binding domain. The N-terminal portion of AppA is a BLUF domain protein that binds flavin which enables the protein to absorb blue light and in turn alter the conformation of the cysteine rich C-terminal domain to release PpsR. The C-terminal domain is an oxygen sensor (17) and the transfer of the blue light signal from the N- to the C-terminal domain is not yet understood. In addition, it is known that the amino terminal domain of AppA (residues 1-125) can be expressed independently of its C-terminus and still function as a sensor of blue light. A significant question in AppA's mechanism is how structural changes propagate from the N-terminal BLUF domain to the C-terminal domain altering the affinity of AppA for PpsR.

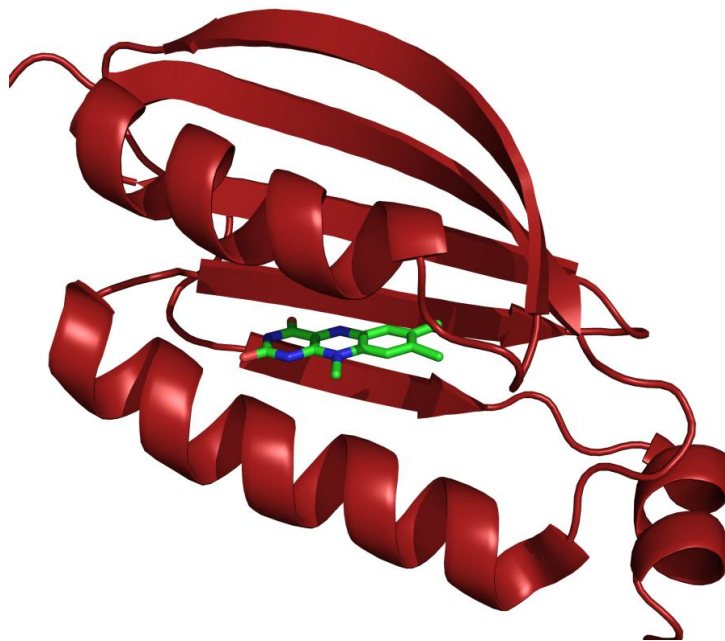


**Figure 1.3:** Crystal structure of AppA<sub>BLUF</sub> bound to the flavin chromophore.

PDBID: **1YRX** (3).

The photocycle of the BLUF domain of AppA has been heavily studied using both steady state and time resolved spectroscopy. Electronic absorption spectroscopy shows photoexcitation with 450 nm light leads to the formation of the light adapted state of the protein and is accompanied by a 10 nm red shifted electronic spectrum of the flavin (**Figure 1.4**). The two states are commonly referred to as dAppA (dark AppA- non irradiated AppA) and lAppA (light

AppA- AppA after irradiation with 450 nm light and is also referred to as the signaling state). Further characterization of AppA was performed using time resolved fluorescence spectroscopy where it was observed the light state of the protein is formed on the picoseconds timescale with a quantum yield of 0.24 for the dAppA to lAppA conversion (*I*). This process is reversible and lAppA will recover to dAppA in approximately 30 minutes (**Figure 1.5**). This is unusual for BLUF proteins, which generally take longer to form the excited state and decay back to the ground state much faster, indicating that the signaling state of AppA (lAppA) is very stable.

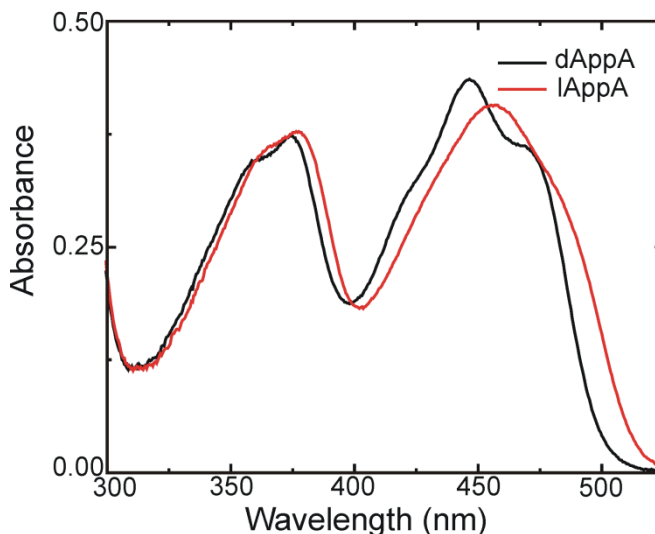


**Figure 1.4:** Photoconversion of dAppA (black) to lAppA (red).

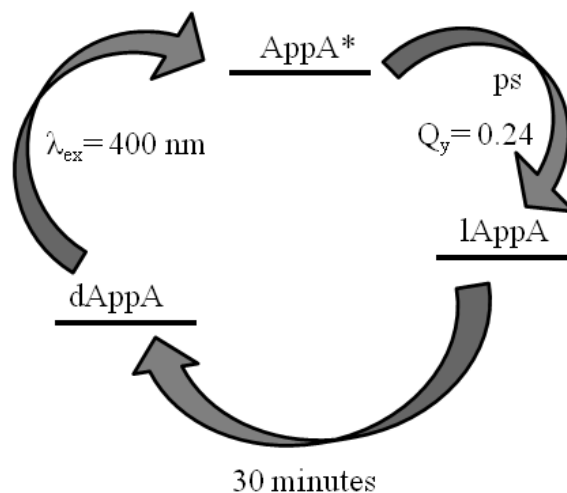


**Figure 1.5:** AppA's photocycle (*I*)



The crystal structure of AppA was solved in 2005 by Anderson *et. al.* and revealed a hydrogen bonding network around the flavin chromophore. Q63 forms a hydrogen bond to the N5 of the flavin ring and to a conserved tyrosine (Y21) and tryptophan (W104). The glutamine is capable of making two different sets of hydrogen bonds depending on its orientation. It has been postulated that the orientation of Q63 changes upon photoexcitation leading to the disruption of the hydrogen bond of the Q63 carbonyl to the flavin, and disrupting the hydrogen bonding with Y21 and W104. Instead Q63 becomes a hydrogen donor to an oxygen atom (O4) on the flavin (3). This state would be less stable because lAppA eventually recovers to dAppA when kept in the dark (1). Anderson *et. al.* claim this structure represents the dark state of the protein (**Figure 1.6**).

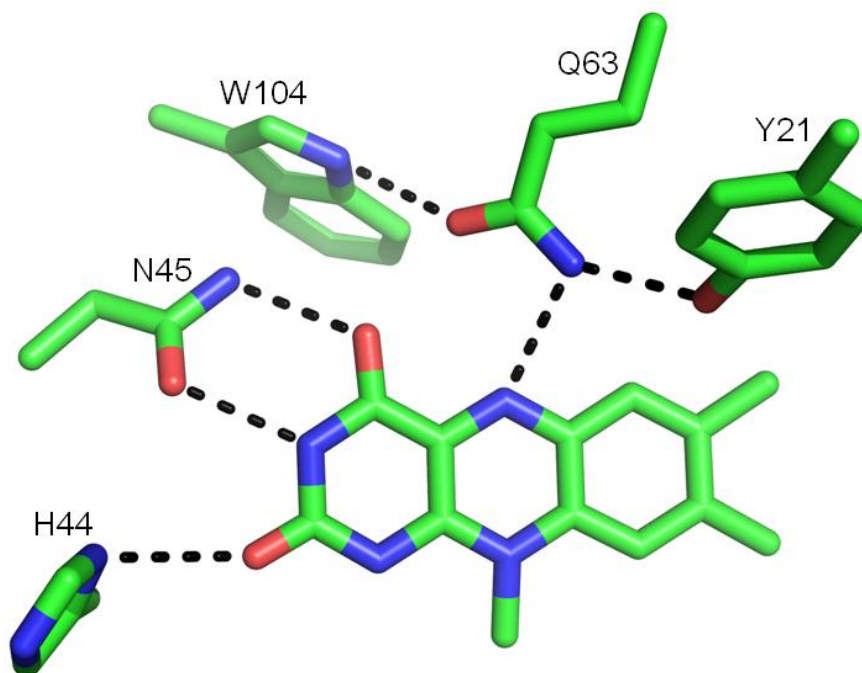


**Figure 1.6:** Anderson *et. al.* crystal structure of AppA reveals a hydrogen bonding network around the flavin chromophore in  $W_{in}$  conformation PDBID: 1YRX (3). This structure is representing the dark state of AppA.

A second crystal structure of AppA was solved in 2006 by Jung *et. al.* and revealed significant differences from the Anderson structure (**Figure 1.7**). The hydrogen bonding network between Q63 and Y21 differs by a 180 degree rotation of the glutamine where Q63 forms a hydrogen bond to the O4 of the flavin ring and Y21 is a hydrogen bond donor to Q63. In addition, this structure shows W104 pointing out towards solution and away from the flavin. Jung *et. al.* suggest motion in W104 can contribute to the formation of the signaling state however, they do not believe W104 flipping to be the direct cause of the formation of lAppA (2).

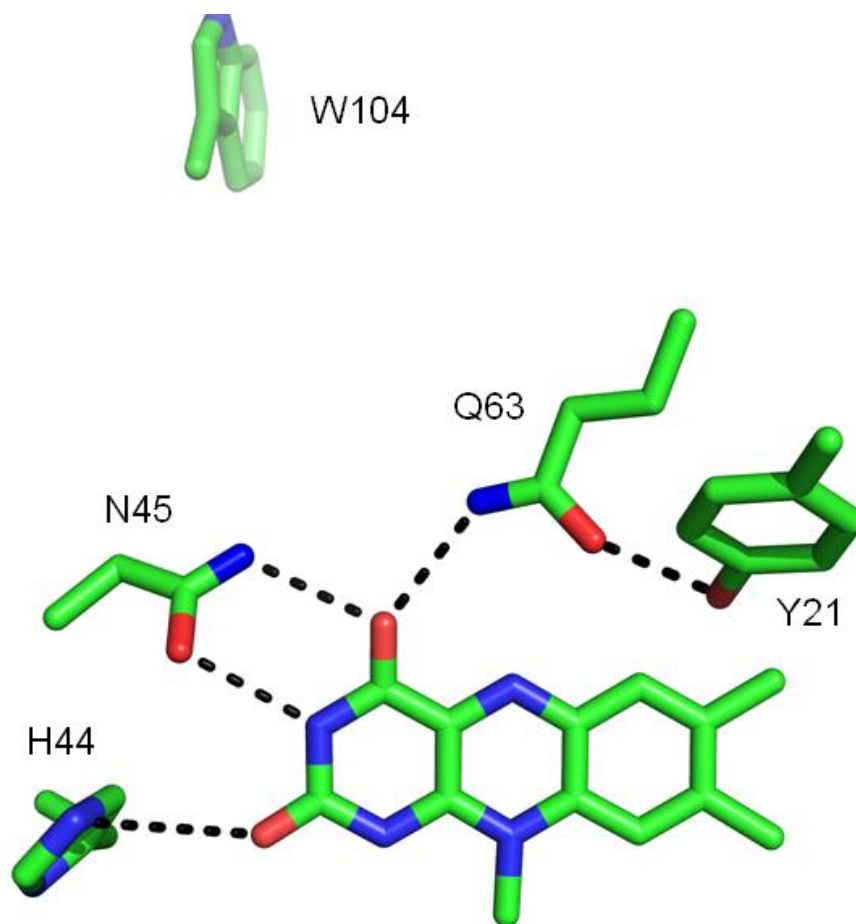


**Figure 1.7:** Jung *et. al.* crystal structure of AppA reveals a hydrogen bonding network around the flavin chromophore in W<sub>out</sub> conformation PDBID: 2IYI (2).

The large difference in the position of W104 in the two crystal structures led to the nomenclature of  $W_{in}$  and  $W_{out}$  referring to the Anderson and Jung structures respectively. There is still much debate centered on the orientation of Q63 and the position of W104 in both lAppA and dAppA and one of the specific aims of my project is to bring clarity to the role of both residues Q63 and W104 in the formation of the signaling state of AppA.

Steady state vibrational Raman spectroscopy has also been used to characterize structural change that results from photoexcitation. The vibrational spectra is sensitive to structure and environment and can be used to probe change pre and post irradiation with 450 nm light. The Raman spectra is shown in **Figure 1.8** and shows major differences between protein and chromophore modes. This spectrum shows lAppA minus dAppA bound to riboflavin. The Raman difference spectrum also shows distinct differences between the dark and light states of the protein. One such feature that is different in the two states of AppA is a  $10\text{ cm}^{-1}$  red shift in the shoulder at  $1696\text{ cm}^{-1}$ . This is hypothesized to be a change in hydrogen bonding around the  $C4=O$  of the flavin chromophore. Additional changes are seen as increased intensities or shifts in the bands at 1632, 1582 and 1551 and below  $1400\text{ cm}^{-1}$  and a  $\sim 15\text{ cm}^{-1}$  blue shift in the  $1390\text{ cm}^{-1}$  peak upon illumination. The mode at  $1390\text{ cm}^{-1}$  is assigned to the methyl deformation in the flavin ring and the  $1342\text{ cm}^{-1}$  mode is assigned to C4-N5 because it shifts upon  $^{15}\text{N5}$  labeling of the flavin (18).

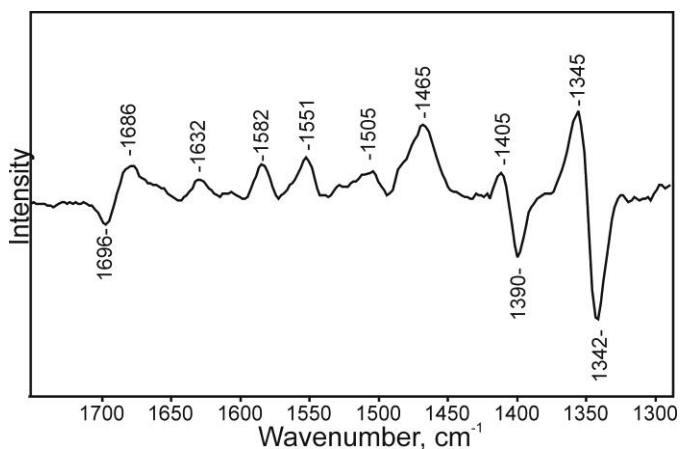


**Figure 1.8:** Steady state Raman difference spectra (light - dark) of wtAppA (pD 8) bound to riboflavin. Concentration 1.5 mM.

In addition to understanding the starting and ending points corresponding to dAppA and lAppA respectively, it is crucial to understand the mechanism of formation of the signaling state from dAppA. Currently, there is intense debate on the structural changes that occur in the protein that lead to the formation of the signaling state of AppA. A variety of experiments, ranging from steady state to ultrafast measurements, have been used to probe the mechanism of formation of lAppA from dAppA. The results of these experiments have led to three different hypotheses on how the signaling state is formed. The first hypothesis proposes a direct proton transfer from Y21 to a nitrogen atom (N5) of the flavin as being responsible for the formation of lAppA (19). The remaining two theories differ mainly on the role of Q63 in the photocycle, where one implicates electron transfer to Y21 from the flavin followed by rotation of Q63 to be the first step upon blue light excitation (3). The last hypothesis was published by our group and states there is formation of a tyrosine-flavin radical followed by a tautomerization of Q63 (20). Each of these proposals is discussed in greater detail below.

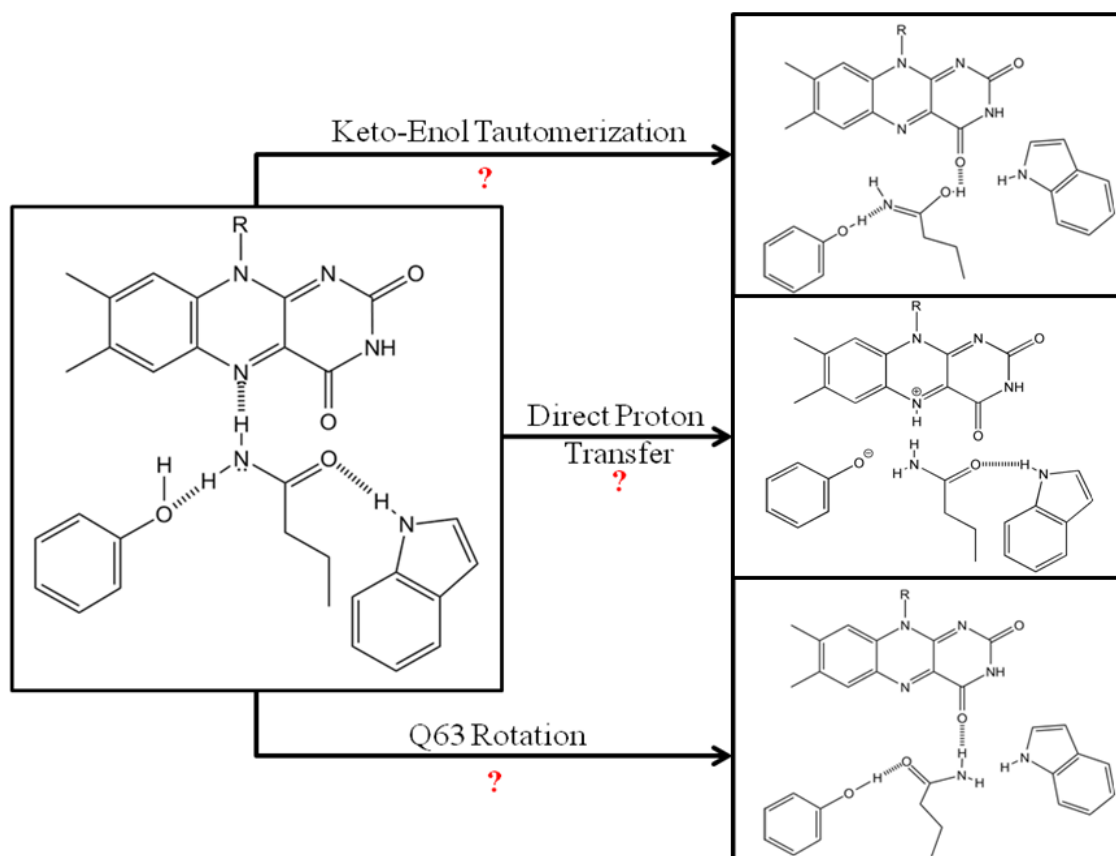


**Figure 1.9:** Proposed mechanisms for the formation of lAppA from dAppA

The first hypothesis for a direct proton transfer from residue Y21 to the flavin was based on steady state UV-visible, FTIR and transient absorption (TA) spectroscopic data. The observation of the shift of the 444 nm flavin peak to 458 nm upon formation of the light state was believed to be due to deprotonation of the N3 atom of the isoalloxazine ring (FAD-  $\lambda_{\text{max}}$  of 454 nm). In the same study the authors created a Y21I mutation which yielded a photoinactive protein, indicating the importance of residue Y21 and its essentiality to the photoactivation mechanism of the protein. In addition, the FTIR data showed differences at  $1451\text{ cm}^{-1}$  and  $1443\text{ cm}^{-1}$  which the authors believed to be due to the formation of tyrosinate (19). However, this explanation did not

account for the shift to the high frequency carbonyl mode ( $1696/1686\text{ cm}^{-1}$ ) in both the FTIR and Raman data.

The next hypothesis of the structural change associated with light absorption was based on the crystal structure of AppA determined in 2005 (3). The structure revealed a hydrogen bonding network with nearly all conserved BLUF domain residues surrounding the flavin chromophore. Most importantly the residue Q63 was at the center of the hydrogen bonding network. The authors suggested this residue serves as a hydrogen bond acceptor for Y21 and a hydrogen bond donor to the N5 of the flavin. From these data, coupled with the FTIR difference analysis by Masuda *et al.*, the authors propose that Q63 is capable of participating in different hydrogen bonding patterns depending on its orientation. They propose that Q63 rotates to form a new set of hydrogen bonds upon photoexcitation, where the amide side chain forms a new hydrogen bond to the O4 of the flavin upon formation of lAppA. This increase in hydrogen bonding explains the shift of  $1696\text{ cm}^{-1}$  to  $1686\text{ cm}^{-1}$  in the dAppA  $\rightarrow$  lAppA transition (3).

The third hypothesis was proposed by our group in 2007 and used time resolved infrared (TRIR) spectroscopy to further investigate the photoactivation mechanism of AppA. Here Stelling *et al.* describe the possibility of a keto-enol tautomerization of Q63 without a formal rotation. This would alter the hydrogen bonding pattern to form a new hydrogen bond to the O4 of the flavin in the light state and cause the shift of the  $1696\text{ cm}^{-1}$  band to lower frequency (21).

My project has focused on further investigation of AppA's photocycle which is essential to disentangle the mechanism of photoactivity. The following chapters discuss the methods we have used in order to propose a new model for photoactivation. Chapter 2 discusses the use of isotope labeling of both the flavin and protein in order to deconvolute the previously reported spectroscopic data. For example, isotope labeling the C4=O carbonyl of the flavin has been

performed in order to assign the high frequency bleach in the vibrational spectra. These data has been used to validate the theory of an increase in hydrogen bonding to the O4 in lAppA. Isotope labeling of the protein has allowed for assignment of specific protein modes observed in the time resolved infrared spectra. Chapter 3 discusses the use of methods, such as mutagenesis, to alter the hydrogen bonding network in order to modify the environment around the flavin. The experiments we performed allowed us to observe the effect of light absorption by the flavin is translated to the protein within 50 femtoseconds of excitation. Chapter 4 focuses on the use of unnatural amino acids that have been incorporated into AppA to be used as probes to monitor structural changes that occur as a result of photoexcitation. Unnatural amino acid replacement has allowed us to gain additional insight into the photoactivation mechanism of AppA by replacing a key tyrosine in the hydrogen bonding network with unnatural fluorotyrosine analogs that have altered pKa values. These data have established the acidity of residue Y21 is crucial in stabilizing the light activated form of the protein.

The following sections will describe the different techniques we have used in order to understand the photoactivation mechanism of AppA. First, there will be a discussion of the various methods that can be used to incorporate unnatural amino acids into proteins. This will be followed by a brief introduction to time resolved infrared (TRIR) spectroscopy, an ultrafast technique to visualize ultrafast events that occur due to photoexcitation. The last section of this chapter will discuss the specific aims for this project.

#### IV. Methods to Incorporate Unnatural Amino Acids into AppA

There a number of different methods used to incorporate unnatural amino acids. These methods include using the cells natural machinery in feeding experiments to incorporate structurally similar amino acids to the natural ones, chemical synthesis of a peptide (solid phase peptide synthesis- SPPS) coupled to native chemical ligation and the 21<sup>st</sup> pair or amber codon method. Each of these methods has advantages and caveats.

SPPS is an *in vitro* method that can be used for generate small peptides. If this method is coupled to chemical ligation of an expressed protein, then it can be extended to larger proteins. One major caveat to this method is that expression of truncated proteins is not always feasible. In addition, decreasing yields with each increasing number of amino acids makes this method only applicable if the amino acids desired to be changed are on the N- or C-terminal of the protein. This is not the case for residue Q63 in AppA and therefore this method was not used in the experimental design to incorporate unnatural amino acids.

A second method is to utilize the cell's existing machinery to incorporate modified amino acids in feeding experiments. Feeding methods to incorporate isotopically labeled amino acids or unnatural amino acid derivatives with similar structure to one of the naturally occurring amino acids have been previously reported (22, 23). This is an *in vivo* method which is fairly straightforward to achieve modified protein. Some examples described are the incorporation of isotopically labeled tyrosine and glutamine, fluorotyrosine derivatives and the incorporation of azidohomoalanine (replaces methionine). In order to specifically label the amino acid of interest, one must start by removing the other residues that exist as multiples in the protein. For example, AppA has seven glutamines in its sequence. It is desirable to incorporate a glutamine with the



side chain nitrogen  $^{15}\text{N}$  labeled specifically into position Q63 to identify peaks in previously reported TRIR data. To accomplish specific labeling of Q63, the remaining glutamines, which are not essential for photoactivity, can be mutated to alternative amino acids. This mutant can be grown in the presence of  $^{15}\text{N}$  labeled glutamine and the cells will uptake the isotope and specifically label Q63. **Figure 1.11** shows the crystal structure of AppA with all glutamines labeled in pink except Q63 which is blue. This structure shows the inactive glutamines are all facing outward toward the solution. The logical choice is to make a hexamutant with the inactive glutamines to asparagines and test activity of the protein. In addition, the mutant could be grown in a transaminase deficient cell line to avoid deamination of the glutamine side chain which could in turn lead to incorporation of  $^{15}\text{N}$  throughout the protein. This protein would then be grown in minimal media and commercially available glutamine isotopes will be added before induction.

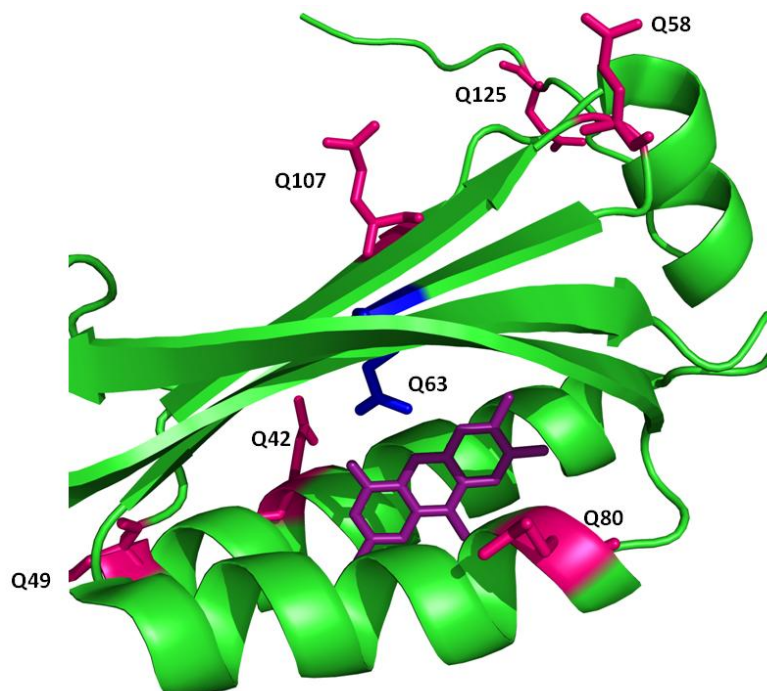


**Figure 1.10:** Crystal structure of AppA highlighting glutamines in pink, the single essential glutamine (Q63) highlighted in blue and riboflavin in purple. PDBID: **1YRX** (3).

The same method can be used for incorporation of fluorinated tyrosines into position Y21. Fluorotyrosine has been used as probe to study the mechanism of electron transfer in numerous systems including photosystem II (24), GFP (25) and ribonucleotide reductase (26-29). The fluorinated derivatives alter both the pKa and the redox potential of the tyrosine with minor perturbation to the structure. The degree to which these two parameters are modified depends on the substitution pattern. We will extend this methodology to AppA and investigate the effect of substitution through TRIR. For example, by modulating the pKa and potential of Y21 in AppA, the tyrosine adjacent to the flavin, will enable us to unravel the interplay between proton transfer (or hydrogen bond breaking) and electron transfer. If a proton coupled electron transfer mechanism proves important in AppA, the incorporation of different substitution patterns will allow a degree of control over the mechanism. There are two tyrosines in AppA which makes mutating out the single inactive tyrosine feasible. Fluorinated tyrosine will be added to the minimal media prior to induction. Importantly, fluorotyrosine acts as a feedback inhibitor of tyrosine and thus prevents the cells from making tyrosine when an excess is added to the media.

Another method to incorporate unnatural amino acids into proteins is using the 21<sup>st</sup> pair or amber codon method (30-33). This method uses engineered amino acyl tRNA synthetases that have been evolved to recognize the amber stop codon and specifically incorporate an unnatural substrate. This method has limitations, one being the small number of amino acids that can be incorporated because of the complex process needed to compliment an amino acyl tRNA synthetase/amino acid pair. However, it has been proved useful for a variety of unnatural amino acids such as azido- and cyanophenylalanine. The cyano and azido groups are ideal reporters because they have a spectroscopically distinct signature, are non-perturbing and sensitive to

structure and environment. The stretching vibration of cyano and azido groups appears at  $\sim 2220$  and  $\sim 2120 \text{ cm}^{-1}$ , respectively, in a region of the IR spectrum that is distinct from the protein (34, 35). Azido and cyanophenylalanine are excellent reporters on protein environment because they are very sensitive to changes in hydrophobicity (32-34, 36). The 21<sup>st</sup> pair method will be used to incorporate cyanophenylalanine into AppA in order to probe structural changes that occur associated with photoexcitation. Initial targets for replacement will be the 4 Phe (F55, F61, F62, F101) and 1 nonessential Tyr (Y56) residues in AppA<sub>BLUF</sub>, since these amino acids are the most structurally similar to cyanophenylalanine and azidophenylalanine.

All of the generated AppA proteins with modifications made to the hydrogen bonding network around the flavin will be studied using time resolved infrared spectroscopy (TRIR).

## V. Ultrafast Studies of AppA – Time Resolved Spectroscopy.

Early structural events in the photoexcitation of AppA been studied by time resolved spectroscopy. This method is made possible by lasers that operate on the femtosecond timescale, which is shorter than an individual bond vibration thus making it possible to monitor excited state dynamics. The time resolved studies use a pump-probe setup. The pump excites the sample with a wavelength of light that it absorbs (450 nm for AppA). The sample is then probed with infrared light. Localized modes may be used as trackers of specific chemical bonds. This allows for the ultrafast reaction of the chromophore decaying from its excited state to be followed on the time scale of individual vibrational modes.

The time resolved data reported are difference spectra. The IR probe will take a spectrum of the ground state, before excitation with the pump. This spectrum is subtracted from each

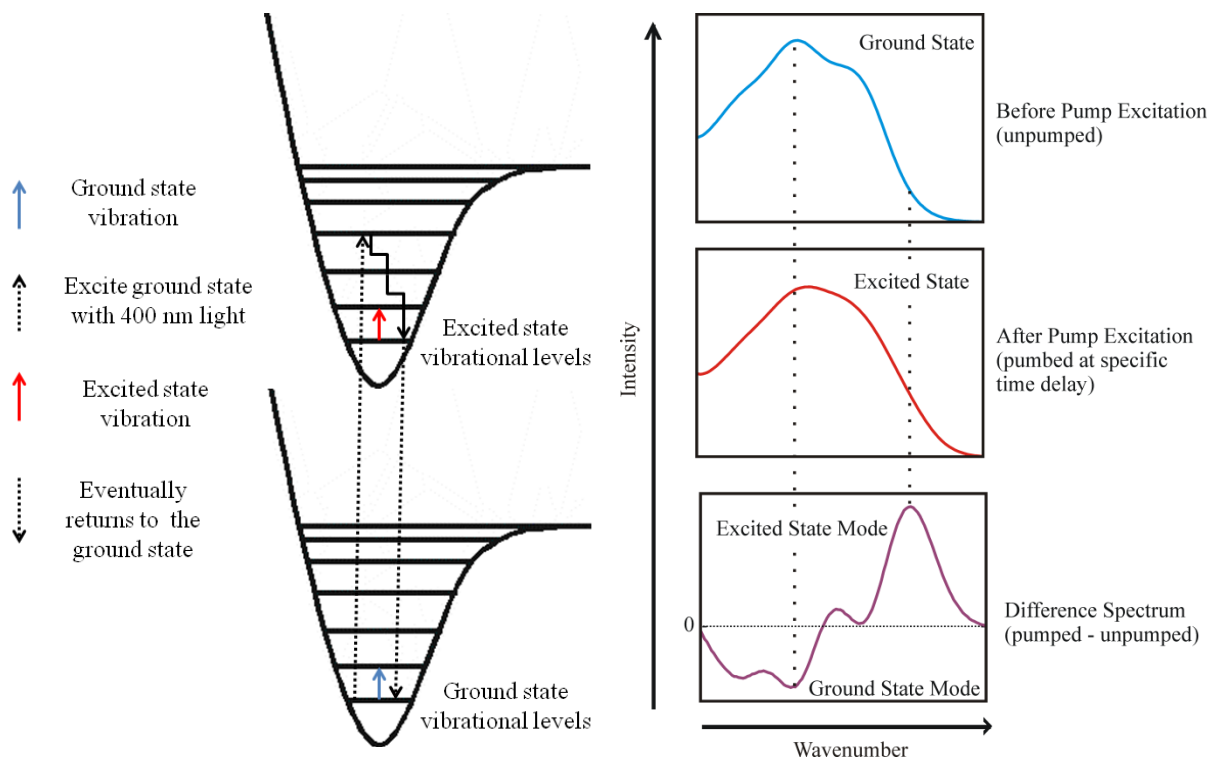


**Figure 1.11:** Schematic of time resolved infrared spectroscopy. Excitation from the ground to excited state with vibrational relaxation to the lowest excited state is shown on the left. The ground state IR spectrum (right, top) is substrated from the excited state IR spectrum (right, middle) after pump excitation and the final spectrum is reported as a difference of excited minus ground state IR (right, bottom).

additional spectrum taken at various time delays after excitation. Modes that are due to the excited state appear as positive peaks and are referred to as transients because they are absent in the ground state. Modes that are not present in the excited state but are present in the ground state appear as negative peaks and referred to as bleaches. Depending on the duration of the excited state the peaks will then decrease as the chromophore relaxes back down to the ground state. This allows one to follow the kinetics of specific bonds that are altered during the photoreaction.

Previous work performed by our group involved the use of time resolved infrared spectroscopy (TRIR) to study the photoactivation mechanism of AppA. TRIR spectra of unbound flavin were obtained and used to determine ground state and excited state modes. In addition, TRIR spectra of dAppA and lAppA were also obtained and the differences between unbound flavin modes and those modes that correlated to protein or protein-flavin interactions were assigned. These studies showed some significant differences between dAppA, lAppA and flavin. It was found that the lAppA as an excited state that has half the lifetime of the excited state in dAppA. Significantly, there is an appearance of a  $1666\text{ cm}^{-1}$  transient in dAppA that is not seen in flavin, lAppA or in any of the studied photo inactive mutants (20). The neutral flavin radical has a  $1660\text{-}1670\text{ cm}^{-1}$  transient (37) however, the  $1666\text{ cm}^{-1}$  transient does not shift upon labeling the flavin. Part of my project has been to use isotope labeling of the protein in order to assign this transient.

## VI. Specific Aims

There are three aims of this project that will be discussed in the following chapters.

- 1. Flavin isotopes will be incorporated into AppA in order to assign the vibrational modes of the TRIR spectrum.** In order to understand the TRIR spectrum it is essential to assign each vibrational mode. The second chapter will discuss time resolved infrared spectra of AppA reconstituted with [4,10a-<sup>13</sup>C<sub>2</sub>]riboflavin, [2-<sup>13</sup>C<sub>1</sub>]-FAD, [uniform-<sup>13</sup>C<sub>17</sub>]-FAD, [xylene-<sup>13</sup>C<sub>8</sub>]-FAD, [uniform-<sup>15</sup>N<sub>4</sub>]-FAD and [4-<sup>18</sup>O<sub>1</sub>]-FAD .
- 2. Reorganization of the hydrogen bonding network surrounding the flavin chromophore.** The third chapter discusses mutations made to the key tyrosine and glutamine residues that are essential to the photocycle of AppA. Mutants, such as Q63E, will be chosen to modulate the photoresponse and structure reactivity relations will be probed by time resolved infrared spectroscopy.
- 3. Unnatural amino acids will be introduced into the AppA BLUF domain in order to probe time dependant structural changes.** The fourth chapter will discuss incorporation of unnatural amino acids into AppA<sub>BLUF</sub> in order to be used as probes to monitor electron transfer and larger conformational changes associated with photoexcitation. Unnatural amino acids such as fluorotyrosines, with reduced pKa values, will be specifically incorporated into residue Y21. In addition, we will introduce p-cyanonophenylalanine to probe time dependant structural changes that occur due to photoexcitation.

## References

1. Gauden, M., Yeremenko, S., Laan, W., van Stokkum, I. H., Ihalainen, J. A., van Grondelle, R., Hellingwerf, K. J., and Kennis, J. T. (2005) Photocycle of the flavin-binding photoreceptor AppA, a bacterial transcriptional antirepressor of photosynthesis genes, *Biochemistry* 44, 3653-3662.
2. Jung, A., Domratcheva, T., Tarutina, M., Wu, Q., Ko, W. H., Shoeman, R. L., Gomelsky, M., Gardner, K. H., and Schlichting, I. (2005) Structure of a bacterial BLUF photoreceptor: insights into blue light-mediated signal transduction, *Proc Natl Acad Sci U S A* 102, 12350-12355.
3. Anderson, S., Dragnea, V., Masuda, S., Ybe, J., Moffat, K., and Bauer, C. (2005) Structure of a novel photoreceptor, the BLUF domain of AppA from *Rhodobacter sphaeroides*, *Biochemistry* 44, 7998-8005.
4. Gomelsky, M., and Klug, G. (2002) BLUF: a novel FAD-binding domain involved in sensory transduction in microorganisms, *Trends Biochem Sci* 27, 497-500.
5. Briggs, W. R. (2007) The LOV domain: a chromophore module servicing multiple photoreceptors, *J Biomed Sci* 14, 499-504.
6. Kort, R., Hoff, W. D., Van West, M., Kroon, A. R., Hoffer, S. M., Vlieg, K. H., Crieland, W., Van Beeumen, J. J., and Hellingwerf, K. J. (1996) The xanthopsins: a new family of eubacterial blue-light photoreceptors, *EMBO J* 15, 3209-3218.
7. Rockwell, N. C., Su, Y. S., and Lagarias, J. C. (2006) Phytochrome structure and signaling mechanisms, *Annu Rev Plant Biol* 57, 837-858.
8. Losi, A. (2004) The bacterial counterparts of plant phototropins, *Photochem Photobiol Sci* 3, 566-574.

9. Briggs, W. R., Christie, J. M., and Salomon, M. (2001) Phototropins: a new family of flavin-binding blue light receptors in plants, *Antioxid Redox Signal* 3, 775-788.
10. Essen, L. O. (2006) Photolyases and cryptochromes: common mechanisms of DNA repair and light-driven signaling?, *Curr Opin Struct Biol* 16, 51-59.
11. van der Horst, M. A., and Hellingwerf, K. J. (2004) Photoreceptor proteins, "star actors of modern times": a review of the functional dynamics in the structure of representative members of six different photoreceptor families, *Acc Chem Res* 37, 13-20.
12. Iseki, M., Matsunaga, S., Murakami, A., Ohno, K., Shiga, K., Yoshida, K., Sugai, M., Takahashi, T., Hori, T., and Watanabe, M. (2002) A blue-light-activated adenylyl cyclase mediates photoavoidance in *Euglena gracilis*, *Nature* 415, 1047-1051.
13. Okajima, K., Yoshihara, S., Fukushima, Y., Geng, X., Katayama, M., Higashi, S., Watanabe, M., Sato, S., Tabata, S., Shibata, Y., Itoh, S., and Ikeuchi, M. (2005) Biochemical and functional characterization of BLUF-type flavin-binding proteins of two species of cyanobacteria, *J Biochem* 137, 741-750.
14. Okajima, K., Fukushima, Y., Suzuki, H., Kita, A., Ochiai, Y., Katayama, M., Shibata, Y., Miki, K., Noguchi, T., Itoh, S., and Ikeuchi, M. (2006) Fate determination of the flavin photoreceptions in the cyanobacterial blue light receptor TePixD (Tll0078), *J Mol Biol* 363, 10-18.
15. Zirak, P., Penzkofer, A., Schiereis, T., Hegemann, P., Jung, A., and Schlichting, I. (2006) Photodynamics of the small BLUF protein BlrB from *Rhodobacter sphaeroides*, *J Photochem Photobiol B* 83, 180-194.



16. Rajagopal, S., Key, J. M., Purcell, E. B., Boerema, D. J., and Moffat, K. (2004) Purification and initial characterization of a putative blue light-regulated phosphodiesterase from *Escherichia coli*, *Photochem Photobiol* 80, 542-547.
17. Han, Y., Meyer, M. H., Keusgen, M., and Klug, G. (2007) A haem cofactor is required for redox and light signalling by the AppA protein of *Rhodobacter sphaeroides*, *Mol Microbiol* 64, 1090-1104.
18. Unno, M., Sano, R., Masuda, S., Ono, T. A., and Yamauchi, S. (2005) Light-induced structural changes in the active site of the BLUF domain in AppA by Raman spectroscopy, *J Phys Chem B* 109, 12620-12626.
19. Laan, W., van der Horst, M. A., van Stokkum, I. H., and Hellingwerf, K. J. (2003) Initial characterization of the primary photochemistry of AppA, a blue-light-using flavin adenine dinucleotide-domain containing transcriptional antirepressor protein from *Rhodobacter sphaeroides*: a key role for reversible intramolecular proton transfer from the flavin adenine dinucleotide chromophore to a conserved tyrosine?, *Photochem Photobiol* 78, 290-297.
20. Stelling, A. L., Ronayne, K. L., Nappa, J., Tonge, P. J., and Meech, S. R. (2007) Ultrafast structural dynamics in BLUF domains: transient infrared spectroscopy of AppA and its mutants, *J Am Chem Soc* 129, 15556-15564.
21. Stelling, A. L., Ronayne, K. L., Nappa, J., Tonge, P. J., and Meech, S. R. (2007) Ultrafast structural dynamics in BLUF domains: transient infrared spectroscopy of AppA and its mutants, *J Am Chem Soc* 129, 15556-15564.
22. Brooks, B., and Benisek, W. F. (1994) Mechanism of the reaction catalyzed by delta 5-3-ketosteroid isomerase of *Comamonas (Pseudomonas) testosteroni*: kinetic properties of a

- modified enzyme in which tyrosine 14 is replaced by 3-fluorotyrosine, *Biochemistry* 33, 2682-2687.
23. Tong, K. I., Yamamoto, M., and Tanaka, T. (2008) A simple method for amino acid selective isotope labeling of recombinant proteins in *E. coli*, *J Biomol NMR* 42, 59-67.
  24. Rappaport, F., Boussac, A., Force, D. A., Peloquin, J., Brynda, M., Sugiura, M., Un, S., Britt, R. D., and Diner, B. A. (2009) Probing the Coupling between Proton and Electron Transfer in Photosystem II Core Complexes Containing a 3-Fluorotyrosine, *J Am Chem Soc* 131, 4425-4433.
  25. Ayyadurai, N., Prabhu, N. S., Deepankumar, K., Kim, A., Lee, S. G., and Yun, H. (2011) Biosynthetic substitution of tyrosine in green fluorescent protein with its surrogate fluorotyrosine in *Escherichia coli*, *Biotechnol Lett* 33, 2201-2207.
  26. Seyedsayamdost, M. R., Reece, S. Y., Nocera, D. G., and Stubbe, J. (2006) Mono-, di-, tri-, and tetra-substituted fluorotyrosines: new probes for enzymes that use tyrosyl radicals in catalysis, *J Am Chem Soc* 128, 1569-1579.
  27. Seyedsayamdost, M. R., Yee, C. S., and Stubbe, J. (2007) Site-specific incorporation of fluorotyrosines into the R2 subunit of *E. coli* ribonucleotide reductase by expressed protein ligation, *Nat Protoc* 2, 1225-1235.
  28. Minnihan, E. C., Young, D. D., Schultz, P. G., and Stubbe, J. (2011) Incorporation of Fluorotyrosines into Ribonucleotide Reductase Using an Evolved, Polyspecific Aminoacyl-tRNA Synthetase, *J Am Chem Soc* 133, 15942-15945.
  29. Reece, S. Y., Seyedsayamdost, M. R., Stubbe, J., and Nocera, D. G. (2006) Electron transfer reactions of fluorotyrosyl radicals, *J Am Chem Soc* 128, 13654-13655.

30. Hammill, J. T., Miyake-Stoner, S., Hazen, J. L., Jackson, J. C., and Mehl, R. A. (2007) Preparation of site-specifically labeled fluorinated proteins for  $^{19}\text{F}$ -NMR structural characterization, *Nat Protoc* 2, 2601-2607.
31. Wang, L., Xie, J., and Schultz, P. G. (2006) Expanding the genetic code, *Annu Rev Biophys Biomol Struct* 35, 225-249.
32. Young, D. D., Young, T. S., Jahnz, M., Ahmad, I., Spraggon, G., and Schultz, P. G. (2011) An evolved aminoacyl-tRNA synthetase with atypical polysubstrate specificity, *Biochemistry* 50, 1894-1900.
33. Chin, J. W., Santoro, S. W., Martin, A. B., King, D. S., Wang, L., and Schultz, P. G. (2002) Addition of p-azido-L-phenylalanine to the genetic code of Escherichia coli, *J Am Chem Soc* 124, 9026-9027.
34. Gai, X. S., Coutifaris, B. A., Brewer, S. H., and Fenlon, E. E. (2011) A direct comparison of azide and nitrile vibrational probes, *Phys Chem Chem Phys* 13, 5926-5930.
35. Waegele, M. M., Culik, R. M., and Gai, F. (2011) Site-Specific Spectroscopic Reporters of the Local Electric Field, Hydration, Structure, and Dynamics of Biomolecules, *J Phys Chem Lett* 2, 2598-2609.
36. Chin, J. W., Cropp, T. A., Anderson, J. C., Mukherji, M., Zhang, Z., and Schultz, P. G. (2003) An expanded eukaryotic genetic code, *Science* 301, 964-967.
37. Wolf, M. M., Schumann, C., Gross, R., Domratcheva, T., and Diller, R. (2008) Ultrafast infrared spectroscopy of riboflavin: dynamics, electronic structure, and vibrational mode analysis, *J Phys Chem B* 112, 13424-13432.

## Chapter 2

### Assignments of Vibrational Modes by FAD and Riboflavin Isotopologue

#### Incorporation into AppA<sub>BLUF</sub>

##### A. Introduction

Flavoproteins are found extensively in biology and are involved in a variety of functions. Most of these proteins are capable of mediating redox chemistry because of the various redox states that the flavin can adopt (1, 2). Some enzymes that use electron transfer both to and from the flavin include cytochrome P450 reductase, flavin-containing monooxygenases and glucose oxidase (3-5). In addition to their use as redox centers, flavin is used as a sensor for light and is found as the chromophore responsible for initial response to blue light absorption in a number of photoreceptors.

Flavin containing photoreceptors constitute a unique class of photosensors because they are only able to undergo small structural changes upon light absorption. This is in contrast to the phytochromes, rhodopsins and xanthopsins where large scale structural changes, such as a cis-trans isomerization, occur in the chromophore when light is absorbed (6-8). Some examples of the known flavin containing photoreceptors are light-oxygen-voltage (LOV) domain proteins (9, 10), photolyase-like cryptochromes (12) and the blue-light using FAD (BLUF) domain proteins (13). The mechanism leading to the signaling state in each class of photoreceptor is unique and for each class there is a desire to understand how the absorption of light leads to the signaling state of the protein. In the LOV domain proteins, a cysteinyl-flavin adduct is transiently formed in the signaling state (14) and in the cryptochromes a single-electron transfer leading to the reduction of the flavin to a neutral radical semiquinone signaling intermediate. The BLUF

proteins undergo a much more subtle change in the chromophore configuration and it is speculated that the absorption of light leads to rearrangement of a hydrogen bonding network which leads to the formation of the signaling state of the protein (15).

Blue light using FAD (BLUF) domain proteins exist in many species with a variety of functions. This class of proteins undergoes a characteristic 10 nm redshift in the absorption spectrum of the flavin upon excitation with 450 nm light. AppA is the first and best characterized BLUF domain photoreceptor and is found in *Rhodobacter sphaeroides* where it acts as an antirepressor of photosystem biosynthesis. In the dark, AppA binds PpsR, a transcription factor, forming an AppA-PpsR<sub>2</sub> complex. When irradiated with high intensity blue light, the complex dissociates releasing PpsR and enabling PpsR to bind to DNA and repress photosystem biosynthesis (13). AppA has two domains, the amino terminal light sensing domain and the carboxy terminal PpsR repressor binding domain. The N-terminal portion of AppA is a BLUF domain protein that binds flavin which enables the protein to absorb blue light and in turn alter the conformation of the cysteine rich C-terminal domain to release PpsR.

The crystal structure of AppA was determined and revealed a hydrogen bonding network around the flavin chromophore. Q63 forms a hydrogen bond to the N5 of the flavin ring and to a conserved tyrosine (Y21) and tryptophan (W104) (**Figure 2.1**). The glutamine is capable of making two different sets of hydrogen bonds depending on its orientation. It has been postulated that the orientation of Q63 changes upon photoexcitation leading to the breaking of the hydrogen bond of the carbonyl of glutamine to the flavin and disrupting the hydrogen bonding with Y21 and W104 and becoming a hydrogen donor to the C4=O on the flavin (11).

Currently there is a debate on how the signaling state of AppA is formed. The two existing theories differ mainly on the role of Q63 in the photocycle. The first theory implicates

electron transfer to Y21 from the flavin followed by rotation of Q63 to be the first step upon blue light excitation (11). The second theory states formation of a tyrosine-flavin radical followed a tautomerization of Q63 (16). In addition a third theory suggests direct proton transfer from Y21 to N5 of the flavin (17).

Both AppA's dark (dAppA) and light (lAppA) excited state dynamics have been studied in this chapter using time resolved infrared spectroscopy (TRIR). TRIR spectra of unbound flavin were obtained and used to determine ground state and excited state modes. In addition, TRIR spectra of dAppA<sub>BLUF</sub> and lAppA<sub>BLUF</sub> were also obtained and the differences between unbound flavin modes and those modes that correlated to protein or protein-flavin interactions were assigned (16). These studies showed some significant differences between dAppA<sub>BLUF</sub>, lAppA<sub>BLUF</sub> and free flavin. Most importantly there is an appearance of a 1666 cm<sup>-1</sup> transient in dAppA<sub>BLUF</sub> that is not seen in flavin, lAppA<sub>BLUF</sub> or in any of the studied photo inactive mutants (16). This section reports time resolved infrared spectra of AppA reconstituted with isotopically-labeled riboflavin and FAD, which permits the first unambiguous assignment of bands to ground and excited state modes associated with the flavin. We report TRIR spectra of [4,10a-<sup>13</sup>C<sub>2</sub>]riboflavin, [2-<sup>13</sup>C<sub>1</sub>]-FAD, [uniform-<sup>13</sup>C<sub>17</sub>]-FAD, [xylene-<sup>13</sup>C<sub>8</sub>]-FAD, [uniform-<sup>15</sup>N<sub>4</sub>]-FAD and [4-<sup>18</sup>O<sub>1</sub>]-FAD both unbound and bound to AppA<sub>BLUF</sub>. This allows for the assignments of vibrational modes to the isoalloxazine ring of the flavin. We complement these AppA<sub>BLUF</sub> measurements with an experimental and theoretical study of the isoalloxazine modes of FAD, riboflavin and their isotopes in aqueous solution, which reveals their sensitivity to isotopic substitution and to their hydrogen bonding environment.

## B. Materials and Methods

The gene encoding the AppA BLUF domain (residues 5-125 AppA<sub>BLUF</sub>) was cloned into a pet15b vector (Novagen) so that the protein is expressed with an N-terminal His-tag. Expression and purification was performed using a modified version the protocol published by Stelling *et al.* (16).

### B.1. Overexpression and Purification of AppA<sub>BLUF</sub>:

Protein expression was performed by transforming the plasmid into BL21DE3 *E. coli* cells which were then grown up in 10 mL cultures of Luria Broth (LB) media containing 0.5 mM ampicillin at 37°C and shaking at 250 RPM. These cultures were used to inoculate 1 L of LB/ampicillin media, in 4L flasks, which was grown to an OD<sub>600</sub> of approximately 1.2 at 30°C for 5 hours. The temperature was then decreased to 18°C for 30 minutes followed by addition of 0.8 mM isopropyl β-D-1-thiogalactopyranoside (IPTG) to induce protein growth overnight in the dark. All purification processes were then performed in the dark. The cells were harvested by centrifugation at 5,000 RPM at 4°C and stored at -20°C. The cell pellet was then resuspended in 40 mL of lysis buffer (10mM NaCl, 50mM NaH<sub>2</sub>PO<sub>4</sub> at pH 8) to which 200 μL of a protease inhibitor, 50 mM phenylmethanesulphonylfluoride (PMSF), and 14 μL of β-mercaptoethanol, a disulfide bond reducing agent, was added. The cells were then lysed using sonication and cell debris was removed using centrifugation (33K for 90 min) and the supernatant was incubated with 1 mL of a 10 mg/mL solution of either FAD or riboflavin for 45 min on ice in the dark. The protein was purified using Ni-NTA chromatography (Qiagen) with 10 mM NaCl, 50 mM NaH<sub>2</sub>PO<sub>4</sub>, pH 8 wash buffer. The bound protein was then washed with increasing amounts of imidazole in buffer and finally eluted with 250 mM imidazole. The fractions collected were dialyzed in 10 mM NaCl, 50 mM NaH<sub>2</sub>PO<sub>4</sub>, pH 8 dialysis buffer overnight. The purity of the

protein was determined using SDS-PAGE electrophoresis. These proteins were then concentrated to 1.5 mM and frozen in liquid N<sub>2</sub> and lyophilized overnight before being exchanged into an equal volume of D<sub>2</sub>O buffer for at least 5 hours. The exchange was repeated 3 to 4 times by dissolving and re-lyophilizing and then stored at -80°C dry.

## B.2. Binding of Riboflavin and FAD Isotopologues to AppA<sub>BLUF</sub>:

*Binding of Riboflavin Isotopologue:* Approximately 5 mg of riboflavin isotopologue was solubilized in 50 µl DMSO. The solution was added to 15 mL of D<sub>2</sub>O buffer (1 mM NaCl, 20 mM Na<sub>2</sub>HPO<sub>4</sub>, pH 8) and allowed to incubate at 60 °C for at least 1.5 hrs. The solution was cooled to 4°C and combined with 0.5-1 mL of 1.5 mM AppA<sub>BLUF</sub> bound to unlabeled riboflavin. The mixture was kept in the dark at 4°C for 1.5 hrs. The protein was then concentrated to between 1.5 and 2 mM by centrifugation using Amicon filters with a MW cutoff of 3,000 Da. To remove unbound ligand the protein was diluted with buffer and then re-concentrated using an Amicon filter.

*Binding of FAD Isotopologues:* The FAD isotopologues were incorporated into AppA<sub>BLUF</sub> by incubating a ~0.5 mM solution of the purified protein with ~1.5 mM isotopically labeled FAD for 45 min. This protein flavin mixture was then washed by repeated cycles of concentration and dilution with buffer using a 3,000 Da Amicon filter until free flavin could not be detected in the eluate. The protein sample (~0.5 mM) was then incubated a second time with an excess of isotopically labeled FAD (~1.5 mM), followed by repeated washing until no free flavin could be detected in the protein solution. Using this method the final incorporation of labeled FAD was estimated to be greater than 90% when the starting isotopologue is 100% labeled.

For example, the <sup>13</sup>C-C2 FAD isotope was bound to AppA<sub>BLUF</sub> by incubation of the purified protein with an excess of <sup>13</sup>C-C2 FAD. AppA<sub>BLUF</sub> at 0.544 mM final concentration was



incubated for one hour at 4°C in the dark with a final concentration of 1.42 mM  $^{13}\text{C}$ -C2 FAD assuming the equilibrium of bound and free FAD, this gave 72% of labeled FAD. This protein flavin mixture was then washed by repeated concentration and dilution with phosphate buffer using filters with a molecular weight cut off of 3,000 daltons until the flavin concentration in flow through was undetectable. This sample was then incubated a second time with an excess of  $^{13}\text{C}$ -C2 FAD at a final concentration 1.42 mM. The final percent isotope incorporation was 92%  $^{13}\text{C}$ -C2 FAD because [ $^{13}\text{C}$ -C2]-FAD is 100 % labeled.

### B.3. Time Resolved Infrared Spectroscopy:

Time resolved IR (TRIR) spectra were taken at the STFC Central Laser Facility and the experimental apparatus and methods have been previously described (18). Measurements on both dAppA<sub>BLUF</sub> and lAppA<sub>BLUF</sub> were performed using a 10 kHz titanium sapphire amplified system pumping OPAs for IR generation. The samples were excited with 200 nJ pulses at 400 nm. It was established that the transient data was independent of pulse energy below 500 nJ. A flow cell system was used in addition to rastering the sample holder in the beam path in order to avoid photobleaching and degradation of the protein and the photoconversion of dAppA<sub>BLUF</sub>. The IR probe then recorded transient difference spectra (pump on – pump off) at time delays between 1 ps and 2 ns. After the measurements were recorded the extent of photoconversion was checked using absorbance spectroscopy. Measurements were also made on light adapted AppA<sub>BLUF</sub>. All photoconversions were performed using a hand held UV illuminator with ca 20 Watts output at 365 nm light for 3 minutes and the light state conversion was checked using absorbance spectroscopy.

#### B.4. Density functional theory (DFT) calculations:

DFT calculations were performed to support the assignments based on isotopic substitution. So as to avoid complications associated with possible multiple conformations of the side chain, and to allow a greater number of calculations, all the frequencies given refer to lumiflavin rather than FAD (R= CH<sub>3</sub> in **Figure 2.1**). The DFT calculations were made for gas phase using the Gaussian 03 software package, B3LYP method, and 6-31G basis set. This can obviously lead to discrepancies between the experimental data and the calculations, so for the purpose of assignment the relative spectral shifts are more relevant than the exact wavenumber. H-bonding effects of the solvent were investigated by adding specific water molecules. For the H<sub>2</sub>O/D<sub>2</sub>O comparison we exchanged the H atom at the N3 position with deuterium. The resulting frequencies were in every case multiplied by 0.9614, the accepted scaling factor for the B3LYP/6-31G calculations (19). Although the theory predicts only maximum  $\pm 34 \text{ cm}^{-1}$  difference between the theoretical and the experimental data, this rule had to be relaxed for the high frequencies (1650  $\text{cm}^{-1}$ , 1700  $\text{cm}^{-1}$ ) where there was strong evidence for a matching vibration that was more than 34  $\text{cm}^{-1}$  away.

## C. Results and Discussion:

### C.1. Isotopically Labeling the Flavin Carbonyls Groups: [4,10a-<sup>13</sup>C<sub>2</sub>]riboflavin and [2-<sup>13</sup>C<sub>1</sub>]-FAD

The TRIR spectra of dark (dAppA<sub>BLUF</sub>) and light-adapted (lAppA<sub>BLUF</sub>) AppA<sub>BLUF</sub> contain a wealth of information on the early structural changes that accompany protein photoexcitation (16). However, in order to fully interpret the TRIR spectra, and thereby enhance our understanding of the mechanism of AppA photoactivation, isotope labels must be incorporated site specifically into both the chromophore and the surrounding amino acids in order to assign vibrational modes associated with changes upon photoexcitation. Obvious targets for site-specific labeling include groups that are involved in direct interactions between chromophore and protein, including the carbonyl groups in the FAD isoalloxazine ring that are hydrogen bonded to amino acids surrounding the chromophore. The isoalloxazine C4=O group is of particular interest since models for AppA activation propose a strengthening of hydrogen bond(s) to this group in the light-activated protein (**Figure 2.1**), and we and others have assigned bands in the vibrational spectra to both the C4=O as well as the adjacent C2=O group, (20), (16), (21-25). These bands alter upon photoconversion, supporting the importance of protein interactions with the carbonyl groups in the AppA photocycle. While DFT calculations have been used to calculate the normal mode composition of each band (26), true band assignments require selective isotope labeling in order, for example, to delineate the degree of vibrational coupling between the two carbonyl groups. In this work we first probe through TRIR measurements and DFT calculations the sensitivity of the carbonyl modes of FAD or riboflavin to isotopic substitution at C2 and C4 and also to H/D exchange at the N3 atom (known to be coupled to the carbonyl stretches) (24, 27). We further probe the environmental sensitivity of these modes by

calculating the effect of specific H-bonding interactions. With these data it becomes possible to investigate the same modes in AppA in both its dark and light adapted states.

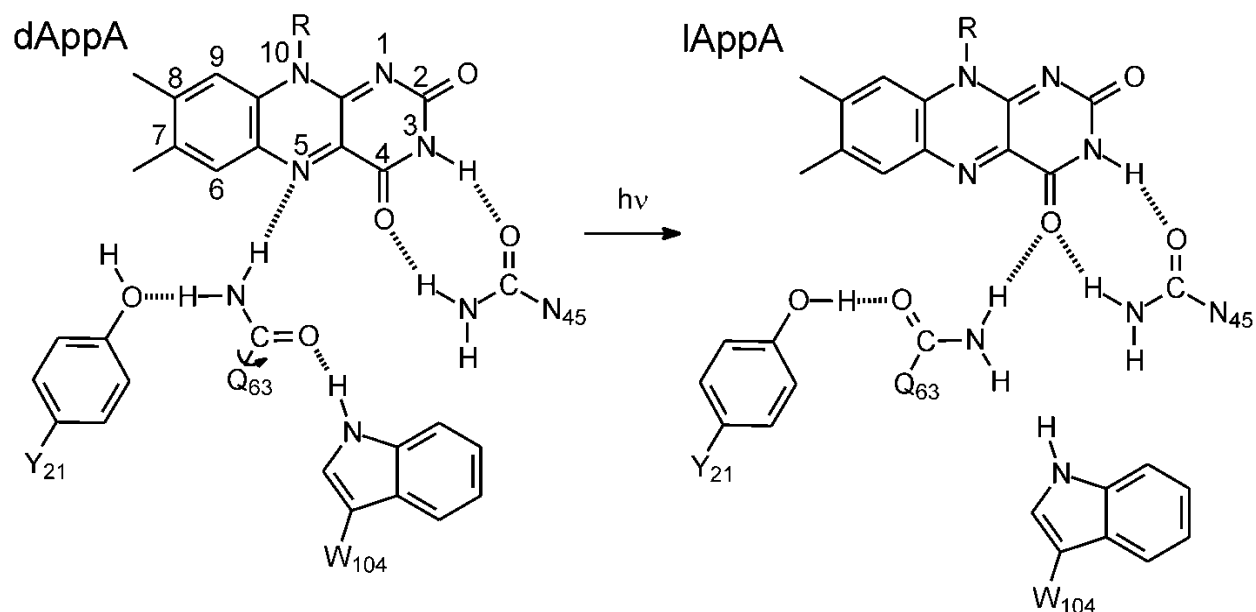
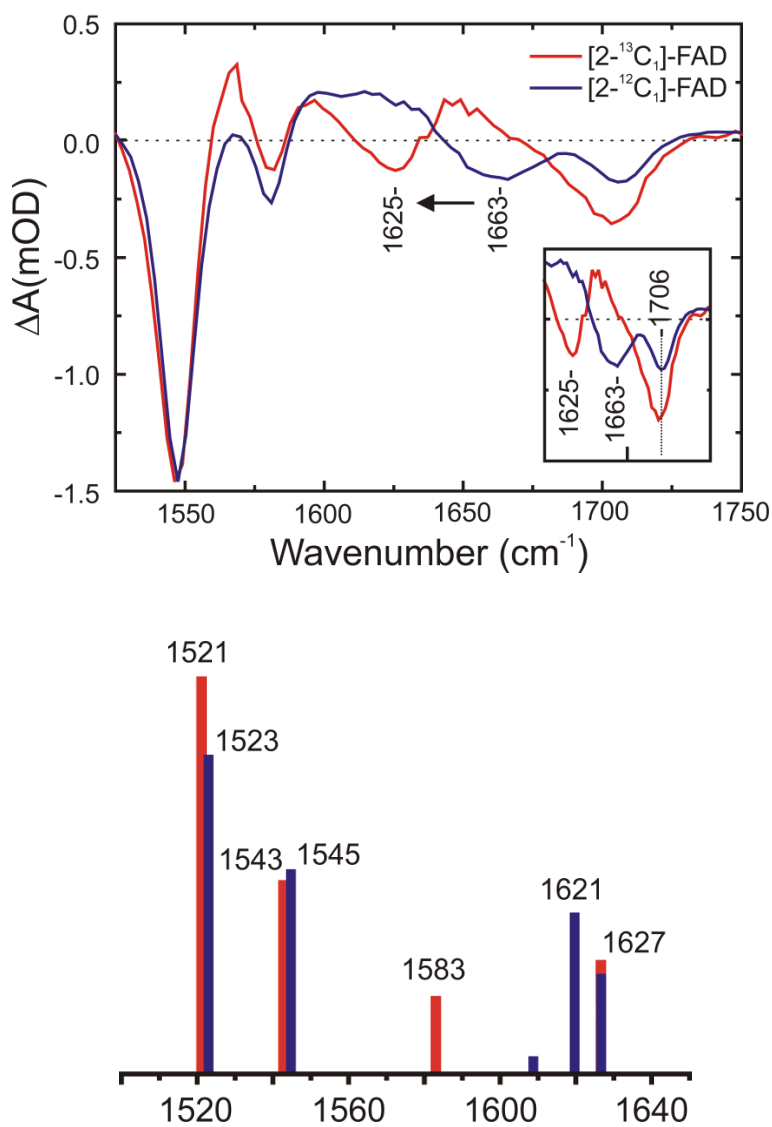


**Figure 2.1: Environment of the isoalloxazine chromophore in AppA.**

Putative hydrogen bonding interactions are shown by dashed lines. Photoexcitation may lead to changes in the hydrogen bond network, one model for which involves a rotation of Q63 (11).

In **Figure 2.2** the transient vibrational spectra at a 3 ps time delay after excitation for FAD and [2-<sup>13</sup>C<sub>1</sub>]-FAD are shown and compared with DFT calculations of the ground state IR transmission spectrum. Experimental data were recorded in H<sub>2</sub>O and calculations were made with a proton at N3. The experimental spectra in **Figure 2.2** are difference spectra of the excited state minus un-excited (ground) state transmission where the negative modes are associated with loss of the ground state and referred to as bleaches and the positive modes are associated with the newly generated excited state. The main observed effect of isotopic substitution is a shift in the band with the second highest frequency from 1663 cm<sup>-1</sup> to 1625 cm<sup>-1</sup>. This compares nicely with the calculated down shift of 38 cm<sup>-1</sup> in the DFT data as a result of the same exchange and is

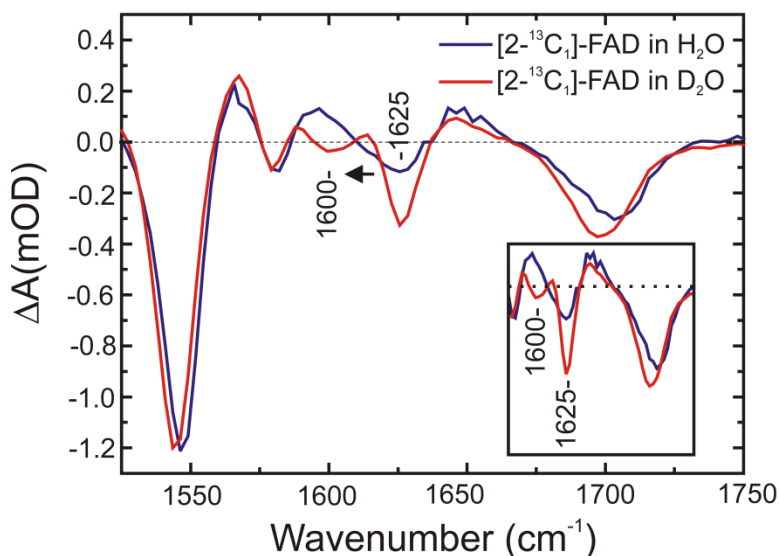
consistent with the assignment of this band to a mode that is principally associated with motions of the C2=O group. Although the DFT calculations reveal that this mode is strongly coupled to the N3H wag, there is no significant movement of C4=O upon isotopic substitution at C2 indicating that the two carbonyl modes are not strongly coupled.



**Figure 2.2: TRIR and calculated spectra of unlabeled FAD and [2-<sup>13</sup>C<sub>1</sub>]FAD in H<sub>2</sub>O**

FAD concentration was 6 mM in phosphate buffer, pH 8, and the TRIR spectra were recorded with a time delay of 3 ps.

In **Figure 2.3** the effect of exchange of N3H for N3D is shown both experimentally for  $[2\text{-}^{13}\text{C}_1]\text{-FAD}$  in water and  $\text{D}_2\text{O}$  and in DFT calculations. Again the agreement between calculated and experimental data is good. Both of the carbonyl localized modes shift down in frequency, with the larger effect being seen for the  $\text{C2=O}$  mode in this case ( $1625$  to  $1600\text{ cm}^{-1}$ ). This result indicates the importance of H/D exchange at N3 and is consistent with the DFT calculations which indicate coupling between  $\text{C2=O}$  and N3H. The effect of deuteration on the vibrational data will be significant when comparing theory and experiment since the vast majority of IR difference spectra are made in  $\text{D}_2\text{O}$ . A consequence of the downshift of  $\text{C2=O}$  is the unexpected appearance of a bleach at  $1625\text{ cm}^{-1}$ . We suggest that this mode can be assigned to the adenine of the FAD (28) and was partially obscured by the excited state absorption of  $\text{C2=O}$ . Support for this assignment comes from the observation (not shown) that no such mode appears for FMN when  $\text{D}_2\text{O}$  is exchanged for  $\text{H}_2\text{O}$ , although all other shifts are very similar; clearly the adenine mode lends some uncertainty to the location of the  $\text{C2=O}$  mode in  $\text{H}_2\text{O}$ , but the importance of the H/D exchange is clear.



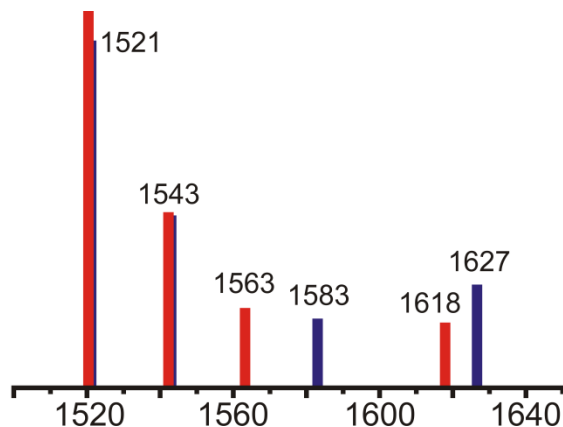


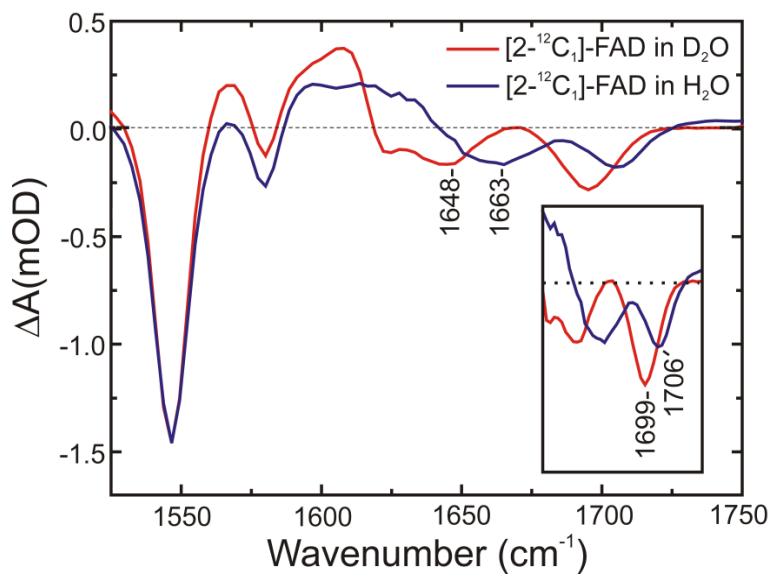
**Figure 2.3: TRIR and calculated spectra of [2-<sup>13</sup>C<sub>1</sub>]-FAD in H<sub>2</sub>O and D<sub>2</sub>O.**

FAD concentration was 6 mM in pH or pD 8 phosphate buffer and the TRIR spectra were recorded with a time delay of 3 ps.

The effect of H/D exchange is even more marked in the case of unlabeled FAD in H<sub>2</sub>O and D<sub>2</sub>O (**Figure 2.4**). Previous Raman studies on riboflavin demonstrated that H/D exchange of FAD resulted in a 13 cm<sup>-1</sup> decrease in the frequency of a band at 1711 cm<sup>-1</sup> (29). This is consistent with the current data where a 7 cm<sup>-1</sup> decrease in the band at 1706 cm<sup>-1</sup> is observed (**Table 1**). In the DFT calculation for the chromophore in H<sub>2</sub>O (N3H) the two highest frequency modes are close in wavenumber with the stretch largely localized on the C4=O (1627 cm<sup>-1</sup>) and C2=O (1620 cm<sup>-1</sup>) modes respectively, and coupled to the N3H wag. In contrast, the DFT calculation of the chromophore in D<sub>2</sub>O (N3D) shows that the two frequencies separate and the character changes to an asymmetric (1594 cm<sup>-1</sup>) and symmetric (1624 cm<sup>-1</sup>) C2/C4=O character pair (again coupled with the N3D wag). The effect seen experimentally is consistent with this result but the modes are already well separated in H<sub>2</sub>O although they do move further apart in D<sub>2</sub>O, as predicted by calculation (**Figure 2.4**). The origin of the apparent discrepancy between N3H experiment and DFT calculations was investigated by including a specific water molecule

in the calculations, H-bonded to the C=O oxygen atoms or to N3H. The largest effect was on H-bonding to N3H, causing the separation of the two carbonyl frequencies in FAD to increase by  $30\text{ cm}^{-1}$ . From this it may be concluded that the pattern of hydrogen bonding modes is not only susceptible to H/D exchange but also to the local H-bonding environment. This will be useful in probing H-bonded interactions in the protein.

The transient spectra in **Figure 2.4** are in good agreement with our previous study in  $\text{D}_2\text{O}$  (26). It is interesting to compare these measurements with the data of Wolf et al (24), who studied riboflavin in the non hydrogen bonding solvent DMSO. The loss in the hydrogen bonding gives rise to a shift of the carbonyl peaks to higher frequencies. The DMSO data has the highest frequency mode at  $1710\text{ cm}^{-1}$  compared to  $\sim 1706\text{ cm}^{-1}$  in aqueous FAD and  $1700\text{ cm}^{-1}$  in riboflavin solution. Hydrogen bonding causes a larger shift in the C2=O localized mode of more than  $20\text{ cm}^{-1}$  from  $1676\text{ cm}^{-1}$  in DMSO to  $\sim 1650$  in both riboflavin and FAD in aqueous solution. The solvent induced shifts in the ring modes at  $1581$  and  $1546$  are much smaller, confirming the sensitivity of the carbonyl modes to H-bonding.





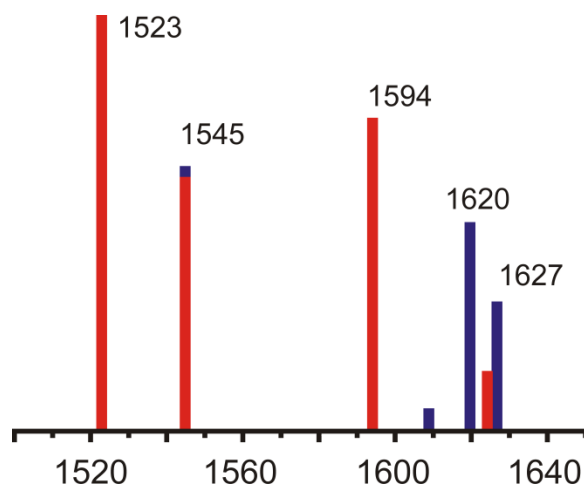


**Figure 2.4: TRIR and calculated spectra of unlabeled FAD in H<sub>2</sub>O and D<sub>2</sub>O.**

FAD concentration was 6 mM in pH or pD 8 phosphate buffer and the TRIR spectra were recorded with a time delay of 3 ps.

In addition to labeling at C2, the effect of <sup>13</sup>C-labeling at C4 has been probed using [4,10a-<sup>13</sup>C<sub>2</sub>]riboflavin. Specific labeling of only C4 is very challenging and synthetic route to the isotopomer studied here resulted in labeling at both C4 and C10a of the isoalloxazine ring. From the TRIR data in **Figure 2.5**, the most obvious effect of labeling in the experimental data is a 37 cm<sup>-1</sup> decrease in the highest observed bleach mode, indicating that this mode has a substantial fraction of C4=O character. This is in agreement with previous steady state Raman spectra on FAD where a 34 cm<sup>-1</sup> shift in this mode was observed upon <sup>13</sup>C labeling of C4=O (21). DFT calculations for [4,10a-<sup>13</sup>C<sub>2</sub>]riboflavin show the same magnitude shift of the peaks at 1523 cm<sup>-1</sup> and 1545 cm<sup>-1</sup> as the respective measured peaks at 1547 cm<sup>-1</sup> and 1575 cm<sup>-1</sup>, i.e. both the higher frequency modes shift down in frequency. The shift of the lower frequency mode of the pair is

less evident experimentally, perhaps because it is poorly resolved (**Figure 2.5**). It may also be that these modes for riboflavin in D<sub>2</sub>O are more localized than suggested by the calculation because of the effect of H-bonding discussed above.

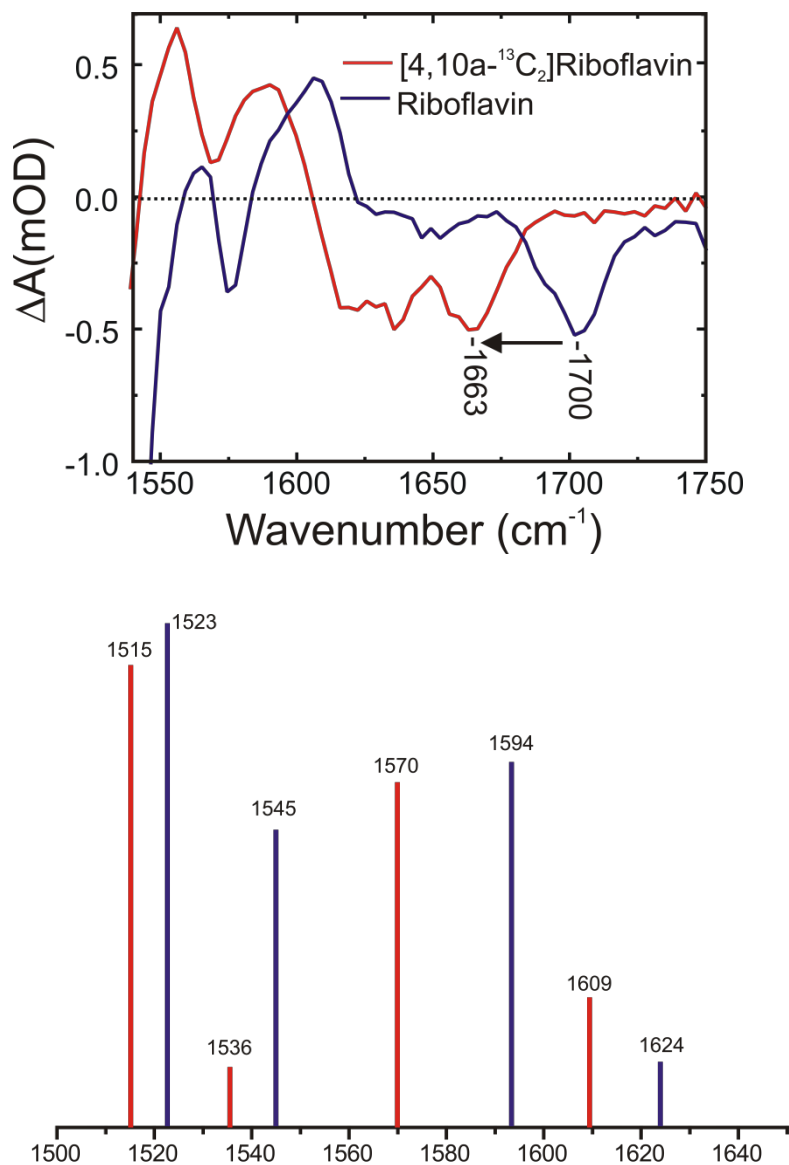


**Figure 2.5: TRIR and calculated spectra of unlabeled riboflavin and [4,10a-<sup>13</sup>C<sub>2</sub>]riboflavin in D<sub>2</sub>O.**

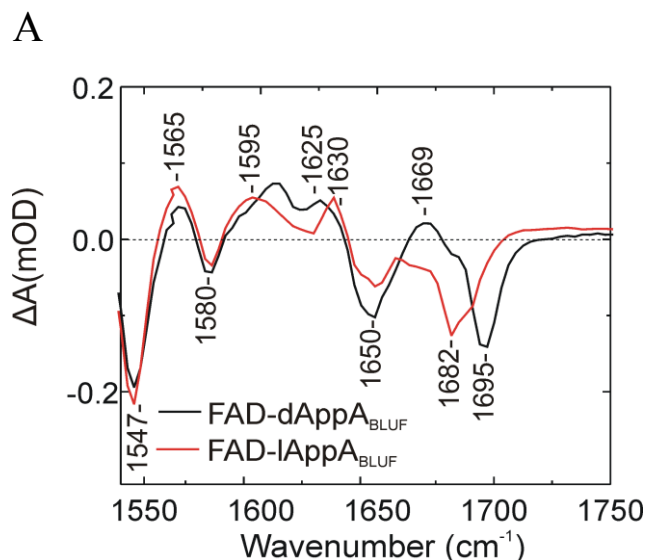
TRIR spectra of 1 mM riboflavin (black) and [4,10a-<sup>13</sup>C<sub>2</sub>]riboflavin (red) in pD 8 phosphate buffer recorded with a time delay of 3 ps.

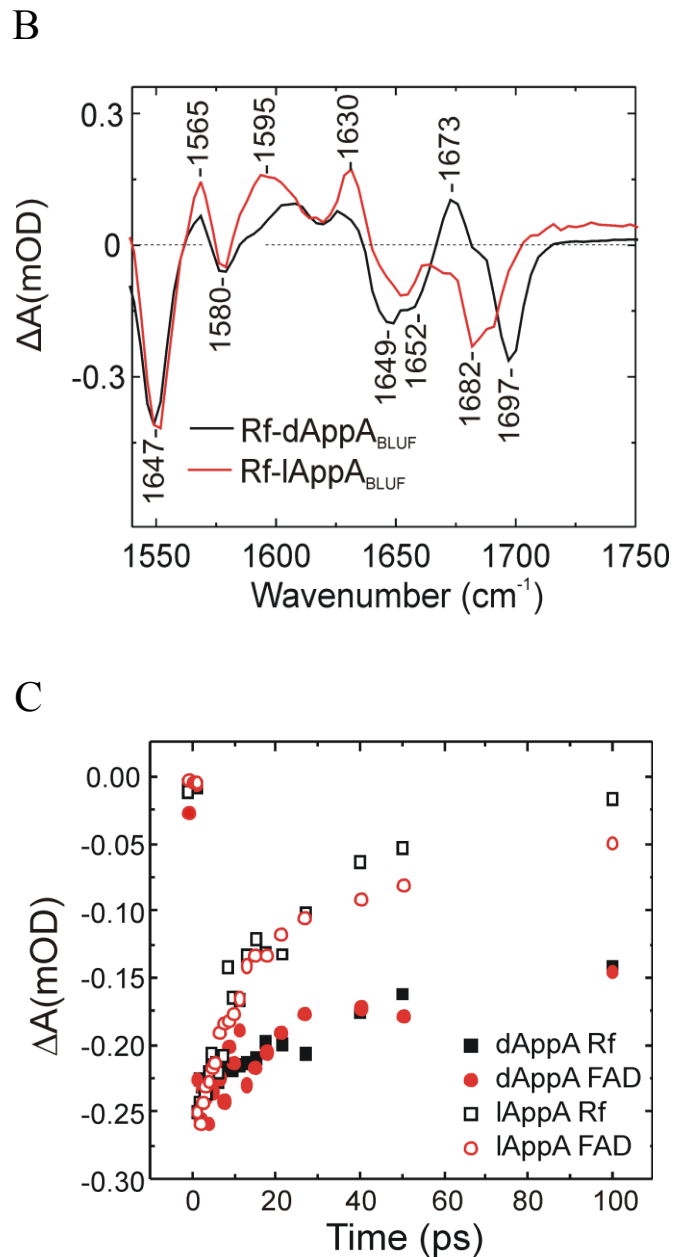
Equipped with the above spectroscopic characterization of isotopically substituted flavins a more detailed discussion of the data for the protein reconstituted with its ligand can be made. We measured TRIR spectra of AppA<sub>BLUF</sub> reconstituted with [2-<sup>13</sup>C<sub>1</sub>]-FAD and [4,10a-<sup>13</sup>C<sub>2</sub>]riboflavin. While FAD is more soluble in aqueous solution than riboflavin, and thus more convenient to work with, previous studies based on electronic spectroscopy suggest that the photocycle of AppA is not affected by replacing FAD with riboflavin (27, 30). To confirm this proposal, we first compared the TRIR spectra of dAppA<sub>BLUF</sub> and lAppA<sub>BLUF</sub> reconstituted with either FAD or riboflavin (**Figure 2.6**). Based on peak position, relative intensity and the kinetic information shown, AppA<sub>BLUF</sub> is not affected by replacing FAD with riboflavin as the flavin chromophore. The dAppA<sub>BLUF</sub> spectra show intense bleaches observed at 1695, 1650, 1580 cm<sup>-1</sup> and 1547 cm<sup>-1</sup> for AppA<sub>BLUF</sub> reconstituted with both riboflavin and FAD. Transient absorptions are observed at 1630, 1595 and 1565 cm<sup>-1</sup> for both FAD and riboflavin in addition to a broad transient at ~1670 cm<sup>-1</sup>. The latter transient has been previously reported by us to be associated with a photoactivatable state of the protein through studies of both light and dark adapted states and photoactive and inactive mutants (16).

The TRIR spectra for lAppA<sub>BLUF</sub> bound to FAD and riboflavin are also shown in **Figure 2.6**. In comparison to the dark state, the high frequency bleach at ~1695 cm<sup>-1</sup> shifts to lower frequency and splits into a doublet at 1691 and 1682 cm<sup>-1</sup>. The bleach at 1650 cm<sup>-1</sup> found in both the dark and light state spectra is lower in intensity in the light state when compared to the dark state. In addition, the transient at ~1670 cm<sup>-1</sup> is no longer observed in the light state which is in agreement with previous measurements (16). The first conclusion that can be drawn from this work is that the similarities reported in the steady state data for AppA<sub>BLUF</sub> bound to either FAD

or riboflavin are also observed in TRIR spectroscopy, demonstrating that riboflavin is a suitable model for FAD in AppA<sub>BLUF</sub>, and that the H-bonding pattern is similar for both chromophores.

In **Figure 2.6c** the ground state recovery kinetics for dAppA<sub>BLUF</sub> and lAppA<sub>BLUF</sub> are compared bound to both FAD and riboflavin. The kinetics for riboflavin and FAD are indistinguishable within experimental error, consistent with the conclusion above. Also immediately noticeable for both chromophores is that the ground state recovery is much faster in lAppA<sub>BLUF</sub>, suggesting faster excited state quenching, as discussed elsewhere (16). A discussion of the ultrafast kinetics is beyond the scope of this chapter, but the non-exponential recovery is evident. For lAppA<sub>BLUF</sub> the fast components dominate. A substantial fraction of the dAppA<sub>BLUF</sub> recovery occurs on a sub 100 ps timescale, as was also observed in earlier studies (16),(31). Measurements of transient electronic spectroscopy however report a dominant 600 ps component (e.g in fluorescence decay), accompanied by faster components (32).

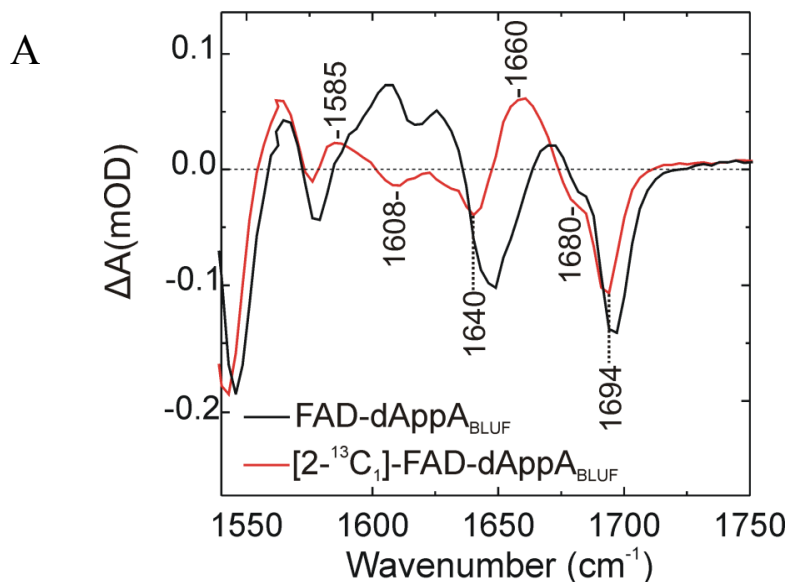




**Figure 2.6: TRIR spectra and kinetic data of dAppA<sub>BLUF</sub> and lAppA<sub>BLUF</sub> bound to riboflavin or FAD in D<sub>2</sub>O.**

- (a) TRIR Spectra of dAppA<sub>BLUF</sub> (black) and lAppA<sub>BLUF</sub> (red) bound to riboflavin. (b) TRIR spectra of dApp<sub>BLUF</sub>A (black) and lAppA<sub>BLUF</sub> (red) bound to FAD. Protein concentration was 2 mM in pD 8 phosphate buffer and the TRIR spectra were recorded with a time delay of 3 ps. (c) Comparison of kinetic measurements of AppA<sub>BLUF</sub> bound to riboflavin and FAD in D<sub>2</sub>O.

The TRIR spectra of AppA<sub>BLUF</sub> bound to [4,10a-<sup>13</sup>C<sub>2</sub>]riboflavin confirm assignments of the high frequency band as involving mainly the C4=O localized stretch and the lower frequency band as mainly arising from the C2=O stretch. First we consider dAppA<sub>BLUF</sub> bound to [2-<sup>13</sup>C<sub>1</sub>]-FAD (**Figure 2.7**) which shows only a small shift in the 1695 cm<sup>-1</sup> bleach. In addition, there is a shift of the 1650 cm<sup>-1</sup> mode to lower frequency (1640 cm<sup>-1</sup>). This bleach is much less intense in comparison to the unlabeled spectra, however, we suggest that the broad positive band spanning from 1630 to 1585 cm<sup>-1</sup> overlaps with the 1640 cm<sup>-1</sup> feature reducing its intensity. These data confirm the assignment of mainly C4=O localized character to the high frequency mode and the C2=O vibration as the main contributor to the low frequency mode, as proposed previously for FAD bound to dAppA<sub>BLUF</sub> (16). These assignments align with our earlier study, and are similar to the one other TRIR study of a BLUF domain, Slr1694 BLUF (31), although in that case a high wavenumber mode of low amplitude was assigned as the highest frequency carbonyl stretch.



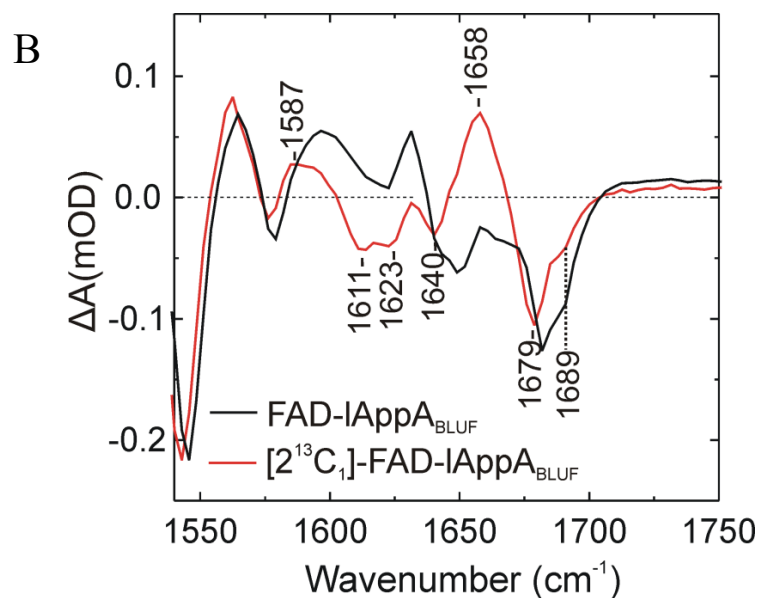


**Figure 2.7: TRIR Spectra of FAD and [2-<sup>13</sup>C<sub>1</sub>]-FAD bound to dAppA<sub>BLUF</sub> and lAppA<sub>BLUF</sub>.**

(a) TRIR spectra of dAppA<sub>BLUF</sub> bound to unlabeled FAD (black) and [2-<sup>13</sup>C<sub>1</sub>]-FAD (red). (b) TRIR spectra of lAppA<sub>BLUF</sub> bound to unlabeled FAD (black) and [2-<sup>13</sup>C<sub>1</sub>]-FAD (red). The protein concentration was 2 mM and the samples were prepared in 50 mM phosphate D<sub>2</sub>O buffer pD 8. The time delay was 3 ps.

**Figure 2.8** shows the TRIR spectra of AppA<sub>BLUF</sub> bound to [4,10a-<sup>13</sup>C<sub>2</sub>]riboflavin and allows assignment of the high frequency carbonyl mode as largely localized on the C4=O stretch. The 1700 cm<sup>-1</sup> peak in dAppA<sub>BLUF</sub> shifts by 20 cm<sup>-1</sup> to 1680 cm<sup>-1</sup>. This isotope shift also appears in lAppA where the 1682 cm<sup>-1</sup> mode shifts by roughly 10 cm<sup>-1</sup> to 1673 cm<sup>-1</sup>. These isotope shifts seen upon <sup>13</sup>C labeling of C4 further validate assignment of 1700 cm<sup>-1</sup> mode in dAppA<sub>BLUF</sub> and the 1682 cm<sup>-1</sup> in lAppA<sub>BLUF</sub> to a mainly C4=O mode of the flavin chromophore.

Another important aspect of both the l and dAppA<sub>BLUF</sub> spectra is the appearance of an intense transient absorption at 1660 – 1670 cm<sup>-1</sup>. This mode is seen in the unlabeled spectra at 1669 cm<sup>-1</sup> in dAppA<sub>BLUF</sub>, and was found earlier (16) to be characteristic of AppA mutants capable of undergoing photocycles, being absent in lAppA<sub>BLUF</sub> and the photoinactivated Q63L mutant. On the basis of those measurements the transient absorption was assigned to a protein mode, most likely Q63, perturbed by flavin excitation. The shift in the 1650 cm<sup>-1</sup> bleach to lower frequency upon labeling removes overlap with the 1669 cm<sup>-1</sup> mode increasing intensity of the transient, making the mode appear slightly red shifted. The same experiment in lAppA<sub>BLUF</sub> reveals for the first time a transient absorption at 1658 cm<sup>-1</sup>. These observations suggest the transient may be associated with an excited state mode of the flavin (localized on C4=O for example). However, such a simple assignment is not consistent with observations on AppA mutants. Further, the spectra in **Figure 2.8a** show that a shift in the C4=O bleach from 1700 cm<sup>-1</sup> to 1680 cm<sup>-1</sup> in dAppA<sub>BLUF</sub> bound to riboflavin is not accompanied by an increase in bleach around 1650 cm<sup>-1</sup>; indeed the opposite is the case. In fact attempts to model the transient absorption in **Figures 2.7** and **2.8** solely on the basis of the isotope shifts seen in the bleach modes was not successful. The data presented here thus raise the possibility that the transient corresponding to that marker mode may reflect photoinduced modifications of flavin excited state - protein coupling. This proposal will be tested by recording TRIR spectra of the AppA<sub>BLUF</sub> protein that has been isotopically edited; such measurements are discussed in chapter 3.



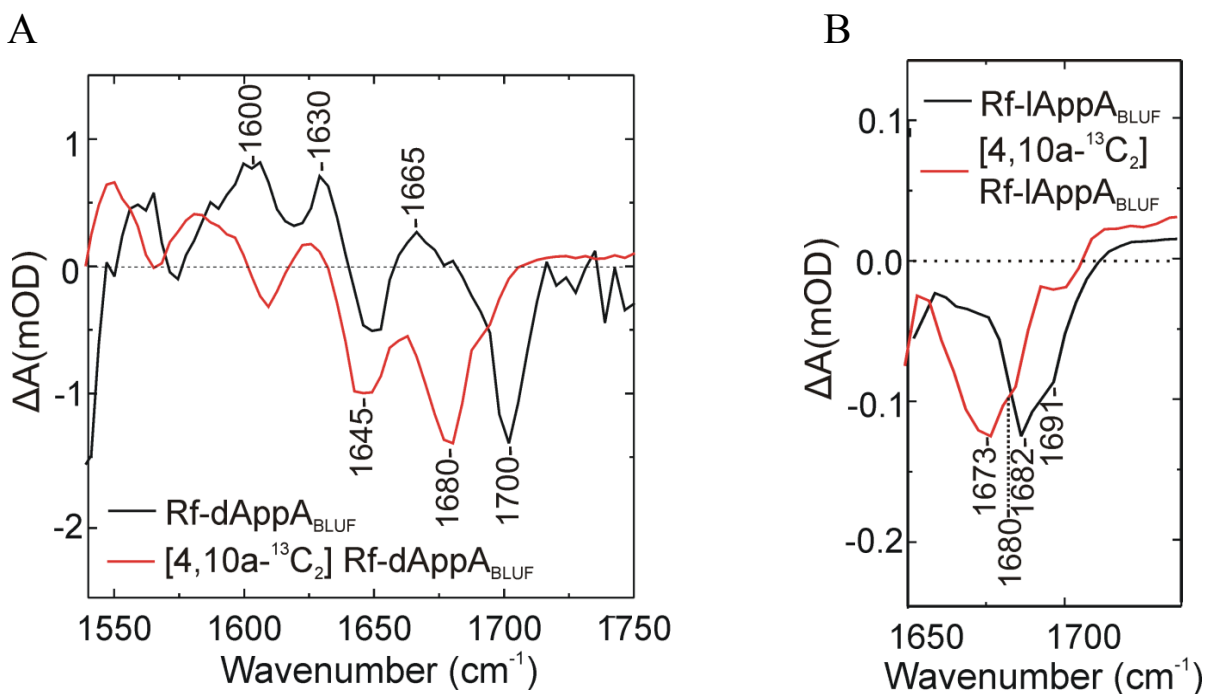


**Figure 2.8: TRIR Spectra of FAD and [4,10a-<sup>13</sup>C<sub>2</sub>]riboflavin bound to dAppA and lAppA.**

(a) TRIR spectra of dAppA<sub>BLUF</sub> bound to unlabeled riboflavin (black) and [4,10a-<sup>13</sup>C<sub>2</sub>]riboflavin (red).

(b) TRIR spectra of lAppA<sub>BLUF</sub> bound to unlabeled riboflavin (black) and [4,10a-<sup>13</sup>C<sub>2</sub>]riboflavin (red). The protein concentration was 2 mM and the samples were prepared in 50 mM phosphate D<sub>2</sub>O buffer pD 8. The time delay was 3 ps.

**Table 2.1: Observed and calculated vibrational modes of FAD, [2-<sup>13</sup>C<sub>1</sub>]-FAD, riboflavin and [4,10a-<sup>13</sup>C<sub>2</sub>]riboflavin in H<sub>2</sub>O and D<sub>2</sub>O**

	[2- <sup>12</sup> C <sub>1</sub> ]-FAD		[2- <sup>13</sup> C <sub>1</sub> ]-FAD		[4,10a- <sup>12</sup> C <sub>2</sub> ]-Rf		[4,10a- <sup>13</sup> C <sub>2</sub> ]-Rf	
	Observed	Calculated	Observed	Calculated	Observed	Calculated	Observed	Calculated
H <sub>2</sub> O	1547 cm <sup>-1</sup>	1523 cm <sup>-1</sup> C10 <sub>a</sub> N <sub>1</sub>	1547 cm <sup>-1</sup>	1521 cm <sup>-1</sup> C10 <sub>a</sub> N <sub>1</sub>				
	1581 cm <sup>-1</sup>	1545 cm <sup>-1</sup> C4 <sub>a</sub> N <sub>5</sub>	1581 cm <sup>-1</sup>	1543 cm <sup>-1</sup> C4 <sub>a</sub> N <sub>5</sub>				
	1663 cm <sup>-1</sup>	1619 cm <sup>-1</sup> C <sub>2</sub> =O+N <sub>3</sub> wag	1625 cm <sup>-1</sup>	1583 cm <sup>-1</sup> C <sub>2</sub> =O+N <sub>3</sub> wag				
	1706 cm <sup>-1</sup>	1627 cm <sup>-1</sup> C <sub>4</sub> =O+N <sub>3</sub> wag	1703 cm <sup>-1</sup>	1627 cm <sup>-1</sup> C <sub>4</sub> =O+N <sub>3</sub> wag				
D <sub>2</sub> O	1547 cm <sup>-1</sup>	1523 cm <sup>-1</sup> C10 <sub>a</sub> N <sub>1</sub>	1545 cm <sup>-1</sup>	1521 cm <sup>-1</sup> C10 <sub>a</sub> N <sub>1</sub>	1547 cm <sup>-1</sup>	1523 cm <sup>-1</sup> C10 <sub>a</sub> N <sub>1</sub>	NA	1515 cm <sup>-1</sup> C10 <sub>a</sub> N <sub>1</sub>
	1581 cm <sup>-1</sup>	1545 cm <sup>-1</sup> C4 <sub>a</sub> N <sub>5</sub>	1581 cm <sup>-1</sup>	1543 cm <sup>-1</sup> C4 <sub>a</sub> N <sub>5</sub>	1575 cm <sup>-1</sup>	1545 cm <sup>-1</sup> C4 <sub>a</sub> N <sub>5</sub>	1565 cm <sup>-1</sup>	1536 cm <sup>-1</sup> C4 <sub>a</sub> N <sub>5</sub>
	1648 cm <sup>-1</sup>	1594 cm <sup>-1</sup> C <sub>2</sub> =O, C <sub>4</sub> =O asym +N <sub>3</sub> wag	1600 cm <sup>-1</sup>	1563 cm <sup>-1</sup> C <sub>2</sub> =O,C <sub>4</sub> = O asym+N <sub>3</sub> wag	1648 cm <sup>-1</sup>	1594 cm <sup>-1</sup> C <sub>2</sub> =O, C <sub>4</sub> =O asym +N <sub>3</sub> wag	1620 cm <sup>-1</sup>	1570 cm <sup>-1</sup> C <sub>4</sub> =O, C <sub>2</sub> =O asym +N <sub>3</sub> wag
	1699 cm <sup>-1</sup>	1624 cm <sup>-1</sup> C <sub>4</sub> =O, C <sub>2</sub> =O sym +N <sub>3</sub> wag	1697 cm <sup>-1</sup>	1618 cm <sup>-1</sup> C <sub>4</sub> =O, C <sub>2</sub> =O sym +N <sub>3</sub> wag	1700 cm <sup>-1</sup>	1624 cm <sup>-1</sup> C <sub>4</sub> =O, C <sub>2</sub> =O sym +N <sub>3</sub> wag	1663 cm <sup>-1</sup>	1608 cm <sup>-1</sup> C <sub>2</sub> =O, C <sub>4</sub> =O sym+N <sub>3</sub> wag

**Table 2.1: Observed and calculated vibrational modes of FAD, [2-<sup>13</sup>C<sub>1</sub>]-FAD, riboflavin and [4,10a-<sup>13</sup>C<sub>2</sub>]riboflavin in H<sub>2</sub>O and D<sub>2</sub>O.**

**Legend:** Observed frequencies are experimental TRIR measurements. Calculated frequencies were measured by Gaussian 03 using the B3LYP method and 6-31G basis set. Both unlabeled FAD and [2-<sup>13</sup>C<sub>1</sub>]-FAD were measured in H<sub>2</sub>O and D<sub>2</sub>O. Unlabeled riboflavin and [4,10a-<sup>13</sup>C<sub>2</sub>]riboflavin were measured in D<sub>2</sub>O only.

## C.2. Additional Assignments of Flavin Vibrational Modes: [uniform- $^{13}\text{C}_{17}$ ]-FAD, [xylene- $^{13}\text{C}_8$ ]-FAD, [uniform- $^{15}\text{N}_4$ ]-FAD and [4- $^{18}\text{O}_1$ ]-FAD

Here we report TRIR spectra of a number of isotopes of FAD, specifically [U- $^{13}\text{C}_{17}$ ]-FAD, [xylene- $^{13}\text{C}_8$ ]-FAD, [U- $^{15}\text{N}_4$ ]-FAD and [4- $^{18}\text{O}_1$ ]-FAD both in solution and bound to AppA<sub>BLUF</sub> (**Figure 2.9**). This allows for a better assignment of the vibrational modes in the isoalloxazine ring of the flavin, and further aids the distinction of protein and flavin modes in the congested  $1500\text{ cm}^{-1} - 1700\text{ cm}^{-1}$  spectral region. In addition, we have used DFT calculations to support our experimental data.

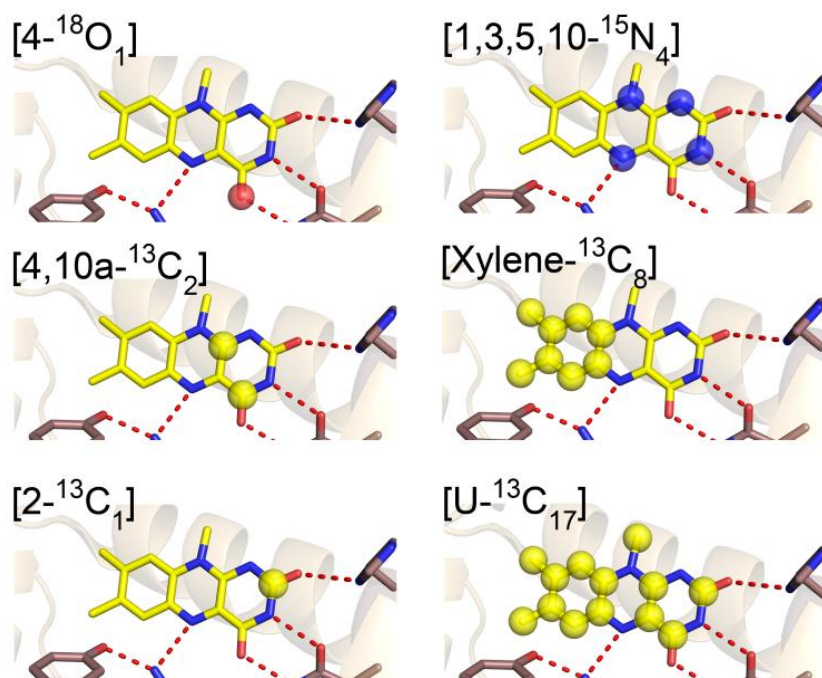


**Figure 2.9: Isotopologues Incorporated into AppA**

[4- $^{18}\text{O}_1$ ]-FAD, [1,3,5,10- $^{15}\text{N}_4$ ]-FAD, [4,10a- $^{13}\text{C}_2$ ]riboflavin, [xylene- $^{13}\text{C}_8$ ]-FAD, [2- $^{13}\text{C}_1$ ]-FAD and [U- $^{13}\text{C}_{17}$ ]-FAD incorporated to AppA<sub>BLUF</sub>.

### FAD Isotopes in Buffer:

In **Figure 2.10a** the TRIR spectra of FAD and [4-<sup>18</sup>O<sub>1</sub>]-FAD measured at a 3 ps time delay after excitation are shown. The high frequency bleach at 1700 cm<sup>-1</sup> in FAD is partially shifted to 1682 cm<sup>-1</sup> in [4-<sup>18</sup>O<sub>1</sub>]-FAD with residual intensity at 1700 cm<sup>-1</sup>. The ratio of the integrals of the 1700 and 1682 cm<sup>-1</sup> peaks is in line with the 60% isotope abundance of [4-<sup>18</sup>O<sub>1</sub>]-FAD (**Figure 2.11c**) so the lower wavenumber mode can be assigned to one involving the C4=O stretch. The effect of <sup>18</sup>O substitution on the mode with the next highest frequency is small and there is a negligible effect on all the lower frequency modes observed in this spectral window. The DFT calculation shown in **Figure 2.10b** is consistent with the observed down shift in the highest frequency mode, but also predicts a similar shift in the second mode (which was shown to be associated with the C2=O stretch from the previous data shown of [2-<sup>13</sup>C<sub>1</sub>]riboflavin). The disagreement between calculated and observed carbonyl frequencies was discussed in the previous section, and arises from the symmetric and anti-symmetric character of the stretching modes associated with the O=C4-N3H-C2=O unit (33). Typically gas phase calculations suggest an assignment of the two highest frequency modes to a symmetric – antisymmetric pair, but, as discussed previously, this is sensitive to the N3H/D exchange and H-bonding with the environment. The <sup>18</sup>O data reported here are consistent with a more localized character for the two C=O stretches in the ground state of FAD, as was suggested in our study of [4,10a-<sup>13</sup>C<sub>2</sub>]riboflavin and [2-<sup>13</sup>C<sub>1</sub>]-FAD.

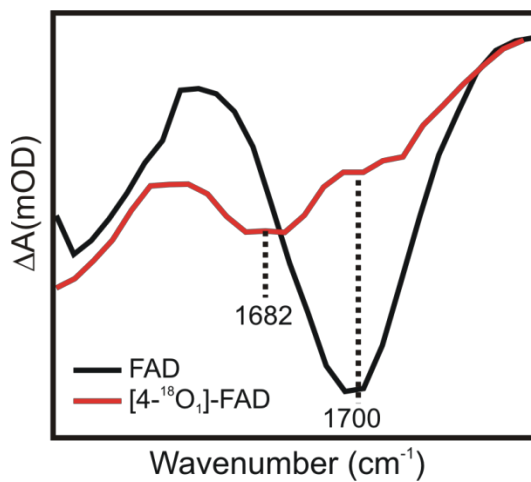
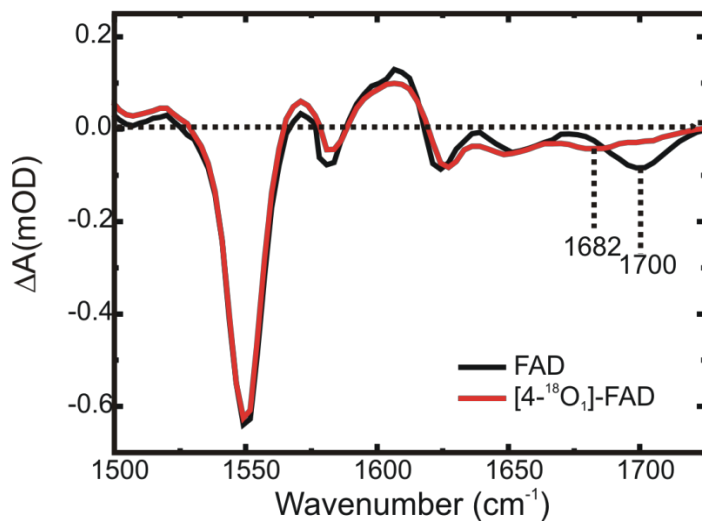


**Figure 2.10a: TRIR spectra of unlabeled FAD and [4-<sup>18</sup>O<sub>1</sub>]-FAD in D<sub>2</sub>O.**

(a) TRIR spectra of 3 mM FAD (black) and [4-<sup>18</sup>O<sub>1</sub>]-FAD (red) in pD 8 phosphate buffer recorded with a time delay of 3 ps. (b) Carbonyl region of TRIR spectra shown in (a).

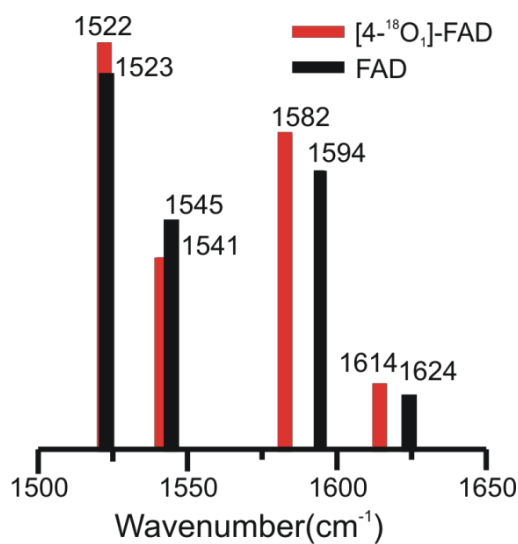


**Figure 2.10b: Calculated spectra of unlabeled FAD and [4-<sup>18</sup>O<sub>1</sub>]-FAD.**

Calculated spectra of FAD (black) and [4-<sup>18</sup>O<sub>1</sub>]-FAD (red) in pD 8 phosphate buffer.

The TRIR spectra of [1,3,5,10-<sup>15</sup>N<sub>4</sub>]-FAD compared to unlabeled FAD are shown in **Figure 2.11a**. The most significant change that occurs is the shift of the 1549 cm<sup>-1</sup> bleach to 1541 cm<sup>-1</sup>. The carbonyl modes are hardly altered by exchange of the N atoms. This is in good agreement with DFT calculations shown in **Figure 2.11b** which show an 8 cm<sup>-1</sup> shift of the most intense bleach upon uniform <sup>15</sup>N labeling. The calculation is summarized in **Table 2** and shows the major contributor to this intense mode is the C10<sub>a</sub>N<sub>1</sub> stretching vibration. In addition, the weaker bleach measured at 1581 cm<sup>-1</sup> shifts to 1578 cm<sup>-1</sup> upon <sup>15</sup>N labeling which is also in agreement with the calculated spectra, which in turn suggest the C4<sub>a</sub>N<sub>5</sub> stretch is a major contributor to this mode.

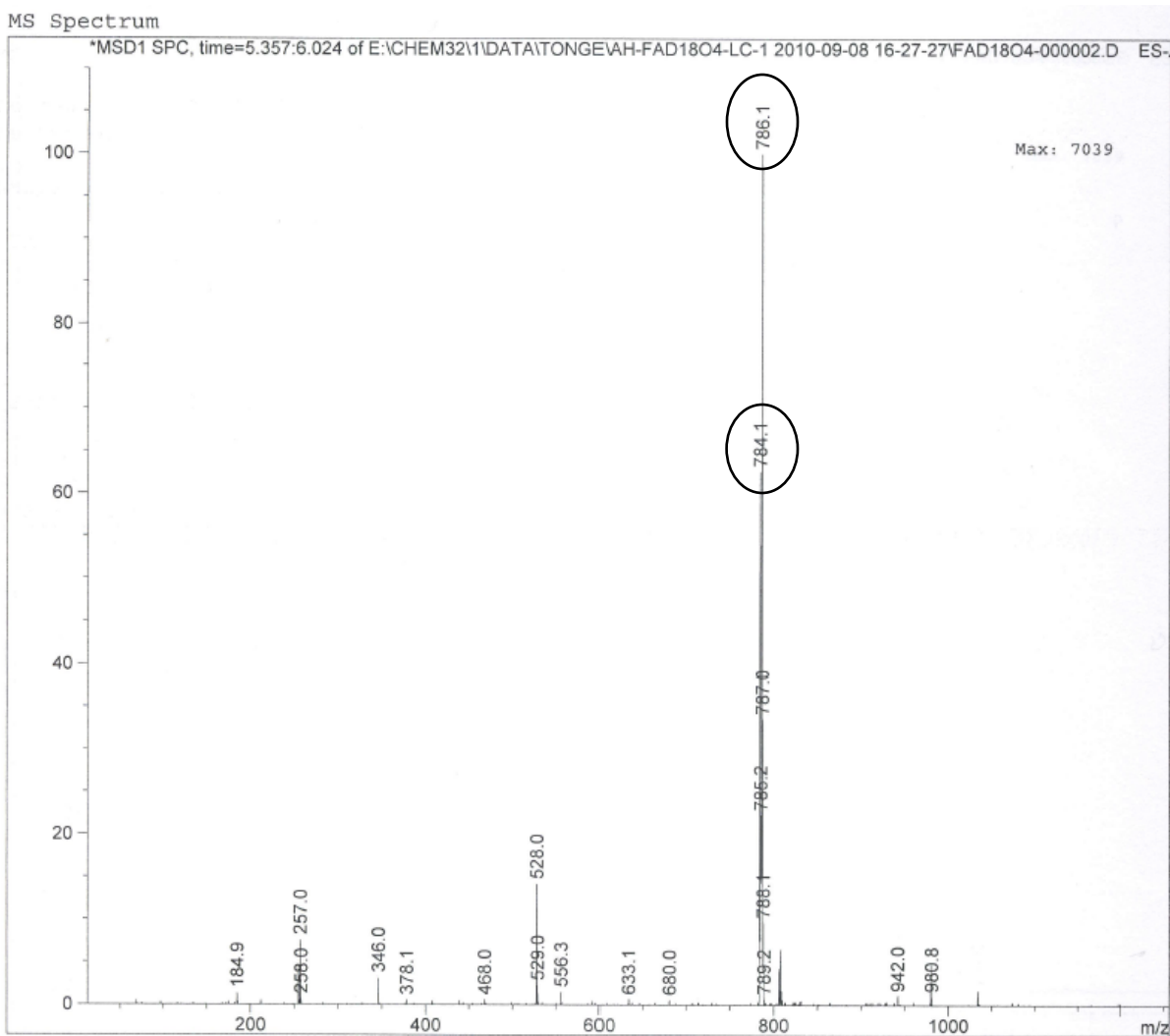


**Figure 2.10c: ES-API in negative mode for [4-<sup>18</sup>O<sub>1</sub>]-FAD:**

Chemical formula C<sub>27</sub>H<sub>32</sub>N<sub>9</sub><sup>16</sup>O<sub>14</sub><sup>18</sup>O<sub>1</sub>P<sub>2</sub><sup>-</sup>: Calculated mass 786.150, found 786.1 and 784.1.

The major peak is mass of FAD +2 and FAD +0. Percent labeled determined from peak ratio is 60% [4-<sup>18</sup>O<sub>1</sub>]-FAD and 40% FAD.

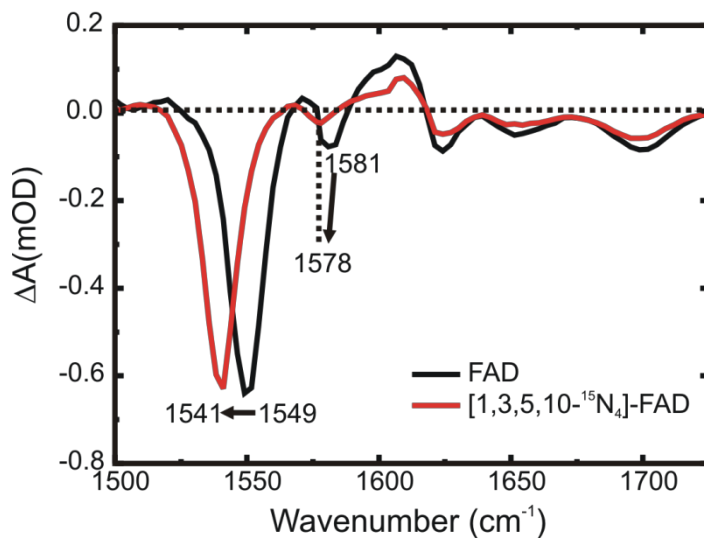


**Figure 2.11a: TRIR spectra of unlabeled FAD and [1,3,5,10-<sup>15</sup>N<sub>4</sub>]-FAD in D<sub>2</sub>O.**

TRIR spectra of 3 mM FAD (black) and [1,3,5,10-<sup>15</sup>N<sub>4</sub>]-FAD (red) in pD 8 phosphate buffer recorded with a time delay of 3 ps.

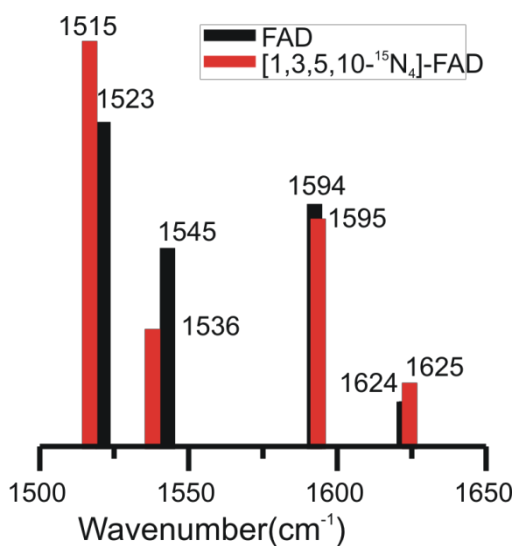


**Figure 2.11b: Calculated spectra of unlabeled FAD and [1,3,5,10-<sup>15</sup>N<sub>4</sub>]-FAD.**

Calculated spectra of FAD (black) and [1,3,5,10-<sup>15</sup>N<sub>4</sub>]-FAD (red) in pD 8 phosphate buffer.



**Figure 2.12a** shows the TRIR spectra of [xylene- $^{13}\text{C}_8$ ]-FAD. Upon labeling of the xylene ring an additional bleach appears in the transient IR spectrum, with three intense peaks appearing between 1500 and 1600  $\text{cm}^{-1}$ . The carbonyl modes are unaffected by isotopic substitution on the xylene ring. The origin of the extra band at 1586  $\text{cm}^{-1}$  can be traced in the DFT calculations, where the modes at 1545 and 1523  $\text{cm}^{-1}$  in FAD are down shifted by 19  $\text{cm}^{-1}$  and 29  $\text{cm}^{-1}$  respectively. The suggested origin of the band calculated at 1564  $\text{cm}^{-1}$  in [xylene- $^{13}\text{C}_8$ ]-FAD is a ring mode calculated as a very weakly allowed IR transition at 1609  $\text{cm}^{-1}$  in FAD. Evidently this mode gains considerably in intensity on decreasing in frequency, possibly from coupling to more intense modes which include the CN stretch.

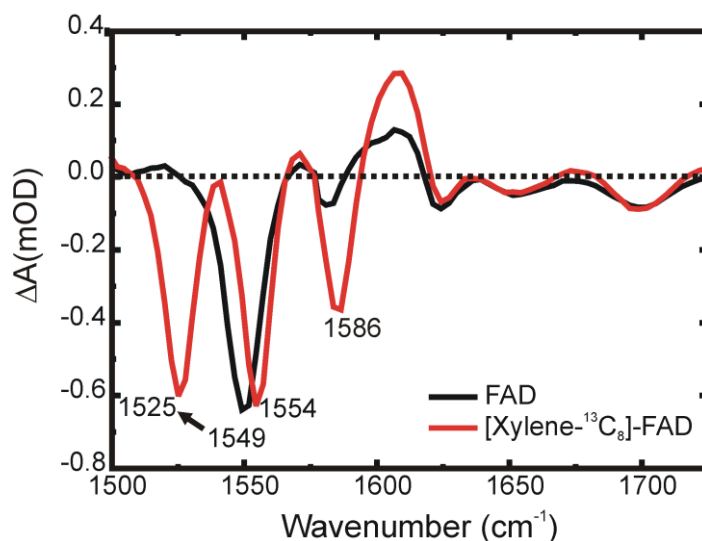


**Figure 2.12a: TRIR spectra of unlabeled FAD and [Xylene- $^{13}\text{C}_8$ ]-FAD in  $\text{D}_2\text{O}$ .**

TRIR spectra of 3 mM FAD (black) [Xylene- $^{13}\text{C}_8$ ]-FAD (red) in pD 8 phosphate buffer recorded with a time delay of 3 ps.

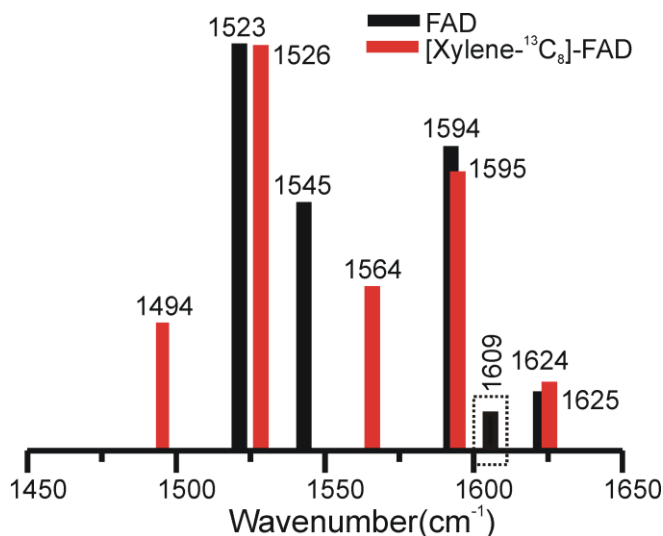


**Figure 2.12b: Calculated spectra of unlabeled FAD and [Xylene-<sup>13</sup>C<sub>8</sub>]-FAD.**

Calculated spectra of FAD (black) and [Xylene-<sup>13</sup>C<sub>8</sub>]-FAD (red) in pD 8 phosphate buffer.

The mode at 1609 cm<sup>-1</sup> has been enhanced by 25X.

The TRIR spectra of [Uniform-<sup>13</sup>C<sub>17</sub>]-FAD are shown in **Figure 2.13**. The 1700 cm<sup>-1</sup> bleach assigned to the C4=O is shifted by 40 cm<sup>-1</sup> to 1660 cm<sup>-1</sup> which is in agreement with data on the [4,10a-<sup>13</sup>C<sub>2</sub>] isotopologue studied earlier (33, 34). This shift is also in good agreement with DFT calculations shown in **Figure 2.13b** which predict a 44 cm<sup>-1</sup> shift of this bleach upon uniform <sup>13</sup>C labeling of FAD. DFT predicts this to be the symmetric stretch of both carbonyls coupled to the N3D. As discussed previously, the extent to which the mode is in fact one of a symmetric/antisymmetric pair or more localized on a particular C=O stretch depends on the environment. The lower frequency of the bleaches associated with C=O modes, at 1651 cm<sup>-1</sup>, was observed to shift by approximately 27 cm<sup>-1</sup> to lower frequency and is observed as a weak bleach mixed with the 1624 cm<sup>-1</sup> feature (**Figure 2.13a**). This is consistent with DFT calculations (**Figure 2.13b**) which show a 43 cm<sup>-1</sup> shift of this bleach upon uniform <sup>13</sup>C labeling (**Table 2.2**). Other shifts observed in the TRIR spectra of [Uniform-<sup>13</sup>C<sub>17</sub>]-FAD include the 1606

$\text{cm}^{-1}$  transient which shifts to approximately  $1568 \text{ cm}^{-1}$ . This band is assigned to the C=N modes in the excited electronic state. **Figure 2.13** also demonstrates that the  $1581 \text{ cm}^{-1}$  and  $1549 \text{ cm}^{-1}$  bleaches shift to  $1536 \text{ cm}^{-1}$  and  $1507 \text{ cm}^{-1}$ , respectively upon uniform  $^{13}\text{C}$  labeling of FAD. This is in agreement with these modes having important contributions from C=C and C=N stretching vibrations. DFT calculations suggest  $44$  and  $34 \text{ cm}^{-1}$  shifts in the most intense IR transitions, which are indeed calculated to have significant CN stretching components.

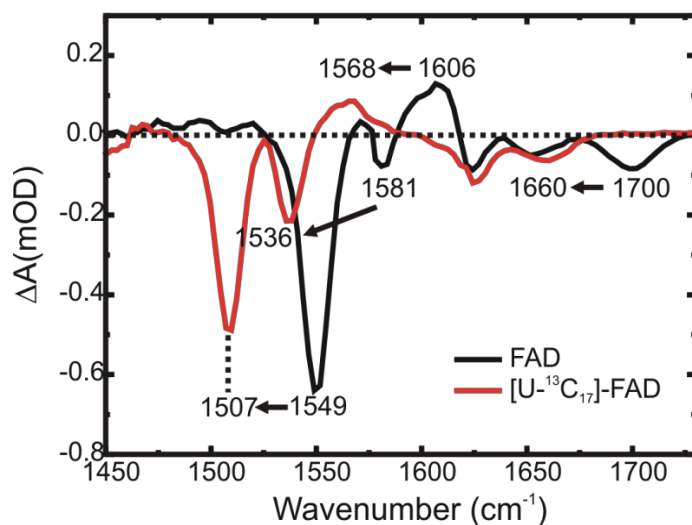


**Figure 2.13a: TRIR spectra of unlabeled FAD and [Uniform- $^{13}\text{C}_{17}$ ]-FAD in  $\text{D}_2\text{O}$ .**

TRIR spectra of  $3 \text{ mM}$  FAD (black) [Uniform- $^{13}\text{C}_{17}$ ]-FAD (red) in  $\text{pD } 8$  phosphate buffer recorded with a time delay of  $3 \text{ ps}$ .

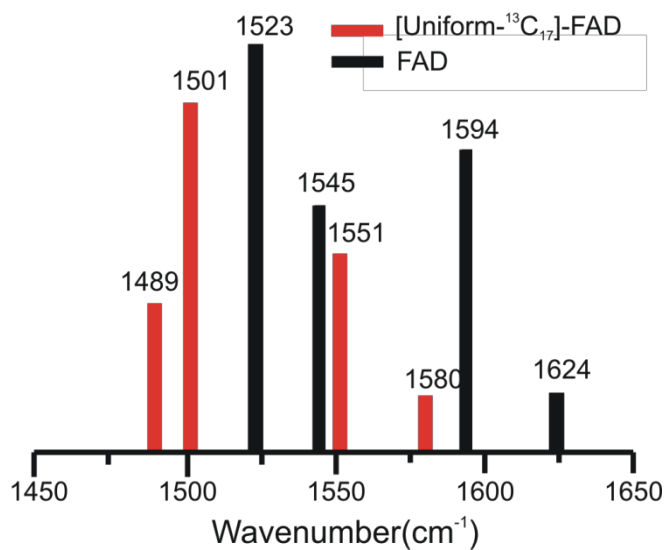
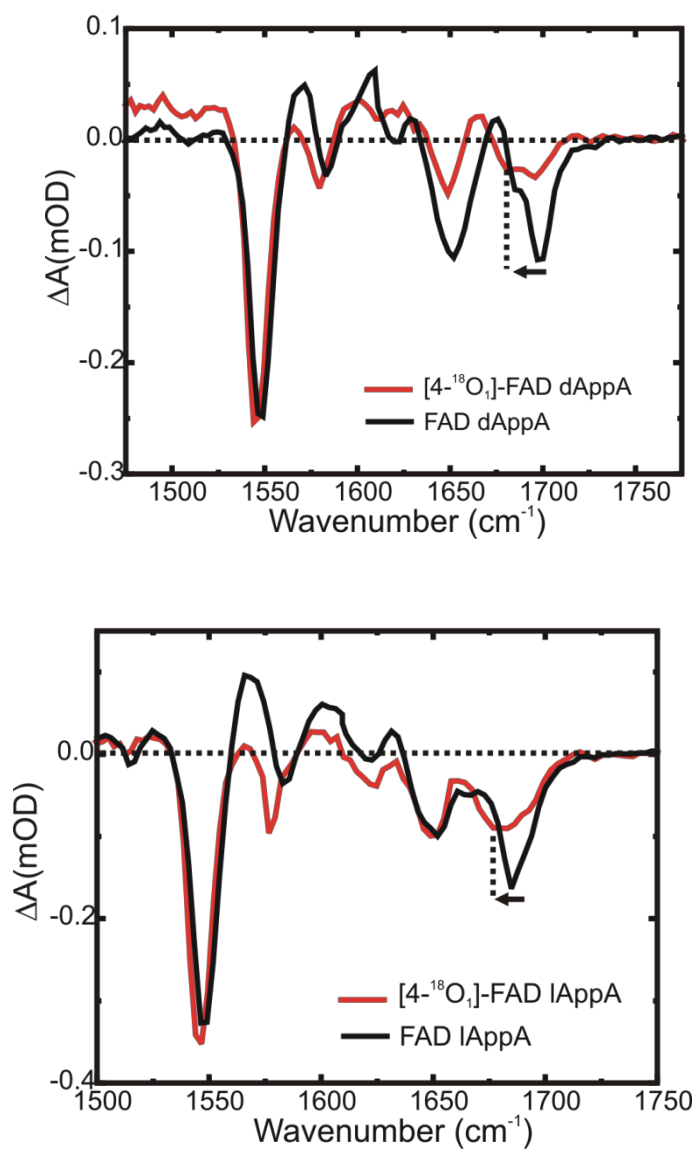


**Figure 2.13b: Calculated spectra of unlabeled FAD and [Uniform-<sup>13</sup>C<sub>17</sub>]-FAD.**

Calculated spectra of FAD (black) and [Uniform-<sup>13</sup>C<sub>17</sub>]-FAD (red) in pD 8 phosphate buffer.

### FAD Isotopes Bound to AppA<sub>BLUF</sub>:

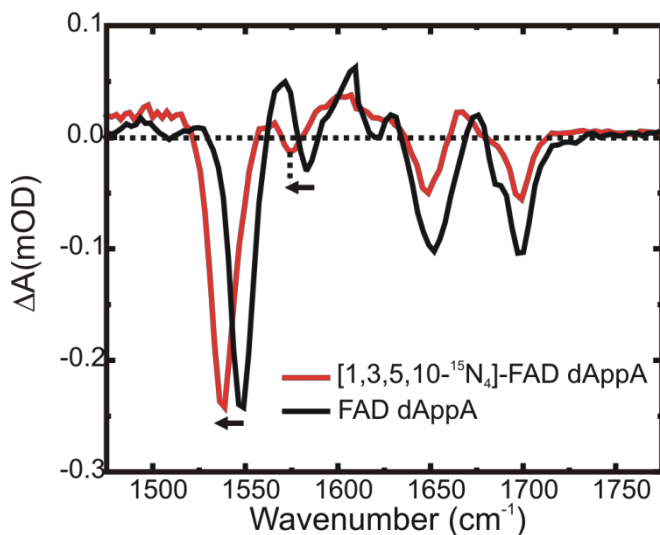
In **Figure 2.14a** TRIR spectra at a 3 ps time delay are shown for dAppA<sub>BLUF</sub> bound to FAD and [4-<sup>18</sup>O<sub>1</sub>]-FAD. The high frequency bleach at 1700 cm<sup>-1</sup> is partially shifted to 1680 cm<sup>-1</sup>. This change in peak position is consistent with 18 cm<sup>-1</sup> shift seen in the TRIR spectra of [4-<sup>18</sup>O<sub>1</sub>]-FAD in buffer. However, the carbonyl modes of the flavin are better resolved when bound to AppA<sub>BLUF</sub>. In addition, a transient that appears at 1672 cm<sup>-1</sup> which shifts to 1664 cm<sup>-1</sup> in the spectra of [4-<sup>18</sup>O<sub>1</sub>]-FAD bound to dAppA<sub>BLUF</sub>.



**Figure 2.14: TRIR spectra of unlabeled FAD and  $[4\text{-}^{18}\text{O}_1]\text{-FAD}$  bound to AppA.**

TRIR spectra of 3 mM FAD (black) and  $[4\text{-}^{18}\text{O}_1]\text{-FAD}$  (red) bound to dAppA (a) and lAppA (b) in pD 8 phosphate buffer recorded with a time delay of 3 ps.

The TRIR spectra of unlabeled FAD and  $[1,3,5,10\text{-}^{15}\text{N}_4]\text{-FAD}$  bound to  $\text{AppA}_{\text{BLUF}}$  are shown in **Figure 2.15**. There is a shift of the major bleach at  $1547\text{ cm}^{-1}$  to  $1536\text{ cm}^{-1}$  in both  $\text{dAppA}_{\text{BLUF}}$  and  $\text{lAppA}_{\text{BLUF}}$  when bound to  $[1,3,5,10\text{-}^{15}\text{N}_4]\text{-FAD}$ . In addition the bleach at  $1581\text{ cm}^{-1}$  shifts to  $1573\text{ cm}^{-1}$ . Both shifts are consistent with the TRIR spectra of solution phase data, although the shift is greater when  $[1,3,5,10\text{-}^{15}\text{N}_4]\text{-FAD}$  is bound to  $\text{AppA}_{\text{BLUF}}$  compared to the buffer solution (**Figure 2.11a**). The major bleach shifts by  $11\text{ cm}^{-1}$  when bound to the protein and  $8\text{ cm}^{-1}$  in solution and the less intense bleach at  $1581\text{ cm}^{-1}$  shifts by  $8\text{ cm}^{-1}$  as opposed to the  $3\text{ cm}^{-1}$  in solution. These differences between isotope shifts are quite small, but nonetheless unexpected. Previously we noted that the character of the flavin vibrational mode is somewhat dependent on the hydrogen bonding environment. This is particularly true for the carbonyl modes. We speculate that the different isotope shifts observed for FAD between buffer solution and bound in the protein reflect an environment sensitivity of the character of the CN/CC ring modes as well.



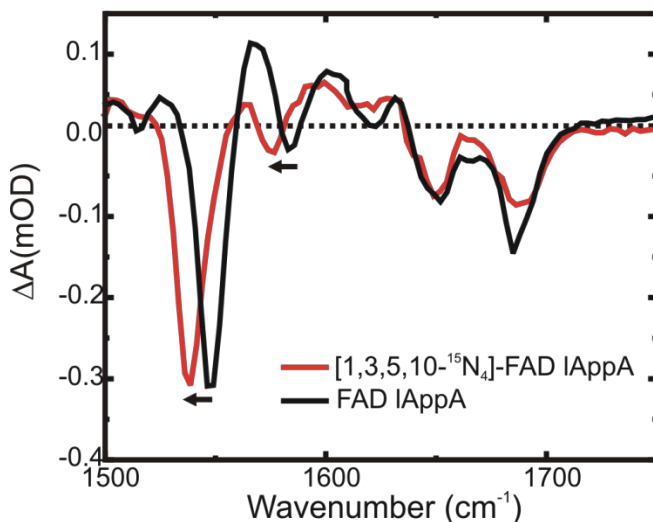


**Figure 2.15: TRIR spectra of unlabeled FAD and [1,3,5,10-<sup>15</sup>N<sub>4</sub>]-FAD bound to AppA.**

TRIR spectra of 3 mM FAD (black) and [1,3,5,10-<sup>15</sup>N<sub>4</sub>]-FAD (red) bound to dAppA (a) and lAppA (b) in pD 8 phosphate buffer recorded with a time delay of 3 ps.

**Figure 2.16** shows the TRIR spectra of unlabeled FAD and [xylene-<sup>13</sup>C<sub>8</sub>]-FAD bound to AppA<sub>BLUF</sub>. The spectra are consistent with those seen in buffer, with an enhanced signal at 1570 cm<sup>-1</sup> assigned to a ring mode with enhanced intensity. Again the spectra are somewhat better resolved than in buffer solution. The isotope shifts are consistent when between dAppA<sub>BLUF</sub> and lAppA<sub>BLUF</sub>, where three intense peaks appear between 1500 and 1600 cm<sup>-1</sup>. There is an appearance of a 1520 cm<sup>-1</sup> mode in addition to the large bleach which is now at 1552 cm<sup>-1</sup>. This is essentially as observed in solution (**Figure 2.12**) with the additional mode arising from an intensity enhancement resulting from the isotope shift. In addition, just as in the unbound isotope spectra of [xylene-<sup>13</sup>C<sub>8</sub>]-FAD, the carbonyl modes are not affected by isotopic substitution on the xylene ring.

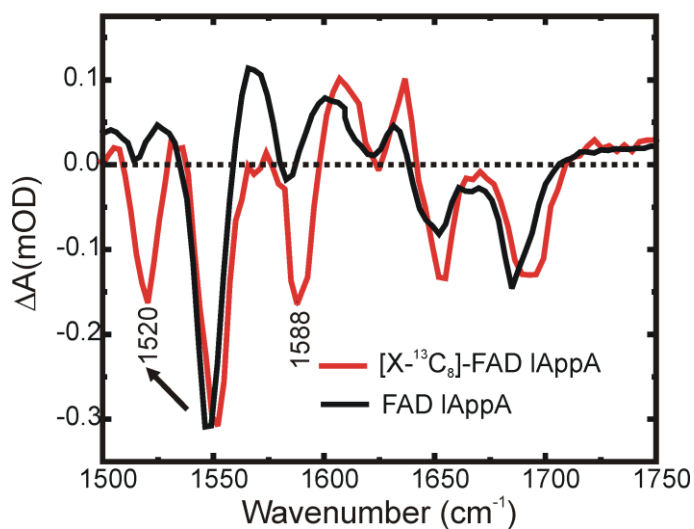
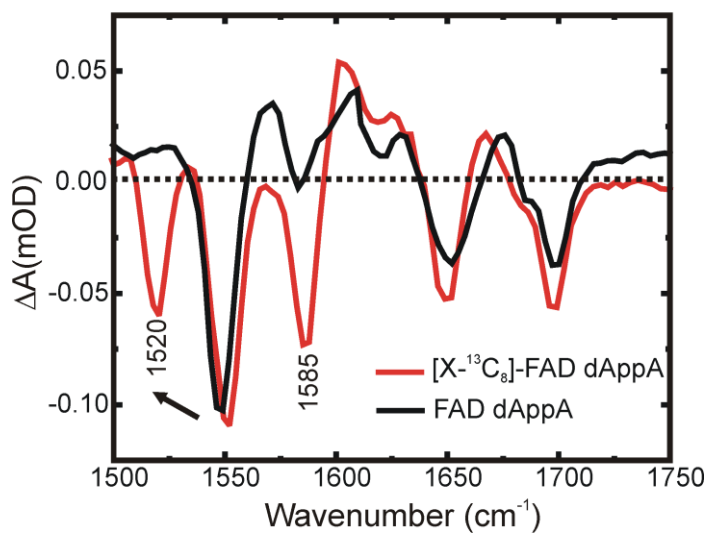


**Figure 2.16: TRIR spectra of unlabeled FAD and  $[X\text{ylene-}^{13}\text{C}_8]\text{-FAD}$  bound to AppA**

TRIR spectra of 3 mM FAD (black) and  $[X\text{ylene-}^{13}\text{C}_8]\text{-FAD}$  (red) bound to dAppA (a) and IAppA (b) in pD 8 phosphate buffer recorded with a time delay of 3 ps.



The TRIR spectra of [Uniform- $^{13}\text{C}_{17}$ ]-FAD and unlabeled FAD bound to AppA<sub>BLUF</sub> at a 3 ps time delay are shown in **Figure 2.17**. For both dAppA<sub>BLUF</sub> and lAppA<sub>BLUF</sub>, the intense bleach at 1549  $\text{cm}^{-1}$  shifts by 44  $\text{cm}^{-1}$  to 1505  $\text{cm}^{-1}$  and the 1582  $\text{cm}^{-1}$  bleach shifts to 1536  $\text{cm}^{-1}$ . These are consistent with the change in frequency seen upon labeling of flavin in solution (**Figure 2.13**). Other shifts are observed in the TRIR spectra of [Uniform- $^{13}\text{C}_{17}$ ]-FAD bound to AppA<sub>BLUF</sub> but are different for dAppA<sub>BLUF</sub> and lAppA<sub>BLUF</sub>, therefore the changes seen in isotope substitution will be discussed separately.

**Figure 2.17a** shows [Uniform- $^{13}\text{C}_{17}$ ]-FAD and unlabeled FAD bound to dAppA<sub>BLUF</sub>. The high frequency bleach at 1700  $\text{cm}^{-1}$  shifts by 30  $\text{cm}^{-1}$  to 1670  $\text{cm}^{-1}$ . The shift is smaller when [Uniform- $^{13}\text{C}_{17}$ ]-FAD is bound to dAppA<sub>BLUF</sub> compared to the buffer solution spectra (**Figure 2.13a**). The bleach shifts by 30  $\text{cm}^{-1}$  when bound to the protein and 40  $\text{cm}^{-1}$  in solution. This difference is attributed to the sensitivity of the carbonyl vibrational mode to the hydrogen bonding environment, as discussed previously (35). In addition, the 1650  $\text{cm}^{-1}$  mode shifts to lower frequency but because of the poor signal to noise in this region we are unable to determine the peak position upon labeling.

**Figure 2.17b** shows the spectra for [Uniform- $^{13}\text{C}_{17}$ ]-FAD bound to lAppA<sub>BLUF</sub> in comparison to unlabeled FAD. In these spectra, it is seen that the high (1682  $\text{cm}^{-1}$ ) and low (1650  $\text{cm}^{-1}$ ) frequency carbonyl modes shifts by 15  $\text{cm}^{-1}$  to 1667  $\text{cm}^{-1}$  and 26  $\text{cm}^{-1}$  to 1624  $\text{cm}^{-1}$  upon  $^{13}\text{C}$  labeling. This is smaller than the shift seen when [U- $^{13}\text{C}_{17}$ ]-FAD is bound to dAppA<sub>BLUF</sub> (30  $\text{cm}^{-1}$ ). This again reflects the high sensitivity of the carbonyl vibrational mode to the hydrogen bonding environment which is very different for the C4=O modes of d and lAppA<sub>BLUF</sub> due to a strengthening of hydrogen bonding upon formation of the lAppA from dAppA (20). Other shifts observed in the TRIR spectra of [Uniform- $^{13}\text{C}_{17}$ ]-FAD bound to

dAppA<sub>BLUF</sub> include the excited state transient at 1631/1603 cm<sup>-1</sup> that shifts by approximately 45 cm<sup>-1</sup> to 1585/1554 cm<sup>-1</sup>.

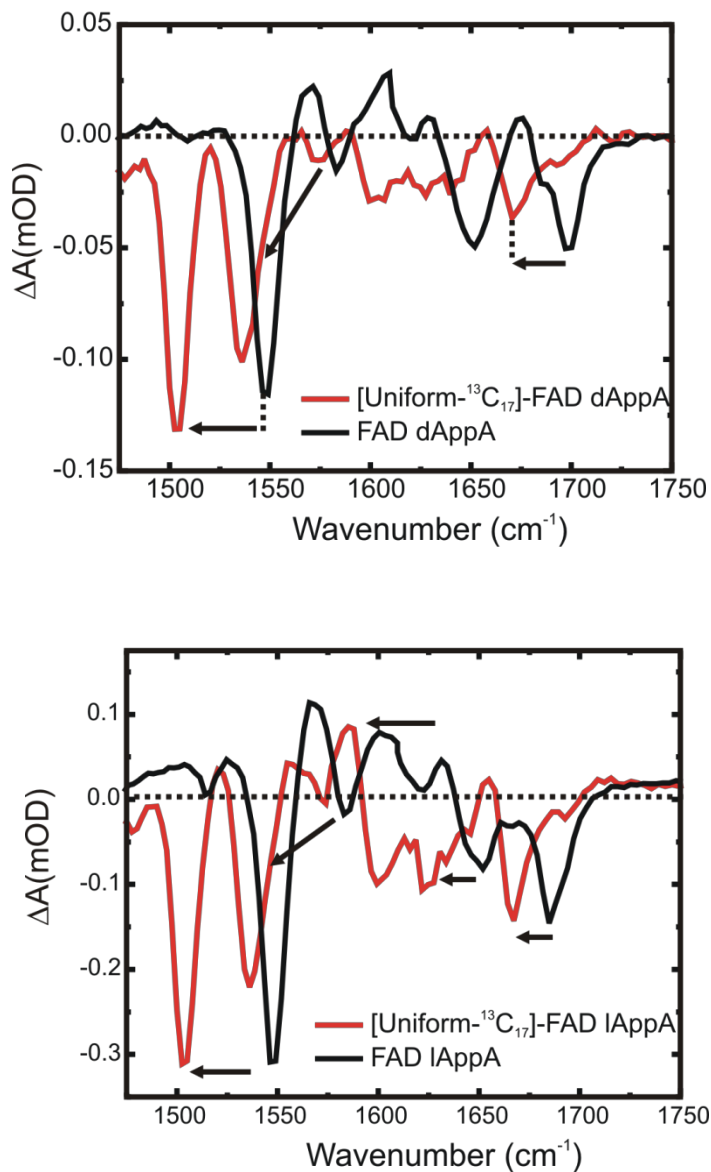


**Figure 2.17: TRIR spectra of unlabeled FAD and [Uniform-<sup>13</sup>C<sub>17</sub>]-FAD bound to AppA.**

TRIR spectra of 3 mM FAD (black) and [Uniform-<sup>13</sup>C<sub>17</sub>]-FAD (red) bound to dAppA (a) and lAppA (b) in pD 8 phosphate buffer recorded with a time delay of 3 ps.

**Table 2.2: Observed and calculated vibrational modes of FAD, [4-<sup>18</sup>O<sub>1</sub>]-FAD, [U-<sup>15</sup>N<sub>4</sub>]-FAD, [U-<sup>13</sup>C<sub>17</sub>]-FAD and [xylene-<sup>13</sup>C<sub>8</sub>]-FAD in D<sub>2</sub>O Buffer.**

FAD (D <sub>2</sub> O)		[4- <sup>18</sup> O <sub>1</sub> ]-FAD		[1,3,5,10- <sup>15</sup> N <sub>4</sub> ]-FAD		[Uniform- <sup>13</sup> C <sub>17</sub> ]-FAD		[Xylene- <sup>13</sup> C <sub>8</sub> ]-FAD	
Observed	Calculated	Observed	Calculated	Observed	Calculated	Observed	Calculated	Observed	Calculated
1549 cm <sup>-1</sup>	1523 cm <sup>-1</sup> C10 <sub>a</sub> N <sub>1</sub>	1549 cm <sup>-1</sup>	1522 cm <sup>-1</sup> C10 <sub>a</sub> N <sub>1</sub>	1541 cm <sup>-1</sup>	1515 cm <sup>-1</sup> C10 <sub>a</sub> N <sub>1</sub>	1509 cm <sup>-1</sup>	1489 cm <sup>-1</sup> C10 <sub>a</sub> N <sub>1</sub>	1525 cm <sup>-1</sup>	1494 cm <sup>-1</sup> C10 <sub>a</sub> N <sub>1</sub> , C <sub>4</sub> <sub>a</sub> N <sub>5</sub> asym
								1554 cm <sup>-1</sup>	1526 cm <sup>-1</sup> C10 <sub>a</sub> N <sub>1</sub>
1581 cm <sup>-1</sup>	1545 cm <sup>-1</sup> C <sub>4</sub> <sub>a</sub> N <sub>5</sub>	1583 cm <sup>-1</sup>	1541 cm <sup>-1</sup> C <sub>4</sub> <sub>a</sub> N <sub>5</sub>	1578 cm <sup>-1</sup>	1536 cm <sup>-1</sup> C <sub>4</sub> <sub>a</sub> N <sub>5</sub>	1535 cm <sup>-1</sup>	1501 cm <sup>-1</sup> C <sub>4</sub> <sub>a</sub> N <sub>5</sub>	1586 cm <sup>-1</sup>	1564 cm <sup>-1</sup> C <sub>4</sub> <sub>a</sub> N <sub>5</sub>
1651 cm <sup>-1</sup>	1594 cm <sup>-1</sup> C <sub>2</sub> =O, C <sub>4</sub> =O asym +N <sub>3</sub> wag	1648 cm <sup>-1</sup>	1582 cm <sup>-1</sup> C <sub>2</sub> =O, C <sub>4</sub> =O asym +N <sub>3</sub> wag	1651 cm <sup>-1</sup>	1591 cm <sup>-1</sup> C <sub>2</sub> =O, C <sub>4</sub> =O asym +N <sub>3</sub> wag	1609 cm <sup>-1</sup>	1551 cm <sup>-1</sup> C <sub>2</sub> =O, C <sub>4</sub> =O asym +N <sub>3</sub> wag	1652 cm <sup>-1</sup>	1595 cm <sup>-1</sup> C <sub>2</sub> =O, C <sub>4</sub> =O asym +N <sub>3</sub> wag
1699 cm <sup>-1</sup>	1624 cm <sup>-1</sup> C <sub>4</sub> =O, C <sub>2</sub> =O sym +N <sub>3</sub> wag	1685 cm <sup>-1</sup>	1614 cm <sup>-1</sup> C <sub>4</sub> =O, C <sub>2</sub> =O sym +N <sub>3</sub> wag	1700 cm <sup>-1</sup>	1622 cm <sup>-1</sup> C <sub>4</sub> =O, C <sub>2</sub> =O sym +N <sub>3</sub> wag	1660 cm <sup>-1</sup>	1580 cm <sup>-1</sup> C <sub>4</sub> =O, C <sub>2</sub> =O sym +N <sub>3</sub> wag	1700 cm <sup>-1</sup>	1625 cm <sup>-1</sup> C <sub>4</sub> =O, C <sub>2</sub> =O sym +N <sub>3</sub> wag

**Table 2.2: Observed and calculated vibrational modes of FAD, [4-<sup>18</sup>O<sub>1</sub>]-FAD, [U-<sup>15</sup>N<sub>4</sub>]-FAD, [U-<sup>13</sup>C<sub>17</sub>]-FAD and [xylene-<sup>13</sup>C<sub>8</sub>]-FAD in D<sub>2</sub>O Buffer.**

**Legend:** Observed frequencies are experimental TRIR measurements. Calculated frequencies were measured by Gaussian 03 using the B3LYP method and 6-31G basis set.

## D. Conclusions

FAD is an important molecule in biology and is used for a variety of functions. In AppA, FAD is used as the chromophore responsible for detecting and responding to the absorption of 450 nm light. Time resolved infrared spectroscopy (TRIR) is a valuable tool to study AppA's mechanism because this technique allows one to observe small scale structural changes that occur in a complex system on a fast timescale because the formation of the excited state is very rapid. In order to further understand where these changes are taking place the use of specific isotope labeling has been used to assign various vibrational modes in the time resolved spectra. We have measured both unbound and bound FAD isotopes and compared the experimental results with DFT calculations. The assignments found experimentally and theoretically are in good agreement with each other and what has been published previously.

The carbonyl modes of the isoalloxazine ring can be used as tools for probing structural dynamics of the primary photoprocesses of AppA. The frequency and character of these modes is a sensitive function of their environment. The time resolved IR data for FAD and riboflavin in solution and bound to AppA are similar in peak position and intensity. This result confirms the assumptions made from steady state experiments that riboflavin is a good model for FAD in the BLUF domain of AppA. Based on this information, we are confident that both riboflavin and FAD can be used interchangeably as models to study flavin excited state dynamics of AppA. Isotope labeling of FAD and riboflavin has enabled the assignment of various ground and excited state modes seen in the TRIR spectra of AppA<sub>BLUF</sub>. Specifically the high frequency and low frequency carbonyl modes are confidently assigned as mainly C4=O and C2=O localized modes, respectively. However, isotopic exchange and DFT calculations showed that these modes have significant mixed character which is medium dependent, in agreement with earlier studies. In

addition, the  $1660 - 1670 \text{ cm}^{-1}$  transient absorption previously reported as a photoactive marker has been designated a protein-chromophore band based on the small shift seen upon isotope labeling. The next chapter discusses methods to isotopically label the protein in order to ensure greater confidence to the assignment of this marker vibrational mode and new mutants that have been prepared to modify the H-bond configuration around the chromophore.

## E. References

1. Kao, Y. T., Saxena, C., He, T. F., Guo, L., Wang, L., Sancar, A., and Zhong, D. (2008) Ultrafast dynamics of flavins in five redox states, *J Am Chem Soc* 130, 13132-13139.
2. Massey, V. (2000) The chemical and biological versatility of riboflavin, *Biochem Soc Trans* 28, 283-296.
3. Aigrain, L., Pompon, D., and Truan, G. (2011) Role of the interface between the FMN and FAD domains in the control of redox potential and electronic transfer of NADPH-cytochrome P450 reductase, *Biochem J* 435, 197-206.
4. Hines, R. N., Cashman, J. R., Philpot, R. M., Williams, D. E., and Ziegler, D. M. (1994) The mammalian flavin-containing monooxygenases: molecular characterization and regulation of expression, *Toxicol Appl Pharmacol* 125, 1-6.
5. Hecht, H. J., Kalisz, H. M., Hendle, J., Schmid, R. D., and Schomburg, D. (1993) Crystal structure of glucose oxidase from *Aspergillus niger* refined at 2.3 Å resolution, *J Mol Biol* 229, 153-172.
6. Rockwell, N. C., Su, Y. S., and Lagarias, J. C. (2006) Phytochrome structure and signaling mechanisms, *Annu. Rev. Plant Biol.* 57, 837-858.
7. Filipek, S., Stenkamp, R. E., Teller, D. C., and Palczewski, K. (2003) G protein-coupled receptor rhodopsin: a prospectus, *Annu Rev Physiol* 65, 851-879.
8. Kort, R., Hoff, W. D., Van West, M., Kroon, A. R., Hoffer, S. M., Vlieg, K. H., Crielaand, W., Van Beeumen, J. J., and Hellingwerf, K. J. (1996) The xanthopsins: a new family of eubacterial blue-light photoreceptors, *Embo J.* 15, 3209-3218.
9. Losi, A. (2004) The bacterial counterparts of plant phototropins, *Photochem Photobiol Sci* 3, 566-574.

10. Briggs, W. R., Christie, J. M., and Salomon, M. (2001) Phototropins: a new family of flavin-binding blue light receptors in plants, *Antioxid Redox Signal* 3, 775-788.
11. Anderson, S., Dragnea, V., Masuda, S., Ybe, J., Moffat, K., and Bauer, C. (2005) Structure of a novel photoreceptor, the BLUF domain of AppA from *Rhodobacter sphaeroides*, *Biochemistry* 44, 7998-8005.
12. Essen, L. O. (2006) Photolyases and cryptochromes: common mechanisms of DNA repair and light-driven signaling?, *Curr Opin Struct Biol* 16, 51-59.
13. Gomelsky, M., and Klug, G. (2002) BLUF: a novel FAD-binding domain involved in sensory transduction in microorganisms, *Trends Biochem Sci* 27, 497-500.
14. Losi, A. (2007) Flavin-based Blue-Light photosensors: a photobiophysics update, *Photochem Photobiol* 83, 1283-1300.
15. van der Horst, M. A., and Hellingwerf, K. J. (2004) Photoreceptor proteins, "star actors of modern times": a review of the functional dynamics in the structure of representative members of six different photoreceptor families, *Acc Chem Res* 37, 13-20.
16. Stelling, A. L., Ronayne, K. L., Nappa, J., Tonge, P. J., and Meech, S. R. (2007) Ultrafast structural dynamics in BLUF domains: transient infrared spectroscopy of AppA and its mutants, *J Am Chem Soc* 129, 15556-15564.
17. Laan, W., van der Horst, M. A., van Stokkum, I. H., and Hellingwerf, K. J. (2003) Initial characterization of the primary photochemistry of AppA, a blue-light-using flavin adenine dinucleotide-domain containing transcriptional antirepressor protein from *Rhodobacter sphaeroides*: a key role for reversible intramolecular proton transfer from the flavin adenine dinucleotide chromophore to a conserved tyrosine?, *Photochem Photobiol* 78, 290-297.

18. Greetham, G. M., Burgos, P., Cao, Q., Clark, I. P., Codd, P. S., Farrow, R. C., George, M. W., Kogimtzis, M., Matousek, P., Parker, A. W., Pollard, M. R., Robinson, D. A., Xin, Z. J., and Towrie, M. (2010) ULTRA: A Unique Instrument for Time-Resolved Spectroscopy, *Appl Spectrosc* 64, 1311-1319.
19. Scott, A. P., and Radom, L. (1996) Harmonic vibrational frequencies: An evaluation of Hartree-Fock, Moller-Plesset, quadratic configuration interaction, density functional theory, and semiempirical scale factors, *J Phys Chem-Us* 100, 16502-16513.
20. Unno, M., Sano, R., Masuda, S., Ono, T. A., and Yamauchi, S. (2005) Light-induced structural changes in the active site of the BLUF domain in AppA by Raman spectroscopy, *J Phys Chem B* 109, 12620-12626.
21. Hazekawa, I., Nishina, Y., Sato, K., Shichiri, M., Miura, R., and Shiga, K. (1997) A Raman study on the C(4)=O stretching mode of flavins in flavoenzymes: hydrogen bonding at the C(4)=O moiety, *J Biochem* 121, 1147-1154.
22. Copeland, R. A., and Spiro, T. G. (1986) Ultraviolet Resonance Raman-Spectroscopy of Flavin Mononucleotide and Flavin Adenine-Dinucleotide, *J Phys Chem-Us* 90, 6648-6654.
23. Abe, M., and Kyogoku, Y. (1987) Vibrational Analysis of Flavin Derivatives - Normal Coordinate Treatments of Lumiflavin, *Spectrochim Acta A* 43, 1027-1037.
24. Wolf, M. M. N., Schumann, C., Gross, R., Domratcheva, T., and Diller, R. (2008) Ultrafast Infrared Spectroscopy of Riboflavin: Dynamics, Electronic Structure, and Vibrational Mode Analysis, *J Phys Chem B* 112, 13424-13432.
25. Alexandre, M. T. A., van Grondelle, R., Hellingwerf, K. J., and Kennis, J. T. M. (2009) Conformational Heterogeneity and Propagation of Structural Changes in the LOV2/J



- alpha Domain from *Avena sativa* Phototropin 1 as Recorded by Temperature-Dependent FTIR Spectroscopy, *Biophysical Journal* 97, 238-247.
26. Kondo, M., Nappa, J., Ronayne, K. L., Stelling, A. L., Tonge, P. J., and Meech, S. R. (2006) Ultrafast vibrational spectroscopy of the flavin chromophore, *J Phys Chem B* 110, 20107-20110.
  27. Masuda, S., Hasegawa, K., and Ono, T. A. (2005) Adenosine diphosphate moiety does not participate in structural changes for the signaling state in the sensor of blue-light using FAD domain of AppA, *FEBS Lett.* 579, 4329-4332.
  28. Li, G., and Glusac, K. D. (2009) The role of adenine in fast excited-state deactivation of FAD: a femtosecond mid-IR transient absorption study, *J Phys Chem B* 113, 9059-9061.
  29. Kim, M. and Carey, P.R. (1993) Observation of a carbonyl feature for riboflavin bound to riboflavin-binding protein in the red-excited raman spectrum, *J Am Chem Soc* 115, 7015–7016.
  30. Laan, W., van der Horst, M. A., van Stokkum, I. H., and Hellingwerf, K. J. (2003) Initial characterization of the primary photochemistry of AppA, a blue-light-using flavin adenine dinucleotide-domain containing transcriptional antirepressor protein from *Rhodobacter sphaeroides*: a key role for reversible intramolecular proton transfer from the flavin adenine dinucleotide chromophore to a conserved tyrosine?, *Photochem. Photobiol.* 78, 290-297.
  31. Alexandre, M. T., Domratcheva, T., Bonetti, C., van Wilderen, L. J., van Grondelle, R., Groot, M. L., Hellingwerf, K. J., and Kennis, J. T. (2009) Primary reactions of the LOV2 domain of phototropin studied with ultrafast mid-infrared spectroscopy and quantum chemistry, *Biophys J* 97, 227-237.

32. Gauden, M., Yeremenko, S., Laan, W., van Stokkum, I. H., Ihalainen, J. A., van Grondelle, R., Hellingwerf, K. J., and Kennis, J. T. (2005) Photocycle of the flavin-binding photoreceptor AppA, a bacterial transcriptional antirepressor of photosynthesis genes, *Biochemistry* 44, 3653-3662.
33. Haigney, A., Lukacs, A., Zhao, R. K., Stelling, A. L., Brust, R., Kim, R. R., Kondo, M., Clark, I., Towrie, M., Greetham, G. M., Illarionov, B., Bacher, A., Romisch-Margl, W., Fischer, M., Meech, S. R., and Tonge, P. J. (2011) Ultrafast infrared spectroscopy of an isotope-labeled photoactivatable flavoprotein, *Biochemistry* 50, 1321-1328.
34. Wolf, M. M., Zimmermann, H., Diller, R., and Domratcheva, T. (2011) Vibrational Mode Analysis of Isotope-Labeled Electronically Excited Riboflavin, *J Phys Chem B*.
35. Unno, M., Kumauchi, M., Sasaki, J., Tokunaga, F., and Yamauchi, S. (2002) Resonance Raman spectroscopy and quantum chemical calculations reveal structural changes in the active site of photoactive yellow protein, *Biochemistry* 41, 5668-5674.

## Chapter 3

# Reorganization of the Hydrogen Bonding Network Surrounding the Flavin Chromophore of AppA

### A. Introduction

Various experimental methods, such as NMR, X-ray crystallography, electronic and infrared spectroscopy have previously shown the AppA BLUF domain requires residues Q63 and Y21 for photoactivity. Additionally, residue W104 was also determined to play a significant role in stabilization of lAppA (W104 mutants exhibit a faster light to dark state recovery). This chapter discusses several structurally conservative AppA mutants that have been generated in order to alter the hydrogen bonding pattern of the flavin chromophore with neighboring protein residues.

### B. Materials and Methods

#### B.1. Overexpression and Purification of AppA and its Mutants:

##### **Preparation of DNA constructs for Q63E, W104M and Y21W AppA<sub>BLUF</sub>:**

AppA mutants were constructed by site directed mutagenesis using Pfu Turbo (Stratagene). Primer sequences for Q63E 5' GGC GTC TTC TTC GAG TGG CTC GAA GGC CGC 3' (Forward) and 5' GCG GCC TTC GAG CCA CTC GAA GAA GAC GCC 3' (Reverse); primer sequences for W104M were 5' CGC CGC TTT GCG GGA ATG CAC ATG CAG CTC TCC 3'(Forward) and 5' GGA GAG CTG CAT GTG CAT TCC CGC AAA GCG GCG 3' (Reverse). All constructs were verified by DNA sequencing.

##### **Methods for Cell Growth and Protein Overexpression:**

The gene encoding the AppA BLUF domain (residues 5-125 AppA<sub>BLUF</sub>) was cloned into a pet15b vector (Novagen) so that the protein is expressed with an N-terminal His-tag. Expression and purification was performed using a modified version the protocol published by Stelling *et. al.* (1).

Protein expression was performed by transforming the plasmid into BL21DE3 *E. coli* cells and then picking a single colony to inoculate 10 mL cultures of Luria Broth (LB) media containing 0.5 mM ampicillin at 37°C at 250 RPM. These cultures were used to infect 1 L of LB/ampicillin media, in 4 L flasks, which was grown to an OD<sub>600</sub> of approximately 1.2 at 30°C for 5 hrs. The temperature was then decreased to 18°C for 30 minutes followed by addition of 0.8 mM isopropyl β-D-1-thiogalactopyranoside (IPTG) to induce protein growth overnight (16 hrs) in the dark.

#### **Protein Purification:**

All purification processes were then performed in the dark. The cells were harvested by centrifugation at 5,000 RPM at 4°C and stored at -20°C. The cell pellet was then resuspended in 40 mL of lysis buffer (10 mM NaCl, 50 mM NaH<sub>2</sub>PO<sub>4</sub> at pH 8) to which 200 μL of a protease inhibitor, 50 mM phenylmethanesulphonylfluoride (PMSF), and 14 μL of β-mercaptoethanol, a disulfide bond reducing agent, was added. The cells were then lysed using sonication and cell debris was removed using centrifugation (33 K for 90 min) and the supernatant was incubated with 1 mL of a 10 mg/mL solution of flavin for 45 min on ice in the dark. The protein was purified using Ni-NTA chromatography (Qiagen) with 10 mM NaCl, 50 mM NaH<sub>2</sub>PO<sub>4</sub>, pH 8 wash buffer. The bound protein is then washed with increasing amounts of imidazole in buffer and finally eluted with 250 mM imidazole. The fractions collected are dialyzed in 10 mM NaCl, 50 mM NaH<sub>2</sub>PO<sub>4</sub>, pH 8 dialysis buffer overnight. The purity of the protein was determined using

SDS-PAGE electrophoresis. These proteins were then concentrated to appropriate concentrations and stored at 4°C.

Uniform  $^{13}\text{C}$  protein labeling was performed by expressing AppA<sub>BLUF</sub> in BL21(DE3) *E. coli* cells that were grown on minimal media containing [U- $^{13}\text{C}_6$ ]-D-glucose as the sole carbon source. Single colonies containing plasmids for either wild-type or Q63E AppA<sub>BLUF</sub> that had been grown on LB/Amp plates were streaked on M9 minimal media/glucose/ampicillin plates containing 200 mg/mL ampicillin, 5 mg/mL glucose. This process is thought to acclimatize the cells to growth in minimal media, therefore leading to higher cell densities than if the cells had been transferred directly from LB media. A single colony from an M9 plate was used to inoculate 500 mL of M9/ampicillin minimal media in a 4 L flask that contained 4.0 grams of glucose (dissolved in 10 mL of water and filtered through a 0.22  $\mu\text{m}$  filter to sterilize) and 5 mL of 100X mem vitamins (added after autoclaving). The cells were grown to an OD<sub>600</sub> of approximately 0.5 at 30°C which took about 24 hrs. The cells were then pelleted and resuspended in fresh media with U-6- $^{13}\text{C}$  glucose replacing the unlabeled glucose after which they were incubated for 30 min at 18°C. After 30 min 0.8 mM IPTG was added to induce protein expression, and the culture was shaken in the dark for 24 hrs to maximize the yield of protein. [U- $^{13}\text{C}$ ]-AppA<sub>BLUF</sub> was then purified using the protocol described above.

## B.2. Photoconversions:

Steady state absorption spectra were recorded using a Cary 100 Bio (Vairian) spectrometer at 25 °C. The protein concentration was roughly 50  $\mu\text{M}$  in 10 mM NaCl, 50 mM  $\text{NaH}_2\text{PO}_4$  pH 8 buffer. All photoconversions were done using a hand held UV illuminator with roughly 20 mW of 365 nm light for times ranging from 1 to 15 minutes.

### B.3. Steady State Raman Spectra:

Steady state Raman spectra were recorded using a model 890 Ti:sapphire laser (Coherent, Santa Clara, CA), pumped by an Innova 308C argon ion laser (Coherent) which provided 550 mW of 752 nm infrared excitation. The measurements were made by focusing the beam on the base of a quartz cuvette containing a solution of protein and collecting at 90° geometry. The Rayleigh scattered light was removed with a super notch plus holographic filter (Kaiser Optical Systems, Inc.). The beam was focused on the 2 mm by 2 mm quartz cell containing 70  $\mu$ L of 500 mM protein and collecting data for 300 accumulations with an exposure time of 2 seconds. Scans of dialysis buffer were taken without changing the optical setup directly after protein data was recorded with the same number of accumulations and exposure time. The buffer scan was then subtracted from the protein scan giving a protein spectrum which was then calibrated using cyclohexanone as a standard. The resolution of the system is 8  $\text{cm}^{-1}$ .

### B.4. Time Resolved Fluorescence Measurements:

Ultrafast fluorescence spectra were measured using a fluorescence up-conversion apparatus at the University of East Anglia. The 800 mW 820 nm output of a titanium sapphire laser was compressed to a pulse width of < 20 fs and focussed into a thin BBO crystal to generate the second harmonic at 410 nm. The second harmonic was sent via a pair of chirped mirrors to focus into the sample contained in a 1 mm cuvette with the excitation power 5 mW. The fluorescence was detected by a reflective microscope objective and imaged onto the surface of a second BBO crystal. The purpose of the chirped mirrors is to compensate for dispersion in the optics and therefore ensure the shortest pulse at the sample. The residual 820 nm gating pulse was sent via a second pair of chirped mirrors to a delay line which controls the delay between

excitation and gate pulses with an accuracy of better than 0.2 fs. The pulse is sent via a half wave plate which sets the polarisation to  $54.7^\circ$  to eliminate any contribution to the measured fluorescence decay from rotational reorientation. The gate pulse was then mixed with the fluorescence in the BBO crystal to generate the sum frequency signal in the ultraviolet. The intensity in the UV signal is linearly related to the instantaneous intensity of the fluorescence. By adjusting the time of the gate pulse the fluorescence decay can be mapped out. The UV frequency is selected by angle tuning the BBO crystal and a monochromator. This gives the fluorescence decay at a specific wavelength. The signal was detected by a photomultiplier tube and a photon counter.

The time resolution of the spectrometer was determined by up-converting the Raman signal scattered from the pure solvent and fitting the result to a Gaussian function. This measurement provides the response function for deconvolution analysis of the up-converted fluorescence. It was measured as having a width of 48 fs under optimum condition, but for the measurements described here, where the fluorescence had to be isolated from scattered excitation light by a glass filter, was measured as 70 fs.

## B.5. Time Resolved Infrared Measurements:

Ultrafast transient IR measurements on dark adapted wild type AppA (dAppA), light adapted AppA (lAppA) and the Q63E mutant were performed using an ultrastable 10 kHz titanium sapphire amplified system pumping OPAs for IR generation. The samples were excited with ~200 nJ linearly polarized pulses at 400 nm. In order to avoid degradation of the protein and the photoconversion of dAppA a raster sample mover was used in conjunction with a flow cell.

Ultrafast fluorescence decays were measured using fluorescence up-conversion with sub 70 fs resolution, exciting the samples with a 5 mW 100 MHz pulse train at 410 nm.

### B.6. Transient Absorption Spectroscopy:

Ultrafast transient absorption measurements were performed using a Clark-MXR 1000 regenerative amplifier providing  $\sim 350 \mu\text{J}$  pulses centered at 800 nm at a repetition rate of 1 kHz. The output of the amplifier was split in two (10/90 %) where the pulse with the smaller energy was used for white light continuum generation in a  $\text{CaF}_2$  crystal for use as the probe. The higher intensity pulse was frequency doubled to 400 nm and attenuated to  $\sim 200\text{-}400 \text{ nJ}$ . The relative angle between the pump and the probe beams was set to the magic angle ( $54.7^\circ$ ) and sample photodegradation was minimized using a Lissajous scanner and peristaltic pump. Absorption changes were measured with an Andor CCD and data collection was performed with Labview data acquisition software.



## C. Results and Discussion

### C.1. Photoexcitation of the Blue Light Using FAD Photoreceptor AppA Results in Ultrafast Changes to the Protein Matrix (Q63E AppA<sub>BLUF</sub>):

Q63 is a critical component of the hydrogen bonding network that surrounds the flavin chromophore in AppA and which provides a mechanism for communication between the flavin chromophore and the protein matrix. Photoexcitation of the flavin results in a modulation in the protein-flavin interactions that are mediated by this hydrogen bond network and that lead ultimately to the light activated state of the protein (**Figure 3.1**). The importance of Q63 was previously shown through the Q63L mutation that renders the protein photoinactive (2). More recently Dragnea et al (3) characterized the Q63E AppA mutant and proposed that this amino acid substitution locks the protein in the light activated state based primarily on HSQC spectra together with the observation that Q63E AppA was unable to bind the PpsR transcriptional repressor. In agreement with this observation we observe that the vibrational spectrum of FAD

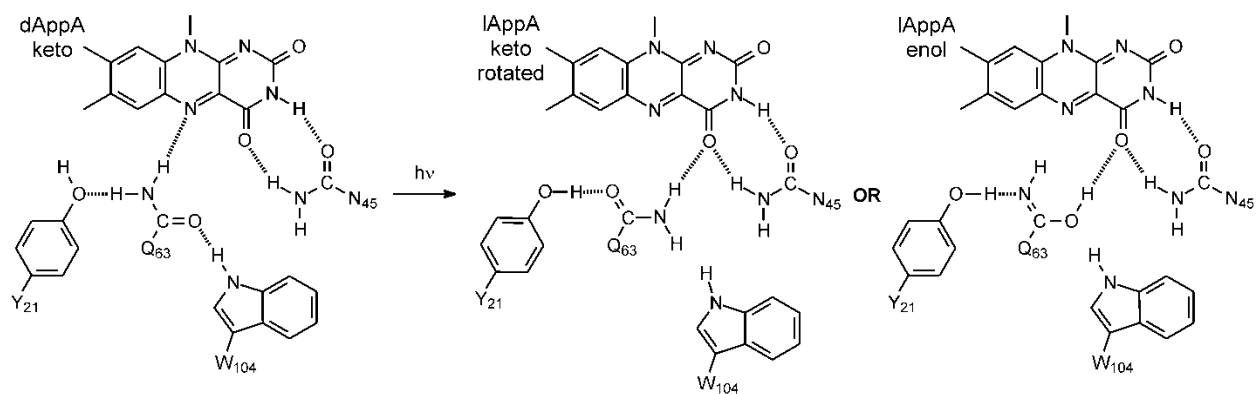


**Figure 3.1. Hydrogen bonding network in dAppA and lAppA.**

Hydrogen bonds are shown as dashed lines and formation of lAppA is based on a proposed keto-enol tautomerism of Q63 leading to formation a new hydrogen bond with the flavin C4=O.

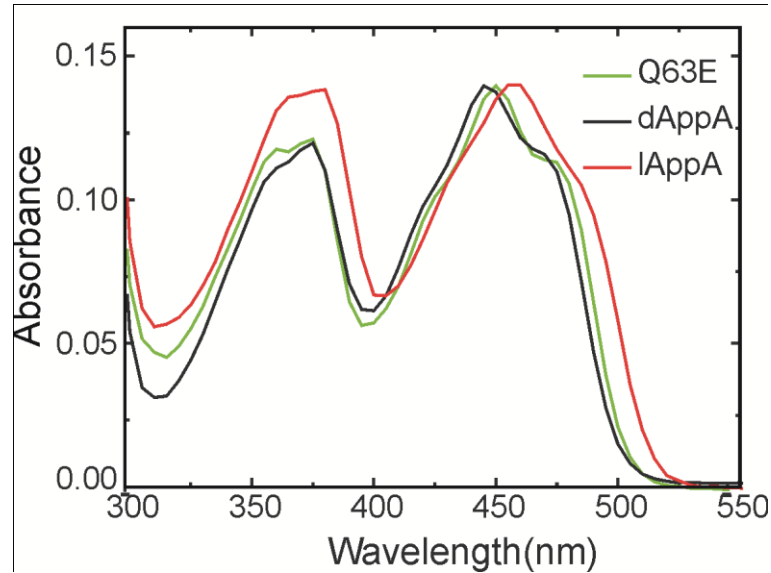


**Figure 3.2. Absorption spectra of wild-type d and lAppA<sub>BLUF</sub> and Q63E AppA<sub>BLUF</sub>.**

Steady state absorption spectra of dAppA<sub>BLUF</sub> (black), lAppA<sub>BLUF</sub> (red) and Q63E AppA<sub>BLUF</sub> (green) bound to FAD. Protein concentration was 20  $\mu$ M in phosphate buffer, pH 8.

in Q63E AppA<sub>BLUF</sub> resembles that of light activated wild-type AppA<sub>BLUF</sub>. In addition we report a vibrational band assigned to the Q63E carboxylic acid side chain that alters hydrogen bond strength within 1 ps of light absorption, indicating that the protein matrix can respond instantaneously to photoexcitation.

In order to evaluate the role of Q63 in the AppA photocycle, we used site-directed mutagenesis to replace Q63 with a glutamate in the AppA5-125 BLUF domain construct (Q63E AppA<sub>BLUF</sub>). The UV-visible absorption spectrum of this AppA mutant is shown in **Figure 3.2** where it can be seen that  $\lambda_{\max}$  for Q63E AppA<sub>BLUF</sub> is red-shifted  $\sim$ 3 nm compared to dAppA<sub>BLUF</sub> from 447 to 450 nm. Based on steady state absorption measurements, this mutant was determined to be photoinactive because the  $\lambda_{\max}$  at 450 nm does not shift when irradiated with 400 nm light as in the wild type protein. As reported previously (3), this change in  $\lambda_{\max}$  is  $\sim$ 25%

of the red-shift observed for wild-type AppA<sub>BLUF</sub> upon light activation (**Figure 3.2**; 447 to 458 nm). To explore changes in the ground state structure of the flavin caused by the Q to E mutation, we used steady state Raman spectroscopy to study Q63E AppA<sub>BLUF</sub>. In the Raman spectrum of dAppA<sub>BLUF</sub>, a weak band can be observed at 1710 cm<sup>-1</sup> which shifts to ~1690 cm<sup>-1</sup> upon irradiation (**Figure 3.3**). This band has previously been assigned to a mode arising from the C4 flavin carbonyl, and the observed ~20 cm<sup>-1</sup> red shift in this band is indicative of a strengthening of hydrogen-bond(s) to the C4=O group caused by light activation (4). In Q63E AppA<sub>BLUF</sub> this weak band appears at about 1695 cm<sup>-1</sup> (**Figure 3.3**). Thus, the absorption and Raman data indicate that the environment of the flavin in Q63E AppA<sub>BLUF</sub> is intermediate between that experienced by the chromophore in d and lAppA<sub>BLUF</sub>.

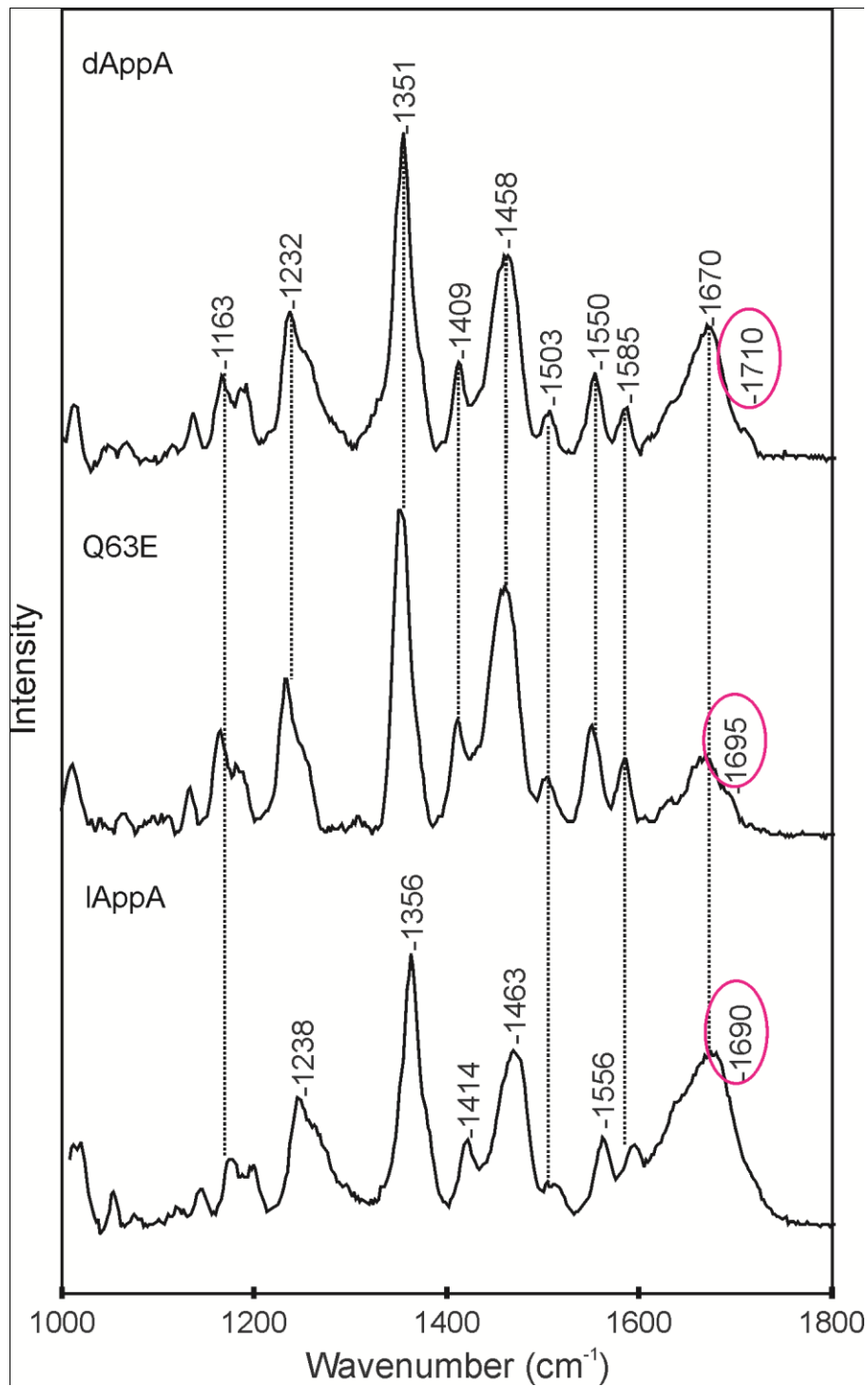


**Figure 3.3. Raman spectra of wild-type d and lAppA<sub>BLUF</sub> and Q63E AppA<sub>BLUF</sub>.**

Raman spectra of dAppA<sub>BLUF</sub> (top), lAppA<sub>BLUF</sub> (bottom) and Q63E<sub>BLUF</sub> AppA (middle) bound to FAD. Protein concentration was 1.5 mM in phosphate buffer, pD 8.

Steady state Raman spectroscopy provides information about the ground state structure but does not provide insight into any potential structural changes caused by photoexcitation. In order to investigate changes that occur rapidly upon absorption of 400 nm light we used ultrafast time-resolved infrared (TRIR) spectroscopy to gain further insight into the structure of Q63E AppA<sub>BLUF</sub>. The TRIR spectrum of Q63E AppA<sub>BLUF</sub> acquired 3 ps following photoexcitation is shown in **Figure 3.4** together with the corresponding spectra of d and lAppA<sub>BLUF</sub>. The most striking feature is the new bleach/transient absorption observed at 1724/1700 cm<sup>-1</sup> only in the Q63E mutant. We consider this new mode in detail below. In contrast, the low frequency range of the Q63E AppA<sub>BLUF</sub> TRIR spectrum is very similar to that of d and lAppA<sub>BLUF</sub> and is characterized by the major bleaches of the FAD chromophore at 1547 cm<sup>-1</sup> and 1581cm<sup>-1</sup>. Important differences exist however between the TRIR spectra of mutant and wild-type proteins between 1600 and 1700 cm<sup>-1</sup>. The TRIR spectrum of dAppA<sub>BLUF</sub> is characterized by two major bleaches in this region at 1700 and 1650 cm<sup>-1</sup> that are assigned to the flavin C4=O and C2=O carbonyl modes, respectively (5-7). Upon irradiation with 400 nm light to form the long lived signaling state, the bands arising from the two carbonyl modes change: the 1700 cm<sup>-1</sup> band decreases in frequency and is replaced by a doublet at 1681/1690 cm<sup>-1</sup> while a shoulder appears on the high frequency side of the 1650 cm<sup>-1</sup> bleach (lAppA<sub>BLUF</sub>, **Figure 3.4**) (1). The TRIR spectrum of Q63E AppA<sub>BLUF</sub> also possesses a bleach at 1650 cm<sup>-1</sup> together with well resolved bleaches at 1663 and 1681 cm<sup>-1</sup>. Based on comparison with the wild-type TRIR spectra together with the steady state data described above, we assign the 1680 cm<sup>-1</sup> bleach in Q63E AppA<sub>BLUF</sub> to the C4=O flavin carbonyl group and suggest that the 1663 cm<sup>-1</sup> bleach has the same origin as the shoulder that appears on the 1650 cm<sup>-1</sup> band in lAppA<sub>BLUF</sub>. Thus the data are consistent with a protein environment that resembles the light activated form of the wild-type protein.

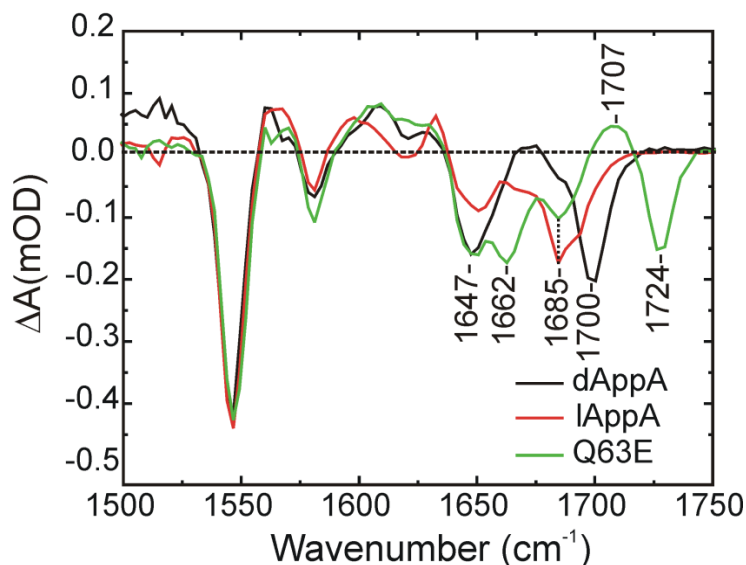


**Figure 3.4. TRIR spectra of wild-type d and lAppA<sub>BLUF</sub> and Q63E AppA<sub>BLUF</sub> measured at 3 ps.**

TRIR spectra of dAppA<sub>BLUF</sub> (black), lAppA<sub>BLUF</sub> (red) and Q63E AppA<sub>BLUF</sub> (green) bound to FAD. Protein concentration was 2 mM in pD 8 phosphate buffer and the TRIR spectra were recorded with a time delay of 3 ps. The spectra have been normalized to the intense FAD ring bleach mode at 1547 cm<sup>-1</sup>.

All the features in the TRIR spectrum of Q63E AppA<sub>BLUF</sub> appear within the time response of the instrument (~100 fs). In **Figure 3.5** we plot the kinetics for the ground state recovery of the intense 1547 cm<sup>-1</sup> bleach to compare Q63E AppA<sub>BLUF</sub> to d and lAppA<sub>BLUF</sub> kinetics. As was observed for d and lAppA<sub>BLUF</sub>, the data for the mutant can be fit with a sum of two exponential decays. The ground state of lAppA<sub>BLUF</sub> is found to recover much more rapidly (mean recovery time of 45 ps) than the dAppA<sub>BLUF</sub> state (249 ps). The ground state recovery kinetics for Q63E AppA<sub>BLUF</sub> are intermediate between these two state (159 ps).

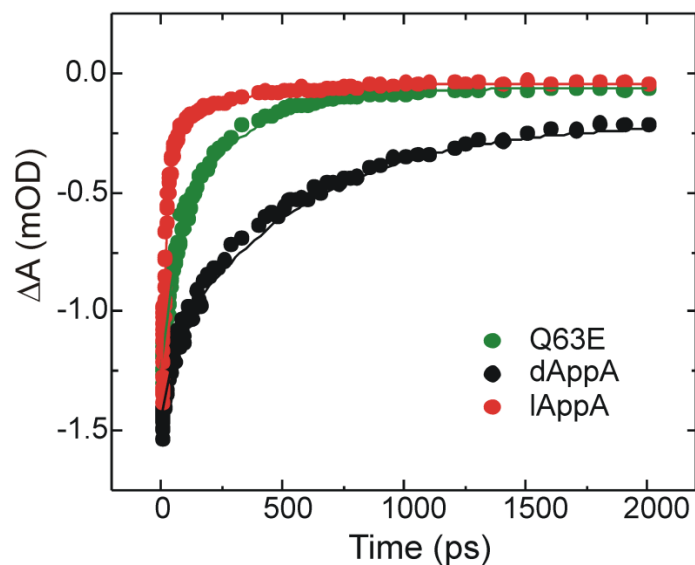


**Figure 3.5. Kinetics of the ground state recovery for wild-type d and lAppA<sub>BLUF</sub> and the Q63E AppA<sub>BLUF</sub> using TRIR spectroscopy measured at 1547 cm<sup>-1</sup>.**

Comparison of kinetic measurements of dAppA<sub>BLUF</sub> (black), lAppA<sub>BLUF</sub> (red), and Q63E AppA<sub>BLUF</sub> (green) bound to FAD. The average lifetime of dAppA<sub>BLUF</sub>, lAppA<sub>BLUF</sub>, and Q63E AppA<sub>BLUF</sub> are 249, 45 and 159 ps respectively. Protein concentration was 2 mM in pD 8 phosphate buffer and the ground state recovery kinetics are measured at the intense bleach at 1547 cm<sup>-1</sup>.

Similar biexponential behavior is observed in the kinetics of the transient absorption spectra for mutant and wild-type AppA<sub>BLUF</sub>. In **Figure 3.6** we show the transient absorption spectra of the three proteins which are each characterized by a bleach at 450 nm and stimulated emission at 550 nm (8). Our visible transient absorption measurements are in good agreement with the data measured by Toh et al. where TA measurements were performed on d and lAppA<sub>BLUF</sub> (9). Recovery of the 450 nm bleach is plotted in **Figure 3.7** for each protein while the rate constants for the biexponential fitting and the mean recovery time are given in **Table 3.1**. The recovery of the major ground state bleach of Q63E again occurs on a time scale between

lAppA<sub>BLUF</sub> and dAppA<sub>BLUF</sub> (**Figure 3.7**). All three kinetics have a short time component which is the same within error for all three (8-11 ps) however, significant differences arise from the long component. Q63E AppA<sub>BLUF</sub> has a slightly slower kinetic decay component (162 ps) than lAppA<sub>BLUF</sub> ( $103 \pm 14$  ps) and approximately half of the long component of dAppA<sub>BLUF</sub> (311 ps). Again, the spectrum of lAppA<sub>BLUF</sub> recovers more quickly than that of the dark adapted protein while the response of Q63E AppA<sub>BLUF</sub> is intermediate between that of the two forms of the wild-type protein. Taken together, the kinetic data reinforce the conclusion that the chromophore environment in the Q63E is intermediate between that of the dark and light states of wild-type AppA, and that the recovery kinetics depart markedly from single exponential behavior.

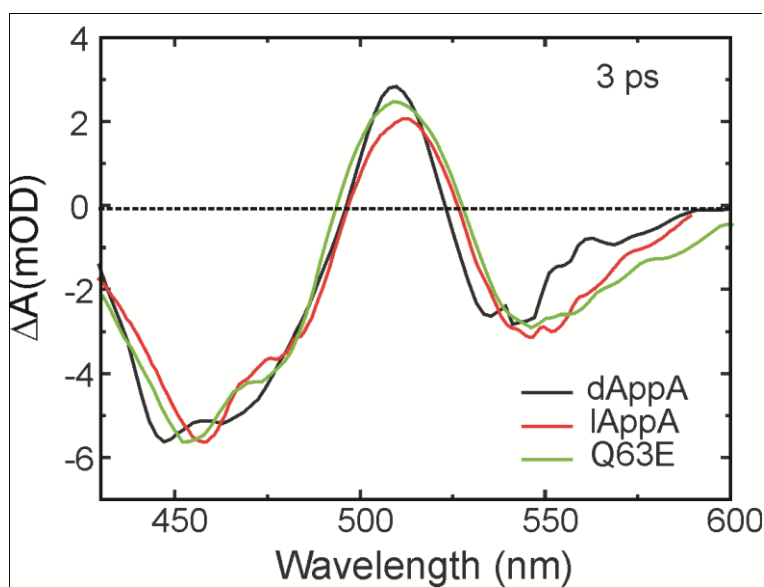


**Figure 3.6. Transient absorption spectra of wild-type d and lAppA<sub>BLUF</sub> and the Q63E AppA<sub>BLUF</sub> measured at 3 ps.**

Transient absorption (TA) spectra of dAppA<sub>BLUF</sub> (black), lAppA<sub>BLUF</sub> (red) and Q63E AppA<sub>BLUF</sub> (green) bound to FAD. Protein concentration was 500  $\mu$ M in pD 8 phosphate buffer and the TA spectra were recorded with a time delay of 3 ps. The spectra have been normalized to the bleach at 450 nm.



The most striking difference between the TRIR spectra of wild-type and mutant AppA<sub>BLUF</sub> is the appearance of the new high frequency bleach at 1724 cm<sup>-1</sup> in the Q63E AppA<sub>BLUF</sub> spectrum together with a transient absorption at 1707 cm<sup>-1</sup>. These bands appear within 100 fs of excitation and thus we initially considered whether the 1724 cm<sup>-1</sup> bleach could arise directly from the flavin chromophore. However, no band is observed at this position in the steady state Raman spectrum of Q63E AppA<sub>BLUF</sub>. In addition, if it were to arise from the flavin then the most likely candidate is the C4=O carbonyl that has blue shifted by 24 cm<sup>-1</sup> upon replacing Q63 with a glutamate. Although Kim and Carey observe the C4=O of riboflavin at 1723 cm<sup>-1</sup> when this molecule is bound to riboflavin binding protein in H<sub>2</sub>O (10), a large blue

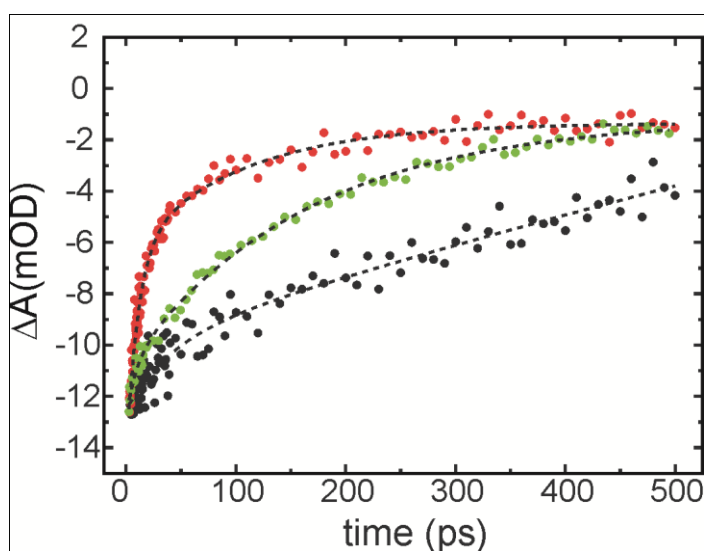


**Figure 3.7. Kinetics of the ground state recovery for wild-type d and lAppA<sub>BLUF</sub> and the Q63E AppA<sub>BLUF</sub> using transient absorption spectroscopy measured at 450 nm.**

Comparison of kinetic measurements of dAppA<sub>BLUF</sub> (black), lAppA<sub>BLUF</sub> (red), and Q63E AppA<sub>BLUF</sub> (green) bound to FAD. The average lifetime of dAppA<sub>BLUF</sub>, lAppA<sub>BLUF</sub>, and Q63E AppA<sub>BLUF</sub> are 236, 46 and 135 ps respectively. Protein concentration was 500 μM in pD 8 phosphate buffer and the ground state recovery kinetics are measured at the bleach at 450 nm.

shift in the corresponding band in Q63E AppA<sub>BLUF</sub> seems unlikely given that other data are consistent with a red shift in this band: from 1700 cm<sup>-1</sup> in dAppA<sub>BLUF</sub> to 1690 cm<sup>-1</sup> in Q63E AppA<sub>BLUF</sub> (**Figure 3.4**). In addition, our data were obtained in D<sub>2</sub>O and we note that the C4=O of riboflavin bound to riboflavin binding protein is at 1710 cm<sup>-1</sup> in D<sub>2</sub>O (10). Since the frequency of the 1724 cm<sup>-1</sup> band is in the region expected for an unconjugated carboxylic acid (11-13), we investigated whether this band could arise from a protein mode that responds to flavin excitation on an ultrafast timescale. To test this hypothesis we uniformly labeled both wild-type and mutant AppA<sub>BLUF</sub> with <sup>13</sup>C and reconstituted the proteins with unlabeled FAD. The resulting TRIR spectra show direct evidence that the vibrational mode observed at 1724 cm<sup>-1</sup> is not the C4=O vibration of the flavin cofactor but a protein mode which shifts by ~36 cm<sup>-1</sup> upon <sup>13</sup>C uniform protein labeling (**Figure 3.8**). In comparison, the flavin carbonyl modes in <sup>13</sup>C labeled wild-type d and lAppA<sub>BLUF</sub> (**Figure 3.9**) are largely insensitive to labeling although it is interesting to note that the absorption at 1660 cm<sup>-1</sup> in dAppA<sub>BLUF</sub> that was previously assigned to Q63 has been reduced in intensity by <sup>13</sup>C labeling. The <sup>13</sup>C labelling also uncovers additional protein modes perturbed by electronic excitation at 1601 cm<sup>-1</sup> and 1505 cm<sup>-1</sup>.

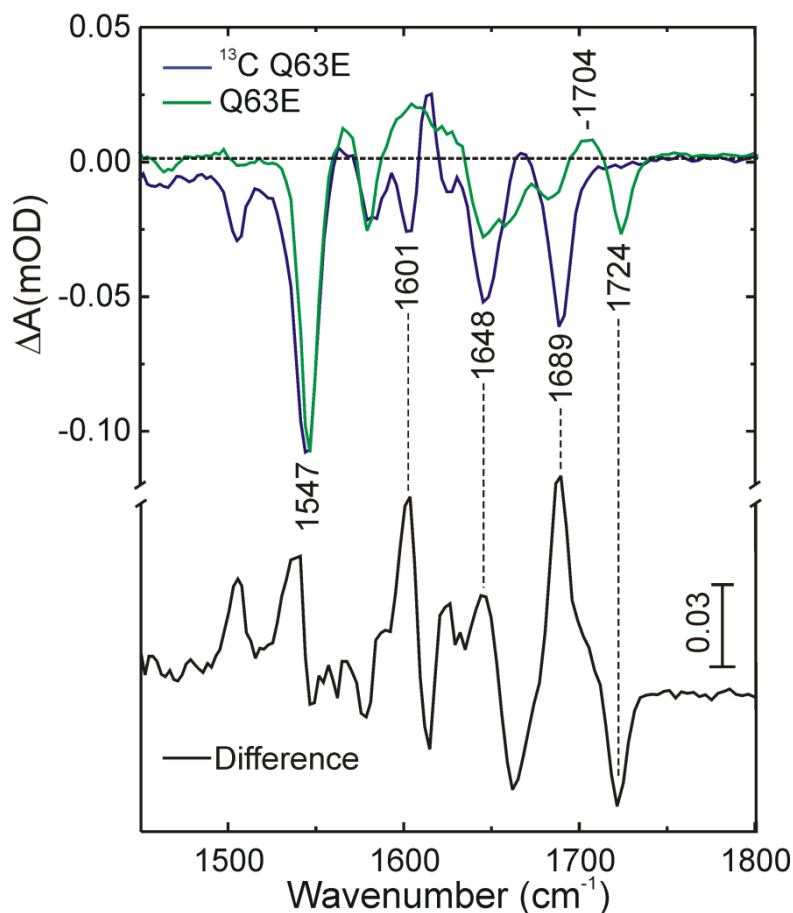


**Figure 3.8. TRIR spectra of unlabeled and  $^{13}\text{C}$  labeled Q63E AppA<sub>BLUF</sub> measured at 3 ps.**

TRIR spectra of unlabeled Q63E AppA<sub>BLUF</sub> (red) and  $^{13}\text{C}$  labeled Q63E AppA<sub>BLUF</sub> (blue) bound to FAD. The difference spectrum is shown on the bottom panel (black). Protein concentration was 2 mM in pD 8 phosphate buffer and the TRIR spectra were recorded with a time delay of 3 ps. The spectra have been normalized to the intense FAD ring bleach mode at  $1547\text{ cm}^{-1}$ .

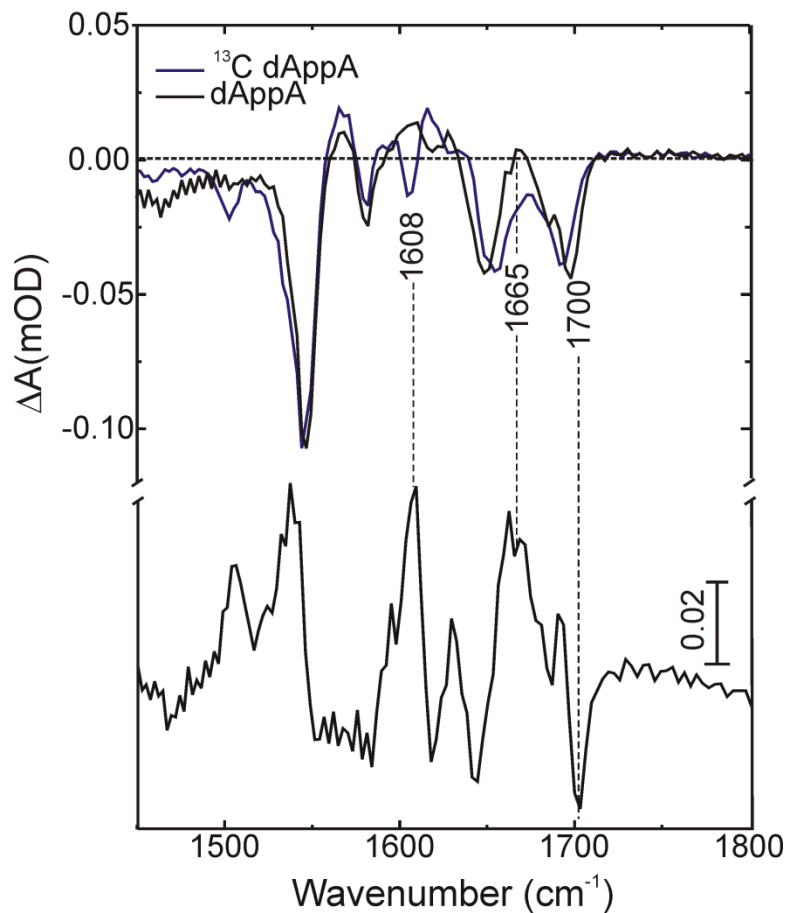


**Figure 3.9. TRIR spectra of unlabeled and <sup>13</sup>C labeled d and lAppA<sub>BLUF</sub> measured at 3 ps.**

(a) TRIR spectra of unlabeled dAppA<sub>BLUF</sub> (red) and <sup>13</sup>C labeled dAppA<sub>BLUF</sub> (blue) bound to FAD. The difference spectrum is shown on the bottom panel (black). Protein concentration was 2 mM in pD 8 phosphate buffer and the TRIR spectra were recorded with a time delay of 3 ps. The spectra have been normalized to the intense FAD ring bleach mode at 1547 cm<sup>-1</sup>.

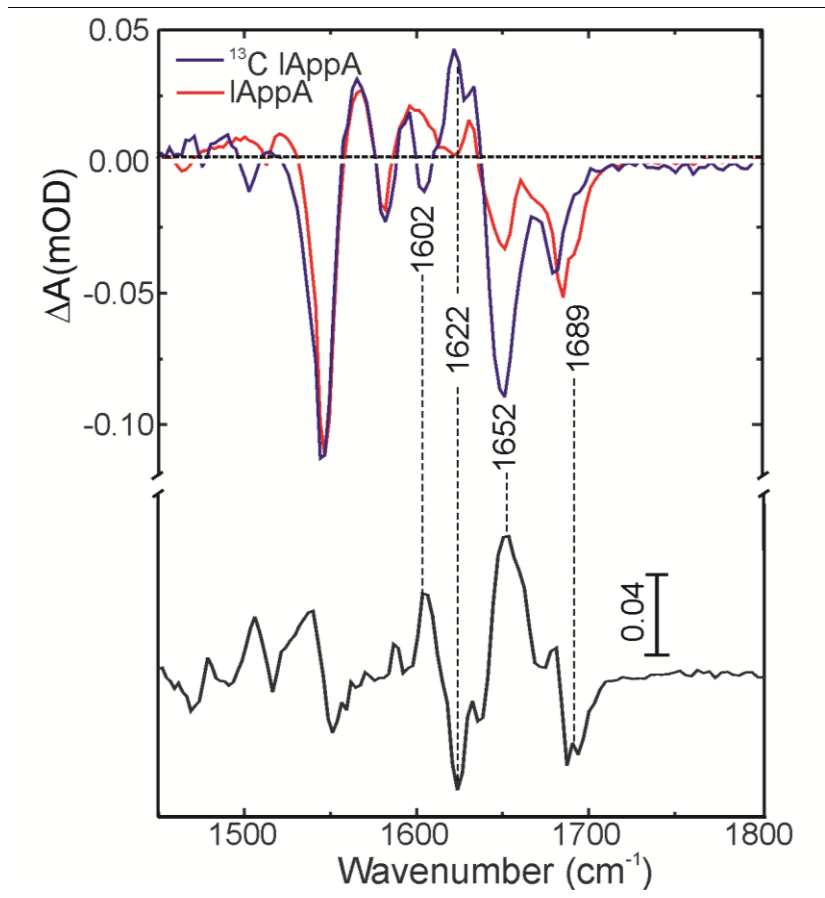


**Figure 3.9. TRIR spectra of unlabeled and  $^{13}\text{C}$  labeled d and lAppA<sub>BLUF</sub> measured at 3 ps.**

(b) TRIR spectra of unlabeled lAppA<sub>BLUF</sub> (red) and  $^{13}\text{C}$  labeled lAppA<sub>BLUF</sub> (blue) bound to FAD. The difference spectrum is shown on the bottom panel (black). Protein concentration was 2 mM in pD 8 phosphate buffer and the TRIR spectra were recorded with a time delay of 3 ps. The spectra have been normalized to the intense FAD ring bleach mode at  $1547\text{ cm}^{-1}$ .

Since the  $1724\text{ cm}^{-1}$  bleach appears within 100 fs of excitation, this group must either be part of the electronic transition associated with light absorption (i.e. a flavin group) or must interact directly with the chromophore so that it responds instantaneously to light absorption. Importantly, the isotope labeling experiments allow us to confidently assign the high frequency  $1724\text{ cm}^{-1}$  bleach and  $1707\text{ cm}^{-1}$  transient in Q63E AppA<sub>BLUF</sub> to a protein residue. Given that the position of the  $1724\text{ cm}^{-1}$  is in the region expected for a protonated carboxylic acid,<sup>(13-15)</sup> we assign this bleach to the E63-COOH(D) group of E63. In order to respond instantaneously to photoexcitation, we propose that E63-COOH(D) is directly hydrogen bonded to the flavin chromophore, or possibly to a group that is itself in direct contact with the flavin such as Y21 or N45. It follows that the change in electronic structure of the flavin caused by photoexcitation must then lead to an instantaneous increase in the strength of the hydrogen bond between the chromophore and E63-COOH(D) leading to loss of the infrared absorption at  $1724\text{ cm}^{-1}$  (bleach) and a new absorption at  $1707\text{ cm}^{-1}$  (transient). Based on model studies that relate changes in carbonyl frequency and hydrogen bond strength, the  $17\text{ cm}^{-1}$  decrease in wavenumber of the carboxylic acid group is consistent with an increase in hydrogen bond enthalpy of  $\sim 3\text{ kcal/mol}$  (16).

The TRIR spectra were acquired at a sample pD of 8 and thus the  $pK_a$  of the Q63E side chain must be at least 3 pH units more basic than the normal value for a carboxylic acid. Such changes in the  $pK_a$  values of buried protein side chains are not unprecedented: for example, the heme propionic acid group in cytochrome c has a  $pK_a$  of 9 (13), while E190 in the thermophilic F<sub>1</sub>-ATPase has a  $pK_a$  of 7 (17). Since the frequency of the C4=O flavin carbonyl in Q63E AppA<sub>BLUF</sub> is similar to that in lAppA<sub>BLUF</sub>, it is reasonable to propose that Q63E is hydrogen bonded directly to C4=O as proposed in the light activated state of the protein (**Figure 3.10**).

This would require that Q63E COOH(D) is a hydrogen bond donor to C4=O and a hydrogen bond acceptor from Y21. Direct interaction of the Q63E-COOH(D) group with C4=O can also account for the instantaneous response of the Q63E side chain to light absorption since an increase in electron density on the C4=O oxygen in the flavin excited state will result in a strengthening of the hydrogen bond with the Q63E side chain (**Figure 3.10**). In one of the models for AppA activation (**Figure 3.1**), Q63 tautomerizes so that the amide nitrogen can accept a hydrogen bond from Y21 while the enol OH forms a hydrogen bond to the C4=O group. Equivalent hydrogen bond interactions are formed by Q63E together with a hydrogen bond to W104. Thus one explanation for the loss of photoactivity in the mutant is that the Q63E side chain is an excellent isostere of the Q63 enol and locks the protein in a state that resembles lAppA and in which W104 is still part of the hydrogen bond network (3). Returning to the wild-type protein, our observation thus suggests that the change in electronic structure of the flavin upon photoexcitation is a driving force for alterations in the hydrogen bonding network, that lead ultimately to photoactivation. In addition, if the hydrogen bonding network in the wild-type protein responds on the same time scale to that observed for Q63E AppA (<1ps), then the TRIR data are consistent with an initial tautomerization of Q63, since the proposed rotation of the Q63 side chain which is expected to occur on a time scale of 10-100 ps (18). However, while we believe that the transient stabilization of the Q63 enol in the AppA excited state is a key step in photoactivation, the keto form of Q63 is expected to predominate in the lAppA ground state. This necessitates that the Q63 side chain must rotate in order to hydrogen bond to the flavin C4=O, since this interaction is present in lAppA, leading also to loss of the hydrogen bond with W104. A model for AppA activation that encompasses both Q63 tautomerization and rotation is shown in **Figure 3.11**. In this new model, we propose that both keto and enol tautomers of Q63

are present in the ground state of dAppA with the equilibrium heavily in favor of the keto tautomer. Upon photoexcitation, the increase in electron density on the C4=O oxygen increases the relative stability of the enol tautomer that then leads ultimately to the light activated form of the protein in which Q63 has rotated.

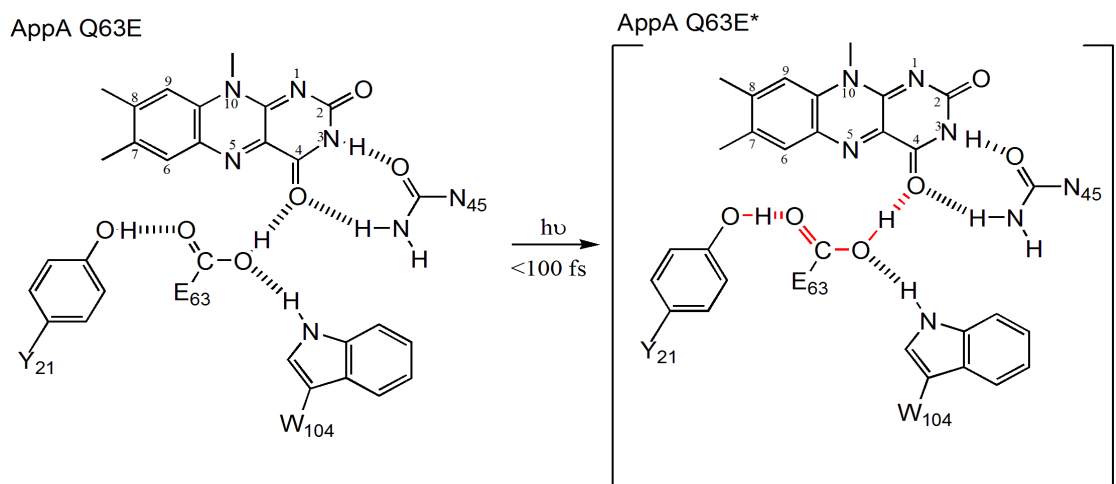


**Figure 3.10. Proposed hydrogen bonding structure of Q63E AppA<sub>BLUF</sub>.**

Replacement of Q63 with a glutamate leads to a hydrogen bond network in which the Q63E mimics the enol form of Q63. The side chain of Q63E is hydrogen bonded to the flavin C4=O in the ground state, explaining the TRIR data in which the vibrational spectrum of the flavin resembles that of lAppA<sub>BLUF</sub>. In the excited state there is an increase in electron density on the C4=O oxygen which will strengthen the hydrogen bond with Q63E and result in polarization of the Q63E C=O and concomitant strengthening of the hydrogen bond between Y21 and Q63E. This change in electronic structure is shown schematically by lengthening of the Q63E C=O and O-H bonds and movement of the Y21 proton so that it is closer to the Q63E C=O group.



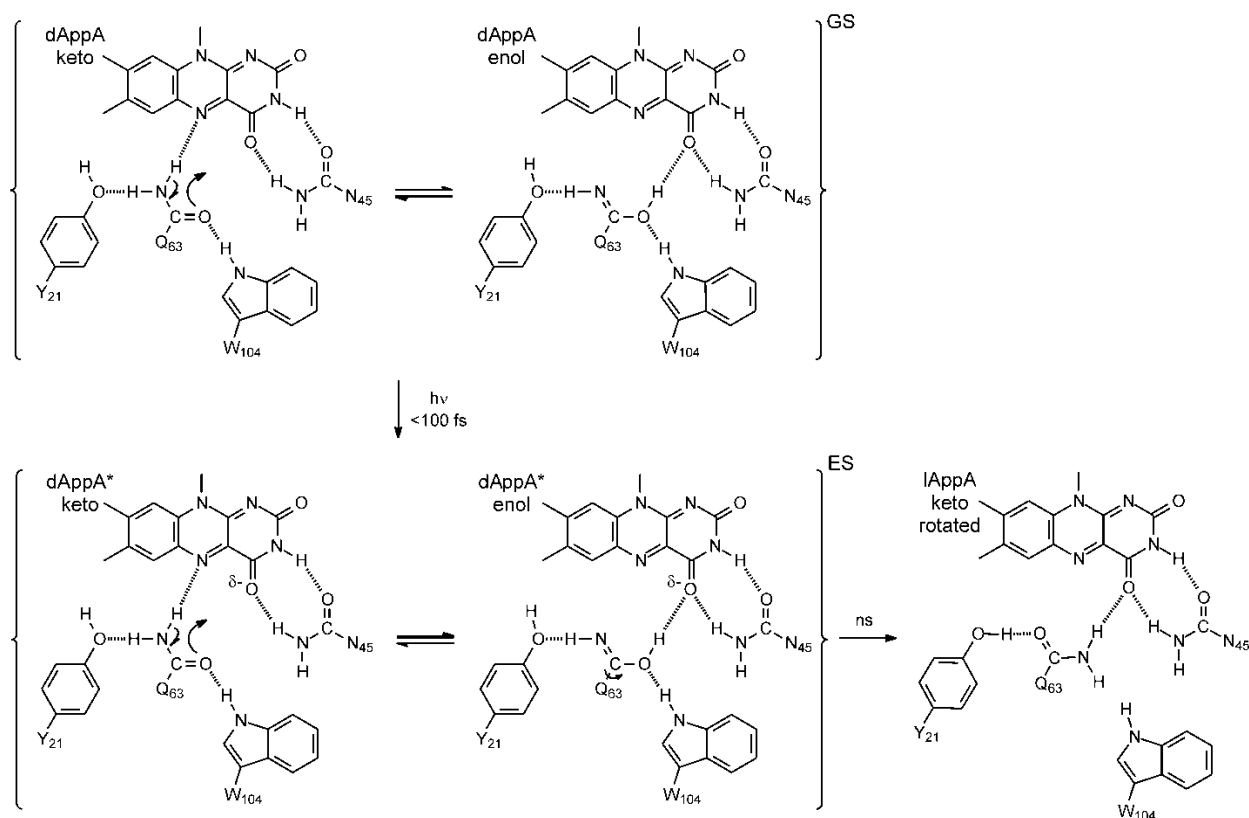


**Figure 3.11. Proposed model for formation of lAppA from dAppA.**

This model encapsulates both proposals for the conversion of dAppA to lAppA in **Figure 3.1**. In the ground state of dAppA the Q63 side chain exists as an equilibrium mixture of keto and enol tautomers. In the enol tautomer there is a hydrogen bond between Q63 and the flavin C4=O by analogy to the structure presented in **Figure 3.10** for Q63E. However, as expected for an amide group, the position of the tautomeric equilibrium strongly favors the keto form which is shown diagrammatically by an equilibrium symbol with disproportionate line widths. Upon photoexcitation there is an increase in electron density on the C4=O which will increase the proportion of the enol tautomer, again shown by an equilibrium symbol with disproportionate line widths. We then propose that this enol tautomer leads to the lAppA ground state in which Q63 has rotated so that the bond to W104 has been broken.

**Table 3.1**

	Transient Absorption (450 nm)					TRIR (1547 cm <sup>-1</sup> )				
	a <sub>1</sub>	τ <sub>1</sub> /ps	a <sub>2</sub>	τ <sub>2</sub> /ps	<τ> /ps	a <sub>1</sub>	τ <sub>1</sub> /ps	a <sub>2</sub>	τ <sub>2</sub> /ps	<τ> /ps
<b>dAppA</b>	-0.25	10 ± 3	-0.75	311 ± 80	236	-0.51	34 ± 4	-0.49	473 ± 73	249
<b>lAppA</b>	-0.62	11 ± 1	-0.38	103 ± 14	46	-0.72	11 ± 1	-0.28	134 ± 24	45
<b>Q63E</b>	-0.17	8 ± 2	-0.83	162 ± 8	135	-0.45	47 ± 6	-0.55	252 ± 30	159

**Table 3.1. Kinetics of dAppA<sub>BLUF</sub>, lAppA<sub>BLUF</sub> and Q63E AppA<sub>BLUF</sub> determined by TRIR and Transient Absorption Spectroscopy.**

The observed kinetic lifetimes of the excited states of dAppA, lAppA and Q63E AppA derived from an analysis of the transient absorption (TA) and time resolved IR (TRIR) spectra. The protein concentration was 500 μM and 2 mM in pD 8 phosphate buffer for the TA and TRIR experiments, respectively. The recovery kinetics have been fit to two exponentials of the 450 nm TA bleach and the 1547 cm<sup>-1</sup> bleach in the TRIR spectra.

## Major Conclusions from Q63E AppA<sub>BLUF</sub>

The mechanism of AppA photoactivation involves the reorganization of a hydrogen bonding network that connects the chromophore to the protein. Q63 is a critical component of this network, and in order to improve our understanding of the role of this residue in photoactivation we replaced Q63 with a glutamate. While the Q63E AppA<sub>BLUF</sub> is not photoactive, steady state and ultrafast spectroscopy indicate that this mutation has trapped the protein in a state that is intermediate between the dark and photoactivated states of AppA<sub>BLUF</sub> in which the flavin C4=O is more strongly hydrogen bonded than in dAppA<sub>BLUF</sub>. Importantly a new vibrational band is observed in the TRIR spectra of Q63E AppA<sub>BLUF</sub> which is assigned to the protonated carboxylic acid side chain of Q63E. This mode appears instantaneously upon photoexcitation indicating that the carboxyl side chain is hydrogen bonded directly to the chromophore. We propose that Q63E is hydrogen bonded to the flavin C4=O and that excitation of the flavin leads to an increase in electron density on the C4=O oxygen which strengthens the interaction with Q63E by ~3 kcal/mol. These data provide conclusive evidence that the hydrogen bond network in the protein environment responds on the ultrafast timescale to light absorption by the flavin chromophore. Thus, independent of any other driving force, electronic excitation of the flavin influences the strength of H-bonds in the network linking the critical Q63 residue to the flavin.

### C.3 Reorganization of the Hydrogen Bonding Network Reveals the Significance of Residue W104 in the Stabilization of lAppA and Shows No Evidence for Electron Transfer During Photoactivation (The W104M and Y21W Mutants):

The importance of W104, as well as Q63 and Y21, is clearly shown by other groups and our lab through the use of site-directed mutagenesis. Mutants of residues Q63 and Y21 yield in photoinactive proteins and mutations to residue W104 result in an increased light to dark state recovery. In addition, residue W104 has been proposed to be important in the structural change leading from the dark to light states (19). The structural change that occurs in W104 is thought to propagate through beta strand 5 (W104-L108) which then relays the light signal to the C-terminal domain of AppA. W104 mutants have been made (W104L and W104F) previously by our group and generate a protein that is photoactive with a fast dark state recovery (W104A is up to approximately 150 fold faster than the wild-type protein). More recent studies by Toh *et. al.* have implicated there is electron transfer from W104 to the flavin chromophore occurs when lAppA is excited with 450 nm light. In addition, the importance of Y21 was previously shown through the Y21F mutation that renders the protein photoinactive (20). It has been proposed by others that photoexcitation of the dark state of AppA triggers electron transfer from residue Y21 to the flavin and that this electron transfer is critical for photoactivation. In order to gain further insight into residues W104 and Y21 involvement in excited state electron transfer, this section discusses the W104M and Y21W AppA<sub>BLUF</sub> mutants.

#### **W104M AppA<sub>BLUF</sub>:**

Other BLUF domain proteins have a methionine where W104 is found in AppA. These proteins exhibit photocycles that relax from the light state to the dark state on a much faster time scale than AppA. in order to investigate if the change to a methioine would cause relaxation to

lAppA on a similar time scale to other BLUF domain proteins, we have made the W104M AppA<sub>BLUF</sub> mutant. This mutant is photoactive and relaxes back to the dark state in 10 minutes after the light state is formed and has a blue shifted spectra ( $\lambda_{\text{max}}$  440 shifts to 447 nm) compared to wild-type ( $\lambda_{\text{max}}$  444 shifts to 454 nm) (**Figures 3.12** and **3.13**). The TRIR spectra for this mutant, shown in **Figure 3.14**, are nearly identical to the wild-type protein suggesting the environment around the flavin does not change significantly by making the W104M mutation.

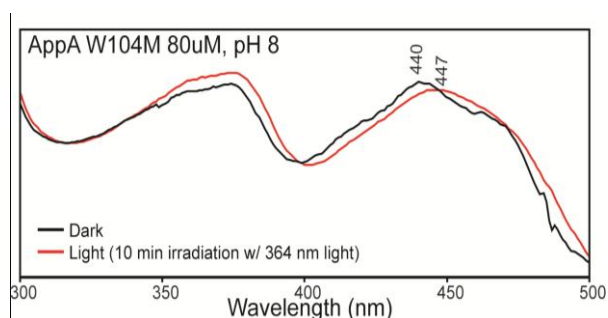


**Figure 3.12. Electronic absorption spectra of W104M photoconversion bound to riboflavin.** The light state of W104M AppA<sub>BLUF</sub> was generated by exciting the sample with 365 nm light Concentrations: 80  $\mu$ M pH 8.

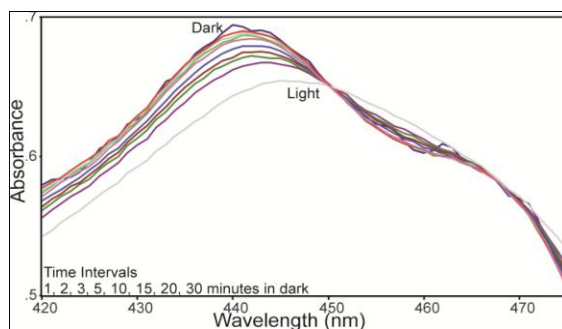


**Figure 3.13. Electronic absorption spectra of W104M recovery from light to dark state bound to riboflavin.**

The light state of W104M AppA<sub>BLUF</sub> was generated by exciting the sample with 365 nm light and the protein was allowed to recover in the dark. Spectra were recorded 1, 2, 3, 5, 10, 15, 20 and 30 minutes to monitor light to dark recovery. Concentration: 80  $\mu$ M pH 8.

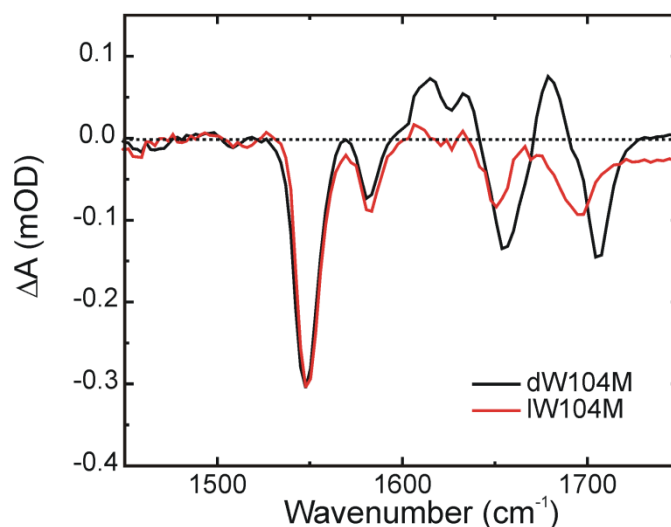


**Figure 3.14. TRIR Spectra of W104M bound to riboflavin.**

The light state is shown in red and the dark state is shown in black. Concentrations: 1.5 mM pD 8.

These data suggest this mutation effects long timescale changes such as conformational change. Because the kinetics of light state recovery for W104M is 3 times faster than the wild type protein, W104 must be involved in stabilizing lAppA. In addition, no radical formation was observed in the TRIR spectra for W104M AppA<sub>BLUF</sub> in either the dark or the light state. In order to gain a better understanding of the role of the tryptophan in AppA, we have generated the Y21W AppA<sub>BLUF</sub> mutant. This mutation was made to enhance radical formation because residue Y21 is closer to the flavin (4.6 Å) than W104 (5.6 Å) in the W<sub>in</sub> crystal structure of AppA.

The Y21W AppA<sub>BLUF</sub> mutant is photoinactive and has ground state recovery kinetics similar to lAppA with the C4=O carbonyl in an environment similar to dAppA. Y21W AppA<sub>BLUF</sub> has a very unique TRIR spectrum (**Figure 3.15**). The frequency of the C4=O flavin carbonyl in Y21W AppA<sub>BLUF</sub> again is similar to that in dAppA<sub>BLUF</sub>, suggesting that Y21W prevents Q63 from

forming a hydrogen bond to the C4=O of the flavin. However, there is an intense transient at  $1634\text{ cm}^{-1}$ . We propose this mutant enhances radical formation of FAD in the excited state and propose this mode belongs to  $\text{FADH}\cdot$  because it appears at the same frequency as  $5\text{-CH}_3\text{ FADH}\cdot$  (submitted). When the absorbance of the  $1634\text{ cm}^{-1}$  transient are plotted as a function of time, the kinetics show a rise during the first few picoseconds (12.8 ps) followed by a decay that last for approximately 300 ps before returning to the ground state (**Figure 3.16**). The bleach that corresponds to the disappearance of  $\text{FAD}_{\text{Ox}}$  is found at  $1623\text{ cm}^{-1}$  and has the same kinetics as the transient at  $1634\text{ cm}^{-1}$ . In addition, the formation of a tryptophan radical is observed at  $1505\text{ cm}^{-1}$  and is described previously by a Blanco-Rodríguez *et al* where it is observed at  $1497\text{ cm}^{-1}$  (21).

By enhancing radical formation in the Y21W mutant we are able to return to the wild type protein to determine if similar behavior is observed. After thorough analysis it becomes obvious the same radical formation occurs in lAppA (**Figure 3.17**). When the absorbance at  $1634\text{ cm}^{-1}$  is plotted as a function of time, the kinetics show the same rise followed by a decay as observed in Y21W AppA<sub>BLUF</sub>. In addition, the bleach that corresponds to the disappearance of  $\text{FAD}_{\text{Ox}}$  is again found at  $1623\text{ cm}^{-1}$  and the formation of a tryptophan radical is observed at  $1505\text{ cm}^{-1}$ . This behavior is not observed in dAppA (**Figure 3.18**) and therefore suggests the position of W104 must be closer in proximity to the flavin in lAppA than in dAppA. The  $1505\text{ cm}^{-1}$  mode assigned to the tryptophan is not observed in the light state of the W104M mutant. In addition, the mode at  $1505\text{ cm}^{-1}$  shifts to  $1490\text{ cm}^{-1}$  upon  $^{13}\text{C}$  protein labeling and therefore can be confidently assigned to a protein mode (**Figure 3.9b**).

When comparing the overall kinetics of the Y21W AppA<sub>BLUF</sub> mutant we observe ground state recovery kinetics that are similar to lAppA (**Figure 3.19**). This is likely due to the

quenching of the excited state by introducing a tryptophan close to the flavin and again suggests Y21W AppA<sub>BLUF</sub> is trapped in a light adapted state in contrast to all the other Y21 mutants studied which resemble the dark state of the protein. This finding is significant and implies the position of the W104 in dAppA is far away from the flavin but after photoexcitation W104 must change orientation and move closer to the flavin in lAppA.

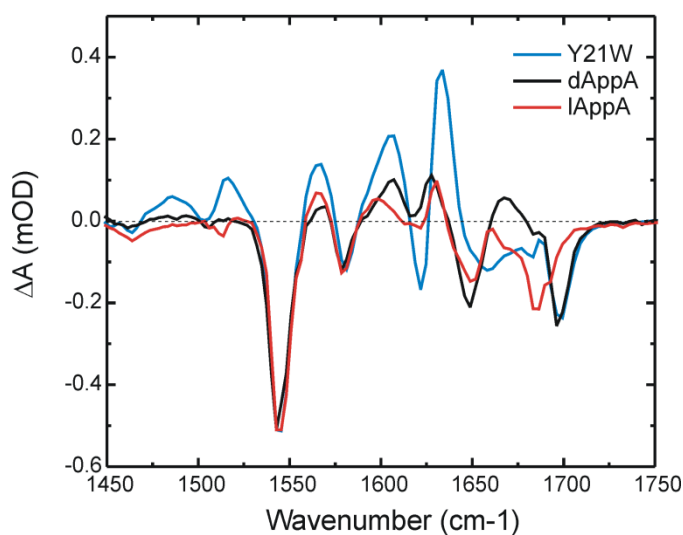


**Figure 3.15. TRIR spectra of wild-type d and lAppA<sub>BLUF</sub> and Y21W AppA<sub>BLUF</sub> measured at 3 ps.**

TRIR spectra of dAppA<sub>BLUF</sub> (black), lAppA<sub>BLUF</sub> (red) and Y21W AppA<sub>BLUF</sub> (blue) bound to FAD. Protein concentration was 2 mM in pD 8 phosphate buffer and the TRIR spectra were recorded with a time delay of 3 ps. The spectra have been normalized to the intense FAD ring bleach mode at 1547 cm<sup>-1</sup>.



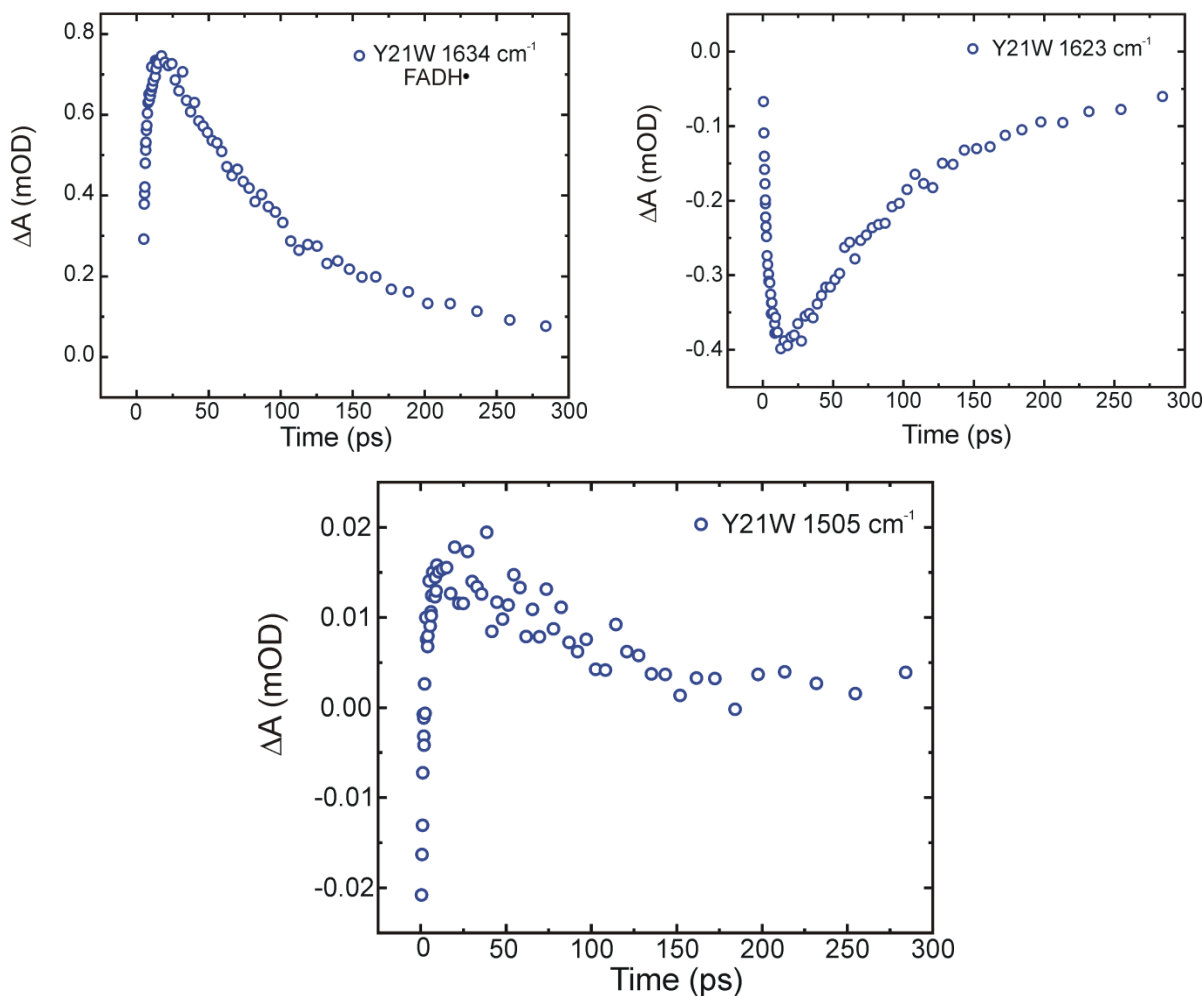


**Figure 3.16. Kinetics of the ground state recovery and excited state decay for Y21W AppA<sub>BLUF</sub> using TRIR spectroscopy measured at 1634, 1623 and 1526 cm<sup>-1</sup>.**

Kinetic measurements of the excited state decay and ground state decay for Y21W AppA<sub>BLUF</sub> using TRIR spectroscopy measured at 1634 and 1623 cm<sup>-1</sup> representing the appearance of FADH• and disappearance of FAD<sub>Ox</sub> (top). The average of the rise and decay fits gives lifetimes of 5 and 136 ps respectively. The kinetics of the excited state decay of Y21W AppA<sub>BLUF</sub> at 1505 cm<sup>-1</sup> represents the formation of a tryptophan radical (bottom). The rise and decay fits gives lifetimes of 3 and 94 ps respectively. Concentrations: 1.5 mM pD 8.

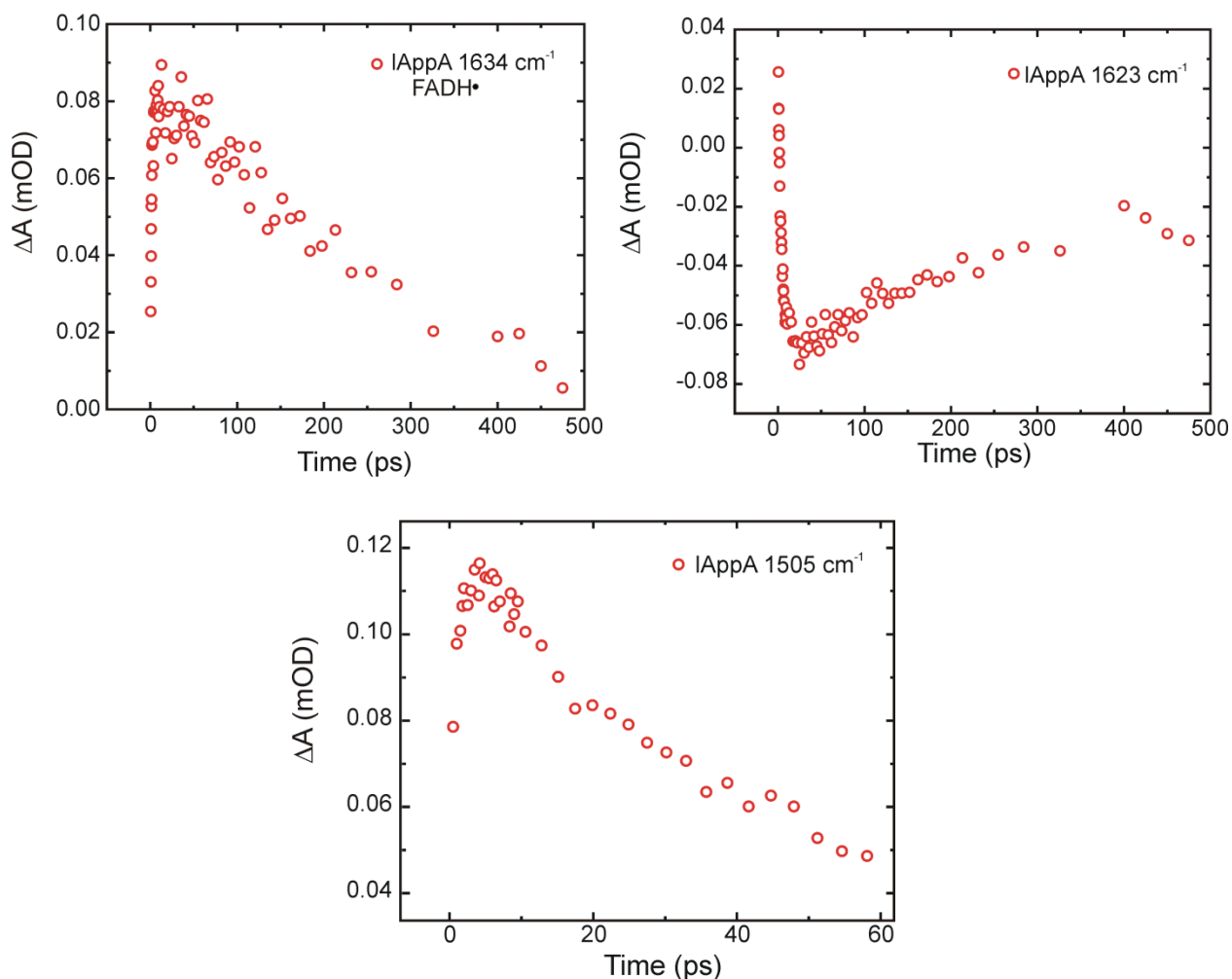


**Figure 3.17. Kinetics of the ground state recovery and excited state decay for lAppA<sub>BLUF</sub> using TRIR spectroscopy measured at 1634, 1623 and 1526  $\text{cm}^{-1}$ .**

Kinetic measurements of the excited state decay and ground state decay for lAppA<sub>BLUF</sub> using TRIR spectroscopy measured at 1634 and 1623  $\text{cm}^{-1}$  representing the appearance of FADH• and disappearance of FAD<sub>Ox</sub> (top). The average of the rise and decay fits gives lifetimes of 4 and 397 ps respectively. The kinetics of the excited state decay of lAppA<sub>BLUF</sub> at 1505  $\text{cm}^{-1}$  represents the formation of a tryptophan radical (bottom). The rise and decay fits gives lifetimes of 3 and 145 ps respectively. Concentrations: 1.5 mM pD 8.

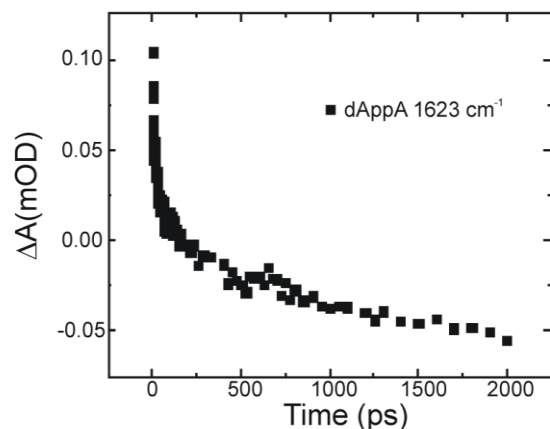


**Figure 3.18. Kinetics of the excited state decay for dAppA<sub>BLUF</sub> using TRIR spectroscopy measured at 1623 cm<sup>-1</sup>.**

Kinetic measurements of the excited state decay for dAppA<sub>BLUF</sub> using TRIR spectroscopy measured at 1623 cm<sup>-1</sup>. Concentrations: 1.5 mM pD 8.

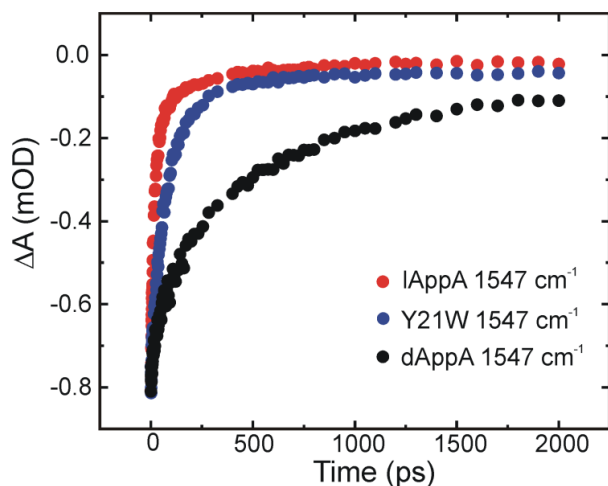


**Figure 3.19. Kinetics of the ground state recovery for wild-type d and lAppA<sub>BLUF</sub> and the Y21W AppA<sub>BLUF</sub> using TRIR spectroscopy measured at 1547 cm<sup>-1</sup>.**

Comparison of kinetic measurements of dAppA<sub>BLUF</sub> (black), lAppA<sub>BLUF</sub> (red) and Y21W (blue) AppA<sub>BLUF</sub> bound to FAD. The lifetimes are determined by fitting to a 2 component exponential and for dAppA<sub>BLUF</sub>, lAppA<sub>BLUF</sub>, and Y21W AppA<sub>BLUF</sub> are 36/559, 21/272 and 62/261 ps respectively. Protein concentration was 2 mM in pD 8 phosphate buffer and the ground state recovery kinetics are measured at the intense bleach at 1547 cm<sup>-1</sup>.

There are two published crystal structures of AppA where the conformation of W104 differs. It has been proposed that one of these structures corresponds to lAppA and the other dAppA. However, intense debate has not allowed for the assignment of either structure to either lAppA or dAppA. The first structure, shown in **Figure 3.20**, shows W104 pointing out to solution, away from the flavin and is referred to as  $W_{out}$ . Our data suggests this structure represents dAppA where residue Q63 is a hydrogen bond donor to both residue Y21 and a nitrogen atom (N5) on the flavin. The second crystal structure (**Figure 3.20**) is referred to as  $W_{in}$  because W104 is pointing into the protein, towards the flavin and is in close proximity to Q63.

The Y21W mutant enhances the characteristics observed in lAppA such as radical formation ( $FADH\cdot$  at  $1628\text{ cm}^{-1}$ ) and quenching of the excited state. This is because we have introduced a tryptophan closer to the flavin than in the  $W_{in}$  structure. Therefore we can confidently assign  $W104_{in}$  to lAppA where Y21 is a hydrogen bond donor to Q63 which also donates a hydrogen bond to an oxygen atom (O4) on the flavin. This also explains the fast light to dark state recovery of W104 mutants because W104 can now form a hydrogen bond to the carbonyl side chain of Q63 in order to stabilize lAppA.

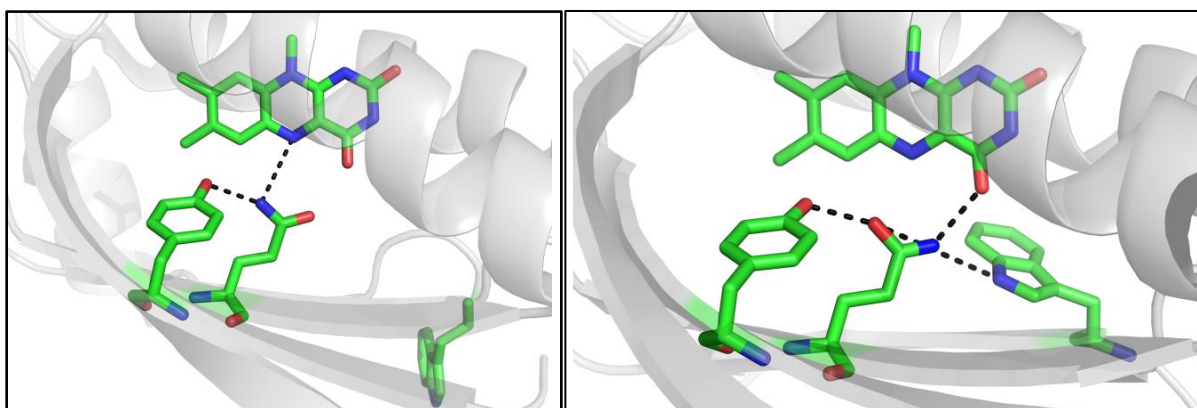


**Figure 3.20. Comparison of Anderson and Jung crystal structures.**

The two existing crystal structure of AppA where  $W_{out}$  is shown on the left and  $W_{in}$  is shown on the right. The  $W_{in}$  structure is consistent with lAppA.

## Major Conclusions from the W104M and Y21W Mutants

The mechanism of AppA photoactivation involves the reorganization of a hydrogen bonding network that connects the chromophore to the protein. Residues Y21 and W104 are a critical component of this network, and in order to improve our understanding of the role of these residues in photoactivation we replaced W104 with a methionine and Y21 with a tryptophan. While W104M AppABLUF retains photoactivity, the rate of recovery from the light to dark state increases suggesting W104 plays an important role in stabilization of lAppA. In order to further investigate the proposed mechanism of electron transfer by W104 we have generated the Y21W mutant to enhance tryptophan radical formation. While Y21W AppABLUF is not photoactive, steady state and ultrafast spectroscopy indicate that this mutation has trapped the protein in a state that resembles the photoactivated states of AppABLUF. The flavin C4=O is more weakly hydrogen bonded than in lAppABLUF suggesting the importance of Y21 in formation of lAppA. Additional studies on residue Y21 will be discussed in the following chapter. Importantly an intense vibrational band is observed in the TRIR spectra of Y21W AppABLUF which is assigned to FADH• and a second vibrational mode indicated tryptophan radical formation. We propose that Y21W places the tryptophan much closer to the flavin than the wild type protein therefore increasing the yield of FADH• formation. By enhancing radical formation we have been able to find similar behavior in lAppA and also omit the proposal of radical formation in dAppA. These data provide conclusive evidence that residue W104 is in the  $W_{out}$  conformation in dAppA and once photoactivation occurs, there is a change in the hydrogen bond network in the protein bringing W104 closer to the flavin in the final light activated state of the protein representing the  $W_{in}$  conformation.

## D. Summary

This chapter discussed various AppA mutants that have been generated in order to alter the hydrogen bonding pattern of the flavin chromophore with neighboring protein residues. Previous experiments have established the importance of residues Y21, Q63 and W104 in the AppA photoactivation mechanism. In this chapter we have discussed the significance of altering the hydrogen bonding network around the chromophore in establishing the role of Q63 and W104.

While the Q63E AppA<sub>BLUF</sub> was generated and is not photoactive, steady state and ultrafast spectroscopy indicate that this mutation has trapped the protein in a state that is intermediate between the dark and photoactivated states of AppA<sub>BLUF</sub> in which the flavin C4=O is more strongly hydrogen bonded than in dAppA<sub>BLUF</sub>. Importantly a new vibrational band is observed in the TRIR spectra of Q63E AppA<sub>BLUF</sub> which is assigned to the protonated carboxylic acid side chain of Q63E by isotopically labelling the protein. This proves communication between the flavin and protein occurs on a femtosecond timescale. From this data we propose of a new mechanism of tautomerization followed by rotation of dAppA in order to form the light state of the wild type protein.

The W104M mutant was created to determine effects on recovery time of the light state to the dark state. Other BLUF domain proteins with short recovery times have a conserved methionine as opposed to the tryptophan in AppA. It was determined the recovery rate by making a W104M mutant was increased by a factor of 3. This is consistent with the W104F mutant and indicates the importance of W104 in stabilization of lAppA.

The photoinactive Y21W mutant has been generated in the N-terminal BLUF domain of AppA (AppA<sub>BLUF</sub>) in order to investigate the mechanism of electron transfer between the protein

and chromophore. This proves the aromatic ring of tyrosine is crucial for the photoactivation mechanism and modifications to residue Y21 will be discussed in chapter 4. All Y21 mutants except Y21W resemble dAppA which is more similar to lAppA. In addition, the TRIR spectrum of Y21W has an intense transient at  $1634\text{ cm}^{-1}$ . This transient is in the same position as FADH• and is also weakly observed in lAppA but not dAppA. This allows us to conclude W104 is essential for formation of FADH•. Because this peak is also observed in lAppA it is apparent that W104 must be closer to the flavin in lAppA than in dAppA. This information combined with the two existing crystal structures of AppA, allow for assignment of dAppA to the W104<sub>Out</sub> structure and lAppA to the W104<sub>In</sub> structure.

The following chapter will probe the role of Y21 in the photoactivation mechanism of AppA by using mutagenesis and unnatural amino acids incorporation to make subtle changes in the protein. In addition, chapter 4 will also discuss further investigation of W104 motion by incorporating cyano and azido probes that are sensitive to structural and environmental changes.

## E. References

1. Stelling, A. L., Ronayne, K. L., Nappa, J., Tonge, P. J., and Meech, S. R. (2007) Ultrafast structural dynamics in BLUF domains: transient infrared spectroscopy of AppA and its mutants, *J Am Chem Soc* *129*, 15556-15564.
2. Masuda, S., Tomida, Y., Ohta, H., and Takamiya, K. (2007) The critical role of a hydrogen bond between Gln63 and Trp104 in the blue-light sensing BLUF domain that controls AppA activity, *J Mol Biol* *368*, 1223-1230.
3. Dragnea, V., Arunkumar, A. I., Lee, C. W., Giedroc, D. P., and Bauer, C. E. (2010) A Q63E *Rhodobacter sphaeroides* AppA BLUF domain mutant is locked in a pseudo-light-excited signaling state, *Biochemistry* *49*, 10682-10690.
4. Masuda, S., Hasegawa, K., Ishii, A., and Ono, T. A. (2004) Light-induced structural changes in a putative blue-light receptor with a novel FAD binding fold sensor of blue-light using FAD (BLUF); Slr1694 of *synechocystis* sp. PCC6803, *Biochemistry* *43*, 5304-5313.
5. Kondo, M., Nappa, J., Ronayne, K. L., Stelling, A. L., Tonge, P. J., and Meech, S. R. (2006) Ultrafast vibrational spectroscopy of the flavin chromophore, *J Phys Chem B* *110*, 20107-20110.
6. Haigney, A., Lukacs, A., Zhao, R. K., Stelling, A. L., Brust, R., Kim, R. R., Kondo, M., Clark, I., Towrie, M., Greetham, G. M., Illarionov, B., Bacher, A., Romisch-Margl, W., Fischer, M., Meech, S. R., and Tonge, P. J. (2011) Ultrafast infrared spectroscopy of an isotope-labeled photoactivatable flavoprotein, *Biochemistry* *50*, 1321-1328.
7. Wolf, M. M., Zimmermann, H., Diller, R., and Domratcheva, T. (2011) Vibrational Mode Analysis of Isotope-Labeled Electronically Excited Riboflavin, *J Phys Chem B*.



8. Brazard, J., Usman, A., Lacomat, F., Ley, C., Martin, M. M., and Plaza, P. (2011) New insights into the ultrafast photophysics of oxidized and reduced FAD in solution, *J Phys Chem A* *115*, 3251-3262.
9. Toh, K. C., van Stokkum, I. H. M., Hendriks, J., Alexandre, M. T. A., Arents, J. C., Perez, M. A., van Grondelle, R., Hellingwerf, K. J., and Kennis, J. T. M. (2008) On the signaling mechanism and the absence of photoreversibility in the AppA BLUF domain, *Biophys. J.* *95*, 312-321.
10. Kim, M. and Carey, P.R. (1993) Observation of a carbonyl feature for riboflavin bound to riboflavin-binding protein in the red-excited raman spectrum, *J Am Chem Soc* *115*, 7015–7016.
11. Kottke, T., Batschauer, A., Ahmad, M., and Heberle, J. (2006) Blue-light-induced changes in Arabidopsis cryptochrome 1 probed by FTIR difference spectroscopy, *Biochemistry* *45*, 2472-2479.
12. Immeln, D., Pokorny, R., Herman, E., Moldt, J., Batschauer, A., and Kottke, T. (2010) Photoreaction of plant and DASH cryptochromes probed by infrared spectroscopy: the neutral radical state of flavoproteins, *J Phys Chem B* *114*, 17155-17161.
13. Tonge, P., Moore, G. R., and Wharton, C. W. (1989) Fourier-transform infra-red studies of the alkaline isomerization of mitochondrial cytochrome c and the ionization of carboxylic acids, *Biochem. J.* *258*, 599-605.
14. Fahmy, K., Jager, F., Beck, M., Zvyaga, T. A., Sakmar, T. P., and Siebert, F. (1993) Protonation states of membrane-embedded carboxylic acid groups in rhodopsin and metarhodopsin II: a Fourier-transform infrared spectroscopy study of site-directed mutants, *Proc Natl Acad Sci U. S. A.* *90*, 10206-10210.

15. Lubben, M., and Gerwert, K. (1996) Redox FTIR difference spectroscopy using caged electrons reveals contributions of carboxyl groups to the catalytic mechanism of haem-copper oxidases, *FEBS Lett.* 397, 303-307.
16. Tonge, P. J. (1996) FTIR studies of hydrogen bonding between  $\alpha,\beta$ -unsaturated esters and alcohols, *J Mol Struct* 379, 135- 142.
17. Tozawa, K., Ohbuchi, H., Yagi, H., Amano, T., Matsui, T., Yoshida, M., and Akutsu, H. (1996) Unusual pKa of the carboxylate at the putative catalytic position of the thermophilic F1-ATPase beta subunit determined by  $^{13}\text{C}$ -NMR, *FEBS Lett.* 397, 122-126.
18. Henzler-Wildman, K., and Kern, D. (2007) Dynamic personalities of proteins, *Nature* 450, 964-972.
19. Rieff, B., Bauer, S., Mathias, G., and Tavan, P. (2011) DFT/MM description of flavin IR spectra in BLUF domains, *J Phys Chem B* 115, 11239-11253.
20. Dragnea, V., Waegele, M., Balascuta, S., Bauer, C., and Dragnea, B. (2005) Time-resolved spectroscopic studies of the AppA blue-light receptor BLUF domain from *Rhodobacter sphaeroides*, *Biochemistry* 44, 15978-15985.
21. Blanco-Rodriguez, A. M., Towrie, M., Sykora, J., Zalis, S., and Vlcek, A., Jr. (2011) Photoinduced intramolecular tryptophan oxidation and excited-state behavior of  $[\text{Re}(\text{L-AA})(\text{CO})_3(\text{alpha-diimine})]^+$  (L = pyridine or imidazole, AA = tryptophan, tyrosine, phenylalanine), *Inorg Chem* 50, 6122-6134.

## Chapter 4

# Modulating the Environment of the Hydrogen Bonding Network of AppA to Probe Time Dependent Structural Changes that Occur with Photoactivation

### A. Introduction

Residue Y21 is a critical component of the hydrogen bonding network that surrounds the flavin chromophore in AppA. Photoexcitation of the flavin results in modulation of the protein-flavin interactions that are mediated by this hydrogen bond network and ultimately lead to the light activated state of the protein. The importance of residue Y21 was previously shown through the Y21F mutation that renders the protein photoinactive and it has been proposed by other groups that electron transfer from Y21 to the flavin may be critical for photoactivation. In order to investigate the proposed mechanism of electron transfer between the protein and chromophore, we have generated various Y21 mutants that will be discussed in detail in this chapter. However, all of the mutations produced photoinactive proteins and in order to modify residue Y21 and retain photoactivity, we have incorporated the unnatural amino acid fluorotyrosine as a probe to alter the pKa and redox potential of tyrosine with minor structural perturbation.

Unnatural amino acids have been used as probes to study a variety of biochemical processes. These include monitoring both large scale conformational changes, such as protein folding, and observing small scale events, such as electron transfer. The benefit to using unnatural amino acids is the ability to retain structure and function while still modulating the protein environment. This chapter mainly focuses on unnatural amino acid probes incorporated into AppA<sub>BLUF</sub>. The unnatural probes we have used include fluorotyrosine analogs and cyanophenylalanine.

Fluorotyrosine has been used as probe to study the mechanism of electron transfer in numerous systems including photosystem II (1), GFP (3) and ribonucleotide reductase (4-7). The fluorinated derivatives alter both the pKa and the redox potential of the tyrosine with minor perturbation to the structure. The degree to which these two parameters are modified depends on the substitution pattern. Modulating the pKa and potential of Y21 in AppA, the tyrosine adjacent to the flavin, will enable us to unravel the interplay between proton transfer (or hydrogen bond breaking) and electron transfer. Incorporation of fluorotyrosines has commonly been used to determine whether proton coupled electron transfer (PCET) is concerted or separate (8, 9). If such a PCET mechanism proves important in AppA the incorporation of different substitution patterns will allow a degree of control over the mechanism. We have successfully generated fluorotyrosines and incorporated them specifically into Y21. These proteins have been studied using steady state and ultrafast spectroscopy. This will allow us to understand the significance of electron transfer in AppA.

Specific incorporation of various fluorinated tyrosines into position Y21 of AppA was completed using the photoactive Y56F AppA<sub>BLUF</sub> mutant. This mutant leaves Y21 as the only tyrosine residue in AppA and is described in the results and discussion section below. In addition, this chapter describes the expression and purification of tyrosine phenol lyase (TPL) which is a promiscuous enzyme capable of using a variety of phenols, ammonia and pyruvic acid to make tyrosine and analogs. In addition, these analogs were fed into cells grown in minimal media for fluorotyrosine incorporation into AppA. The percent incorporation was checked using MALDI mass spectroscopy.

In addition to using fluorotyrosine analogs to probe electron transfer, the unnatural amino acid cyanophenylalanine has been incorporated into AppA as an IR reporter. The azido and

cyano stretching frequencies are known to be sensitive to environment and structure. These probes are ideal reporter groups because they have a spectroscopically distinct signature, are non-perturbing to structure and are sensitive to changes in protein structure and environment. The stretching vibration of cyano and azido groups appears at  $\sim 2220$  and  $\sim 2120$   $\text{cm}^{-1}$ , respectively, in a region of the IR spectrum that is distinct from the protein (10, 11). Such spectral separation has of course historically been used to study the binding of CN and  $\text{N}_3$  ligands to heme proteins (12-15), and is now being used to study protein dynamics through site-specific incorporation of cyano and azido groups on amino acids. For example, the azido group has been used as an IR probe to study protein dynamics (11, 16, 17), while cyanophenylalanine is an excellent reporter on protein environment because it is very sensitive to changes in hydrophobicity (10, 18-20).

Three amino acids were chosen as initial replacements for cyanophenylalanine. These were two phenylalanine (F62 and F101) residues and one tyrosine (Y56) residue in AppA<sub>BLUF</sub>, since these amino acids are the most structurally similar to cyanophenylalanine. Importantly, cyanophenylalanine can be introduced site selectively at any position using the 21<sup>st</sup> pair (amber codon) methodology (19-22).

## B. Materials and Methods

### B.1. Tyrosine Phenol Lyase Purification:

The gene encoding the tyrosine phenol lyase (TPL) was cloned into a pet23b vector (Novagen) by Eduard Melief so that the protein is expressed with an N-terminal His-tag. TPL was expressed BL21DE3 PlyS *E. coli* cells which were then grown up in 10 mL cultures of LB media containing 0.5 mM ampicillin and 0.5 mM chloramphenicol at 37°C at 250 RPM. These cultures were used to inoculate 1 L of LB/ampicillin/chloramphenicol media, in 4 L flasks, which were grown to an OD<sub>600</sub> of approximately 0.8 at 37°C for 2.5 hrs. The temperature was then decreased to 25°C for 30 min followed by addition of 0.5 mM IPTG to induce protein growth overnight. The cells were harvested by centrifugation at 5,000 RPM at 4°C and immediately purified to ensure maximal protein yield. The cell pellet was then resuspended in lysis buffer (150 mM NaCl, 0.1 M NaH<sub>2</sub>PO<sub>4</sub>, 5 mM imidazole, 5 mM β-mercaptoethanol, 0.1 mM pyridoxal 5' phosphate buffer at pH 7). The cells were then lysed using sonication (sonicate 6x 45 seconds at 18 W and 1 min on ice between cycles). The cell debris was removed using centrifugation (33 K for 90 min). The protein was purified using Ni-NTA chromatography (Qiagen) with 150 mM NaCl, 0.1 M NaH<sub>2</sub>PO<sub>4</sub>, 5 mM β-mercaptoethanol at pH 7.00 wash buffer. The bound protein was then washed with a step gradient of 10 mM and 20 mM imidazole in buffer and eluted with 5 mL increments of 250 mM imidazole. The protein was immediately diluted by a factor of 2 with 150 mM NaCl, 0.1 M NaH<sub>2</sub>PO<sub>4</sub> at pH 7 and dialyzed overnight into 0.1 M NaH<sub>2</sub>PO<sub>4</sub>, 5 mM β-mercaptoethanol buffer at pH 7. The purity of the protein was determined using SDS-PAGE electrophoresis (**Figure 4.5**). These proteins were then concentrated to approximately 5 mg/mL and stored at 4°C in 20% glycerol for no more than 7 days.

## B.2. Enzymatic synthesis of Fluorinated Tyrosine Analogs:

The activity of TPL was determined using phenol, the natural substrate of the enzyme. The reaction mixture contained 360 mg phenol, 325 mg pyruvic acid, 1.5 mg pyridoxal-5'-phosphate and 570 mg ammonium acetate in 50 mL H<sub>2</sub>O. The pH of the reaction mixture was adjusted to 8 using NH<sub>4</sub>OH. This solution was then filtered using a 22 µm sterile filter and 8 units (.53 mg = 1 unit) of purified TPL were added to catalyze the reaction.

The reaction mixture was then stored in the dark at room temperature for a minimum of 4 days. Purification of tyrosine was performed by first acidifying the mixture using 5% trichloroacetic acid to precipitate out TPL. The precipitated protein was then removed by centrifugation at 5K RPM for 25 min at 4°C. An extraction using an equal volume of ethyl acetate was performed twice in order to remove excess phenol. The aqueous layer was heated until the tyrosine was solubilized. Purification was performed on a 10 cm ion exchange amberlite column activated with 50 mL of 2 N HCl. When cooled to room temperature the aqueous layer was poured on the column and air pressure was used if necessary to get a steady flow from the column. The tyrosine was then washed with 500 mL distilled deionized water and then the tyrosine was eluted with 250 mL of 4% NH<sub>4</sub>OH and 10 mL fractions were collected. The fractions were tested with a 4% ninhydrin solution for amine. Those fractions that tested positive were combined and lyophilized after freezing with liquid N<sub>2</sub> to give a solid white powder and a mass spectrum was attained to verify purity (**Figure 4.2**).

Production of 3-fluoro-L-tyrosine, 2-fluoro-L-tyrosine, 2,6-difluoro-L-tyrosine, 3,5-difluoro-L-tyrosine, 2,3,5,6-tetrafluoro-L-tyrosine and 2-nitro-L-tyrosine was also completed using the previously described protocol. However the aqueous layer was not heated because the lower pK<sub>a</sub> enabled solubility of the modified tyrosines at room temperature.

### B.3. AppA overexpression protocols for mutants and fluorotyrosine incorporation:

#### **Preparation of DNA constructs for AppA mutants:**

AppA mutants were constructed by site directed mutagenesis using Pfu Turbo (Stratagene). Primer sequences for Y56F were 5' ACC GGC GCG CTC TTC TTC AGC CAG GGC GTC TTC 3' (Forward) and 5' GAA GAC GCC CTG GCT GAA GAA GAG CGC GCC GGT 3' (Backward); primer sequences for Y21C were 5' CTG GTT TCC TGC TGC TGC CGC AGC CTG GCG GCC 3' (Forward) and 5' GGC CGC CAG GCT GCG GCA GCA GCA GGA AAC CAG 3' (Backward); primer sequences for Y21S were 5' CTG GTT TCC TGC TGC AGC CGC AGC CTG GCG GCC 3' (Forward) and 5' GGC CGC CAG GCT GCG GCT GCA GCA GGA AAC CAG 3' (Backward). primer sequences for Y21I were 5' CTG GTT TCC TGC TGC ATC CGC AGC CTG GCG GCC 3' (Forward) and 5' GGC CGC CAG GCT GCG CAT GCA GCA GGA AAC CAG 3' (Backward). All constructs were verified by DNA sequencing.

#### **Methods for Cell Growth and Protein Overexpression:**

Protein expression was performed by transforming the plasmid into BL21DE3 *E.coli* cells which were then grown up in 10 mL cultures of LB media containing 0.5 mM ampicillin at 37°C at 250 RPM. These cultures were used to infect 1 L of LB/ampicillin media, in 4 L flasks, which was grown to an OD<sub>600</sub> of approximately 1.2 at 30°C for 5 hrs. The temperature was then decreased to 18°C for 30 min followed by addition of 0.8 mM IPTG to induce protein expression overnight (16 hrs) in the dark.

#### **Methods for to Incorporate Fluorotyrosine:**

In order to incorporate fluorinated tyrosine specifically into position Y21, the mutant AppA Y56F was used to leave Y21 as the sole tyrosine in AppA. Protein expression for Y56F AppA in minimal media was carried out by transforming the plasmid containing Y56F



AppA<sub>BLUF</sub> in BL21DE3 *E. coli* cells and plating on LB/ampicillin agar. A single colony from this plate was then streaked on an M9 minimal media/glucose/ampicillin plate. A 500 mL of M9/ampicillin minimal media with 5 grams sterile glucose and 5 mL of 100X mem vitamins added after autoclaving, in 4 L flasks was inoculated with a colony from the M9 plate. The cells were grown to an OD<sub>600</sub> of approximately 0.8 at 30°C for 24 hrs. These cells were then spun down and resuspended in fresh media with 300 mg of fluorotyrosine and incubated for 30 min at 18°C. Subsequently 0.8 mM IPTG was used to induce protein expression for 5 hrs in the dark before harvesting. The cell pellet resulting from a 1 L culture was resuspended in 40 mL of buffer A (50 mM NaH<sub>2</sub>PO<sub>4</sub> buffer pH 8 containing 10 mM NaCl) to which was added 200 µL of the protease inhibitor phenylmethanesulphonylfluoride (50 mM stock solution in ethanol), and 14 µL of β-mercaptoethanol. The cells were then lysed using sonication, cell debris was removed by centrifugation (33K rpm for 90 min), and the supernatant was incubated with a 1 mL of 10 mg/mL of FAD for 45 min on ice in the dark to ensure a homogeneous population of protein bound chromophore (23). Following incubation, the solution was loaded onto a Ni-NTA column (1x10 cm) that had been preequilibrated with pH 8 phosphate buffer, and then washed with 50 mL of buffer A. The column was then washed with buffer A containing increasing concentrations of imidazole until AppA<sub>BLUF</sub> eluted at 250 mM imidazole. The fractions containing protein were pooled, dialyzed against buffer A overnight, and concentrated to 1.5 mM. Protein purity was assessed by SDS-PAGE electrophoresis and UV-vis spectroscopy (protein,  $\epsilon_{270} = 35,800 \text{ M}^{-1} \text{ cm}^{-1}$ ; FAD  $\epsilon_{446} = 8,500 \text{ M}^{-1} \text{ cm}^{-1}$ ). Chromophore content was determined by the ratio of protein to FAD absorbance (4.2 for wild-type AppA<sub>BLUF</sub> with FAD bound (24)). To exchange the protein into D<sub>2</sub>O, samples of AppA were frozen in liquid N<sub>2</sub>, lyophilized overnight, redissolved in pH 8 buffer, and allowed to incubate for 5 hrs after which

this process was repeated 3-4 times. Both exchanged and unexchanged proteins were stored as lyophilized powders at -80°C until needed. Percent incorporation of fluorination at position Y21 was determined using a trypsin digest and MALDI mass spectroscopy.

#### B.4. Incorporation of cyanophenylalanine using amber codon methodology:

In order to use the 21<sup>st</sup> pair method AppA must be cloned into a pBAD vector. The DNA encoding AppA<sub>BLUF</sub> (residues 5-125) was excised from the pET15b vector with the restriction enzymes NcoI and BamHI and purified using PCR product purification kit (Roche). Using these restriction sites the N-terminal hexahistidine tag is retained. The new vector, pBADmyc His (Invitrogen), was then digested with NcoI and BglII. This vector was then ligated to AppA<sub>BLUF</sub> with the remaining N-terminal hexahistidine tag. In order to avoid 21<sup>st</sup> pair incorporation, the amber stop codon (TAG) at the end of the gene was replaced using mutagenesis to TAA using the following primer: 5' GCC GAG AGC CGG CAG TAA GGA TCT GCA GAT GGT 3'. The amber mutants were generated at positions Y56, F62 and F101 by mutagenesis using the following primers: 5' ACC GGC GCG CTC TTC TAG AGC CAG GGC GTC TTC 3', 5' AGC CAG GGC GTC TTC TAG CAG TGG CTC GAA GGC 3' and 5' ATC GCC AAG CGC CGC TAG GCG GGA TGG CAC ATG 3' respectively.

The protein was expressed in BL21AI *E. coli* cells using the construct described above in which the AppA<sub>BLUF</sub> coding sequence had been inserted into a pBAD vector. Protein expression and purification was performed in the dark in auto induction media as described by Hammill *et al.* (21) Each amber mutant was cotransformed with the pDule vector (kindly obtained from the Raleigh lab) that encoded for the tRNA/synthetase pair that recognizes cyanophenylalanine into BL21AI *E. coli* cells and plated on an LB/ampicillin/spectinomycin agar. A single colony from

this plate was then used to make a 6 mL overnight culture in LB media with added ampicillin and spectinomycin. After 12 hrs, 3 mL of this overnight was used to inoculate 500 mL of auto induction media. The cells were grown at 30°C for 24 hrs and then harvested by centrifugation at 5K RPM for 15 min. The cell pellet resulting from a 1 L culture was resuspended in 40 mL of buffer A (50 mM NaH<sub>2</sub>PO<sub>4</sub> buffer pH 8 containing 10 mM NaCl) to which was added 200 µL of the protease inhibitor phenylmethanesulphonylfluoride (50 mM stock solution in ethanol), and 14 µL of β-mercaptoethanol. The cells were then lysed using sonication, cell debris was removed by centrifugation (33K RPM for 90 min), and the supernatant was incubated with 1 mL of a 10 mg/mL solution of FAD for 45 min on ice in the dark to ensure a homogeneous population of protein bound chromophore (23). Following incubation, the solution was loaded onto a Ni-NTA column (1x10 cm) that had been preequilibrated with pH 8 phosphate buffer, and then washed with 50 mL of buffer A. The column was then washed with buffer A containing increasing concentrations of imidazole until AppA<sub>BLUF</sub> eluted at 250 mM imidazole. The fractions containing protein were pooled, dialyzed against buffer A overnight, and concentrated to 1.5 mM. Protein purity was assessed by SDS-PAGE electrophoresis and UV-vis spectroscopy (protein,  $\epsilon_{270} = 35,800 \text{ M}^{-1} \text{ cm}^{-1}$ ; FAD  $\epsilon_{446} = 8,500 \text{ M}^{-1} \text{ cm}^{-1}$ ). Chromophore content was determined by the ratio of protein to FAD absorbance (4.2 for wild-type AppA<sub>BLUF</sub> with FAD bound (24)). To exchange the protein into D<sub>2</sub>O, samples of AppA were frozen in liquid N<sub>2</sub>, lyophilized overnight, redissolved in pD 8 buffer, and allowed to incubate for 5 hrs after which this process was repeated 3-4 times. Both exchanged and unexchanged proteins were stored as lyophilized powders at -80°C until needed. Percent incorporation of cyanophenylalanine was determined using a trypsin digest and MALDI mass spectroscopy.

#### B.4. Time-Resolved Infrared Spectroscopy:

Ultrafast time-resolved IR (TRIR) spectra were measured at the STFC Central Laser Facility using a TRIR system exploited a recently developed high sensitivity 10 kHz repetition rate source with  $\sim 100$  fs time resolution. The apparatus will be described in detail elsewhere (Greetham et al Submitted). The key differences compared to the 1 kHz source were an improved signal to noise resulting from the faster repetition rate and more stable source and a wider spectral bandwidth permitting the  $1400 - 1800 \text{ cm}^{-1}$  wavenumber range to be measured in one experiment. For this source the excitation spot size was  $\sim 100 \text{ }\mu\text{m}$  radius and the pulse energy was kept below 400 nJ. The possible effect of the higher repetition rate on the photokinetics of the photoactive samples should be considered. For this 10 kHz source photoactive proteins were studied in a flow cell which was used in addition to rastering of the sample holder in the beam path, thus minimizing photobleaching and degradation of the protein and the photoconversion of dark adapted AppA<sub>BLUF</sub>. Even under these condition if the pump pulse energy exceeded 600 nJ the transient spectrum measured at 3 ps was observed to be a mixture of dark and light adapted AppA<sub>BLUF</sub>. Below 400 nJ the dark adapted AppA<sub>BLUF</sub> spectrum was independent of pump intensity. Under these conditions the spectra and the kinetics (ground state recovery) were compared with those measured on the 1 kHz spectrum and were seen to be the same within the signal – to noise. The IR probe again recorded transient difference spectra (pump on – pump off) at time delays between 1 ps and 2 ns. After the measurements were recorded the extent of photoconversion was shown to be negligible using absorbance spectroscopy. To retain the same spectral resolution as for the 1 kHz system the probe was measured by two carefully matched 128 pixel detectors, yielding a resolution of  $3 \text{ cm}^{-1}$  per pixel.

Spectra were calibrated relative to the IR transmission of a pure *cis* stilbene standard sample placed at the sample position.

Light adapted AppA<sub>BLUF</sub> was prepared by irradiating dAppA<sub>BLUF</sub> at 365 nm using a hand held UV illuminator. Photoconversion was monitored using UV-vis spectroscopy and was found to be complete within 3 min.

## C. Results and Discussion

### C.1. Y21 Mutants (Y21C, Y21S and Y21I):

Y21 is a critical component of the hydrogen bonding network that surrounds the flavin chromophore in AppA. Photoexcitation of the flavin results in modulation of the protein-flavin interactions that are mediated by this hydrogen bond network and that ultimately lead to the light activated state of the protein. The importance of Y21 was previously shown through the Y21F mutation that renders the protein photoinactive (25) and it has been proposed by other groups that electron transfer from Y21 to the flavin may be critical for photoactivation. The Y21C, Y21S and Y21I AppA<sub>BLUF</sub> mutants have generated in order to investigate the mechanism of electron transfer between the protein and chromophore. These mutants are all photoinactive and are trapped in a dark like conformation of the protein.

In order to investigate structural changes that occur rapidly upon absorption of 450 nm light, we used ultrafast TRIR spectroscopy to gain further insight into the structure of the Y21 AppA<sub>BLUF</sub> mutants. The TRIR spectrum of Y21C AppA<sub>BLUF</sub> acquired 3 ps after photoexcitation is shown in **Figure 4.1** together with the corresponding spectra of d and lAppA<sub>BLUF</sub>. Since the frequency of the C4=O flavin carbonyl in Y21C AppA<sub>BLUF</sub> is similar to that in dAppA<sub>BLUF</sub>, it is reasonable to propose that Y21C prevents Q63 from forming a hydrogen bond to C4=O as proposed in the light activated state of the protein. In order to form the lAppA, Q63 must tautomerize and then rotate to form a new set of hydrogen bonds to residue Y21 and an oxygen atom (O4) on the flavin. It is critical for residue Y21 to act as a hydrogen bond donor in order to stabilize this orientation of Q63. This is consistent with what is observed for the Y21S and Y21I mutant shown in **Figure 4.2** and **Figure 4.3**. Therefore, all the Y21 mutants resemble dAppA where the high frequency carbonyl (C4=O) is found at 1700 cm<sup>-1</sup> confirming the carbonyl is not

forming a hydrogen bond to Q63. In addition, the photoactive marker at  $1666\text{ cm}^{-1}$  is no longer seen in the spectrum of Y21C.

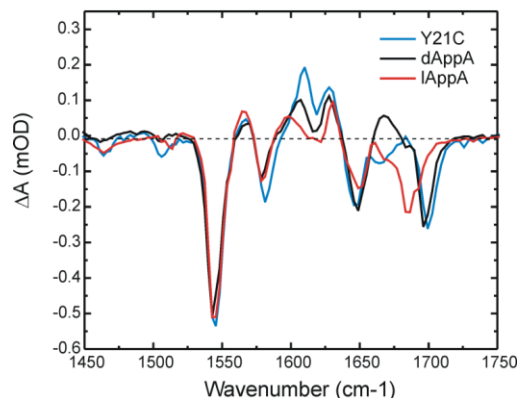


**Figure 4.1. TRIR spectra of wild-type d and lAppA<sub>BLUF</sub> and Y21C AppA<sub>BLUF</sub> measured at 3 ps.** TRIR spectra of dAppA<sub>BLUF</sub> (black), lAppA<sub>BLUF</sub> (red) and Y21C AppA<sub>BLUF</sub> (blue) bound to FAD. Protein concentration was 2 mM in pD 8 phosphate buffer and the TRIR spectra were recorded with a time delay of 3 ps. The spectra have been normalized to the intense FAD ring bleach mode at  $1547\text{ cm}^{-1}$ .

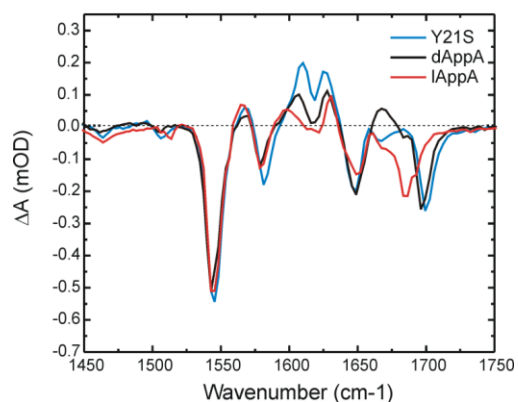


**Figure 4.2. TRIR spectra of wild-type d and lAppA<sub>BLUF</sub> and Y21S AppA<sub>BLUF</sub> measured at 3 ps.** TRIR spectra of dAppA<sub>BLUF</sub> (black), lAppA<sub>BLUF</sub> (red) and Y21S AppA<sub>BLUF</sub> (blue) bound to FAD. Protein concentration was 2 mM in pD 8 phosphate buffer and the TRIR spectra were recorded with a time delay of 3 ps. The spectra have been normalized to the intense FAD ring bleach mode at  $1547\text{ cm}^{-1}$ .

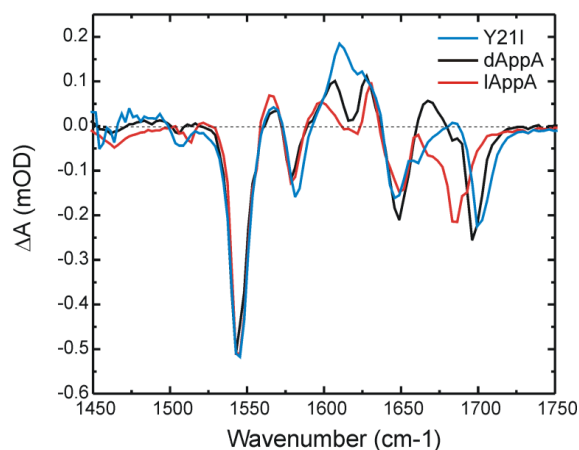


**Figure 4.3. TRIR spectra of wild-type d and lAppA<sub>BLUF</sub> and Y21I AppA<sub>BLUF</sub> measured at 3 ps.** TRIR spectra of dAppA<sub>BLUF</sub> (black), lAppA<sub>BLUF</sub> (red) and Y21I AppA<sub>BLUF</sub> (blue) bound to FAD. Protein concentration was 2 mM in pD 8 phosphate buffer and the TRIR spectra were recorded with a time delay of 3 ps. The spectra have been normalized to the intense FAD ring bleach mode at 1547 cm<sup>-1</sup>.

When comparing the ground state recovery kinetics of AppA<sub>BLUF</sub> mutants, there is common theme. Either the kinetics of the 1547 cm<sup>-1</sup> bleach for each mutant is similar to dAppA or lAppA (**Figure 4.4**). The Y21C, Y21S and Y21I mutants have kinetics similar to dAppA. This indicates these mutations have trapped the protein in a dark state conformation around the flavin. This is in consistent with the position of the flavin C4=O mode of Y21C, Y21S and Y21I AppA<sub>BLUF</sub> in which the flavin C4=O arises at the same frequency as dAppA<sub>BLUF</sub> (1700 cm<sup>-1</sup>) which is more weakly hydrogen bonded than lAppA<sub>BLUF</sub>.

Returning to the wild-type protein, our observation thus suggests that residue Y21 must be able to act as a hydrogen bond donor to Q63 in order to stabilize lAppA. The change in electronic structure of the flavin upon photoexcitation ultimately leads to a tautomerization followed by a rotation of residue Q63 in the wild-type protein and it is necessary for residue Y21



to make a hydrogen bond to the final rotated conformation of Q63 which is hydrogen bonded to the flavin C4=O in lAppA (**Figure 4.5**).

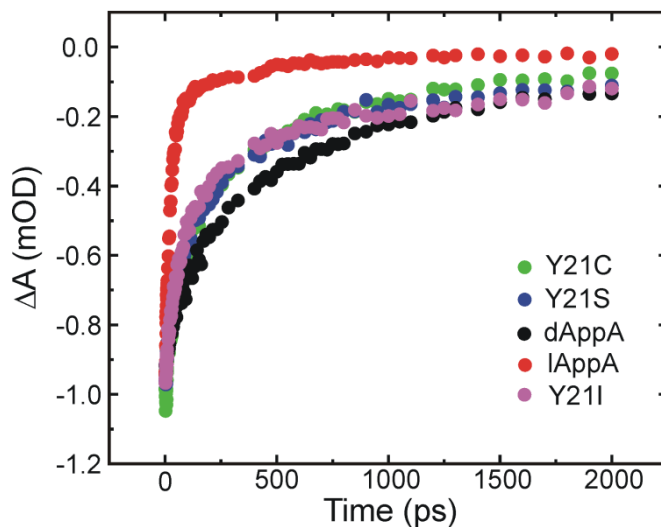


**Figure 4.4. Kinetics of the ground state recovery for wild-type d and lAppA<sub>BLUF</sub> and the Y21 AppA<sub>BLUF</sub> mutants using TRIR spectroscopy measured at 1547 cm<sup>-1</sup>.**

Comparison of kinetic measurements of dAppA<sub>BLUF</sub> (black), lAppA<sub>BLUF</sub> (red), Y21C (green), Y21S (blue) and Y21I (pink) AppA<sub>BLUF</sub> bound to FAD. The ground state recovery kinetics were fit to a 2 component exponential decay where the lifetimes of dAppA<sub>BLUF</sub>, lAppA<sub>BLUF</sub>, Y21C, Y21S and Y21I AppA<sub>BLUF</sub> were 36/559, 21/272, 55/502, 52/491, 56/456 ps for the short and long components respectively. Protein concentration was 2 mM in pD 8 phosphate buffer and the ground state recovery kinetics are measured at the intense bleach at 1547 cm<sup>-1</sup>.

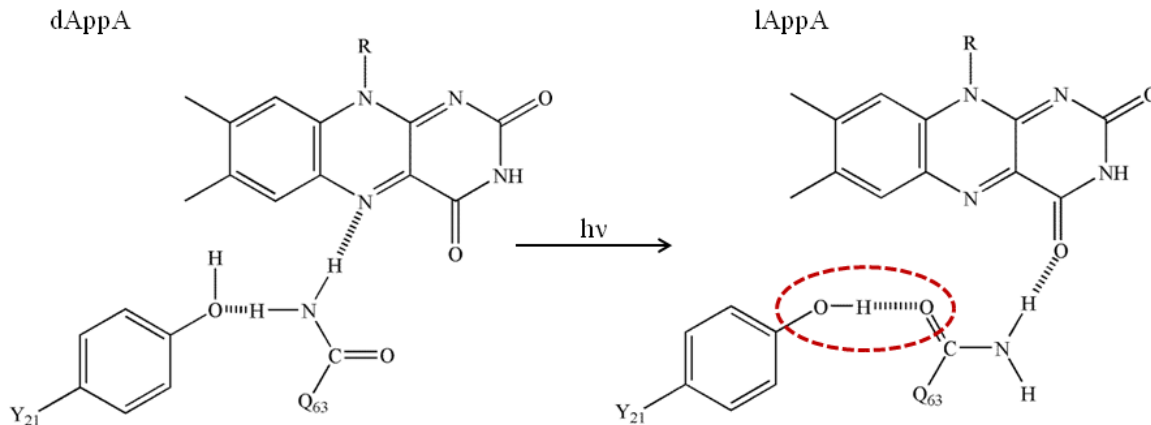


**Figure 4.5. Protein configuration of residues Y21 and Q63 in wild-type d and lAppA<sub>BLUF</sub>.**

The change in electronic structure of the flavin upon photoexcitation ultimately leads to a tautomerization followed by a rotation of residue Q63. This reorganization lead to Q63 forming a new hydrogen bond to the C4=O of the flavin in lAppA. It is essential for residue Y21 to create a hydrogen bond to the final rotated conformation of Q63 in order to stabilize lAppA.

Further investigation of the role of residue Y21 in the photoactivation mechanism of AppA will be probed by incorporating fluorotyrosine analogs specifically into residue Y21. Fluorotyrosines are isosteric to tyrosine and therefore offer minimal structural perturbation to AppA. Fluorination at different positions on tyrosine allow for a large range of pKa values and the effect of these more subtle changes to Y21 will be discussed in the following section.

## C.2. Tyrosine Phenol Lyase- Enzymatic production of fluorinated and nitro tyrosine:

### Tyrosine Phenol Lyase (TPL):

TPL is an enzyme that catalyzes the reversible breakdown of L-tyrosine to phenol, pyruvic acid and ammonia (26). This enzyme has been used to make tyrosine enzymatically. In addition, fluorinated phenols have been used instead of phenol to produce tyrosine analogs (27). We have cloned, expressed and purified TPL to enzymatically produce a variety of fluorinated tyrosine analogs. These include 2,6-difluorotyrosine, 3,5-difluorotyrosine, 3-fluorotyrosine and 2-fluorotyrosine. The SDS-PAGE gel of the purification of TPL is shown in **Figure 4.6**. After the protein was purified, a reaction was set up using fluorophenol derivatives to produce the corresponding fluorotyrosine analog. Each fluorotyrosine analog was purified and electrospray ionization mass spectrometry was performed to detect product formation and purity. A ESI mass spectrum is shown in **Figure 4.7** for 2,6-difluorotyrosine and the correct mass of 218 was observed. These unnatural amino acids were then used in feeding experiments in the Y56F mutant in order to specifically incorporate fluorotyrosine analogs into position Y21.

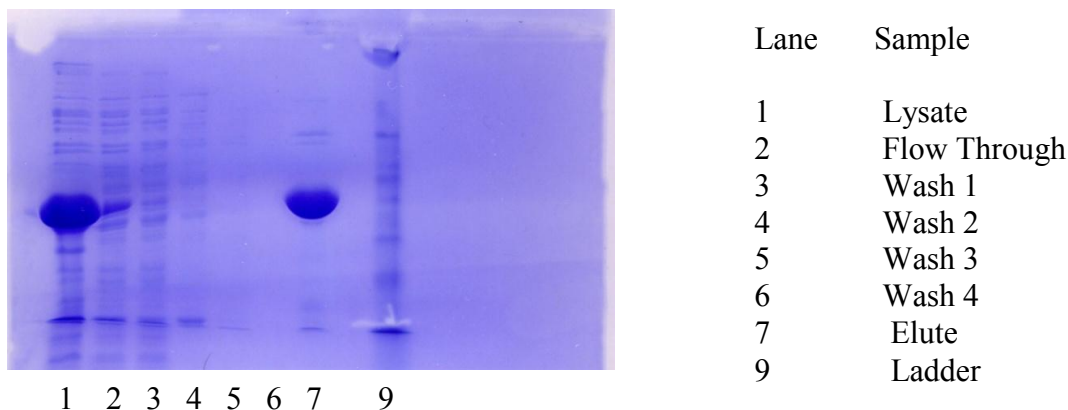


**Figure 4.6. SDS PAGE gel illustrating the purification of TPL.**

15% acrylimide gel of TPL purification. This gel was run at 90 volts for 135 minutes.

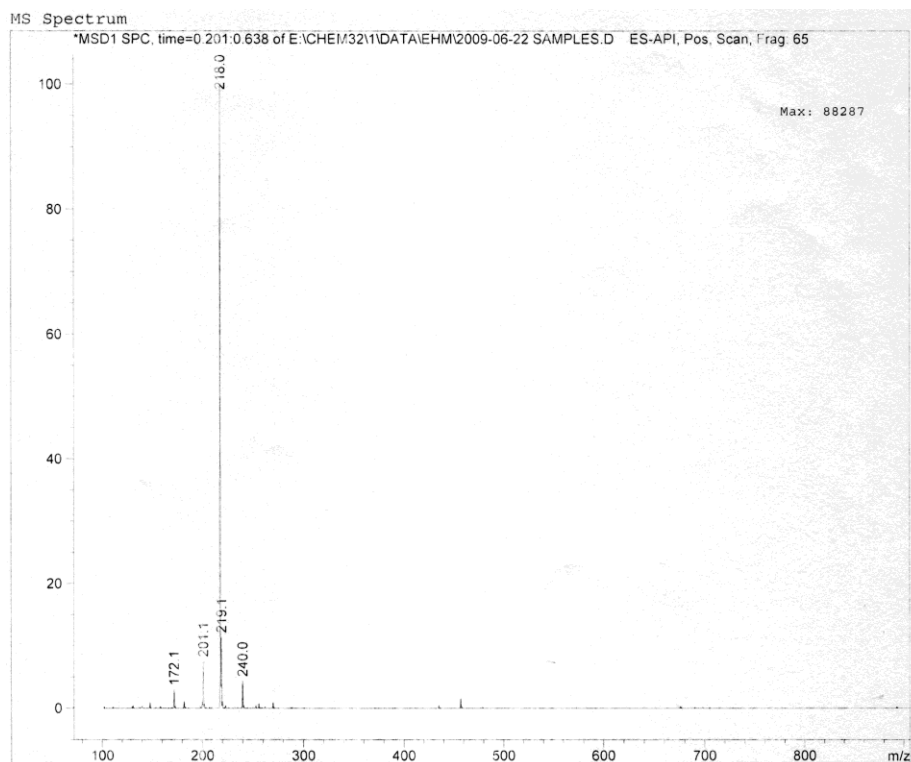


**Figure 4.7. Mass spectrum of 2,6-difluorotyrosine.**

Calculated mass is 217.1 g/mol. Experimental mass from MS is 218.0 g/mol.

### C.3. Y56F AppA<sub>BLUF</sub>:

AppA<sub>BLUF</sub> has only two tyrosines residues (Y21, which is essential for photoexcitation and Y56). We have generated Y56F AppA<sub>BLUF</sub> in order to specifically incorporate fluorotyrosine analogs into residue Y21. This mutant allows for specific labeling of Y21 by feeding cells with fluorinated tyrosine derivatives that have been made enzymatically. The preliminary data shows the Y56F mutant is photoactive (**Figure 4.8**) and exhibits a photocycle (ie recovers to the dark state in 30 minutes) similar to wild-type AppA. In addition, the TRIR spectra shown in **Figure 4.9** of both d and lY56F AppA overlay perfectly with wild-type AppA.

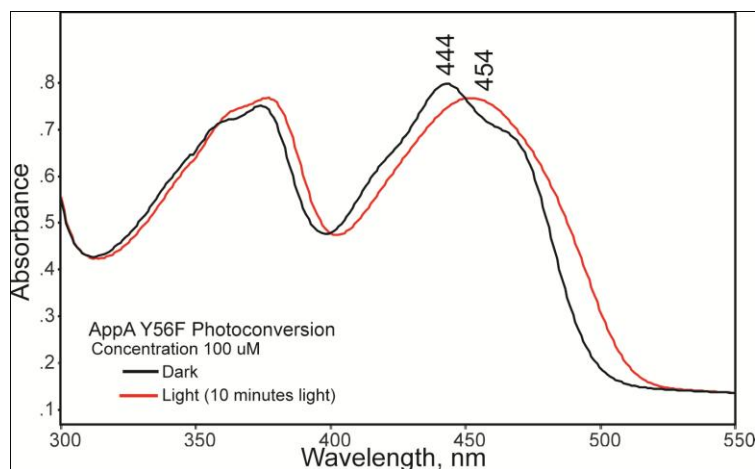


**Figure 4.8. Electronic absorption spectra of Y56F AppA<sub>BLUF</sub>.**

The light state of Y56F AppA<sub>BLUF</sub> was generated by exciting the sample with 365 nm light.

Concentration: 100  $\mu$ M pH 8.

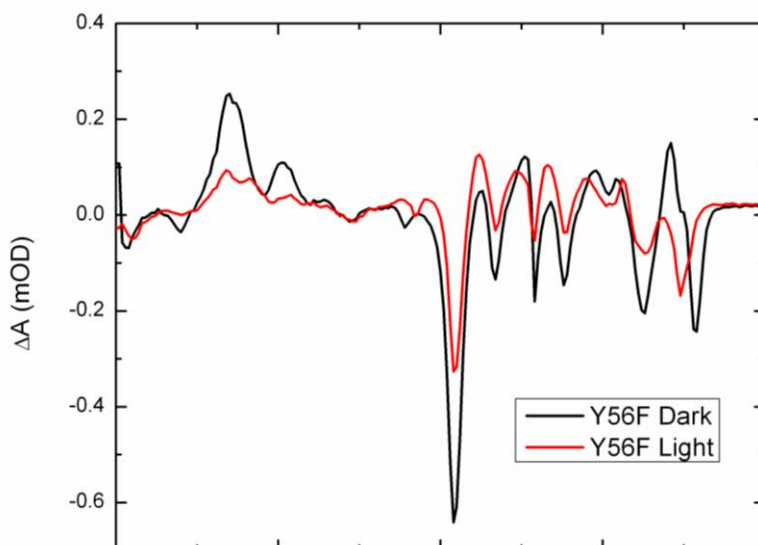


**Figure 4.9. TRIR spectra of Y56F d and lAppA<sub>BLUF</sub> measured at 3 ps.**

TRIR spectra of dY56F AppA<sub>BLUF</sub> (black), lY56F AppA<sub>BLUF</sub> (red) bound to FAD. Protein concentration was 2 mM in pD 8 phosphate buffer and the TRIR spectra were recorded with a time delay of 3 ps.

#### C.4. Incorporation of fluorinated tyrosines into Y56F AppA:

Growth in minimal media enables the incorporation of isotopically labeled and modified amino acids into proteins. The current opinion on the formation of the signaling state of AppA involves the transfer of a hydrogen from Y21 to either a neighboring residue (Q63) or directly to the flavin chromophore. Introducing a fluorine atom into the phenol ring of Y21 will reduce the pKa of the tyrosine hydroxyl. The lower pKa could therefore have the effect of changing kinetics of the photocycle in AppA leading to a better understanding of Y21's role in photoactivity.

The Y56F AppA<sub>BLUF</sub> mutant was shown to have a photocycle similar to wild-type and we have successfully replaced Y21 in Y56F AppA<sub>BLUF</sub> with 3,5-difluorotyrosine, 2,6-difluorotyrosine, 3-fluorotyrosine and 2-fluorotyrosine. The percent incorporation of 3-fluorotyrosine into AppA<sub>BLUF</sub> was determined by MALDI-TOF Mass spectrometry of a trypsin digest of the protein and was calculated to be 93 % (**Figures 4.10** and **4.11**). Both steady state (UV-vis) and ultrafast (TRIR) spectroscopy were used to characterize these proteins.

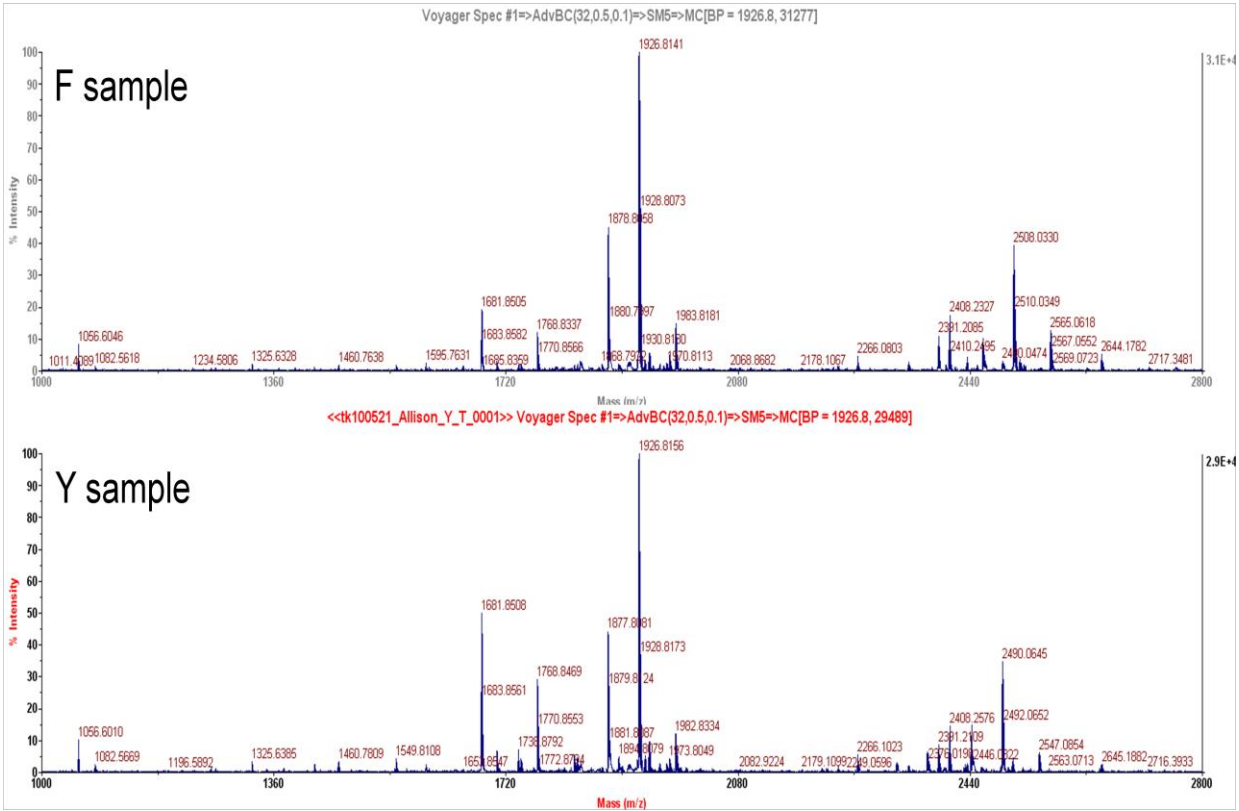


**Figure 4.10. MALDI mass spectra of fluorotyrosine incorporation.**

MALDI mass spectra of trypsin digested Y56F containing Y21 with (F) and without (Y) added 3-fluoro-L-tyrosine allowing for percent incorporated calculation. A blown up version of the region with the peptide containing residue Y21 is shown in **Figure 4.11**.

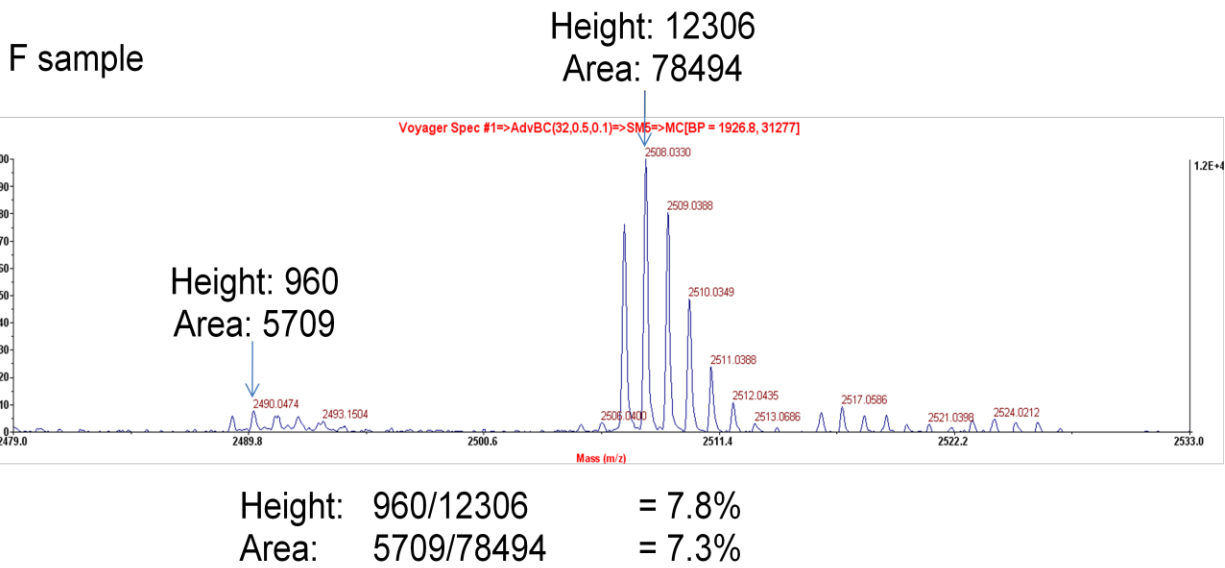
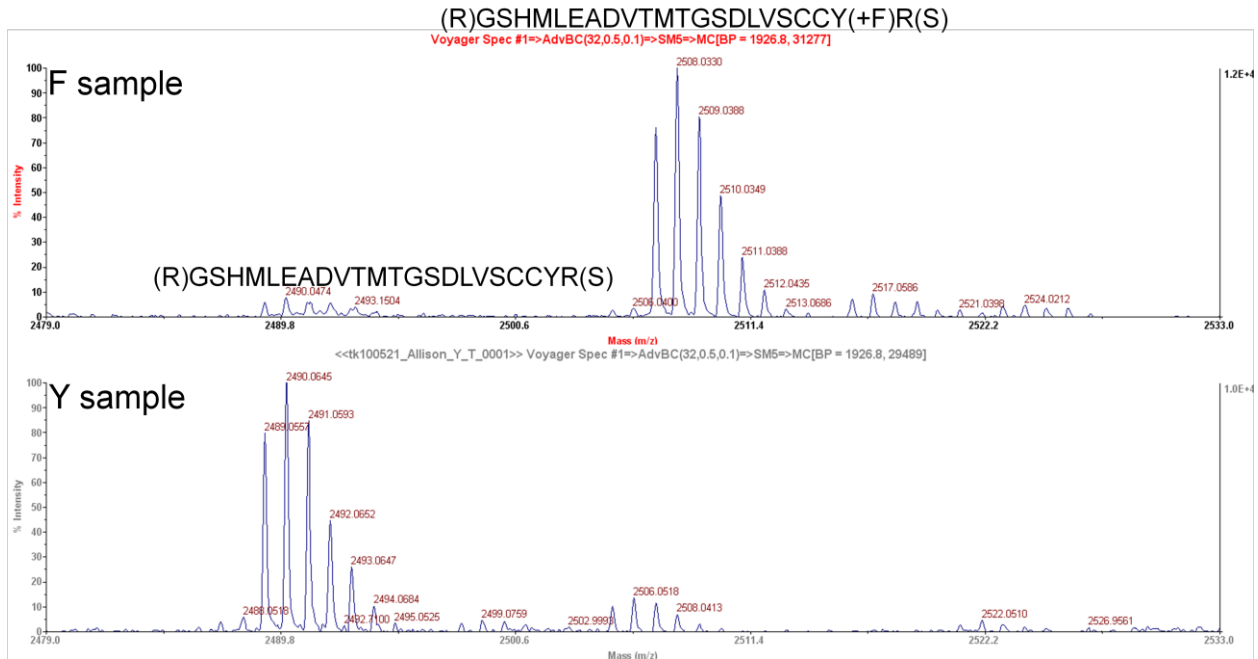
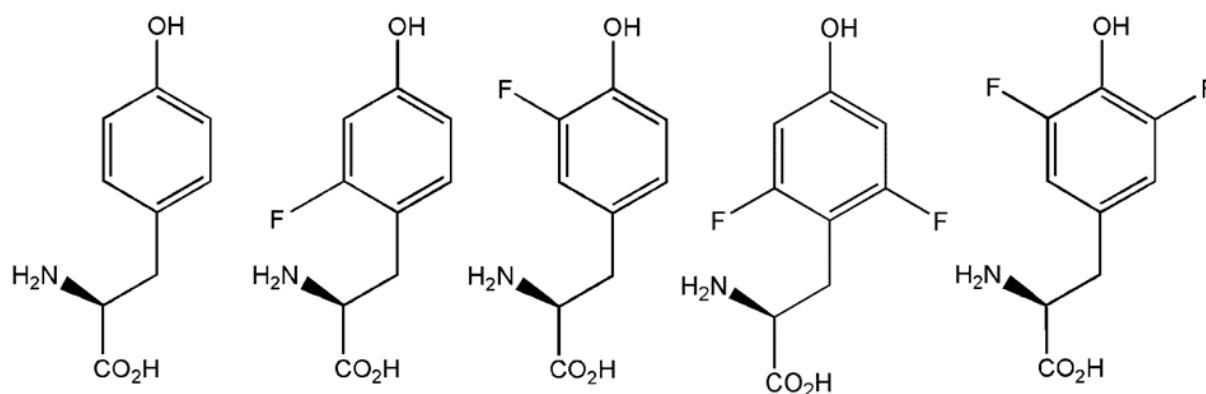


**Figure 4.11. MALDI mass spectra of peptide containing fluorotyrosine.**

MALDI mass spectra of trypsin digested Y56F zoomed in of the peptide GSHMLEADV TMTGSDLVSCCYRS containing Y21 with (F) and without (Y) added 3-fluoro-L-tyrosine allowing for percent incorporated calculation. Calculated mass of peptide without fluorine is 2463 g/mol and experimental mass is 2490 g/mol. Calculated mass of peptide with fluorine is 2481 g/mol and experimental mass is 2508 g/mol.





	Tyrosine (Y)	2FY	3FY	2,6dFY	3,5dFY
pK <sub>a</sub>	10	9.0	8.4	8.1	6.8
Binds Flavin	Yes	Yes	Yes	Yes	No
Photoactive	Yes	Yes	Yes	ND	No

**Table 4.1. Fluorotyrosine analogs incorporated into residue Y21.**

Summary of fluorotyrosine derivatives incorporated specifically into residue Y21 of AppA<sub>BLUF</sub> including theoretical pK<sub>a</sub> values for the hydroxyl group. 3,5dFY21 does not bind flavin, The 3FY21 and 2FY21 AppA<sub>BLUF</sub> proteins retained photoactivity. 2,6dFY21 has either a very fast light to dark recovery or is not photoactive.

### C.5. Incorporation of 3,5-difluorotyrosine into residue Y21

When residue Y21 was replaced with 3,5-difluorotyrosine (3,5-dFY21) the protein did not bind flavin. This was determined by electronic absorption spectroscopy where the spectrum of the protein did not have absorbance intensity at either 450 or 350 nm corresponding to the  $S_0$  to  $S_1$  and  $S_0$  to  $S_2$  transitions respectively of oxidized flavin. In order to favor the bound state of the protein, 3,5-dFY21 AppA<sub>BLUF</sub> was incubated with a 10 fold excess of flavin for 45 minutes and then was washed with buffer using serial dilution and concentration in order to remove the unbound flavin. However, 3,5-dFY21 AppA<sub>BLUF</sub> did not bind flavin under these conditions either. A possible explanation for absence of flavin is that the electrostatics in the binding pocket of 3,5-dFY21 AppA<sub>BLUF</sub> cause an unfavorable environment for the isoalloxazine ring. In addition, it is possible the large decrease in pKa (3,5-difluorotyrosine has a pKa of 6.8) creates a completely anionic state of the tyrosine which destabilizes the binding pocket of the flavin.

### C.6. Incorporation of 3-fluorotyrosine into residue Y21

When residue Y21 was replaced with 3-fluorotyrosine (3FY21) the protein bound flavin and is photoactive with a very fast light to dark state recovery. The electronic spectrum of the light to dark recovery is shown in **Figure 4.12** and when the absorbance at 495 nm is plotted as a function of time the lifetime of l3FY21 AppA<sub>BLUF</sub> is calculated to be 2.34 minutes in D<sub>2</sub>O buffer. This is approximately 20 times faster than wild-type AppA in D<sub>2</sub>O. The rate of recovery had to be calculated in D<sub>2</sub>O buffer because no shift of the flavin 450 nm transition was observed in H<sub>2</sub>O where the sample recovers ~2.5 fold faster. The increased rate of recovery suggests the acidity of Y21 plays an important role in the stabilization of lAppA and will be discussed in greater detail later.

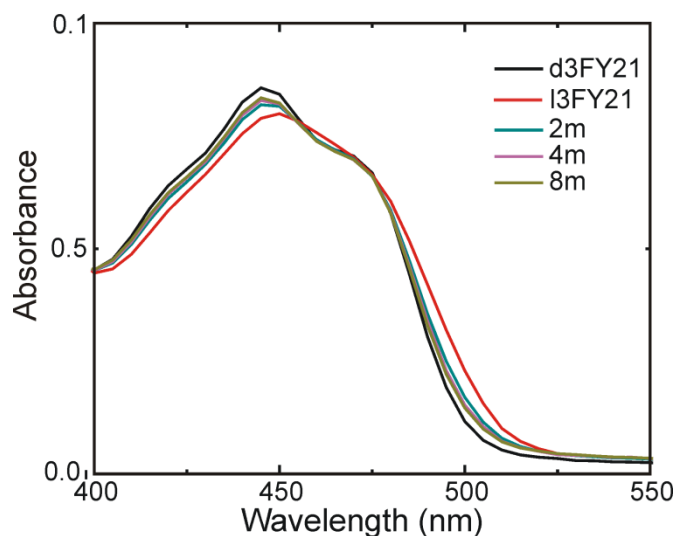


**Figure 4.12. Electronic absorption spectra of 3FY21 AppA<sub>BLUF</sub> recovery from light to dark state bound to FAD.** The light state of 3FY21 AppA<sub>BLUF</sub> was generated by exciting the sample with 365 nm light and the protein was allowed to recover in the dark. Spectra were recorded 1, 2, 4, and 8 minutes after light absorption to monitor light to dark recovery. Concentration: 80  $\mu$ M pH 8.

The TRIR spectra of 3FY21 AppA<sub>BLUF</sub> are shown in **Figure 4.13**. The spectra are similar to the wild-type protein, suggesting there is either little or no change to the protein due to the addition of a fluorine atom. The kinetics of the 1547  $\text{cm}^{-1}$  intense bleach of dAppA<sub>BLUF</sub>, lAppA<sub>BLUF</sub>, l3FY21 AppA<sub>BLUF</sub> and d3FY21 AppA<sub>BLUF</sub> are shown in **Figure 4.14** and again are comparable to the wild-type protein where the ground state recovery for light state both samples recovers approximately 3 times faster than the dark state.

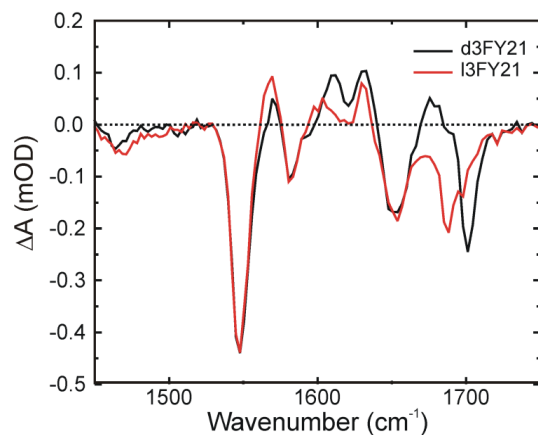


**Figure 4.13. TRIR spectra of d and l3FY21 AppA<sub>BLUF</sub> measured at 3 ps.** TRIR spectra of d3FY21AppA<sub>BLUF</sub> (black) and l3FY21AppA<sub>BLUF</sub> (red) bound to FAD. Protein concentration was 2 mM in pD 8 phosphate buffer and the TRIR spectra were recorded with a time delay of 3 ps. The spectra have been normalized to the intense FAD ring bleach mode at 1547 cm<sup>-1</sup>.

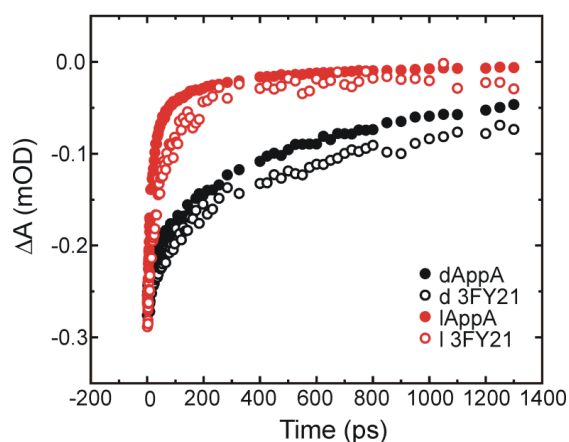


**Figure 4.14. Kinetics of the ground state recovery for wild-type d and lAppA<sub>BLUF</sub> and d and l3FY21 AppA<sub>BLUF</sub> using TRIR spectroscopy measured at 1547 cm<sup>-1</sup>.**

Comparison of kinetic measurements of dAppA<sub>BLUF</sub> (black, filled), lAppA<sub>BLUF</sub> (red, filled), d3FY21 AppA<sub>BLUF</sub> (black, hollow) and l3FY21AppA<sub>BLUF</sub> (red, hollow) bound to FAD. The lifetimes of dAppA<sub>BLUF</sub>, lAppA<sub>BLUF</sub>, 3FY21 dAppA<sub>BLUF</sub> and 3FY21 lAppA<sub>BLUF</sub> were 36/559, 21/272, 68/559 and 25/141 ps for the short and long components respectively. Protein concentration was 2 mM in pD 8 phosphate buffer and the ground state recovery kinetics are measured at the intense bleach at 1547 cm<sup>-1</sup>.

### C.7. Incorporation of 2-fluorotyrosine into Residue Y21

When 2-fluorotyrosine was incorporated into Y21 (2FY21) of AppA<sub>BLUF</sub> the protein bound flavin and was photoactive. This was determined by electronic absorption spectroscopy where the spectrum showed a shift in the 450 nm absorbance characteristic of photoactivity (**Figure 4.16a**). 2FY21AppA<sub>BLUF</sub> has smaller shift in absorbance (2 nm) upon formation of the light state in comparison to wild-type AppA<sub>BLUF</sub> (13 nm, **Figure 4.16b**) at the same concentration and pH and a faster light to dark state recovery (**Table 2**). The lifetime of 12FY21AppA<sub>BLUF</sub> is calculated to be 7.02 minutes in D<sub>2</sub>O buffer. This is approximately 5.6 times faster than wild-type AppA<sub>BLUF</sub> in D<sub>2</sub>O. This increased rate was also observed in 3FY21 AppA<sub>BLUF</sub> and is likely due to a change in the acidity of residue Y21.

In order to investigate how the acidity of residue Y21 affects the rate of recovery, control light to dark recovery experiments were performed on the wild-type protein at varying pH values (**Figure 4.16b**). The general trend is as the pH increases, there is an increase in the rate of dark

pH	t (minutes)
7	23
8	16
10	8
11	3
2FY21 pH8	5
Wild-type pD8	39.33
2FY21 pD8	7.02
3FY21 pD 8	2.34

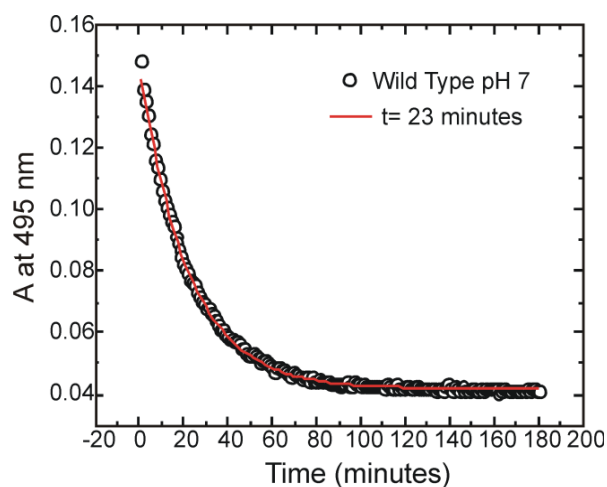


**Figure 4.15.** An example of a kinetic measurement of wild-type AppABLUF at pH 7.

Kinetics of the light to dark state recovery are measured at 495 nm. Lifetimes for each pH are shown in the table.

state recovery. In addition, the shift in the 450 nm peak upon formation of the light state decreases with increasing pH (12 nm at pH 7 to 6 nm at pH 10). The experiment performed at pH 11 show a very small shift in absorbance upon formation of the light state (2 nm) but when a second photoconversion was attempted on the same sample, no shift in absorbance was observed. These data were reproduced 3 times and is most likely due to protein instability at high pH. However, the general trend shows both 2FY21 and 3FY21 AppA<sub>BLUF</sub> are mimicking a high pH environment.

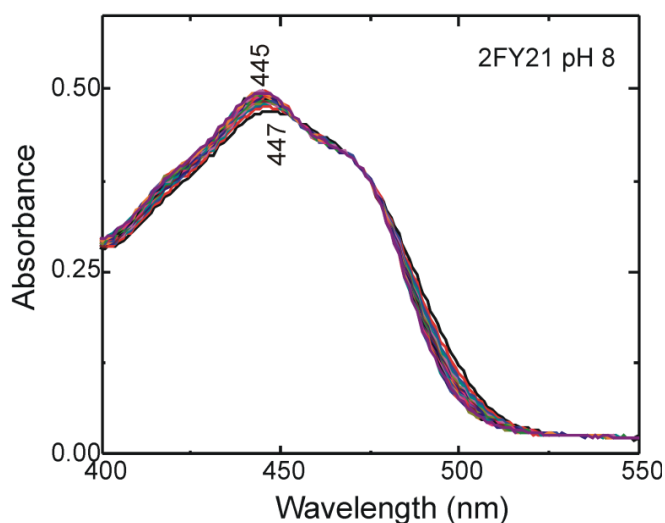


**Figure 4.16a. Electronic absorption spectra of 2FY21 AppA<sub>BLUF</sub> light to dark state recovery.** The light state of 2FY21 AppA<sub>BLUF</sub> was generated by exciting the sample with 365 nm light and the protein was allowed to recover in the dark. Spectra were recorded every 30 seconds after light absorption to monitor light to dark recovery. Concentration: 80  $\mu$ M pH 8.

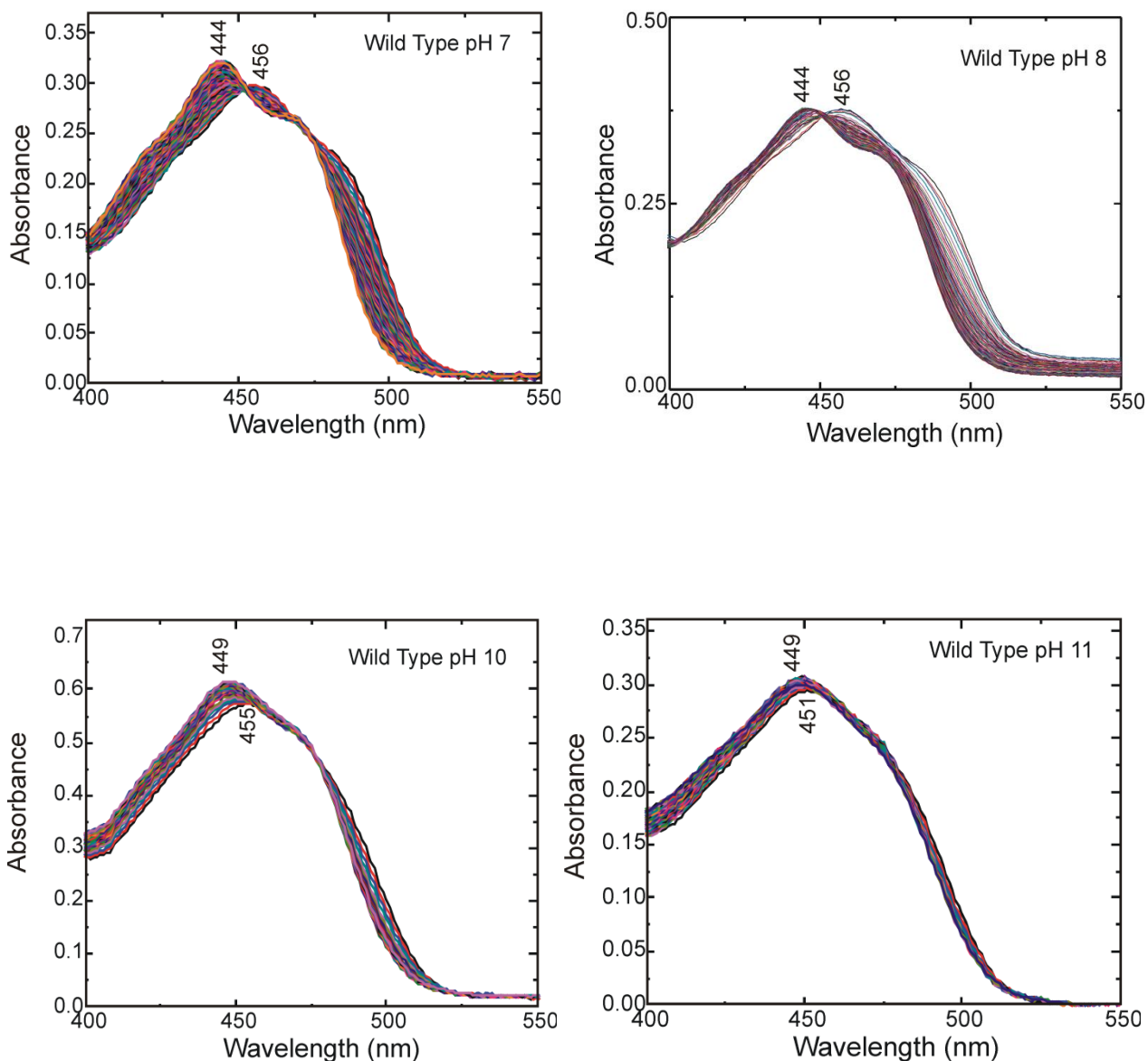


**Figure 4.16b. Electronic absorption spectra of wild-type AppA<sub>BLUF</sub> light to dark state recovery at various pH values.** The light state of AppA<sub>BLUF</sub> was generated by exciting the sample with 365 nm light and the protein was allowed to recover in the dark. Spectra were recorded every 30 seconds after light absorption to monitor light to dark recovery. Protein concentration was between 50 and 100  $\mu$ M in pH 7, 8, 10 and 11 in phosphate buffer.

The TRIR spectra of 2FY21 AppA<sub>BLUF</sub> are shown in **Figure 4.17**. These spectra are similar to the wild-type protein, suggesting there is either little or no change to the protein due to the addition of a fluorine atom. The kinetics of the 1547 cm<sup>-1</sup> intense bleach of dAppA<sub>BLUF</sub>, lAppA<sub>BLUF</sub>, l2FY21 AppA<sub>BLUF</sub> and d2FY21 AppA<sub>BLUF</sub> are shown in **Figure 4.18** and again are comparable to the wild-type protein where the ground state recovery for light state both samples recovers approximately 3 times faster than the dark state. This result suggests the kinetics of the both the dark and light state is unaffected by altering the pKa of Y21. This indicates residue Y21 is most likely does not participate in electron transfer in either dAppA or lAppA.

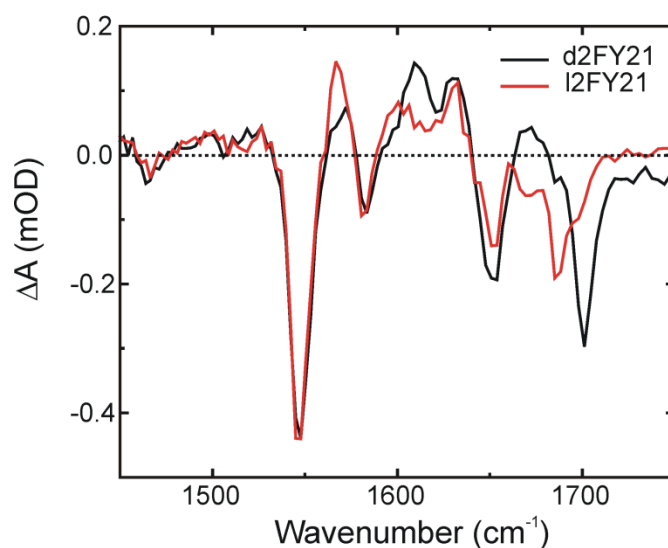


**Figure 4.17. TRIR spectra of 2FY21 d and lAppA<sub>BLUF</sub> measured at 3 ps.**

TRIR spectra of 2FY21 dAppA<sub>BLUF</sub> (black) and 2FY21 lAppA<sub>BLUF</sub> (red) bound to FAD. Protein concentration was 2 mM in pD 8 phosphate buffer and the TRIR spectra were recorded with a time delay of 3 ps. The spectra have been normalized to the intense FAD ring bleach mode at 1547 cm<sup>-1</sup>.



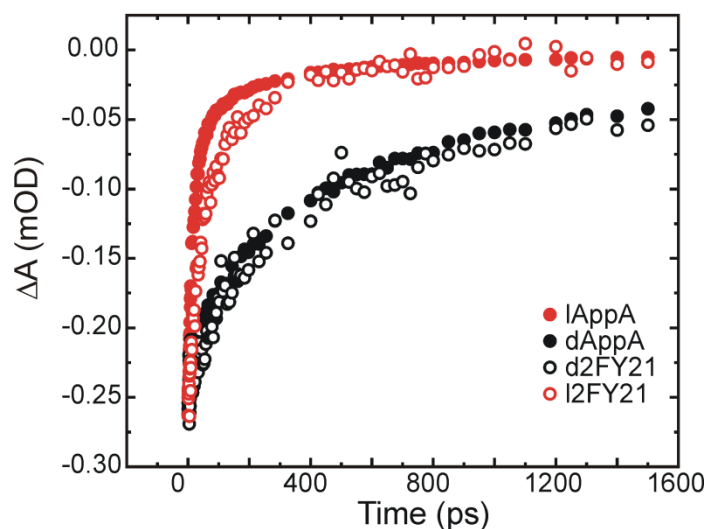


**Figure 4.18. Kinetics of the ground state recovery for wild-type d and lAppA<sub>BLUF</sub> and 2FY21 d and lAppA<sub>BLUF</sub> using TRIR spectroscopy measured at 1547 cm<sup>-1</sup>.**

Comparison of kinetic measurements of dAppA<sub>BLUF</sub> (black solid), lAppA<sub>BLUF</sub> (red solid), 2FY21 dAppA<sub>BLUF</sub> (black hollow) and 2FY21 lAppA<sub>BLUF</sub> (red hollow) bound to FAD. The ground state recovery kinetics were fit to a 2 component exponential decay where the lifetimes of dAppA<sub>BLUF</sub>, lAppA<sub>BLUF</sub>, 2FY21 dAppA<sub>BLUF</sub> and 2FY21 lAppA<sub>BLUF</sub> were 36/559, 21/272, 143/1214 and 39/239 ps for the short and long components respectively. Protein concentration was 2 mM in pD 8 phosphate buffer and the ground state recovery kinetics are measured at the intense bleach at 1547 cm<sup>-1</sup>.

## C.8. Incorporation of 2,6-difluorotyrosine into Residue Y21

When 2,6-difluorotyrosine was incorporated into Y21 (2,6-dFY21) of AppA the protein bound flavin. The electronic absorption spectrum of this protein does not show a shift in the 450 nm absorbance which is characteristic of photoactivity (**Figure 4.19**). However, it is possible this mutant is photoactive with a very fast recovery that is not observed in the steady state electronic absorption spectrum. Unfortunately, this sample over expresses with very poor yield and it was not possible to measure the TRIR spectrum which would be a good method to determine if 2,6-dFY21 AppA is photoactive because it is possible to irradiate the sample for the duration of the measurement. From our previous experiments we predict this analog is photoactive with an extremely fast light to dark recovery.

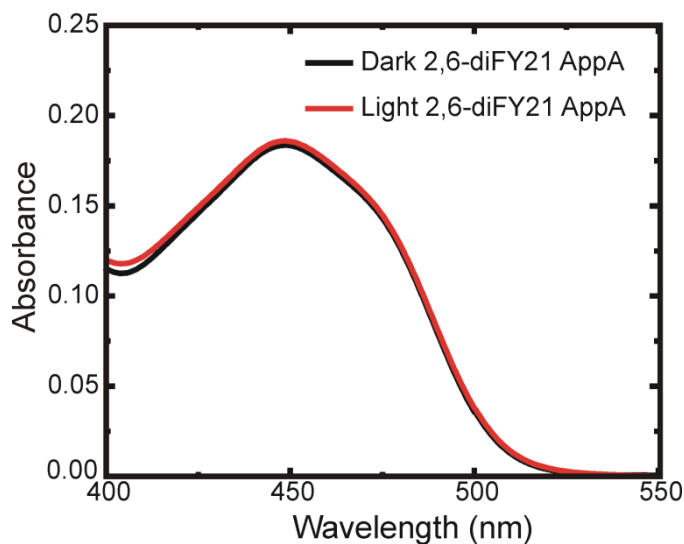


**Figure 4.19. Photoconversion of 2,6-difluoroY21 AppA<sub>BLUF</sub>**

Electronic absorption spectra of d and l 2,6dFY21 AppA<sub>BLUF</sub>. Protein concentration was 50  $\mu$ M in pH 8 phosphate buffer.

## C.9. Major Conclusions from Fluorotyrosine Incorporation

The mechanism of AppA photoactivation involves the reorganization of the protein's hydrogen bonding network that surrounds the flavin chromophore. Y21 is a critical component of this network, and in order to improve our understanding of the role of this residue in photoactivation we replaced Y21 with fluorotyrosine analogs. In the wild-type protein, photoexcitation of AppA to form the signaling state is known to involve strengthening of hydrogen bonds between the C4=O group of the chromophore and the protein as shown in **Figure 4.20**. Mutations to residue Y21 lead to the generation of photoinactive proteins that are trapped in a dark state environment and thus indicate the significance of Y21 in the photocycle of AppA. Therefore, it is plausible that Y21 must act as a hydrogen bond donor to residue Q63 in order to stabilize the light state of AppA.

3FY21 AppA<sub>BLUF</sub> is photoactive and time resolved infrared spectroscopy indicate that this mutation is structurally similar to the wild-type protein. However, 3FY21 AppA<sub>BLUF</sub> has a light to dark state recovery that is 20 times faster than in wild-type AppA. One plausible explanation for the fast recovery of 3FY21 AppA<sub>BLUF</sub> is that the reduction in pKa by adding a fluorine atom to the tyrosine causes a destabilization of the light state decreasing the energy barrier for light to dark recovery.

An increase in the light to dark recovery rate is also observed in 2FY21 AppA<sub>BLUF</sub> where recovery is 6 fold faster than the wild-type protein. The same decrease in recovery time is observed when the pH is increased in the wild-type protein and thus indicates that 3FY21 and 2FY21 AppA<sub>BLUF</sub> are mimicking a high pH environment of the protein. In addition, the light to dark recovery rate of AppA is 2.5 fold slower when the protein is in deuterated buffer demonstrating a normal isotope effect.

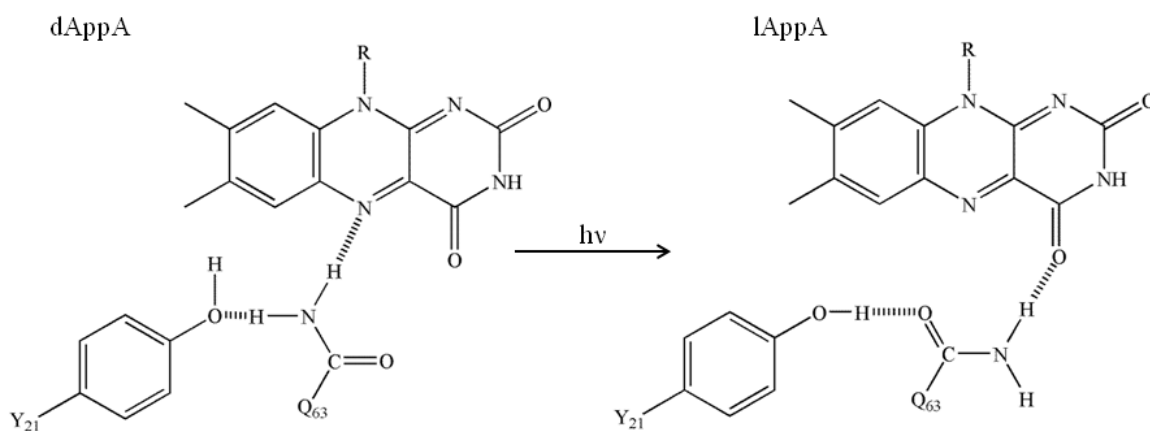


**Figure 4.20. Hydrogen bonding network in dAppA and lAppA.**

Hydrogen bonds are shown as dashed lines and formation of lAppA is based on a proposed keto-enol tautomerism followed by rotation of Q63 leading to formation a new hydrogen bond with the flavin C4=O.

In order to investigate the relationship between the acidity of residue Y21 with the rate of light to dark state recovery, a Brønsted analysis was used to plot the  $\log k$  vs. pKa and is shown in **Figure 4.21**. This plot establishes there is a direct correlation between the pKa of residue Y21 and the rate of light to dark state recovery implying proton transfer must be proportional to the activation energy for light to dark recovery. In addition, the slope of the plot of  $\log k$  vs pKa (termed  $-\alpha$ ) is calculated to be -0.76 suggesting the proton is almost fully transferred in the transition state.

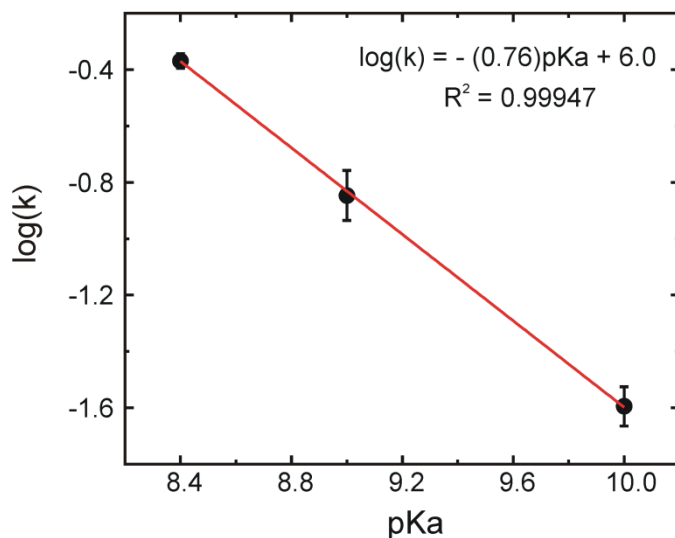


**Figure 4.21. Bronsted plot of log k versus the pKa of residue Y21.**

The Bronsted plot of log k versus the pKa of residue Y21 shows a direct correlation between the acidity of residue Y21 and the light to dark state recovery. This demonstrates proton transfer of residue Y21 is proportional to the activation energy. The slope ( $-\alpha$ ) is calculated to be -0.76 indicating the proton is almost fully transferred in the rate determining step.

These data allow us to propose a mechanism for the light to dark state recovery of wild-type AppA (**Figure 4.22**) where proton transfer from Y21 is the rate determining step in the recovery. After the formation of lAppA, residue Q63 tautomerizes so that the side chain deprotonated alcohol remains hydrogen bonded to the hydroxyl side chain of Y21. This enol conformation of Q63 allows the glutamine to act as a base and abstract a proton from residue Y21. After protonation of the enol, Q63 will rotate thus breaking the hydrogen bond to the C4=O of the flavin and form a new hydrogen bond with the flavin N5 atom. The last step involves a second tautomerization to return to the more stable keto state of Q63. Residue Y21 will now be solvent accessible and be able to abstract a proton from the solvent. Abstraction of the proton

from Y21 by Q63 is the rate determining step of the light to dark recovery. This mechanism also explains the observed normal isotope effect in deuterated buffer.

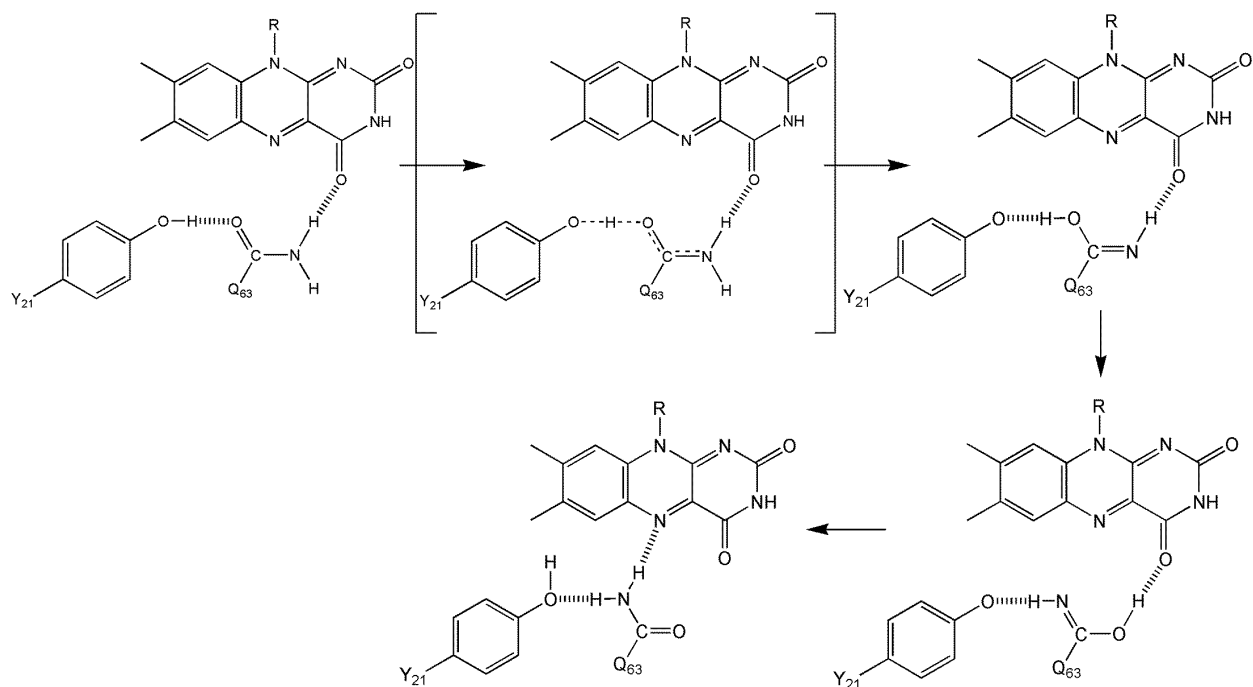


**Figure 4.22. Proposed Model for the recovery of lAppA to dAppA.**

In the ground state of lAppA the Q63 side chain exists as an equilibrium mixture of keto and enol tautomers. In the enol tautomer there is a hydrogen bond between Q63 and the Y21 that is essential for stabilization of lAppA. Upon recovery the enol tautomer, will abstract a hydrogen from residue Y21 in the rate determining step of relaxation back to the dark state. This enol tautomer will then rotate breaking the hydrogen bond with the C4=O of the flavin and form a new hydrogen bond with the N5 atom of the flavin. This rotated state of Q63 will then return to the more stable keto form and Y21 will abstract a proton from the solvent.

## C.10. Cyanophenylalanine Incorporation

A method has been developed by Schultz *et. al.* to incorporate a variety of unnatural amino acids specifically into a protein. This method relies on an orthogonal aminoacyl-tRNA synthetase/tRNA that recognizes the amber stop codon UAG in *E. coli* and incorporates an unnatural amino acid (in our case p-cyanophenylalanine). The protocol uses two plasmids: the pDule vector resistant to spectinomycin encoding for the aminoacyl-tRNA synthetase/tRNA and the pBAD vector resistant to ampicillin containing the gene of interest (AppA) allowing for selection of both vectors.

The first step of the protocol is to clone AppA into a pBAD vector. The pBAD vector used had a C-terminal his-tag but the current protocol to overexpress/purify AppA uses an N-terminal his-tag. Taking into account our existing reagents, the method used to insert AppA into a pBAD vector was digested to remove AppA<sub>BLUF</sub> from the pet15b vector while retaining the N-terminal his-tag from this vector. The stop codon at the end of the gene will prevent the C-terminal his-tag from the commercial pBAD vector from being expressed.

The DNA encoding for AppA<sub>BLUF</sub> was digested and excised from a pET15b vector with NcoI and BamHI and N-terminal His-AppA was purified. Next, pBADmyc His was cut with NcoI and BglII and this vector was ligated to N-terminal His-AppA. The final gene sequence is shown in **Figure 4.23** where the N-terminal His-tag with thrombin cleavage site is shown in pink and the nucleotide sequence encoding for the AppA protein sequence is shown in yellow. In addition, the original amber stop codon, shown in red, used was replaced with TAA, in order to prevent undesired cyanophenylalanine incorporation.

The final step in plasmid generation is to insert the amber stop codon (TAG) to replace the natural amino acid where cyanophenylalanine is desired. Three amino acids were chosen as

initial replacements for cyanophenylalanine. These were 2 phenylalanine (F62 and F101) residues and one tyrosine (Y56) residue in AppA<sub>BLUF</sub>, since these amino acids are the most structurally similar to cyanophenylalanine. The crystal structure highlighting each natural amino acid that was replaced is shown in **Figure 4.24**. Of the amino acids chosen for replacement, the most interesting choice is F101. This residue is in close proximity to W104 which, in one of the models for photoactivation, moves resulting in structural changes to the  $\beta$ -sheet which are then transmitted to the C-terminal domain.

```

CGG  TAC  ATT  CCC  CTC  TAG  AAA  TAA  TTT  TGT  TTA  ACT  TTA  AGA
AGG  AGA  TAT  ACC  ATG  GGC  AGC  AGC  CAT  CAT  CAT  CAT  CAT  CAC  AGC
AGC  GGC  CTG  GTG  CCG  CGC  GGC  AGC  CAT  ATG  CTC  GAG  GCG  GAC  GTC
ACG  ATG  ACG  GGC  TCG  GAT  CTG  GTT  TCC  TGC  TGC  TAC  CGC  AGC  CTG
GCG  GCC  CCG  GAT  CTG  ACG  CTG  CGC  GAC  CTC  CTC  GAC  ATC  GTC  GAG
ACC  TCG  CAG  GCG  CAC  AAT  GCC  CGG  GCG  CAG  CTG  ACC  GGC  GCG  CTC
TTC  TAC  AGC  CAG  GGC  GTC  TTC  TTC  CAG  TGG  CTC  GAA  GGC  CGC  CCC
GCC  GCC  GTG  GCG  GAG  GTC  ATG  ACC  CAC  ATC  CAG  CGG  GAC  CGG  CGC
CAC  AGC  AAC  GTC  GAG  ATC  CTC  GCA  GAG  GAA  CCG  ATC  GCC  AAG  CGC
CGC  TTT  GCG  GGA  TAC  CAC  ATG  CAG  CTC  TCC  TGC  TCG  GAG  GCC  GAC
ATG  CGC  AGC  CTC  GGG  CTG  GCC  GAG  AGC  CGG  CAG  TAG  GGA  TCT  GCA
GAT  GGT

```

**Figure 4.23. The gene sequence of AppA BLUF in pBAD myc His Vector.** N-terminal His-tag with thrombin cleavage site is shown in pink, the nucleotide sequence encoding for the AppA<sub>BLUF</sub> protein sequence is shown in yellow. The original Amber stop codon is shown in red but was later mutated to TAA.



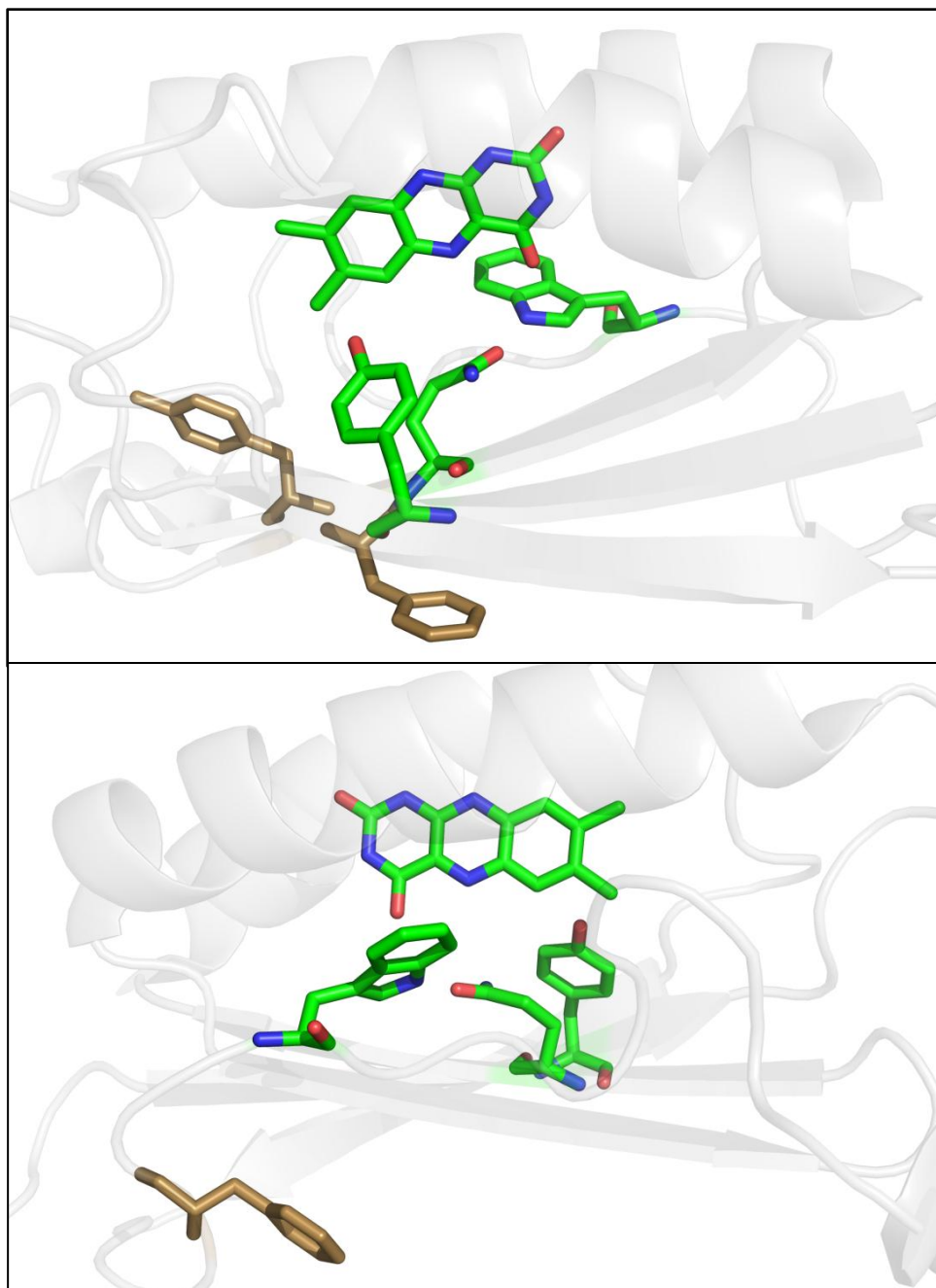


**Figure 4.24.** The crystal structure of AppA<sub>BLUF</sub> showing positions where cyanophenylalanine was inserted. The residues chosen for replacement with cyanophenylalanine are shown in tan. The top highlights residues Y56 and F62 and the bottom highlights residue F101 which is in close proximity to W104. This figure was made using pymol PDBID: [1YRX](#) (2).

The protein was over expressed in autoinduction media using BL21AI *E. coli* cells where each amber mutant was co transformed with the pDule vector. Time points were taken every hour for 12 hours after inoculation for an autoinduction profile (**Figure 4.25**). F101cyanophenylalanine had the best overexpression when compared to Y56 and F62cyanophenylalanine. The percent incorporation into AppA was calculated by MALDI-TOF mass spectrometry of a trypsin digest of the protein and was calculated to be greater than 95% (**Figure 4.26**) for each amber mutant. Steady state UV-Vis spectroscopy was used to characterize these proteins.

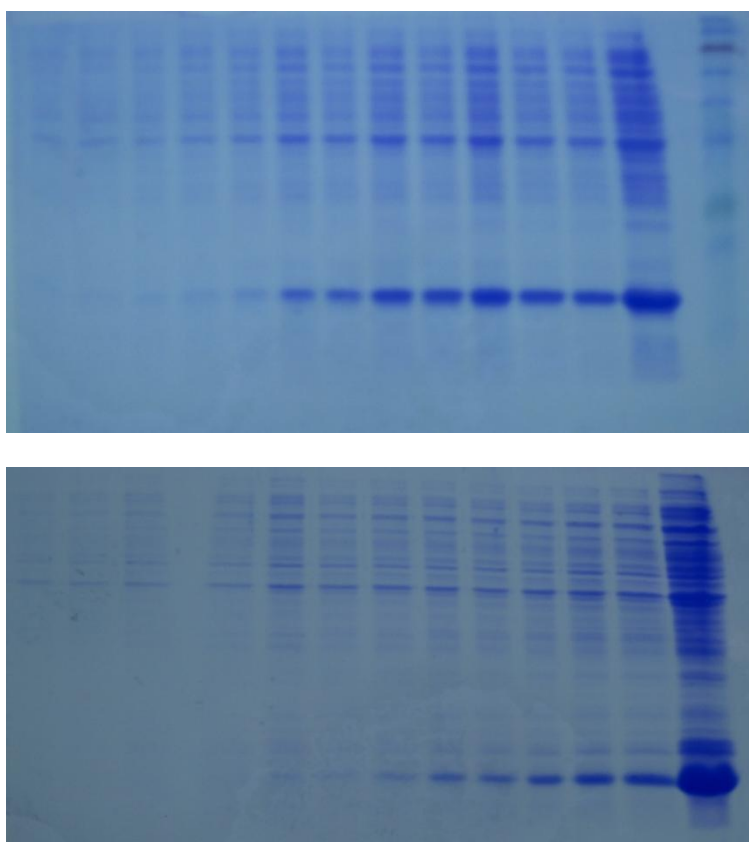


**Figure 4.25. Overexpression gel of wild-type (top) and F101cyanophenylalanine (bottom) AppA<sub>BLUF</sub> expressed in BL21AI cells.** Lane 1 is at time zero after inoculation followed by 1 hour time points until 12 hours. Lane 13 contains the whole cells right before harvesting at 24 hours.

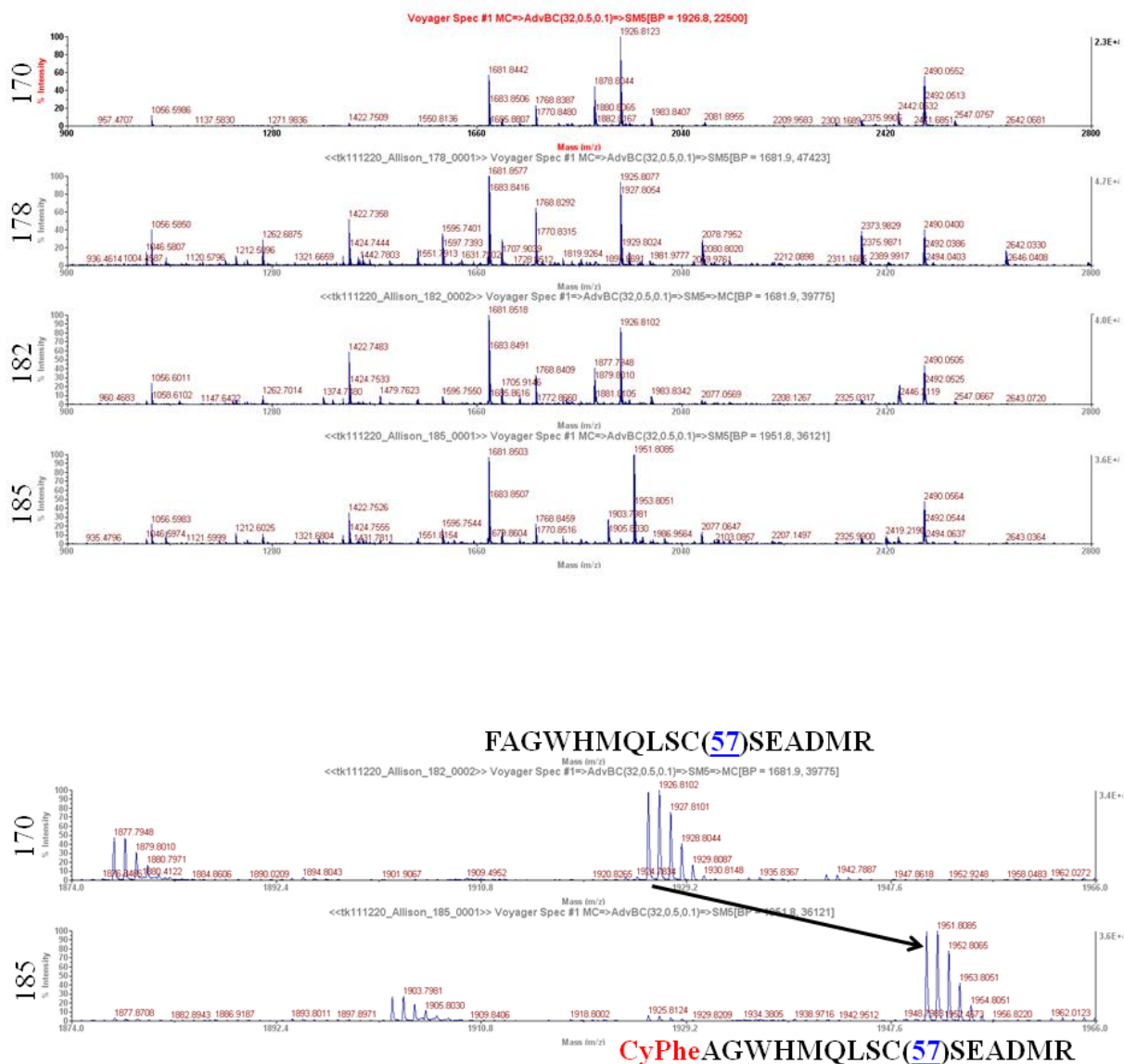


**Figure 4.26. MALDI mass spectra of peptide containing cyanophenylalanine.**

MALDI mass spectra of trypsin digested App<sub>A</sub>BLUF zoomed in of peptide FAGWHMQLSCSEADMR containing F101 with (185) and without (170) cyanophenylalanine allowing for percent incorporated calculation. Calculated mass of peptide without fluorine is 1869 g/mol and experimental mass is 1926.8 g/mol. Calculated mass of peptide with cyanophenylalanine is 1894 g/mol and experimental mass is 1951.8 g/mol.

From the electronic absorption spectra, all three cyanophenylalanine labeled proteins are photoactive with recovery times of ~30 min similar to wild-type AppA (**Figures 4.27, 4.28, 4.29** and **4.30**). In addition, the steady state FTIR spectra of both dark and light AppA<sub>BLUF</sub> was obtained for F101cyanophenylalanine. This mutant was chosen for further characterization because it over expressed with high yields and the cyano group is in a position likely associated with structural change upon photoexcitation. The steady state FTIR spectrum of free cyanophenylalanine in buffer is shown in **Figure 4.31** and was used to determine the peak position of the cyano group (found at 2236 cm<sup>-1</sup>). Unfortunately, there was no signal observed for the cyano probe in the protein either dAppA or lAppA. In addition, the cyano stretching mode was not observed in TRIR measurements. Future experiments are planned to place to use azidophenylalanine, which has a higher extinction coefficient compared to cyanophenylalanine, in order to observe large structural changes associated with photexcitation.

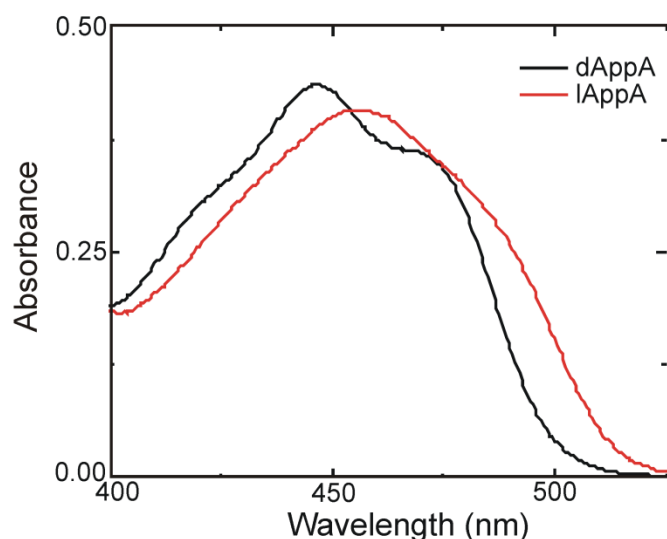


**Figure 4.27. Absorption spectra of wild-type d and lAppA<sub>BLUF</sub>.**

Steady state absorption spectra of dAppA<sub>BLUF</sub> (black) and lAppA<sub>BLUF</sub> (red) bound to FAD.

Protein concentration was 60  $\mu$ M in phosphate buffer, pH 8.

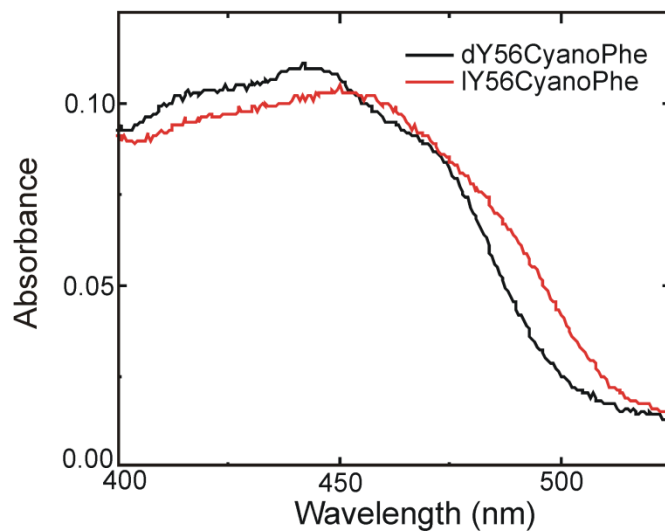


**Figure 4.28. Absorption spectra of d and IY56cyanophenylalanine AppA<sub>BLUF</sub>.**

Steady state absorption spectra of dY56cyanophenylalanine AppA<sub>BLUF</sub> (black) and IY56 cyanophenylalanine AppA<sub>BLUF</sub> (red). Protein concentration was 15  $\mu$ M in pH 8 phosphate buffer.

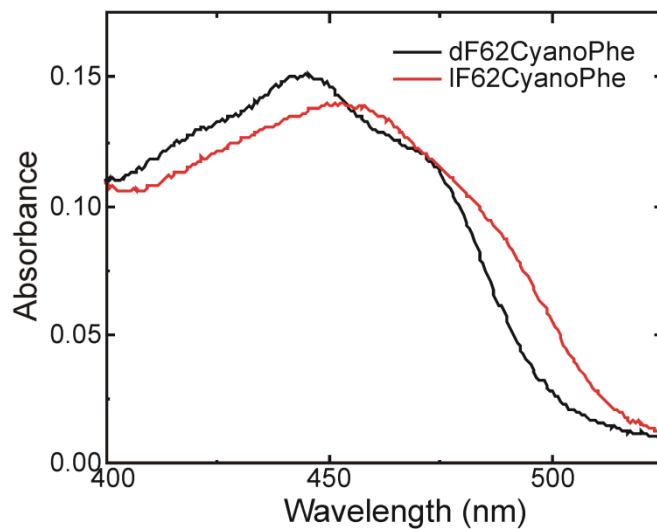


**Figure 4.29. Absorption spectra of d and IY56cyanophenylalanine AppA<sub>BLUF</sub>.**

Steady state absorption spectra of dF62cyanophenylalanine AppA<sub>BLUF</sub> (black) and IF62 cyanophenylalanine AppA<sub>BLUF</sub> (red). Protein concentration was 20  $\mu$ M in pH 8 phosphate buffer.

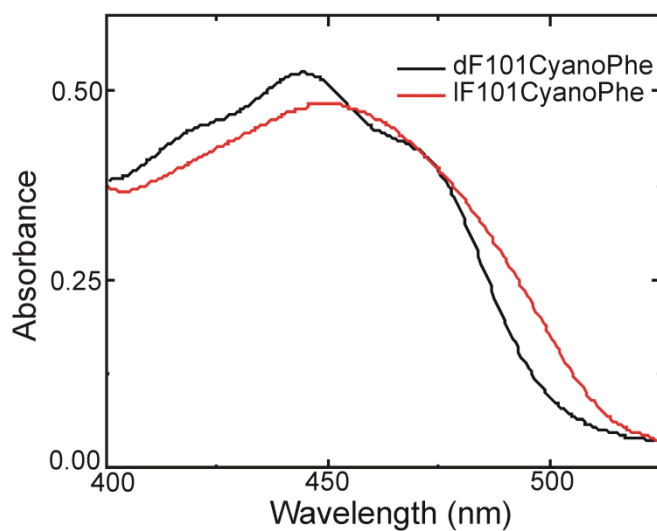


**Figure 4.30. Absorption spectra of d and IF101cyanophenylalanine AppA<sub>BLUF</sub>.**

Steady state absorption spectra of dF101cyanophenylalanine AppA<sub>BLUF</sub> (black) and IF101cyanophenylalanine AppA<sub>BLUF</sub> (red). Protein concentration was 70  $\mu$ M in pH 8 phosphate buffer.

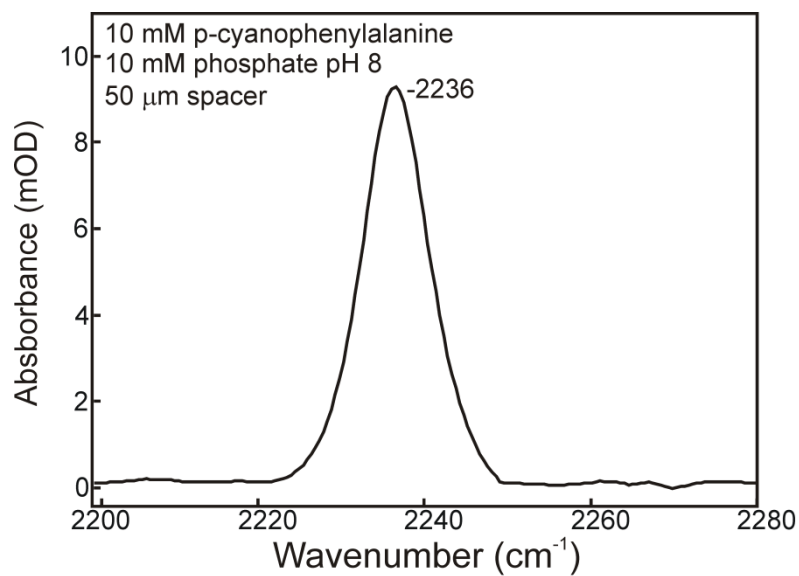
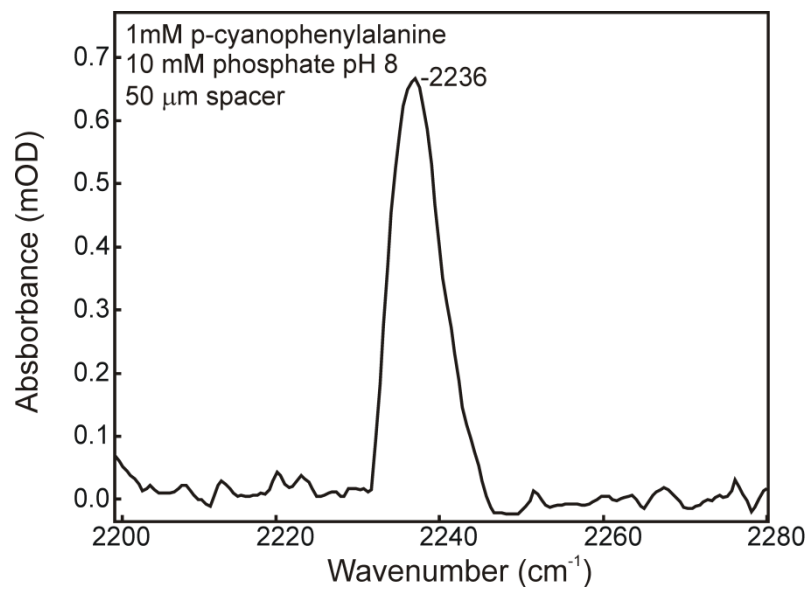


**Figure 4.31. FTIR spectrum of cyanophenylalanine in buffer.**

FTIR spectrum of cyanophenylalanine in buffer. Concentration was 1 mM (top) and 10 mM (bottom). The extinction coefficient for the CN mode in cyanophenylalanine at  $2236\text{ cm}^{-1}$  is  $220\text{ M}^{-1}\text{ cm}^{-1}$ . Buffer conditions: 10 mM phosphate pH 8 in  $50\text{ }\mu\text{m}$  spacer.

## D. Summary

The photoinactive Y21C, Y21S, and Y21I AppA<sub>BLUF</sub> mutants have been generated in order to investigate the role of residue Y21. These mutants are all photoinactive thus proving the tyrosine is crucial for formation of the light state of the protein. All Y21 mutants (except Y21W discussed in chapter 3) resemble dAppA where the C4 carbonyl of the flavin is less hydrogen bonded than in lAppA. This suggests the protein is trapped in a dark state conformation and it is plausible the reason for photodeactivation is the inability to donate a hydrogen bond to the enol form of residue Q63 after irradiation with 450 nm light. In order to further probe the role of residue Y21, we have incorporated fluorotyrosine analogs which cause minor structural perturbations to AppA.

The Y56F AppA<sub>BLUF</sub> mutant was generated to specifically incorporate fluorotyrosines into position Y21. This mutant behaves identically to the wild-type protein and therefore we are able to monitor changes directly from the addition of the fluorine atom. In addition, an overexpression and purification protocol was developed for the enzyme TPL and a protocol to maximize yields in minimal media was performed on AppA Y56F. Purified TPL was then used to catalyze the reaction to produce a variety of fluorinated tyrosine analogs from corresponding fluorinated phenols to be used for feeding experiments into residue Y21 of Y56F AppA<sub>BLUF</sub>.

When residue Y21 was replaced with 3,5-difluorotyrosine (3,5-dFY21) the protein did not bind flavin. A possible explanation for absence of flavin is that the electrostatics in the binding pocket of 3,5-dFY21 AppA cause an unfavorable environment for the isoalloxazine ring. In addition, it is possible the large decrease in pKa creates a completely anionic state of the tyrosine which destabilizes the binding pocket of the flavin.



3FY21 AppA<sub>BLUF</sub> is photoactive and time resolved infrared spectroscopy indicate that this mutation is structurally similar to the wild-type protein. However, 3FY21 AppA<sub>BLUF</sub> has a light to dark state recovery that is 20 times faster than in wild-type AppA. The increase in light to dark recovery rate is also observed in 2FY21 AppA<sub>BLUF</sub> where recovery is 6 fold faster than the wild-type protein. The same decrease in recovery time is observed when the pH is increased in the wild-type protein and thus indicates that 3FY21 and 2FY21 AppA<sub>BLUF</sub> are mimicking a high pH environment of the protein. In addition, the light to dark recovery rate of AppA is 2.5 fold slower when the protein is in deuterated buffer demonstrating a normal isotope effect.

Additionally, a Brønsted type plot established there is a direct correlation between the pKa of residue Y21 and the rate of recovery. This implies proton transfer must be proportional to the activation energy for light to dark recovery. These data allow us to propose a mechanism for the light to dark state recovery of wild-type AppA where abstraction of the proton from Y21 by Q63 is the rate determining step of the light to dark recovery. This also explains the observed normal isotope effect in deuterated buffer.

Preliminary studies have been performed on AppA<sub>BLUF</sub> with cyanophenylalanine incorporated into three positions, Y56, F62 and F101. All three cyanophenylalanine labeled proteins are photoactive with recovery times of ~30 min similar to wild-type AppA. There was no signal observed from the cyano group in the FTIR or TRIR measurements of F101cyanophenylalanine AppA. This indicates the low extinction coefficient of cyanophenylalanine is not large enough to observe if there is a change in environment around F101 during photoexcitation. Future experiments will involve placing azidophenylalanine, which has a higher extinction coefficient, in different various positions, including W104, which might be associated with larger structural changes upon photoexcitation.

## E. References

1. Rappaport, F., Boussac, A., Force, D. A., Peloquin, J., Brynda, M., Sugiura, M., Un, S., Britt, R. D., and Diner, B. A. (2009) Probing the Coupling between Proton and Electron Transfer in Photosystem II Core Complexes Containing a 3-Fluorotyrosine, *J Am Chem Soc* 131, 4425-4433.
2. Anderson, S., Dragnea, V., Masuda, S., Ybe, J., Moffat, K., and Bauer, C. (2005) Structure of a novel photoreceptor, the BLUF domain of AppA from *Rhodospira rubra*, *Biochemistry* 44, 7998-8005.
3. Ayyadurai, N., Prabhu, N. S., Deepankumar, K., Kim, A., Lee, S. G., and Yun, H. (2011) Biosynthetic substitution of tyrosine in green fluorescent protein with its surrogate fluorotyrosine in *Escherichia coli*, *Biotechnol Lett* 33, 2201-2207.
4. Seyedsayamdost, M. R., Reece, S. Y., Nocera, D. G., and Stubbe, J. (2006) Mono-, di-, tri-, and tetra-substituted fluorotyrosines: new probes for enzymes that use tyrosyl radicals in catalysis, *J Am Chem Soc* 128, 1569-1579.
5. Seyedsayamdost, M. R., Yee, C. S., and Stubbe, J. (2007) Site-specific incorporation of fluorotyrosines into the R2 subunit of *E. coli* ribonucleotide reductase by expressed protein ligation, *Nat Protoc* 2, 1225-1235.
6. Minnihan, E. C., Young, D. D., Schultz, P. G., and Stubbe, J. (2011) Incorporation of Fluorotyrosines into Ribonucleotide Reductase Using an Evolved, Polyspecific Aminoacyl-tRNA Synthetase, *J Am Chem Soc* 133, 15942-15945.
7. Reece, S. Y., Seyedsayamdost, M. R., Stubbe, J., and Nocera, D. G. (2006) Electron transfer reactions of fluorotyrosyl radicals, *J Am Chem Soc* 128, 13654-13655.

8. Bonin, J., Costentin, C., Robert, M., Saveant, J. M., and Tard, C. (2011) Hydrogen-Bond Relays in Concerted Proton-Electron Transfers, *Acc Chem Res*.
9. Reece, S. Y., Hodgkiss, J. M., Stubbe, J., and Nocera, D. G. (2006) Proton-coupled electron transfer: the mechanistic underpinning for radical transport and catalysis in biology, *Philos Trans R Soc Lond B Biol Sci* 361, 1351-1364.
10. Gai, X. S., Coutifaris, B. A., Brewer, S. H., and Fenlon, E. E. (2011) A direct comparison of azide and nitrile vibrational probes, *Phys Chem Chem Phys* 13, 5926-5930.
11. Waegele, M. M., Culik, R. M., and Gai, F. (2011) Site-Specific Spectroscopic Reporters of the Local Electric Field, Hydration, Structure, and Dynamics of Biomolecules, *J Phys Chem Lett* 2, 2598-2609.
12. Lim, M., Hamm, P., and Hochstrasser, R. M. (1998) Protein fluctuations are sensed by stimulated infrared echoes of the vibrations of carbon monoxide and azide probes, *PNAS USA* 95, 15315-15320.
13. Tsubaki, M., Mogi, T., and Hori, H. (1999) Fourier-transform infrared studies on azide-binding to the binuclear center of the Escherichia coli bo-type ubiquinol oxidase, *FEBS letters* 449, 191-195.
14. Tsubaki, M., Mogi, T., and Hori, H. (1999) Azide- and cyanide-binding to the Escherichia coli bd-type ubiquinol oxidase studied by visible absorption, EPR and FTIR spectroscopies, *JBC* 126, 510-519.
15. Yoshikawa, S., O'Keeffe, D. H., and Caughey, W. S. (1985) Investigations of cyanide as an infrared probe of heme protein ligand binding sites, *JBC* 260, 3518-3528.
16. Taskent-Sezgin, H., Chung, J., Banerjee, P. S., Nagarajan, S., Dyer, R. B., Carrico, I., and Raleigh, D. P. (2010) Azidohomoalanine: a conformationally sensitive IR probe of

- protein folding, protein structure, and electrostatics, *Angew Chem Int Ed Engl* 49, 7473-7475.
17. Choi, J. H., Raleigh, D., and Cho, M. (2011) Azido Homocysteine is a Useful Infrared Probe for Monitoring Local Electrostatics and Side-Chain Solvation in Proteins, *J Phys Chem Lett* 2, 2158-2162.
  18. Chin, J. W., Cropp, T. A., Anderson, J. C., Mukherji, M., Zhang, Z., and Schultz, P. G. (2003) An expanded eukaryotic genetic code, *Science* 301, 964-967.
  19. Chin, J. W., Santoro, S. W., Martin, A. B., King, D. S., Wang, L., and Schultz, P. G. (2002) Addition of p-azido-L-phenylalanine to the genetic code of Escherichia coli, *J Am Chem Soc* 124, 9026-9027.
  20. Young, D. D., Young, T. S., Jahnz, M., Ahmad, I., Spraggon, G., and Schultz, P. G. (2011) An evolved aminoacyl-tRNA synthetase with atypical polysubstrate specificity, *Biochemistry* 50, 1894-1900.
  21. Hammill, J. T., Miyake-Stoner, S., Hazen, J. L., Jackson, J. C., and Mehl, R. A. (2007) Preparation of site-specifically labeled fluorinated proteins for <sup>19</sup>F-NMR structural characterization, *Nat Protoc* 2, 2601-2607.
  22. Wang, L., Xie, J., and Schultz, P. G. (2006) Expanding the genetic code, *Annu Rev Biophys Biomol Struct* 35, 225-249.
  23. Laan, W., Gauden, M., Yeremenko, S., van Grondelle, R., Kennis, J. T., and Hellingwerf, K. J. (2006) On the mechanism of activation of the BLUF domain of AppA, *Biochemistry* 45, 51-60.

24. Laan, W., Bednarz, T., Heberle, J., and Hellingwerf, K. J. (2004) Chromophore composition of a heterologously expressed BLUF-domain, *Photochem. Photobiol. Sci.* 3, 1011-1016.
25. Dragnea, V., Waegele, M., Balascuta, S., Bauer, C., and Dragnea, B. (2005) Time-resolved spectroscopic studies of the AppA blue-light receptor BLUF domain from *Rhodobacter sphaeroides*, *Biochemistry* 44, 15978-15985.
26. Kumagai, H., Yamada, H., Matsui, H., Ohkishi, H., and Ogata, K. (1970) Tyrosine phenol lyase. I. Purification, crystallization, and properties, *J Biol Chem* 245, 1767-1772.
27. Nagasawa, T., Utagawa, T., Goto, J., Kim, C. J., Tani, Y., Kumagai, H., and Yamada, H. (1981) Syntheses of L-tyrosine-related amino acids by tyrosine phenol-lyase of *Citrobacter intermedius*, *Eur J Biochem* 117, 33-40.

## Chapter 5

### Summary of Proposed Models for Dark to Light Formation and Light to Dark

#### Recovery of AppA<sub>BLUF</sub>

My project has focused on further investigation of AppA's photocycle which is essential to disentangle the mechanism of photoactivity. In the previous chapters we have discussed the methods we have used in order to propose a new model for photoactivation. Chapter 2 discussed the use of isotope labeling of the flavin in order to deconvolute the previously reported spectroscopic data. Reconstitution of the protein with isotopically labeled flavin has permitted unambiguous assignment of the ground and excited state modes associated with the flavin C2=O and C4=O groups which participate in a hydrogen bonding network that surrounds the flavin. This approach has allowed us to probe the role of the hydrogen bonding network in AppA activation.

The reorganization of the hydrogen bonding network surrounding the flavin chromophore of AppA by generation of Q63E AppA<sub>BLUF</sub>, W104M AppA<sub>BLUF</sub> and Y21W AppA<sub>BLUF</sub> was discussed in chapter 3. Isotope labeling of the Q63E mutant allowed assignment of a protein mode that appears within 100 fs of excitation, demonstrating that the protein matrix responds instantaneously to flavin excitation. These data have led to a detailed understanding of the photoexcitation mechanism, which involves a tautomerization followed by rotation of residue Q63 (**Figure 5.1**). In addition, the role of residue W104 in AppA<sub>BLUF</sub> was investigated by generating the W104M AppA<sub>BLUF</sub> mutant which retains photoactivity but the rate of recovery from the light to dark state increases. These data suggests W104 plays an important role in stabilization of lAppA. The Y21W AppA<sub>BLUF</sub> mutant was then created to enhance tryptophan radical formation and while this mutant is not photoactive, steady state and ultrafast spectroscopy

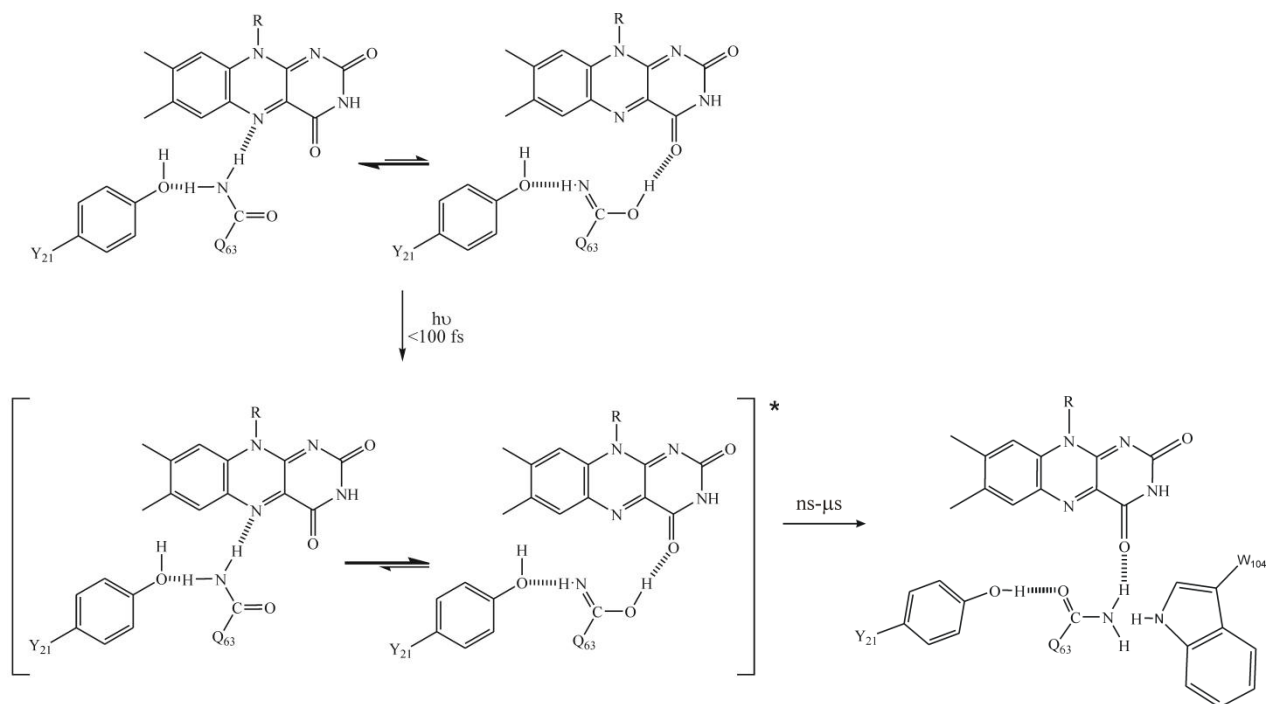


**Figure 5.1. Proposed model for formation of lAppA from dAppA.**

In the ground state of dAppA the Q63 side chain exists as an equilibrium mixture of keto and enol tautomers. In the enol tautomer there is a hydrogen bond between Q63 and the flavin C4=. However, as expected for an amide group, the position of the tautomeric equilibrium strongly favors the keto form. Upon photoexcitation there is an increase in electron density on the C4=O which will increase the proportion of the enol tautomer, again shown by an equilibrium symbol with disproportionate line widths. We then propose that this enol tautomer leads to the lAppA ground state in which Q63 has rotated and residue W104 has moved closer to the flavin stabilizing the lAppA.

indicate that this mutation has trapped the protein in a state that resembles the photoactivated states of AppA<sub>BLUF</sub> (with an intense vibrational band assigned to FADH• is observed). These data provide conclusive evidence that residue W104 is in the W<sub>out</sub> conformation in dAppA and once photoactivation occurs, there is a change in the hydrogen bond network in the protein bringing W104 closer to the flavin in the final light activated state of the protein representing the W<sub>in</sub> conformation (**Figure 5.1**).

Additional insight into photoactivation of AppA has also been obtained by replacing a key tyrosine in the hydrogen bonding network with unnatural fluorotyrosine analogs that have altered pKa values. A Brønsted type plot established there is a direct correlation between the pKa of residue Y21 and the rate of recovery. This implies proton transfer must be proportional to the activation energy for light to dark recovery. These data have established the acidity of residue Y21 is crucial in stabilizing the light activated form of the protein. This allows us to propose a mechanism for the light to dark state recovery of wild-type AppA (**Figure 5.2**) where abstraction of the proton from Y21 by Q63 is the rate determining step of the light to dark recovery.



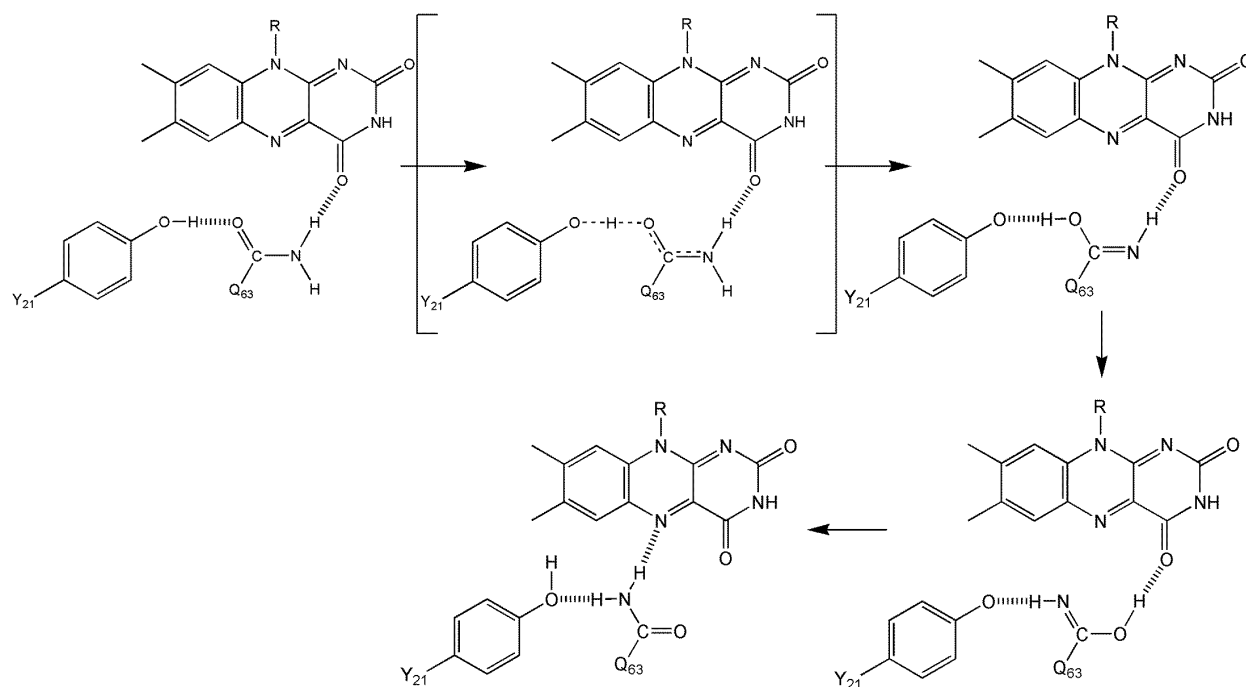


**Figure 5.2. Proposed model for the recovery of lAppA to dAppA.**

In the ground state of lAppA the Q63 side chain exists as an equilibrium mixture of keto and enol tautomers. In the enol tautomer there is a hydrogen bond between Q63 and the Y21 that is essential for stabilization of lAppA. Upon recovery the enol tautomer, will abstract a hydrogen from residue Y21 in the rate determining step of relaxation back to the dark state. This enol tautomer will then rotate breaking the hydrogen bond with the C4=O of the flavin and form a new hydrogen bond with the N5 atom of the flavin. This rotated state of Q63 will then return to the more stable keto form and Y21 will abstract a proton from the solvent.

## Bibliography

### Chapter 1

1. Gauden, M., Yeremenko, S., Laan, W., van Stokkum, I. H., Ihalainen, J. A., van Grondelle, R., Hellingwerf, K. J., and Kennis, J. T. (2005) Photocycle of the flavin-binding photoreceptor AppA, a bacterial transcriptional antirepressor of photosynthesis genes, *Biochemistry* 44, 3653-3662.
2. Anderson, S., Dragnea, V., Masuda, S., Ybe, J., Moffat, K., and Bauer, C. (2005) Structure of a novel photoreceptor, the BLUF domain of AppA from *Rhodospira rubra*, *Biochemistry* 44, 7998-8005.
3. Gomelsky, M., and Klug, G. (2002) BLUF. a novel FAD-binding domain involved in sensory transduction in microorganisms, *Trends Biochem Sci* 27, 497-500.
4. Briggs, W. R. (2007) The LOV domain. a chromophore module servicing multiple photoreceptors, *J Biomed Sci* 14, 499-504.
5. Kort, R., Hoff, W. D., Van West, M., Kroon, A. R., Hoffer, S. M., Vlieg, K. H., Crielaand, W., Van Beeumen, J. J., and Hellingwerf, K. J. (1996) The xanthopsins. a new family of eubacterial blue-light photoreceptors, *EMBO J* 15, 3209-3218.
6. Rockwell, N. C., Su, Y. S., and Lagarias, J. C. (2006) Phytochrome structure and signaling mechanisms, *Annu Rev Plant Biol* 57, 837-858.
7. Losi, A. (2004) The bacterial counterparts of plant phototropins, *Photochem Photobiol Sci* 3, 566-574.
8. Briggs, W. R., Christie, J. M., and Salomon, M. (2001) Phototropins. a new family of flavin-binding blue light receptors in plants, *Antioxid Redox Signal* 3, 775-788.

9. Essen, L. O. (2006) Photolyases and cryptochromes. common mechanisms of DNA repair and light-driven signaling?, *Curr Opin Struct Biol* 16, 51-59.
10. van der Horst, M. A., and Hellingwerf, K. J. (2004) Photoreceptor proteins, "star actors of modern times". a review of the functional dynamics in the structure of representative members of six different photoreceptor families, *Acc Chem Res* 37, 13-20.
11. Iseki, M., Matsunaga, S., Murakami, A., Ohno, K., Shiga, K., Yoshida, K., Sugai, M., Takahashi, T., Hori, T., and Watanabe, M. (2002) A blue-light-activated adenylyl cyclase mediates photoavoidance in *Euglena gracilis*, *Nature* 415, 1047-1051.
12. Okajima, K., Yoshihara, S., Fukushima, Y., Geng, X., Katayama, M., Higashi, S., Watanabe, M., Sato, S., Tabata, S., Shibata, Y., Itoh, S., and Ikeuchi, M. (2005) Biochemical and functional characterization of BLUF-type flavin-binding proteins of two species of cyanobacteria, *J Biochem* 137, 741-750.
13. Okajima, K., Fukushima, Y., Suzuki, H., Kita, A., Ochiai, Y., Katayama, M., Shibata, Y., Miki, K., Noguchi, T., Itoh, S., and Ikeuchi, M. (2006) Fate determination of the flavin photoreceptions in the cyanobacterial blue light receptor TePixD (Tll0078), *J Mol Biol* 363, 10-18.
14. Zirak, P., Penzkofer, A., Schiereis, T., Hegemann, P., Jung, A., and Schlichting, I. (2006) Photodynamics of the small BLUF protein BlrB from *Rhodobacter sphaeroides*, *J Photochem Photobiol B* 83, 180-194.
15. Rajagopal, S., Key, J. M., Purcell, E. B., Boerema, D. J., and Moffat, K. (2004) Purification and initial characterization of a putative blue light-regulated phosphodiesterase from *Escherichia coli*, *Photochem Photobiol* 80, 542-547.

16. Han, Y., Meyer, M. H., Keusgen, M., and Klug, G. (2007) A haem cofactor is required for redox and light signalling by the AppA protein of *Rhodobacter sphaeroides*, *Mol Microbiol* 64, 1090-1104.
17. Unno, M., Sano, R., Masuda, S., Ono, T. A., and Yamauchi, S. (2005) Light-induced structural changes in the active site of the BLUF domain in AppA by Raman spectroscopy, *J Phys Chem B* 109, 12620-12626.
18. Stelling, A. L., Ronayne, K. L., Nappa, J., Tonge, P. J., and Meech, S. R. (2007) Ultrafast structural dynamics in BLUF domains. transient infrared spectroscopy of AppA and its mutants, *J Am Chem Soc* 129, 15556-15564.
19. Wolf, M. M., Schumann, C., Gross, R., Domratcheva, T., and Diller, R. (2008) Ultrafast infrared spectroscopy of riboflavin. dynamics, electronic structure, and vibrational mode analysis, *J Phys Chem B* 112, 13424-13432.
20. Laan, W., van der Horst, M. A., van Stokkum, I. H., and Hellingwerf, K. J. (2003) Initial characterization of the primary photochemistry of AppA, a blue-light-using flavin adenine dinucleotide-domain containing transcriptional antirepressor protein from *Rhodobacter sphaeroides*. a key role for reversible intramolecular proton transfer from the flavin adenine dinucleotide chromophore to a conserved tyrosine?, *Photochem Photobiol* 78, 290-297.
21. Stelling, A. L., Ronayne, K. L., Nappa, J., Tonge, P. J., and Meech, S. R. (2007) Ultrafast structural dynamics in BLUF domains. transient infrared spectroscopy of AppA and its mutants, *J Am Chem Soc* 129, 15556-15564.
22. Brooks, B., and Benisek, W. F. (1994) Mechanism of the reaction catalyzed by delta 5-3-ketosteroid isomerase of *Comamonas (Pseudomonas) testosteroni*. kinetic properties of a

- modified enzyme in which tyrosine 14 is replaced by 3-fluorotyrosine, *Biochemistry* 33, 2682-2687.
23. Tong, K. I., Yamamoto, M., and Tanaka, T. (2008) A simple method for amino acid selective isotope labeling of recombinant proteins in *E. coli*, *J Biomol NMR* 42, 59-67.
  24. Rappaport, F., Boussac, A., Force, D. A., Peloquin, J., Brynda, M., Sugiura, M., Un, S., Britt, R. D., and Diner, B. A. (2009) Probing the Coupling between Proton and Electron Transfer in Photosystem II Core Complexes Containing a 3-Fluorotyrosine, *Journal of the American Chemical Society* 131, 4425-4433.
  25. Ayyadurai, N., Prabhu, N. S., Deepankumar, K., Kim, A., Lee, S. G., and Yun, H. (2011) Biosynthetic substitution of tyrosine in green fluorescent protein with its surrogate fluorotyrosine in *Escherichia coli*, *Biotechnol Lett* 33, 2201-2207.
  26. Seyedsayamdost, M. R., Reece, S. Y., Nocera, D. G., and Stubbe, J. (2006) Mono-, di-, tri-, and tetra-substituted fluorotyrosines. new probes for enzymes that use tyrosyl radicals in catalysis, *J Am Chem Soc* 128, 1569-1579.
  27. Seyedsayamdost, M. R., Yee, C. S., and Stubbe, J. (2007) Site-specific incorporation of fluorotyrosines into the R2 subunit of *E. coli* ribonucleotide reductase by expressed protein ligation, *Nat Protoc* 2, 1225-1235.
  28. Minnihan, E. C., Young, D. D., Schultz, P. G., and Stubbe, J. (2011) Incorporation of Fluorotyrosines into Ribonucleotide Reductase Using an Evolved, Polyspecific Aminoacyl-tRNA Synthetase, *J Am Chem Soc* 133, 15942-15945.
  29. Reece, S. Y., Seyedsayamdost, M. R., Stubbe, J., and Nocera, D. G. (2006) Electron transfer reactions of fluorotyrosyl radicals, *J Am Chem Soc* 128, 13654-13655.

30. Hammill, J. T., Miyake-Stoner, S., Hazen, J. L., Jackson, J. C., and Mehl, R. A. (2007) Preparation of site-specifically labeled fluorinated proteins for  $^{19}\text{F}$ -NMR structural characterization, *Nat Protoc* 2, 2601-2607.
31. Wang, L., Xie, J., and Schultz, P. G. (2006) Expanding the genetic code, *Annu Rev Biophys Biomol Struct* 35, 225-249.
32. Young, D. D., Young, T. S., Jahnz, M., Ahmad, I., Spraggon, G., and Schultz, P. G. (2011) An evolved aminoacyl-tRNA synthetase with atypical polysubstrate specificity, *Biochemistry-Us* 50, 1894-1900.
33. Chin, J. W., Santoro, S. W., Martin, A. B., King, D. S., Wang, L., and Schultz, P. G. (2002) Addition of p-azido-L-phenylalanine to the genetic code of Escherichia coli, *J Am Chem Soc* 124, 9026-9027.
34. Gai, X. S., Coutifaris, B. A., Brewer, S. H., and Fenlon, E. E. (2011) A direct comparison of azide and nitrile vibrational probes, *Phys Chem Chem Phys* 13, 5926-5930.
35. Waegele, M. M., Culik, R. M., and Gai, F. (2011) Site-Specific Spectroscopic Reporters of the Local Electric Field, Hydration, Structure, and Dynamics of Biomolecules, *J Phys Chem Lett* 2, 2598-2609.
36. Chin, J. W., Cropp, T. A., Anderson, J. C., Mukherji, M., Zhang, Z., and Schultz, P. G. (2003) An expanded eukaryotic genetic code, *Science* 301, 964-967.

## Chapter 2

1. Anderson, S., Dragnea, V., Masuda, S., Ybe, J., Moffat, K., and Bauer, C. (2005) Structure of a novel photoreceptor, the BLUF domain of AppA from *Rhodobacter sphaeroides*, *Biochemistry-Us* 44, 7998-8005.

2. Kao, Y. T., Saxena, C., He, T. F., Guo, L., Wang, L., Sancar, A., and Zhong, D. (2008) Ultrafast dynamics of flavins in five redox states, *J Am Chem Soc* 130, 13132-13139.
3. Massey, V. (2000) The chemical and biological versatility of riboflavin, *Biochem Soc Trans* 28, 283-296.
4. Aigrain, L., Pompon, D., and Truan, G. (2011) Role of the interface between the FMN and FAD domains in the control of redox potential and electronic transfer of NADPH-cytochrome P450 reductase, *Biochem J* 435, 197-206.
5. Hines, R. N., Cashman, J. R., Philpot, R. M., Williams, D. E., and Ziegler, D. M. (1994) The mammalian flavin-containing monooxygenases: molecular characterization and regulation of expression, *Toxicol Appl Pharmacol* 125, 1-6.
6. Hecht, H. J., Kalisz, H. M., Hendle, J., Schmid, R. D., and Schomburg, D. (1993) Crystal structure of glucose oxidase from *Aspergillus niger* refined at 2.3 Å resolution, *J Mol Biol* 229, 153-172.
7. Rockwell, N. C., Su, Y. S., and Lagarias, J. C. (2006) Phytochrome structure and signaling mechanisms, *Annu. Rev. Plant Biol.* 57, 837-858.
8. Filipek, S., Stenkamp, R. E., Teller, D. C., and Palczewski, K. (2003) G protein-coupled receptor rhodopsin: a prospectus, *Annu Rev Physiol* 65, 851-879.
9. Kort, R., Hoff, W. D., Van West, M., Kroon, A. R., Hoffer, S. M., Vlieg, K. H., Crieland, W., Van Beeumen, J. J., and Hellingwerf, K. J. (1996) The xanthopsins: a new family of eubacterial blue-light photoreceptors, *Embo J.* 15, 3209-3218.
10. Losi, A. (2004) The bacterial counterparts of plant phototropins, *Photochem Photobiol Sci* 3, 566-574.

11. Briggs, W. R., Christie, J. M., and Salomon, M. (2001) Phototropins: a new family of flavin-binding blue light receptors in plants, *Antioxid Redox Signal* 3, 775-788.
12. Essen, L. O. (2006) Photolyases and cryptochromes: common mechanisms of DNA repair and light-driven signaling?, *Curr Opin Struct Biol* 16, 51-59.
13. Gomelsky, M., and Klug, G. (2002) BLUF: a novel FAD-binding domain involved in sensory transduction in microorganisms, *Trends Biochem Sci* 27, 497-500.
14. Losi, A. (2007) Flavin-based Blue-Light photosensors: a photobiophysics update, *Photochem Photobiol* 83, 1283-1300.
15. van der Horst, M. A., and Hellingwerf, K. J. (2004) Photoreceptor proteins, "star actors of modern times": a review of the functional dynamics in the structure of representative members of six different photoreceptor families, *Acc Chem Res* 37, 13-20.
16. Stelling, A. L., Ronayne, K. L., Nappa, J., Tonge, P. J., and Meech, S. R. (2007) Ultrafast structural dynamics in BLUF domains: transient infrared spectroscopy of AppA and its mutants, *J Am Chem Soc* 129, 15556-15564.
17. Laan, W., van der Horst, M. A., van Stokkum, I. H., and Hellingwerf, K. J. (2003) Initial characterization of the primary photochemistry of AppA, a blue-light-using flavin adenine dinucleotide-domain containing transcriptional antirepressor protein from *Rhodobacter sphaeroides*: a key role for reversible intramolecular proton transfer from the flavin adenine dinucleotide chromophore to a conserved tyrosine?, *Photochem Photobiol* 78, 290-297.
18. Stelling, A. L., Ronayne, K. L., Nappa, J., Tonge, P. J., and Meech, S. R. (2007) Ultrafast structural dynamics in BLUF domains: transient infrared spectroscopy of AppA and its mutants, *J. Am. Chem. Soc.* 129, 15556-15564.



19. Greetham, G. M., Burgos, P., Cao, Q., Clark, I. P., Codd, P. S., Farrow, R. C., George, M. W., Kogimtzis, M., Matousek, P., Parker, A. W., Pollard, M. R., Robinson, D. A., Xin, Z. J., and Towrie, M. (2010) ULTRA: A Unique Instrument for Time-Resolved Spectroscopy, *Appl Spectrosc* 64, 1311-1319.
20. Scott, A. P., and Radom, L. (1996) Harmonic vibrational frequencies: An evaluation of Hartree-Fock, Moller-Plesset, quadratic configuration interaction, density functional theory, and semiempirical scale factors, *J Phys Chem-Us* 100, 16502-16513.
21. Unno, M., Sano, R., Masuda, S., Ono, T. A., and Yamauchi, S. (2005) Light-induced structural changes in the active site of the BLUF domain in AppA by Raman spectroscopy, *J. Phys. Chem. B* 109, 12620-12626.
22. Hazekawa, I., Nishina, Y., Sato, K., Shichiri, M., Miura, R., and Shiga, K. (1997) A Raman study on the C(4)=O stretching mode of flavins in flavoenzymes: hydrogen bonding at the C(4)=O moiety, *J Biochem* 121, 1147-1154.
23. Copeland, R. A., and Spiro, T. G. (1986) Ultraviolet Resonance Raman-Spectroscopy of Flavin Mononucleotide and Flavin Adenine-Dinucleotide, *J Phys Chem-Us* 90, 6648-6654.
24. Abe, M., and Kyogoku, Y. (1987) Vibrational Analysis of Flavin Derivatives - Normal Coordinate Treatments of Lumiflavin, *Spectrochim Acta A* 43, 1027-1037.
25. Wolf, M. M. N., Schumann, C., Gross, R., Domratcheva, T., and Diller, R. (2008) Ultrafast Infrared Spectroscopy of Riboflavin: Dynamics, Electronic Structure, and Vibrational Mode Analysis, *J. Phys. Chem. B* 112, 13424-13432.
26. Alexandre, M. T. A., van Grondelle, R., Hellingwerf, K. J., and Kennis, J. T. M. (2009) Conformational Heterogeneity and Propagation of Structural Changes in the LOV2/J

- alpha Domain from *Avena sativa* Phototropin 1 as Recorded by Temperature-Dependent FTIR Spectroscopy, *Biophysical Journal* 97, 238-247.
27. Kondo, M., Nappa, J., Ronayne, K. L., Stelling, A. L., Tonge, P. J., and Meech, S. R. (2006) Ultrafast vibrational spectroscopy of the flavin chromophore, *J Phys Chem B* 110, 20107-20110.
  28. Masuda, S., Hasegawa, K., and Ono, T. A. (2005) Adenosine diphosphate moiety does not participate in structural changes for the signaling state in the sensor of blue-light using FAD domain of AppA, *FEBS Lett.* 579, 4329-4332.
  29. Li, G., and Glusac, K. D. (2009) The role of adenine in fast excited-state deactivation of FAD: a femtosecond mid-IR transient absorption study, *J Phys Chem B* 113, 9059-9061.
  30. Kim, M. a. C., P.R. (1993) Observation of a carbonyl feature for riboflavin bound to riboflavin-binding protein in the red-excited raman spectrum, *J. Am. Chem. Soc.*, 115, 7015–7016
  31. Kondo, M., Nappa, J., Ronayne, K. L., Stelling, A. L., Tonge, P. J., and Meech, S. R. (2006) Ultrafast vibrational spectroscopy of the flavin chromophore, *J. Phys. Chem. B* 110, 20107-20110.
  32. Laan, W., van der Horst, M. A., van Stokkum, I. H., and Hellingwerf, K. J. (2003) Initial characterization of the primary photochemistry of AppA, a blue-light-using flavin adenine dinucleotide-domain containing transcriptional antirepressor protein from *Rhodobacter sphaeroides*: a key role for reversible intramolecular proton transfer from the flavin adenine dinucleotide chromophore to a conserved tyrosine?, *Photochem. Photobiol.* 78, 290-297.

33. Alexandre, M. T., Domratcheva, T., Bonetti, C., van Wilderen, L. J., van Grondelle, R., Groot, M. L., Hellingwerf, K. J., and Kennis, J. T. (2009) Primary reactions of the LOV2 domain of phototropin studied with ultrafast mid-infrared spectroscopy and quantum chemistry, *Biophys J* 97, 227-237.
34. Gauden, M., Yeremenko, S., Laan, W., van Stokkum, I. H., Ihalainen, J. A., van Grondelle, R., Hellingwerf, K. J., and Kennis, J. T. (2005) Photocycle of the flavin-binding photoreceptor AppA, a bacterial transcriptional antirepressor of photosynthesis genes, *Biochemistry* 44, 3653-3662.
35. Haigney, A., Lukacs, A., Zhao, R. K., Stelling, A. L., Brust, R., Kim, R. R., Kondo, M., Clark, I., Towrie, M., Greetham, G. M., Illarionov, B., Bacher, A., Romisch-Margl, W., Fischer, M., Meech, S. R., and Tonge, P. J. (2011) Ultrafast infrared spectroscopy of an isotope-labeled photoactivatable flavoprotein, *Biochemistry* 50, 1321-1328.
36. Wolf, M. M., Zimmermann, H., Diller, R., and Domratcheva, T. (2011) Vibrational Mode Analysis of Isotope-Labeled Electronically Excited Riboflavin, *J Phys Chem B*.
37. Unno, M., Kumauchi, M., Sasaki, J., Tokunaga, F., and Yamauchi, S. (2002) Resonance Raman spectroscopy and quantum chemical calculations reveal structural changes in the active site of photoactive yellow protein, *Biochemistry* 41, 5668-5674.

### Chapter 3

1. Masuda, S., Tomida, Y., Ohta, H., and Takamiya, K. (2007) The critical role of a hydrogen bond between Gln63 and Trp104 in the blue-light sensing BLUF domain that controls AppA activity, *J. Mol. Biol.* 368, 1223-1230.

2. Dragnea, V., Arunkumar, A. I., Lee, C. W., Giedroc, D. P., and Bauer, C. E. (2010) A Q63E Rhodobacter sphaeroides AppA BLUF domain mutant is locked in a pseudo-light-excited signaling state, *Biochemistry* 49, 10682-10690.
3. Masuda, S., Hasegawa, K., Ishii, A., and Ono, T. A. (2004) Light-induced structural changes in a putative blue-light receptor with a novel FAD binding fold sensor of blue-light using FAD (BLUF); Slr1694 of synechocystis sp. PCC6803, *Biochemistry* 43, 5304-5313.
4. Kondo, M., Nappa, J., Ronayne, K. L., Stelling, A. L., Tonge, P. J., and Meech, S. R. (2006) Ultrafast vibrational spectroscopy of the flavin chromophore, *J. Phys. Chem. B* 110, 20107-20110.
5. Haigney, A., Lukacs, A., Zhao, R. K., Stelling, A. L., Brust, R., Kim, R. R., Kondo, M., Clark, I., Towrie, M., Greetham, G. M., Illarionov, B., Bacher, A., Romisch-Margl, W., Fischer, M., Meech, S. R., and Tonge, P. J. (2011) Ultrafast infrared spectroscopy of an isotope-labeled photoactivatable flavoprotein, *Biochemistry* 50, 1321-1328.
6. Wolf, M. M., Zimmermann, H., Diller, R., and Domratcheva, T. (2011) Vibrational Mode Analysis of Isotope-Labeled Electronically Excited Riboflavin, *J Phys Chem B*.
7. Stelling, A. L., Ronayne, K. L., Nappa, J., Tonge, P. J., and Meech, S. R. (2007) Ultrafast structural dynamics in BLUF domains: transient infrared spectroscopy of AppA and its mutants, *J. Am. Chem. Soc.* 129, 15556-15564.
8. Brazard, J., Usman, A., Lacomat, F., Ley, C., Martin, M. M., and Plaza, P. (2011) New insights into the ultrafast photophysics of oxidized and reduced FAD in solution, *J Phys Chem A* 115, 3251-3262.

9. Toh, K. C., van Stokkum, I. H. M., Hendriks, J., Alexandre, M. T. A., Arents, J. C., Perez, M. A., van Grondelle, R., Hellingwerf, K. J., and Kennis, J. T. M. (2008) On the signaling mechanism and the absence of photoreversibility in the AppA BLUF domain, *Biophys. J.* *95*, 312-321.
10. Kim, M. a. C., P.R. (1993) Observation of a carbonyl feature for riboflavin bound to riboflavin-binding protein in the red-excited raman spectrum, *J. Am. Chem. Soc.* *115*, 7015–7016
11. Kottke, T., Batschauer, A., Ahmad, M., and Heberle, J. (2006) Blue-light-induced changes in Arabidopsis cryptochrome 1 probed by FTIR difference spectroscopy, *Biochemistry* *45*, 2472-2479.
12. Immeln, D., Pokorny, R., Herman, E., Moldt, J., Batschauer, A., and Kottke, T. (2010) Photoreaction of plant and DASH cryptochromes probed by infrared spectroscopy: the neutral radical state of flavoproteins, *J. Phys. Chem. B* *114*, 17155-17161.
13. Tonge, P., Moore, G. R., and Wharton, C. W. (1989) Fourier-transform infra-red studies of the alkaline isomerization of mitochondrial cytochrome c and the ionization of carboxylic acids, *Biochem. J.* *258*, 599-605.
14. Fahmy, K., Jager, F., Beck, M., Zvyaga, T. A., Sakmar, T. P., and Siebert, F. (1993) Protonation states of membrane-embedded carboxylic acid groups in rhodopsin and metarhodopsin II: a Fourier-transform infrared spectroscopy study of site-directed mutants, *Proc. Natl. Acad. Sci. U. S. A.* *90*, 10206-10210.

15. Lubben, M., and Gerwert, K. (1996) Redox FTIR difference spectroscopy using caged electrons reveals contributions of carboxyl groups to the catalytic mechanism of haem-copper oxidases, *FEBS Lett.* 397, 303-307.
16. Tonge, P. J. (1996) FTIR studies of hydrogen bonding between  $\alpha,\beta$ -unsaturated esters and alcohols, *J. Mol. Struct.* 379, 135- 142.
17. Tozawa, K., Ohbuchi, H., Yagi, H., Amano, T., Matsui, T., Yoshida, M., and Akutsu, H. (1996) Unusual pKa of the carboxylate at the putative catalytic position of the thermophilic F1-ATPase beta subunit determined by  $^{13}\text{C}$ -NMR, *FEBS Lett.* 397, 122-126.
18. Henzler-Wildman, K., and Kern, D. (2007) Dynamic personalities of proteins, *Nature* 450, 964-972.
19. Dragnea, V., Waegelé, M., Balascuta, S., Bauer, C., and Dragnea, B. (2005) Time-resolved spectroscopic studies of the AppA blue-light receptor BLUF domain from *Rhodobacter sphaeroides*, *Biochemistry* 44, 15978-15985.

#### Chapter 4

1. Rappaport, F., Boussac, A., Force, D. A., Peloquin, J., Brynda, M., Sugiura, M., Un, S., Britt, R. D., and Diner, B. A. (2009) Probing the Coupling between Proton and Electron Transfer in Photosystem II Core Complexes Containing a 3-Fluorotyrosine, *Journal of the American Chemical Society* 131, 4425-4433.
2. Anderson, S., Dragnea, V., Masuda, S., Ybe, J., Moffat, K., and Bauer, C. (2005) Structure of a novel photoreceptor, the BLUF domain of AppA from *Rhodobacter sphaeroides*, *Biochemistry* 44, 7998-8005.

3. Ayyadurai, N., Prabhu, N. S., Deepankumar, K., Kim, A., Lee, S. G., and Yun, H. (2011) Biosynthetic substitution of tyrosine in green fluorescent protein with its surrogate fluorotyrosine in *Escherichia coli*, *Biotechnol Lett* 33, 2201-2207.
4. Seyedsayamdost, M. R., Reece, S. Y., Nocera, D. G., and Stubbe, J. (2006) Mono-, di-, tri-, and tetra-substituted fluorotyrosines: new probes for enzymes that use tyrosyl radicals in catalysis, *J Am Chem Soc* 128, 1569-1579.
5. Seyedsayamdost, M. R., Yee, C. S., and Stubbe, J. (2007) Site-specific incorporation of fluorotyrosines into the R2 subunit of *E. coli* ribonucleotide reductase by expressed protein ligation, *Nat Protoc* 2, 1225-1235.
6. Minnihan, E. C., Young, D. D., Schultz, P. G., and Stubbe, J. (2011) Incorporation of Fluorotyrosines into Ribonucleotide Reductase Using an Evolved, Polyspecific Aminoacyl-tRNA Synthetase, *J Am Chem Soc* 133, 15942-15945.
7. Reece, S. Y., Seyedsayamdost, M. R., Stubbe, J., and Nocera, D. G. (2006) Electron transfer reactions of fluorotyrosyl radicals, *J Am Chem Soc* 128, 13654-13655.
8. Bonin, J., Costentin, C., Robert, M., Saveant, J. M., and Tard, C. (2011) Hydrogen-Bond Relays in Concerted Proton-Electron Transfers, *Acc Chem Res*.
9. Reece, S. Y., Hodgkiss, J. M., Stubbe, J., and Nocera, D. G. (2006) Proton-coupled electron transfer: the mechanistic underpinning for radical transport and catalysis in biology, *Philos Trans R Soc Lond B Biol Sci* 361, 1351-1364.
10. Gai, X. S., Coutifaris, B. A., Brewer, S. H., and Fenlon, E. E. (2011) A direct comparison of azide and nitrile vibrational probes, *Phys Chem Chem Phys* 13, 5926-5930.

11. Waegele, M. M., Culik, R. M., and Gai, F. (2011) Site-Specific Spectroscopic Reporters of the Local Electric Field, Hydration, Structure, and Dynamics of Biomolecules, *J Phys Chem Lett* 2, 2598-2609.
12. Lim, M., Hamm, P., and Hochstrasser, R. M. (1998) Protein fluctuations are sensed by stimulated infrared echoes of the vibrations of carbon monoxide and azide probes, *Proceedings of the National Academy of Sciences of the United States of America* 95, 15315-15320.
13. Tsubaki, M., Mogi, T., and Hori, H. (1999) Fourier-transform infrared studies on azide-binding to the binuclear center of the Escherichia coli bo-type ubiquinol oxidase, *FEBS letters* 449, 191-195.
14. Tsubaki, M., Mogi, T., and Hori, H. (1999) Azide- and cyanide-binding to the Escherichia coli bd-type ubiquinol oxidase studied by visible absorption, EPR and FTIR spectroscopies, *Journal of biochemistry* 126, 510-519.
15. Yoshikawa, S., O'Keeffe, D. H., and Caughey, W. S. (1985) Investigations of cyanide as an infrared probe of heme protein ligand binding sites, *The Journal of biological chemistry* 260, 3518-3528.
16. Taskent-Sezgin, H., Chung, J., Banerjee, P. S., Nagarajan, S., Dyer, R. B., Carrico, I., and Raleigh, D. P. (2010) Azidohomoalanine: a conformationally sensitive IR probe of protein folding, protein structure, and electrostatics, *Angew Chem Int Ed Engl* 49, 7473-7475.
17. Choi, J. H., Raleigh, D., and Cho, M. (2011) Azido Homoalanine is a Useful Infrared Probe for Monitoring Local Electrostatics and Side-Chain Solvation in Proteins, *J Phys Chem Lett* 2, 2158-2162.



18. Chin, J. W., Cropp, T. A., Anderson, J. C., Mukherji, M., Zhang, Z., and Schultz, P. G. (2003) An expanded eukaryotic genetic code, *Science* 301, 964-967.
19. Chin, J. W., Santoro, S. W., Martin, A. B., King, D. S., Wang, L., and Schultz, P. G. (2002) Addition of p-azido-L-phenylalanine to the genetic code of Escherichia coli, *J Am Chem Soc* 124, 9026-9027.
20. Young, D. D., Young, T. S., Jahnz, M., Ahmad, I., Spraggon, G., and Schultz, P. G. (2011) An evolved aminoacyl-tRNA synthetase with atypical polysubstrate specificity, *Biochemistry* 50, 1894-1900.
21. Hammill, J. T., Miyake-Stoner, S., Hazen, J. L., Jackson, J. C., and Mehl, R. A. (2007) Preparation of site-specifically labeled fluorinated proteins for <sup>19</sup>F-NMR structural characterization, *Nat Protoc* 2, 2601-2607.
22. Wang, L., Xie, J., and Schultz, P. G. (2006) Expanding the genetic code, *Annu Rev Biophys Biomol Struct* 35, 225-249.
23. Laan, W., Gauden, M., Yeremenko, S., van Grondelle, R., Kennis, J. T., and Hellingwerf, K. J. (2006) On the mechanism of activation of the BLUF domain of AppA, *Biochemistry* 45, 51-60.
24. Laan, W., Bednarz, T., Heberle, J., and Hellingwerf, K. J. (2004) Chromophore composition of a heterologously expressed BLUF-domain, *Photochem. Photobiol. Sci.* 3, 1011-1016.
25. Kumagai, H., Yamada, H., Matsui, H., Ohkishi, H., and Ogata, K. (1970) Tyrosine phenol lyase. I. Purification, crystallization, and properties, *J Biol Chem* 245, 1767-1772.

26. Nagasawa, T., Utagawa, T., Goto, J., Kim, C. J., Tani, Y., Kumagai, H., and Yamada, H. (1981) Syntheses of L-tyrosine-related amino acids by tyrosine phenol-lyase of *Citrobacter intermedius*, *Eur J Biochem* 117, 33-40.